Joelson Fernandes Silva

Many-body correlations and Majorana fermions in quantum impurity problems

Uberlândia, Minas Gerais, Brasil

2021

Joelson Fernandes Silva

Many-body correlations and Majorana fermions in quantum impurity problems

Tese apresentada ao Programa de Pós-Graduação em Física da Universidade Federal de Uberlândia, como requisito parcial para obtenção do título de doutor em Física. Área de Concentração: Física da Matéria Condensada.

Universidade Federal de Uberlândia – UFU

Instituto de Física

Programa de Pós-Graduação

Supervisor: Prof. Dr. Edson Vernek

Uberlândia, Minas Gerais, Brasil

2021

Ficha Catalográfica Online do Sistema de Bibliotecas da UFU
com dados informados pelo(a) próprio(a) autor(a).

S586 Silva, Joelson Fernandes, 1992-
2021 Many-body correlations and Majorana fermions in quantum impurity problems [recurso eletrônico] / Joelson Fernandes Silva. - 2021.

Orientador: Edson Vernek.
Tese (Doutorado) - Universidade Federal de Uberlândia, Pós-graduação em Física.
Modo de acesso: Internet.
Disponível em: http://doi.org/10.14393/ufu.te.2021.182
Inclui bibliografia.
Inclui ilustrações.

1. Física. I. Vernek, Edson,1973-, (Orient.). II. Universidade Federal de Uberlândia. Pós-graduação em Física. III. Título.

CDU: 53

Bibliotecários responsáveis pela estrutura de acordo com o AACR2:

Gizele Cristine Nunes do Couto - CRB6/2091

UNIVERSIDADE FEDERAL DE UBERLÂNDIA
Coordenação do Programa de Pós-Graduação em Física
Av. João Naves de Ávila, 2121, Bloco 1A, Sala 213 - Bairro Santa Mônica, Uberlândia-MG, CEP 38400-902
Telefone: (34) 3239-4309 - www.infis.ufu.br - cpgfisica@ufu.br

ATA DE DEFESA - PÓS-GRADUAÇÃO

Programa de Pós-Graduação em:	Física				
Defesa de:	Tese de Doutorado				
Data:	03 de Março de 2021	Hora de início:	15:50	Hora de encerramento:	19:15
Matrícula do Discente:	11713FIS002				
Nome do Discente:	Joelson Fernandes Silva				
Título do Trabalho:	Many-body correlations and Majorana fermions in quantum impurity problems				
Área de concentração:	Física				
Linha de pesquisa:	Sistemas Fortemente Correlacionados				
Projeto de Pesquisa de vinculação:	Manybody physics in Majorana and Weyl fermion systems, Agência de Fomento: CNPq				

Reuniu-se por meio de vídeo conferência , a Banca Examinadora, designada pelo Colegiado do Programa de Pós-graduação em Física, assim composta: Professores Doutores: George Balster Martins - INFIS/UFU, José de los Santos Guerra - INFIS/UFU, Luis G. G. V. Dias da Silva- IF/USP, Tobias Micklitz - CBPF e Edson Vernek- INFIS/UFU , orientador do candidato.

Iniciando os trabalhos o presidente da mesa, Prof. Dr. Edson Vernek, apresentou a Comissão Examinadora e o candidato, agradeceu a presença do público, e concedeu ao Discente a palavra para a exposição do seu trabalho. A duração da apresentação do Discente e o tempo de arguição e resposta foram conforme as normas do Programa.

A seguir o senhor(a) presidente concedeu a palavra, pela ordem sucessivamente, aos(às) examinadores(as), que passaram a arguir o(a) candidato(a). Ultimada a arguição, que se desenvolveu dentro dos termos regimentais, a Banca, em sessão secreta, atribuiu o resultado final, considerando o(a) candidato(a):

Aprovado.

Esta defesa faz parte dos requisitos necessários à obtenção do título de Doutor

O competente diploma será expedido após cumprimento dos demais requisitos, conforme as normas do Programa, a legislação pertinente e a regulamentação interna da UFU.

Nada mais havendo a tratar foram encerrados os trabalhos. Foi lavrada a presente ata que após lida e achada conforme foi assinada pela Banca Examinadora.

Documento assinado eletronicamente por **José de los Santos Guerra**, **Professor(a) do Magistério Superior**, em 16/03/2021, às 12:47, conforme horário oficial de Brasília, com fundamento no art. 6º, § 1º, do Decreto nº 8.539, de 8 de outubro de 2015.

Documento assinado eletronicamente por **Luis Gregório Godoy de Vasconcellos Dias da Silva**, **Usuário Externo**, em 16/03/2021, às 13:04, conforme horário oficial de Brasília, com fundamento no art. 6º, § 1º, do Decreto nº 8.539, de 8 de outubro de 2015.

Documento assinado eletronicamente por **Tobias Micklitz**, **Usuário Externo**, em 16/03/2021, às 15:24, conforme horário oficial de Brasília, com fundamento no art. 6º, § 1º, do Decreto nº 8.539, de 8 de outubro de 2015.

Documento assinado eletronicamente por **George Balster Martins**, **Professor(a) do Magistério Superior**, em 16/03/2021, às 16:09, conforme horário oficial de Brasília, com fundamento no art. 6º, § 1º, do Decreto nº 8.539, de 8 de outubro de 2015.

Documento assinado eletronicamente por **Edson Vernek**, **Professor(a) do Magistério Superior**, em 16/03/2021, às 16:14, conforme horário oficial de Brasília, com fundamento no art. 6º, § 1º, do Decreto nº 8.539, de 8 de outubro de 2015.

A autenticidade deste documento pode ser conferida no site https://www.sei.ufu.br/sei/controlador_externo.php?acao=documento_conferir&id_orgao_acesso_externo=0, informando o código verificador **2642017** e o código CRC **8334BC07**.

Referência: Processo nº 23117.014487/2021-39 SEI nº 2642017

Essa tese é dedicada ao meu filho Rafael,
minha mãe Maria de Fátima
e minha esposa Paola.

Acknowledgements

Primeiramente agradeço à Deus, dono de todo conhecimento e sabedoria.

Agradeço à minha mãe, Maria de Fátima, por todo amor, carinho, apoio, por ser a mulher guerreira que é, meu maior exemplo de vida, a melhor mãe que alguém poderia ter, te amo mãe.

Agradeço ao meu pai, Joel e minha irmã, Jéssica.

Agradeço à minha esposa, Paola, por todo amor e companheirismo, por me suportar nos dias bons e dias ruins, e por ter me dado o maior presente que poderia ter, nosso amado filho.

Agradeço ao meu filho, Rafael. Antes de você nascer eu desconhecia o que realmente significava a palavra amor, hoje eu sei que você é a resposta.

Agradeço à todos meus amigos, não são muitos, mas com certeza são os melhores, em especial à Nayara (maninha), ao grande Gilmar, Dionattan, Gabriel, Marcos, ao Caio pelos memes que salvam o dia, enfim, todos vocês. Agradeço também à todos meus colegas de laboratório.

Agradesço à todos os professores que possibilitaram a minha formação, desde o primário até os professores do PPFIS.

Agradeço ao Prof. Luis Gregório pela parceria e disponibilização do seu código de NRG, fundamental para os resultados da primeira parte da presente tese.

Por último, mas não menos importante, agradeço ao meu orientador e mentor Prof. Edson Vernek, pelo apoio, paciência e por todos os anos me orientando e provocando reflexões profundas e fundamentais para minha formação como homem e como físico.

Durante o doutorado o presente aluno foi fomentado pela Fundação de Amparo à Pesquisa do Estado de Minas Gerais (FAPEMIG).

"The miracle of appropriateness of the language of mathematics for the formulation of the laws of physics is a wonderful gift which we neither understand nor deserve."
(Eugene Wigner)

Abstract

In this thesis we study the physical properties of quantum magnetic impurities in condensed matter systems. More precisely, we are interested in the quantum many-body phenomena emerging in metallic quantum wires with spin-orbit coupling (SOC) in the presence of magnetic impurities. In particular, we investigate Kondo effect in topological superconducting quantum wires sustaining Majorana zero modes (MZMs) bound to their edges. The first part of this work is dedicated to a general digression on the formation of localized magnetic moments in solid state materials and the emergence of the Kondo effect in single-impurity systems. We further study a system composed by a single level quantum dot coupled to a metallic reservoir and to two MZMs with opposite polarizations. The system is described by a version of single impurity Anderson model (SIAM) adapted to account for the MZMs. To access the Kondo physics we used the projection approach to derive an effective Kondo-like Hamiltonian from the SIAM. We show the coexistence of the many-body Kondo singlet and a local Majorana singlet which results from the robustness of the Kondo fixed points even in the presence local Majorana operators. Moreover, we show that the free MZMs of the system are responsible for the impurity residual entropy $S_{\rm res} = \frac{N_0}{2} k_B \ln(2)$, where N_0 is the number of free MZMs. This result reveals a fractional residual entropy for an odd number of free MZMs associated with a local non-Fermi liquid behavior. Both results were confirmed by the perturbative Anderson's Poor Man's scaling (PMS), and the nonperturbative Wilson's numerical renormalization group (NRG). The second part of the thesis is dedicated to the low-temperature physics of two-impurity systems. We revisit the well known Ruderman-Kittel-Kasuya-Yosida (RKKY) interaction between two spatially separated magnetic impurities in a quantum wire with SOC. To compute the RKKY coupling we use the original Ruderman-Kittel approach, based on the traditional second-order perturbation theory. This allows us find also the Dzaloshinskii-Moriya and Ising interactions between the impurities, both originated from the SOC. Our results show that due to momentum-spin-lock, provided by the SOC, the RKKY coupling does not decay with the inverse of the inter-impurities distance, as in the usual case. Instead, the coupling survives even at large distances oscillating with a characteristic wave-vector $2k_{\rm R}$, where $k_{\rm R}$ is proportional to the Rashba SOC.

Keywords: Quantum magnetic impurities, Majorana zero modes, quantum wires, Kondo effect, RKKY interaction, spin-orbit coupling.

Resumo

Na presente tese estudamos as propriedades físicas de impurezas magnéticas quânticas em sistemas de matéria condensada. Mais precisamente, estamos interessados em fenômenos de muitos corpos em fios quânticos metálicos com acoplamento spin-órbita (SOC) na presença de impurezas magnéticas. Particularmente, investigamos o efeito Kondo em fios quânticos supercondutores com fases topológicas que apresentem modos de Majorana de energia zero (MZMs) ligados à suas pontas. A primeira parte da tese é dedicada à discussão geral da formação de momentos magnéticos localizados e a emergência do efeito Kondo em sístemas de única impureza. Posteriormente, estudamos um sistema composto por um ponto quântico de um nível acoplado à um reservatório metálico e dois MZMs polarizados. O sistema é descrito por um modelo de Anderson de uma única impureza (SIAM) adaptado para comportar os dois MZMs. Para acessar a física de Kondo utilizamos o método projeção para deduzir um Hamiltoniano do tipo Kondo extraído do SIAM. Nós mostramos a coexistência do singleto de muitos corpos de Kondo e do singleto local de Majorana que resulta da robustez dos pontos fixos de Kondo, mesmo na presença de operadores locais de Majorana. Além disso, mostramos que os MZMs livres do sistema são responsáveis por uma entropia residual da impureza $S_{\rm res} = \frac{N_0}{2} k_B \ln(2)$, onde N_0 é o número de MZMs livres. Esse resultado revela uma entropia residual fracionária para um número impar de MZMs livres associado com um comportamento local de *non-Fermi liquid*. Ambos os resultados foram confirmados usando o método perturbativo de Anderson, Poor Man's scaling (PMS), e o método não perturbativo de Wilson, o grupo de renormalização numérico (NRG). A segunda parte da tese é dedicada à física de baixas temperaturas de sistemas de duas impurezas. Nós revisitamos a tradicional interação de Ruderman-Kittel-Kasuya-Yosida (RKKY) entre duas impurezas quânticas em um fio quântico com SOC. Para calcular o acoplamento RKKY usamos a abordagem original de Ruderman e Kittel, baseada na teoria quântica de perturbação. Além da interação RKKY, encontramos também interações adicionais do tipo Dzyaloshinskii-Moriya e Ising entre as impurezas originada do SOC. Nossos resultados mostram que devido ao "spin-lock" do momento, devido ao SOC, o acoplamento RKKY não decai com o inverso da distância entre as impurezas, como no caso usual. Ao invés disso, ele sobrevive a distâncias significativamente grandes e possui um comportamento oscilatório com o vetor de onda característico $2k_{\rm R}$, onde $k_{\rm R}$ é o proporcional ao acoplamento spin-órbita de Rashba.

Palavras-chave: Impurezas magnéticas quânticas, modos de Majorana de energia zero, fios quânticos, efeito Kondo, interação RKKY, acoplamento spin-órbita.

List of Figures

List of abbreviations and acronyms

SIAM	Single impurity Anderson model
MAM	Molecular Anderson model
PHS	Particle-hole symmetry
QD	Quantum dot
QW	Quantum wire
TQW	Topological quantum wire
TSQW	Topological superconducting quantum wire
SOC	Spin-orbit coupling
MZM	Majorana zero mode
RG	Renormalization group
NRG	Numerical renormalization group
PMS	Poor Man's scaling
RKKY	Ruderman-Kittel-Kasuya-Yosida

Contents

1 Introduction

One of the most interesting physical effect is magnetism (MEYER, 1971). Classical statistics calculations for a gas in the presence of a magnetic field showed that the system's thermodynamic properties are not affected by the magnetic field (ROSENFELD; NIELSEN, 1972). This fact was a prelude to the genuine quantum nature of magnetic effects in matter. Heisenberg and Neél were the first physicists to study magnetism from a true quantum mechanical perspective (Heisenberg, 1928; NÉEL, 1932), and developed a theory that is still widely used to study several magnetic effects of matter (AUERBACH, 2012) .

Another fascinating phenomenon associated with magnetism is the formation of localized magnetic moments in metallic systems. This process is fundamental to an important class of strongly correlated materials. In these materials, one component of the electronic system is highly localized, inside of partially filled d- or f-orbitals (COLEMAN, 2015). The interaction between the localized magnetic moment and the electronic sea gives rise to strong correlations in the system. These correlations are responsible for important physical phenomena, as the physical behavior of heavy-fermions materials and cuprate superconductors, the Kondo effect and many others (KRONMÜLLER; PARKIN, 2007). The microscopic origin of localized magnetic moments was developed by Anderson in the 1960s (ANDERSON, 1961) and will be summarized in section 2.1.

The Kondo effect plays a central role in phenomena associated with the influence of diluted magnetic impurities in metallic alloys (HEWSON, 1997). Experimentally discovered in the 1930s (de Haas; de Boer; van dën Berg, 1934), the Kondo effect is responsible for the increase of the resistivity of metals doped with magnetic ions at low-temperatures. This observation was counter-intuitive within the microscopic explanation for the resistivity at that time, based on the scattering of conduction electrons with the lattice ions (KITTEL, 2004). In fact, the magnetic nature of the impurities gives rise to a new strong coupling at low-temperatures between the localized magnetic moment and the spin of conduction electrons. As a result, the magnetic impurities becomes large scattering centers, producing the increase of the resistivity at low-temperatures. In the 1990s a renewed interest in the Kondo effect was motived by the discovery of the effect in quantum dots (QD) (GOLDHABER-GORDON et al., 1998; INOSHITA, 1998). The Kondo effect in metals and QDs is explained in detail in section 2.2.

Besides Kondo effect, several other interesting phenomena occurs in condensed matter systems. Over the recent years, the so-called topological materials received attention because their exotic properties and its potential application to new technologies (LIU; WILLIAMS; CHA, 2019). One of the most interesting physics associated with topological

phases in matter are the so-called Majorana zero modes. The MZMs are excitations in topological superconductors which have the astonishing property to be their own antiparticles (or anti-quasiparticles), see section 2.6. The Majorana particle concept was conceived by Etore Majorana in the search for a real solution of the Dirac equation (MAJORANA, 1937). In condensed matter system, MZMs received attention because their prominent potential for applications in quantum information theory (SARMA; FREEDMAN; NAYAK, 2015).

The search for experimental signatures of MZMs in topological superconductors demanded intensive effort in the last years (MOURIK et al., 2012; DENG et al., 2012; DAS et al., 2012; CHURCHILL et al., 2013; NADJ-PERGE et al., 2014). The first claim of a true experimental MZMs measurement was made by Mourik (MOURIK et al., 2012). However, those results were quite controversial. The zero-bias conductance pointed as the signature of the MZM also can be produced by other phenomena, for example the Kondo effect, see section 2.2, and Andreev bound states (LAW; LEE; NG, 2009; CHURCHILL et al., 2013). These effects were not totally distinguished from the possible zero-bias MZM influence (FRANZ, 2013). Moreover, the interplay between MZMs and Andreev bound states was studied by us in (SILVA; VERNEK, 2016).

To clarify distinct zero-bias contributions to the conductance, Vernek *et al.* proposed a system composed by a Kitaev chain coupled to a quantum dot in one of the chain edges (VERNEK et al., 2014). In the proposed system, the QD is also coupled to a metallic lead, and it was shown that the MZMs in the Kitaev chain "leaks" to the QD. This is an important result considering that the QD transport properties can be controlled with high experimental precision (FÖLSCH et al., 2014). This proposed setup is, therefore, very attractive from an experimental perspective. Moreover, Vernek's work also shows that the zero-bias contribution of MZMs to the conductance occurs when the QD energy level is far above (or far bellow) the metallic lead Fermi level. This establishes a clear distinction from the Kondo effect, that occurs only when the QD level is bellow the lead Fermi level, section 2.2.2.

More recently, in 2018 a highly reliable measurement of MZM was reported on *InSb-Al* hybrid semiconductor-superconductor nanowire devices (ZHANG et al., 2018). However, in 2021 these experimental results were re-analyzed and other effects which can mimic topological induced MZMs have not been discarded, leading to a retraction (ZHANG et al., 2021). The principal reason for this is disorder-induced subgap bound states and low-energy Andreev states which can appear in semiconductor-superconductor systems (PAN et al., 2021). Therefore, an unquestionable experimental signature of MZMs has not yet been reported. On the other hand, the fact of that MZM signature in the conductance be robust for a large range of the gate-controlled dot energy level is one of the main advantages of indirect MZM measurement using QDs which possible may avoid misleadings

as the reported in the 2018 experiment.

In the aforementioned Vernek's paper (VERNEK et al., 2014), local Coulomb interaction U in the QD was not taken into account. This was latter addressed in the Tijerina's work (RUIZ-TIJERINA et al., 2015). It was shown that even in the interacting QD, MZMs zero-bias contribution still survives coexisting with the Kondo contribution. Moreover, the results showed the coexistence of a Majorana local singlet, composed by the MZM and the metallic lead conduction electrons, and the traditional many-body Kondo singlet. However, the question of *why* Kondo screening still takes place in the presence of MZMs is still not well understood. In this context, the first part of the present thesis is dedicated to the study of the Kondo effect in the presence of two polarized MZMs with opposite polarization. This is a natural generalization of the previous scenario of an interacting QD in the presence of one MZM (RUIZ-TIJERINA et al., 2015). The main results from the first part of the thesis were published in (SILVA; SILVA; VERNEK, 2020).

The essence of the Kondo effect is the interaction between a magnetic impurity and the conduction electrons. It is observed in systems with few diluted magnetic impurities, or an isolated impurity connected to metallic leads, as in single QD experiments (BERA et al., 2010). When the density of impurities becomes large, the interaction between the impurities can not be neglected. Two or more magnetic impurities can interact between themselves even at large distances indirectly via the host conduction electrons. This indirect interaction is called Ruderman-Kittel-Kasuya-Yosida (RKKY) interaction (RUDERMAN; KITTEL, 1954; KASUYA, 1956; YOSIDA, 1957). The physical mechanism responsible for the RKKY interaction is a magnetic polarization of the conduction electrons around a magnetic impurity. This polarization can be "felt" by another magnetic impurity, giving rise to an indirect interaction between them. The magnetic polarization has an oscillatory behavior, with a characteristic wave-vector $2k_F$, analogue to the Friedel oscillations promoted by charged impurities (GROSSO; PARRAVICINI, 2000). The oscillations are damped as distance between the impurities R increases. The interaction decays essentially with $1/R^D$, where D is the dimension of the impurity host.

Nowadays, expedited by the advance of the experimental techniques and increase of technological developments, low-dimensional (1D and 2D) systems are accessible experimentally. Low-dimensional physics has interesting features from both fundamental science perspective and technological applications (DAVIES, 1997). One of the most interesting low-dimensional system are the so-called quantum wires (QW), also known as nanowires due to their nanoscopic length (BAND; AVISHAI, 2013). The quantum nature of QW gives rise to several physical phenomena (DAVIES, 1997). In the last few years, superconducting topological quantum wires (TQWs) have attracted attention due their ability to host Majorana Fermions, see section 2.6. The most prominent experimental realizations of TQWs have as essential keys the application of an external magnetic field,

the proximity to a superconducting material and a QW with strong intrinsic spin-orbit coupling (SOC) (ALICEA, 2012).

Indeed, perfect quality samples are almost impossible to be obtained in practice, even in extreme controlled environments impurities can be present. Sometimes the presence of impurities is desirable and originates novel physical phenomena. For example, the influence in magnetic processes in metallic and superconducting systems (WATTS et al., 2019; MöCKLI; HAIM; KHODAS, 2020). While scalar impurities affects only the linear moment of the incident particles, the magnetic impurities can affect both linear and magnetic moment (spin) of an incident particle. However, most of the theoretical calculations of QW's physical properties assume perfect QWs without any kind of imperfection (BAND; AVISHAI, 2013). Therefore, to a better understanding of experimental realizations of QWs it is necessary to consider impurities and how they affect the physics of the QW or TQWs. Generically, we have more than one single impurity, for this reason, other important aspect to be considered is the mutual interaction between the impurities, as the aforementioned RKKY interaction. Within these perspectives, the objective of the second part of the thesis is the understanding of how the RKKY interaction is modified in QWs in the presence of SOC. The main results of the second part of the present thesis were published in (SILVA; VERNEK, 2019).

This thesis is organized as follows. The first part is dedicated to the study of the Kondo effect in the presence of MZMs. The theoretical background of the physics of the localized magnetic moment, such as the Kondo effect and MZMs is given in Chapter 2. The first part results are given in Chapter 3 followed by the conclusion and an outlook (Chapter 4). The second part is dedicated to the study of the RKKY interaction in QWs with SOC. The theoretical background of the RKKY physics in different dimensions, as well the SOC in solids, are given in Chapter 5. The results of the second part are presented in Chapter 6. Finally, the conclusion of the second part is given in Chapter 7. Complementary appendices are presented after the thesis body.

Part I

Local magnetic moments, the Kondo effect, and Majorana zero modes

2 Background

2.1 Magnetic impurities

2.1.1 The Anderson model for magnetic impurities

The microscopic formation of localized magnetic moments in metals was explained in 1961 by P.W. Anderson (ANDERSON, 1961), inspired by the phenomenological work of Friedel (FRIEDEL, 1958). The simple model proposed by Anderson consisted of a single impurity in a metallic host, for this reason is called single impurity Anderson model (SIAM).

Nowadays, more than six decades after the original Anderson's work, the SIAM is still one of the most fundamental model to the study of quantum impurity problems (HEWSON, 1997). The Hamiltonian proposed by Anderson can be written as

$$H = \sum_{\sigma} \varepsilon_d n_{d\sigma} + U n_{d\uparrow} n_{d\downarrow} + \sum_{\mathbf{k}\sigma} \varepsilon_{\mathbf{k}} c^{\dagger}_{\mathbf{k}\sigma} c_{\mathbf{k}\sigma} + \sum_{\mathbf{k}\sigma} V_{\mathbf{k}d} (c^{\dagger}_{\mathbf{k}\sigma} d_{\sigma} + d^{\dagger}_{\sigma} c_{\mathbf{k}\sigma}). \tag{2.1}$$

In the above, $c^{\dagger}_{\mathbf{k}\sigma}(c_{\mathbf{k}\sigma})$ creates (annihilates) a electron with moment $\mathbf{k}$, spin σ and energy $\varepsilon_{\mathbf{k}}$, $d^{\dagger}_{\sigma}(d_{\sigma})$ creates (annihilates) an electron in the impurity with spin σ and energy ε_d, $n_{d\sigma} = d^{\dagger}_{\sigma} d_{\sigma}$ is the impurity number operator. The impurity local Coulomb interaction is denoted by U, and the last term describes the hybridization of the impurity and the conduction electrons of the metallic host, with the hybridization matrix element $V_{\mathbf{k}d}$.

Despite its simplicity, the SIAM is a surprisingly good model for metals, such as Au, Ag, Cu, etc, doped with magnetic impurities with the d-orbitals half-filled, for example Fe, Co and Ni (SMITH; KMETKO, 1983). Let us start by exposing an important feature of the SIAM. Performing the particle-hole transformation, $d_{\sigma} \to d^{\dagger}_{\sigma}$, to the Hamiltonian (2.1), the operator number modifies as $n_{d\sigma} \to (1 - n_{d\sigma})$ and the SIAM becomes

$$\begin{aligned} H \;\; &\to \;\; \sum_{\sigma} [\varepsilon_d - (\varepsilon_d + U) n_{d\sigma}] + U n_{d\uparrow} n_{d\downarrow} + \sum_{\mathbf{k}\sigma} \varepsilon_{\mathbf{k}} c^{\dagger}_{\mathbf{k}\sigma} c_{\mathbf{k}\sigma} + \sum_{\mathbf{k}\sigma} V_{\mathbf{k}d} (c^{\dagger}_{\mathbf{k}\sigma} d_{\sigma} + d^{\dagger}_{\sigma} c_{\mathbf{k}\sigma}) + U \\ &= \;\; \sum_{\sigma} [-(\varepsilon_d + U) n_{d\sigma}] + U n_{d\uparrow} n_{d\downarrow} + \sum_{\mathbf{k}\sigma} \varepsilon_{\mathbf{k}} c^{\dagger}_{\mathbf{k}\sigma} c_{\mathbf{k}\sigma} + \sum_{\mathbf{k}\sigma} V_{\mathbf{k}d} (c^{\dagger}_{\mathbf{k}\sigma} d_{\sigma} + d^{\dagger}_{\sigma} c_{\mathbf{k}\sigma}) + 2\varepsilon_d + U. \end{aligned}$$

Note now that if $\varepsilon_d = -U/2$ the SIAM is invariant under the particle-hole transformations. In this case the SIAM is called *symmetric SIAM*.

Let us now analyze the non-interacting limit of the SIAM ($U = 0$), for with the Hamiltonian (2.1)

$$H = \sum_{\sigma} \varepsilon_d n_{d\sigma} + \sum_{\mathbf{k}\sigma} \varepsilon_{\mathbf{k}} c^{\dagger}_{\mathbf{k}\sigma} c_{\mathbf{k}\sigma} + \sum_{\mathbf{k}\sigma} V_{\mathbf{k}d} (c^{\dagger}_{\mathbf{k}\sigma} d_{\sigma} + d^{\dagger}_{\sigma} c_{\mathbf{k}\sigma}). \tag{2.2}$$

Clearly, the Hamiltonian above is quadratic, and have exact solution. To compute the impurity occupation we will use the Green functions approach[1]. Following the Zubarev's approach (ZUBAREV, 1960), the impurity Green's function can be denoted as $\langle\langle d_\sigma; d_\sigma^\dagger\rangle\rangle_\omega$ and obey the equation of motion (EOM)

$$\omega\langle\langle d_\sigma; d_\sigma^\dagger\rangle\rangle = 1 + \langle\langle [d_\sigma, H]_-; d_\sigma^\dagger\rangle\rangle. \tag{2.3}$$

The commutation in the EOM can be calculated using the fermionic canonical algebra[2] $[d_\alpha, d_\beta^\dagger]_+ = \delta_{\alpha,\beta}$ and the relation $[A, BC]_- = [A, B]_+C - B[A, C]_+$, which leads to

$$[d_\sigma, H]_- = \varepsilon_{d\sigma} d_\sigma + \sum_{k\sigma} V_k c_{k\sigma}.$$

Replacing this expression into Eq.(2.3) we obtain

$$\omega\langle\langle d_\sigma; d_\sigma^\dagger\rangle\rangle = 1 + \varepsilon_d\langle\langle d_\sigma; d_\sigma^\dagger\rangle\rangle + \sum_{\mathbf{k}\sigma} V_{\mathbf{k}d}\langle\langle c_{\mathbf{k}\sigma}; d_\sigma^\dagger\rangle\rangle.$$

Note that a new Green's function $\langle\langle c_{k\sigma}; d_\sigma^\dagger\rangle\rangle$ appears on the right hand side of the equation above. The EOM for this new Green function is given by

$$\omega\langle\langle c_{\mathbf{k}\sigma}; d_\sigma^\dagger\rangle\rangle = \langle\langle [c_{\mathbf{k}\sigma}, H]_-; d_\sigma^\dagger\rangle\rangle.$$

Now

$$[c_{\mathbf{k}\sigma}, H]_- = \varepsilon_{\mathbf{k}} c_{k\sigma} + V_{\mathbf{k}d} d_\sigma,$$

rendering the set of coupled equations for the Green functions

$$\begin{aligned} G_{d\sigma}(\omega) &= g_{d\sigma}(\omega) + g_{d\sigma}(\omega)\sum_{\mathbf{k}\sigma} V_{\mathbf{k}d} G_{\mathbf{k}\sigma,d\sigma}(\omega), \\ G_{\mathbf{k}\sigma,d\sigma}(\omega) &= g_{\mathbf{k}\sigma}(\omega) V_{\mathbf{k}d} G_{d\sigma}(\omega), \end{aligned}$$

where we define $G_{d\sigma}(\omega) \equiv \langle\langle d_\sigma; d_\sigma^\dagger\rangle\rangle$, denoting the full impurity Green function, $G_{k\sigma,d\sigma}(\omega) \equiv \langle\langle c_{k\sigma}; d_\sigma^\dagger\rangle\rangle$ is the host full Green function, and $g_{d\sigma}(\omega) \equiv (\omega - \varepsilon_{d\sigma})^{-1}$, $g_{\mathbf{k}\sigma}(\omega) \equiv (\omega - \varepsilon_{\mathbf{k}\sigma})^{-1}$ are the impurity and host free propagators, respectively. Combining the two equations above we get

$$G_{d\sigma}(\omega) = g_{d\sigma}(\omega) + g_{d\sigma}(\omega)\Sigma(\omega)G_{d\sigma}(\omega). \tag{2.4}$$

This is the known Dyson's equation for the impurity with the self-energy

$$\Sigma(\omega) = \sum_{\mathbf{k}\sigma} V_{\mathbf{k}d}(\omega - \varepsilon_{\mathbf{k}})^{-1} V_{\mathbf{k}d}. \tag{2.5}$$

Required by analytical continuation, we must take $\omega \to \omega + i\eta$, with $\eta \to 0^+$, hence the self-energy can be written as

$$\Sigma(\omega) = \sum_{\mathbf{k}\sigma} \frac{|V_{\mathbf{k}d}|^2}{\omega + i\eta - \varepsilon_{\mathbf{k}}}. \tag{2.6}$$

[1] Further information about the Green's functions methods in condensed matter problems can be found in the nicely article (ODASHIMA; PRADO; VERNEK, 2017).

[2] Here $[A, B]_- = AB - BA$, stands for the usual commutation and $[A, B]_+ = AB + BA$ denotes the anti-commutation relation.

The self-energy can be decomposed in real and imaginary parts as

$$\Sigma(\omega) = \Lambda(\omega) + i\Delta(\omega), \tag{2.7}$$

with

$$\Lambda(\omega) = \sum_{\mathbf{k}} \frac{|V_{\mathbf{k}d}|^2(\omega - \varepsilon_{\mathbf{k}})}{(\omega - \varepsilon_{\mathbf{k}})^2 + \eta^2}, \qquad \Delta(\omega) = -\eta \sum_{\mathbf{k}} \frac{|V_{\mathbf{k}d}|^2}{(\omega - \varepsilon_{\mathbf{k}})^2 + \eta^2}. \tag{2.8}$$

The impurity Green function can be extracted from the Dyson equation (2.4) and acquires the form

$$\begin{aligned} G_{d\sigma}(\omega) &= \frac{1}{\omega - \varepsilon_d - \Sigma(\omega)} \\ &= \frac{1}{\omega - \varepsilon_d - [\Lambda(\omega) + i\Delta(\omega)]} \\ &= \frac{\omega - \varepsilon_d - \Lambda(\omega)}{[\omega - \varepsilon_d - \Lambda(\omega)]^2 + [\Delta(\omega)]^2} + \frac{i\Delta(\omega)}{[\omega - \varepsilon_d - \Lambda(\omega)]^2 + [\Delta(\omega)]^2}. \end{aligned}$$

From now we assume $V_{\mathbf{k}d} = V$, the moment sum in the self-energy can be computed in the energy space using that $\sum_{\mathbf{k}} g_{\mathbf{k}} \to \int \rho(\varepsilon) g(\varepsilon) d\varepsilon$, where $\rho(\varepsilon)$ is the density of states (DOS) of the conduction electrons. If we consider a constant DOS $\rho(\varepsilon) = \rho_0 \theta(D - |\varepsilon|)$, where $\rho_0 = 1/2D$, and D is the half of the conduction bandwidth. Then, for the real part of the self-energy we obtain

$$\Lambda(\omega) = \sum_{k} \frac{|V_k|^2(\omega - \varepsilon_{k\sigma})}{(\omega - \varepsilon_{k\sigma})^2 + \eta^2} = \rho_0 |V|^2 \int_{-D}^{D} \frac{\omega - \varepsilon}{(\omega - \varepsilon)^2 + \eta^2} d\varepsilon = \rho_0 |V|^2 ln \left[\frac{(\omega + D)^2 + \eta^2}{(\omega - D)^2 + \eta^2} \right]^{1/2},$$

and for the imaginary one

$$\begin{aligned} \Delta(\omega) &= -\eta \sum_{k} \frac{|V_k|^2}{(\omega - \varepsilon_{k\sigma})^2 + \eta^2} \\ &= -\rho_0 |V|^2 \int_{-D}^{D} \frac{\eta}{(\omega - \varepsilon)^2 + \eta^2} d\varepsilon \\ &= -\rho_0 |V|^2 \pi \int_{-D}^{D} \delta(\omega - \varepsilon) d\varepsilon \\ &= -\pi \rho_0 |V|^2, \end{aligned}$$

where we have used

$$\lim_{\eta \to 0} \frac{1}{\pi} \frac{\eta}{(\omega - \varepsilon)^2 + \eta^2} = \delta(\omega - \varepsilon). \tag{2.9}$$

Note that if $D \gg \omega$, the real part of the self-energy reduces to $\Lambda(\omega) \approx \rho_0 |V|^2 \ln(1)^{1/2} = 0$ and only the imaginary part contributes for the self-energy which becomes

$$\Sigma(\omega) = -i\Gamma, \tag{2.10}$$

where $\Gamma = \pi \rho_0 |V|^2$. This is an important limit known as *wide band limit* (WBL). The impurity local density of states (LDOS) can be computed by the relation

$$\rho_{d\sigma}(\omega) = -\frac{1}{\pi} \mathrm{Im}[G_{d\sigma}(\omega)]. \tag{2.11}$$

In the WBL, the impurity LDOS is

$$\rho_{d\sigma}(\omega) = \frac{1}{\pi}\frac{\Gamma}{(\omega-\varepsilon_d)^2+\Gamma^2}. \tag{2.12}$$

The impurity occupations for an individual spin is given by

$$\langle n_{d\sigma}\rangle = \int_{-\infty}^{\infty} f(\omega)\rho_{d\sigma}(\omega)d\omega, \tag{2.13}$$

where $f(\omega)$ is the Fermi-Dirac distribution. For $T=0$, the Fermi-Dirac distribution is the step-function $f(\omega)=\theta(E_F-\omega)$, where E_F is the Fermi level. Then, at the zero temperature the impurity occupation is

$$\langle n_{d\sigma}\rangle = \int_{-\infty}^{\varepsilon_F} \rho_{d\sigma}(\omega)d\omega.$$

By setting the Fermi level $\varepsilon_F=0$ and using the LDOS (2.12) together with

$$\int dx \frac{b}{(x-a)^2+b^2} = \mathrm{tg}^{-1}\left[\frac{x-a}{b}\right] + \text{constant}$$

we obtain

$$\langle n_{d\sigma}\rangle = \frac{1}{\pi}\int_{-\infty}^{E_F=0} d\omega \frac{\Gamma}{(\omega-\varepsilon_d)^2+\Gamma^2} = \frac{1}{\pi}\left[\mathrm{tg}^{-1}\left(\frac{-\varepsilon_d}{\Gamma}\right)+\frac{\pi}{2}\right].$$

The result above can be written in a more compact form noting that $\mathrm{tg}^{-1}\alpha+\pi/2=\theta$, so $\alpha=\mathrm{tg}(\theta-\pi/2)$, and using $\mathrm{tg}(\theta-\pi/2)=\cot(-\theta)$. Then, $\theta=\cot^{-1}(-\alpha)$, so we have for the impurity occupation

$$\langle n_{d\sigma}\rangle = \frac{1}{\pi}\cot^{-1}\left(\frac{\varepsilon_d}{\Gamma}\right). \tag{2.14}$$

In the interacting case, Anderson solved the aforementioned model using a mean-field approach to the quartic Coulomb interaction. To do so, Anderson performed the decoupling $Un_{d\uparrow}n_{d\downarrow} \to U\langle n_{d\uparrow}\rangle n_{d\downarrow} + U\langle n_{d\downarrow}\rangle n_{d\uparrow}$. Then, the Hamiltonian (A.1) becomes

$$H_{HF} = \sum_\sigma E_{d\sigma}n_{d\sigma} + \sum_{\mathbf{k}\sigma}\varepsilon_{\mathbf{k}}c^\dagger_{\mathbf{k}\sigma}c_{\mathbf{k}\sigma} + \sum_{\mathbf{k}\sigma}V_{\mathbf{k}d}(c^\dagger_{\mathbf{k}\sigma}d_\sigma + d^\dagger_\sigma c_{\mathbf{k}\sigma}), \tag{2.15}$$

where

$$E_{d\sigma} = \varepsilon_d + U\langle n_{d\bar{\sigma}}\rangle. \tag{2.16}$$

The mean-field Hamiltonian has the same structure of the non-interacting case (2.2), but now the impurity energy is spin-dependent. The same procedure used above leads to the coupled self-consistent equations for the impurity occupation

$$\langle n_{d\uparrow}\rangle = \frac{1}{\pi}\cot^{-1}\left(\frac{\varepsilon_d+U\langle n_{d\downarrow}\rangle}{\Gamma}\right), \tag{2.17}$$

$$\langle n_{d\downarrow}\rangle = \frac{1}{\pi}\cot^{-1}\left(\frac{\varepsilon_d+U\langle n_{d\uparrow}\rangle}{\Gamma}\right). \tag{2.18}$$

Magnetic solution are those for which $\langle n_{d\uparrow}\rangle \neq \langle n_{d\downarrow}\rangle$. Note that for $U=0$ the set of equations above recovered the non-interacting result (2.14). Other important limit is

when $\Gamma \to \infty$, so using that $\cot^{-1}(x) = \mathrm{tg}^{-1}(1/x)$ in the mean-field equations results in $\langle n_{d\uparrow}\rangle = \langle n_{d\downarrow}\rangle = 1/2$ which is other non-magnetic solution. In this limit, the impurity is strongly hybridized with the host and the local moment formation is not possible. We must find the critical size of the Coulomb interaction which allows the local moment formation. To do so, let us define $n_d = \sum_\sigma \langle n_\sigma\rangle$ and the local magnetization $M = \langle n_{d\uparrow}\rangle - \langle n_{d\downarrow}\rangle$, then $\langle n_{d\sigma}\rangle = \frac{1}{2}(n_d + \sigma M)$, with $\sigma = \pm 1$. These new definitions results in the novel self-consistent equations

$$n_d = \frac{1}{\pi}\sum_{\sigma=\pm 1}\cot^{-1}\Big(\frac{\varepsilon_d + U(n_d - \sigma M)/2}{\Gamma}\Big), \tag{2.19}$$

$$M = \frac{1}{\pi}\sum_{\sigma=\pm 1}\sigma\cot^{-1}\Big(\frac{\varepsilon_d + U(n_d - \sigma M)/2}{\Gamma}\Big). \tag{2.20}$$

When $M \to 0^+$ an infinitesimal magnetization rises up, and in this limit the equation for n_d becomes

$$\begin{aligned} n_d &= \frac{1}{\pi}\lim_{M\to 0^+}\sum_{\sigma=\pm 1}\cot^{-1}\Big(\frac{\varepsilon_d + U(n_d - \sigma M)/2}{\Gamma}\Big) \\ &= \frac{2}{\pi}\cot^{-1}\Big(\frac{\varepsilon_d + (U_c n_d)/2}{\Gamma}\Big), \end{aligned}$$

which leads to the condition

$$\cot\Big(\frac{n_d\pi}{2}\Big) = \frac{\varepsilon_d + (U_c n_d)/2}{\Gamma}, \tag{2.21}$$

where U_c is the critical size of the Coulomb interaction for the local moment formation. Now, for an infinitesimal change of the magnetization, we have

$$\begin{aligned} \frac{d}{dM}M &= \frac{1}{\pi}\lim_{M\to 0^+}\frac{d}{dM}\frac{1}{\pi}\sum_{\sigma=\pm 1}\sigma\cot^{-1}\Big(\frac{\varepsilon_d + U(n_d - \sigma M)/2}{\Gamma}\Big) \\ &= \frac{1}{\pi}\sum_{\sigma=\pm 1}\sigma^2\Big(\frac{U_c}{2\Gamma}\Big)\frac{1}{1 + \Big(\frac{\varepsilon_d + (U_c n_d)/2}{\Gamma}\Big)^2}. \end{aligned}$$

The result above results in the algebraic equation

$$1 = \frac{U_c}{\pi\Gamma}\frac{1}{1 + \Big(\frac{\varepsilon_d + (U_c n_d)/2}{\Gamma}\Big)^2}, \tag{2.22}$$

but using the fact that $\cot(n_d\pi/2) = \frac{\varepsilon_d + (U_c n_d)/2}{\Gamma}$ we obtain

$$1 = \frac{U_c}{\pi\Gamma}\frac{1}{1 + \Big(\frac{\varepsilon_d + (U_c n_d)/2}{\Gamma}\Big)^2} = \frac{U_c}{\pi\Gamma}\frac{1}{1 + \cot^2\Big(\frac{n_d\pi}{2}\Big)} = \frac{U_c}{\pi\Gamma}\sin^2\Big(\frac{n_d\pi}{2}\Big).$$

At least, in the half filling we have $n_d = 1$, which finally results in

$$U_c = \pi\Gamma, \tag{2.23}$$

this is the critical size of the Coulomb interaction where the local moment develops. The formation of local moments in diluted magnetic ions dissolved in metallic hosts depends on the ratio $U/\pi\Gamma$ be smaller or bigger than 1. As we saw that Γ is associated with the DOS of the metallic host, then hosts with large DOS are more unfavorable to the local moment formation (CLOGSTON et al., 1962). Even though the Anderson mean-field approach can be able to predict the local moment formation, it neglects spin fluctuations, which are fundamental for many important phenomena, as the Kondo effect, the main subject of the next section.

2.1.2 Local moment in quantum dots

The local moment formation is not restricted to magnetic ions dissolved in metals, but is also a key ingredient in the physics of the so called *quantum dots* (QDs). Quantum dots are artificial structures where the electrons are confined in the three spacial dimensions, leading to a discrete energy spectrum. For this reason, QDs are also known as artificial atoms (MARCOVICH; SHINN, 2014; SCHROER; PETTA, 2008; KOUWENHOVEN; MARCUS, 1998). One of the main advantages of QDs, in comparison with natural atoms, is the precisely fine-tuning control of the QDS energy-levels. The energy-levels can be experimentally changed with an external gate voltage V_g. A simple model for a multi-level QD is

$$H_{\text{dot}} = \sum_{\lambda\sigma}(\varepsilon_\lambda + eV_g)n_{d\lambda\sigma} + \frac{U}{2}N(N-1), \tag{2.24}$$

where $n_{d\sigma\lambda}$ is the QD number operator for the λ level with energy ε_λ, and $N = \sum_{\lambda\sigma} n_{d\lambda\sigma}$ is the total number of electrons in the QD. Notice that the QD Hamiltonian is a generalization of the atomic part of the Anderson model (2.1). Due to the spatial confinement, the Coulomb repulsion is an important energy scale in QD physics and it is responsible for the formation of local magnetic moment. The QD can be coupled to a metallic reservoir, as schematically illustrated in figure [1]. The contact here behaves as the metallic host in the SIAM, as said, the QD occupation can be precisely controlled by an external gate voltage V_g. For an even occupation all the QD energy levels are fully filled and the QD do not have magnetic moment ($S = 0$). However, for odd occupation the highest energy level is partially filled and the QD have a finite magnetic moment ($S = 1/2$)[3]. In the doubly occupied state, the Coulomb repulsion acts on the electrons at the same energy-level. For this reason, for large Coulomb repulsion the partial occupation is more energetically favorable. In this case, the QD have finite magnetic moment and behaves as a magnetic ion. We saw that for $U_c > \pi\Gamma$ we have a moment local formation. Then, when the Coulomb repulsion in the QD is larger than the hybridization with the metallic leads (Γ), the same physics described by the SIAM is expected.

[3] Here we consider a single particle QD, the situation is quite different for multi-particle QDs.

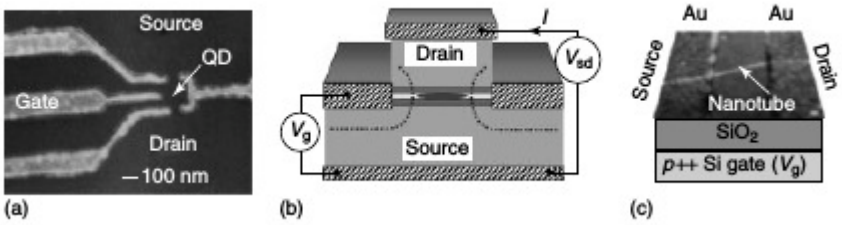

Figure 1 – Experimental realization of quantum dots in different configurations. (a) lateral quantum dot (STM image). (b) Vertical quantum dot. (c) Carbon nanotube quantum dots. Figure extracted from S. Sasaki et all., Nature, 405, 764–767 (2000).

2.2 The Kondo effect

Although the local moment formation can be explained by the Anderson mean-field approach, the spin scattering process cannot be described by this limit. This occurs because in the mean-field treatment the spin fluctuations are neglected. However, spin dynamics plays a fundamental role in the physics of magnetic ions diluted in metals. Indeed, spin-dependent process are the heart of one of the most important physical phenomena associated with magnetic ions, the so-called *Kondo effect*, the main subject of this section.

2.2.1 The Kondo effect in metals

One of the most surprising effects in magnetic ion diluted in metals is the minimum of the resistivity occurring at low temperatures. This fact was experimental known since 1930's when the freezing techniques was developed by the important physicist Onnes (ONNES, 1991). Following the Drude model, the metal resistivity results from atomic collisions and for $T = 0$ the system presents only a residual constant resistivity $R(0)$ (de Haas; de Boer; van dën Berg, 1934; MACDONALD; MENDELSSOHN; SIMON, 1950). Experimental results showed that this scenario was completely changed in metals doped with magnetic ions, see figure [2].

The theoretical explanation of the increase of the resistivity was absent until the middle of the 1960's, when Jun Kondo proposed the first theoretical model to explain the experimental results (KONDO, 1964). For this reason, this phenomena nowadays is called *Kondo effect* (KONDO, 1970; HEWSON, 1997). In the Kondo model, the ion's magnetic moment and the metallic host conduction electrons interacts by a local Heisenberg exchange as

$$H_K = J\delta(\mathbf{r})\mathbf{s} \cdot \mathbf{S}. \tag{2.25}$$

Where $\delta(\mathbf{r})$ is the Dirac delta function, $\mathbf{s}$ is the conduction electron magnetic moment (spin) and $\mathbf{S}$ is the ion magnetic moment. For $J > 0$ we have an antiferromagnetic interaction and

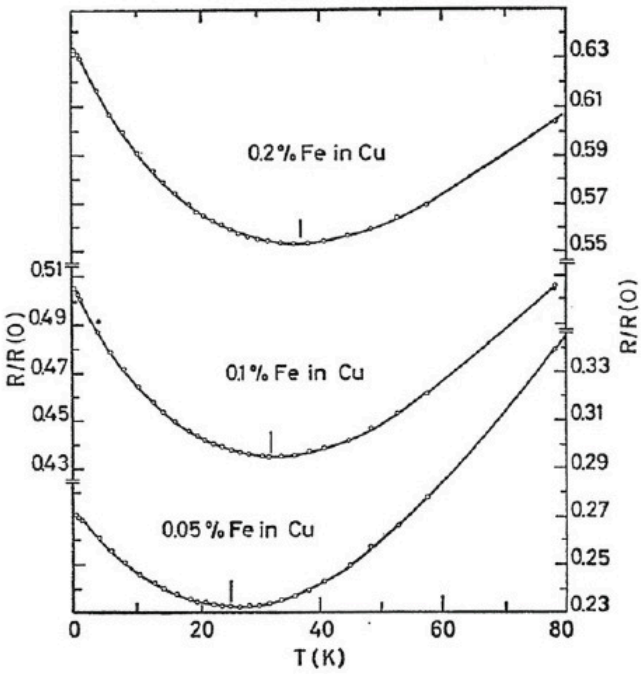

Figure 2 – Resistivity for low temperatures for coper (Cu) doped with iron (Fe) for different concentrations. Figure extracted from J. P. Franck, F. D. Manchester and D. L. Martin, Proc. Roy. Soc. (London) A 263, 494 (1961).

for $J < 0$ the interaction is ferromagnetic. Using spin-dependent second order perturbation theory, Kondo showed that the resistivity as function of the temperature in the presence of a magnetic ion is given by

$$R(T) = C\left[1 + 2Jn_0 \ln\frac{\Delta_c}{k_B T}\right], \tag{2.26}$$

where C is a constant, Δ_c is a high-energy cutoff and $n_0 = \rho(E_F)/N$ is the density of states per electron. Notice that only for antiferromagnetic interactions the resistivity increases. Then, from the Kondo model the resistivity increase is explained by a coupling between the magnetic moment of the ion and the spin of the conduction electrons; the ion with the surrounding electrons becomes a scattering center with a large extension which is responsible for the resistivity increase experimentally observed.

The logarithmic dependence in the perturbative Kondo result is a prelude for the nonperturbative behavior of the problem at low temperatures. The divergence occurs for temperatures in the order of $k_B T_K$; for this reason this energy scale is called *Kondo temperature* T_K.[4] For temperatures $T \gtrsim T_K$ the conduction electrons are weakly coupled with the magnetic ion and perturbative calculations gives qualitative aspects of the system. However, for temperatures $T < T_K$ the conduction electrons are strongly coupled with the magnetic impurity and in this regime the situation is more complicated. This

[4] Despite the name, the Kondo temperature is an energy scale, but is widely denoted only as T_K with the omission of the Boltzmann constant k_B.

fact is known as the *Kondo problem* (HEWSON, 1997). The Kondo problem is one of the most intriguing questions in condensed matter. To address the Kondo problem several techniques were applied over the years (ANDERSON; YUVAL; HAMANN, 1970; ANDERSON, 1970; ANDERSON; YUVAL, 1971; FOWLER; ZAWADOWSKI, 1971). Nevertheless, it was exactly solved only with the nonperturbative Wilson's numerical renormalization group (WILSON, 1975), and later with rigorous analytical tools (ANDREI, 1980; ANDREI; FURUYA; LOWENSTEIN, 1983). In the upcoming sections we will see some of the techniques used to approach the Kondo physics.

2.2.2 The Kondo effect in quantum dots

In the Section 2.1.2 we argued that quantum dots can behave as magnetic impurities. As such, at low temperatures is expected the manifest of the Kondo effect for QDs coupled to metallic leads. Indeed, for low temperatures the Kondo effect was observed in QDs experiments for the first time in experiments conducted by Goldhaber-Gordon (GOLDHABER-GORDON et al., 1998). In systems composed by QDs the Kondo effect has a different physical signature, which is not associated with the increase of the resistivity, but with the increase of the conductance. This fundamental difference between the Kondo effect in metals and in QDs results from the geometrical difference between the systems.

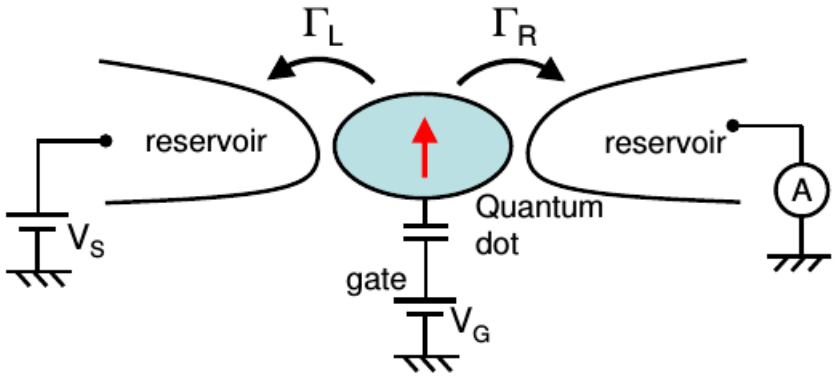

Figure 3 – Schematic representation of a single level quantum dot coupled to two metallic reservoir. The quantum dot energy level is controlled by the gate potencial V_G. Figure adapted from the talk "Quantum Noise of a Carbon Nanotube Quantum Dot in the Kondo Regime", R. Deblock, Orsay, 2001.

To see how the Kondo effect takes place in QDs, let us consider the schematic single level QD coupled to two metallic reservoir with the Fermi energy E_F, showed in the figure 3. At finite bias an electron can go from the left to the right reservoir across the QD, whose energy level ε_0 can be controlled by the gate potential V_G. For $\varepsilon_0 < E_F$ and large Coulomb repulsion U the double occupation is energetically unfavorable and the QD remains filled

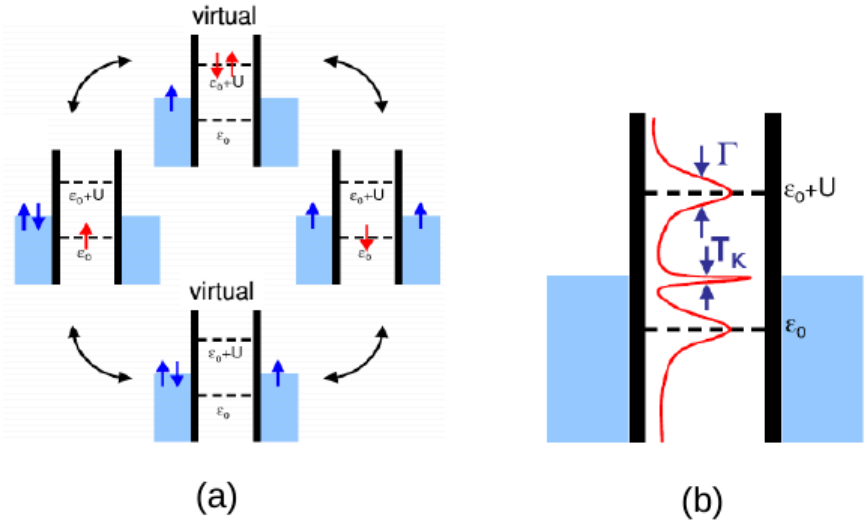

Figure 4 – (a) "Spin-flip" virtual charge fluctuation between the QD and the reservoir. (b) Formation of the Kondo resonance at the Fermi level. Figure adapted from the talk "Quantum Noise of a Carbon Nanotube Quantum Dot in the Kondo Regime", R. Deblock, Orsay, 2001.

with only one trapped electron and the current trough the two reservoir is blocked by the QD. This phenomenon is called *Coulomb blockage*. The conductance measured between the two reservoir will be finite only when $|e|V_G = \varepsilon_0 + U$. At low temperatures, even for $\varepsilon_0 + U > E_F$,"spin-flip" virtual charge fluctuations between the reservoir and the QD take place and gives rise to a resonance at the Fermi level. This is the famous Kondo resonance, see figure [4][5]. The resonance opens up a channel between the two reservoirs. Thus, enhancing the conductance even in the Coulomb blockage regime. This remarkable effect is the experimental signature of the Kondo effect in QDs. An experimental result is showed in figure 5.

The Kondo resonance described in the previous paragraph is one of the most prominent signatures of the Kondo effect (SUHL, 1965; ABRIKOSOV, 1965). The hybridization between a localized state and the continuum conduction band states results in a characteristic spectral line shape, the so-called Fano shape (FANO, 1961). The presence of a Kondo impurity modifies the Fano shape and provide a good experimental observation of physical effects related with the Kondo effect (ÚJSÁGHY et al., 2000). Scanning tunneling microscopy and spectroscopy techniques utilized Fano shapes to the determination of the Kondo temperature of magnetic impurities at the bulk and surfaces of metallic systems (ÚJSÁGHY et al., 2000; KNORR et al., 2002; WAHL et al., 2004).

[5] At low temperatures spin-independent charge fluctuation also occurs, however these process only renormalizes the scalar scattering potential which is not responsible for important physical effects in the system, see Appendix A.

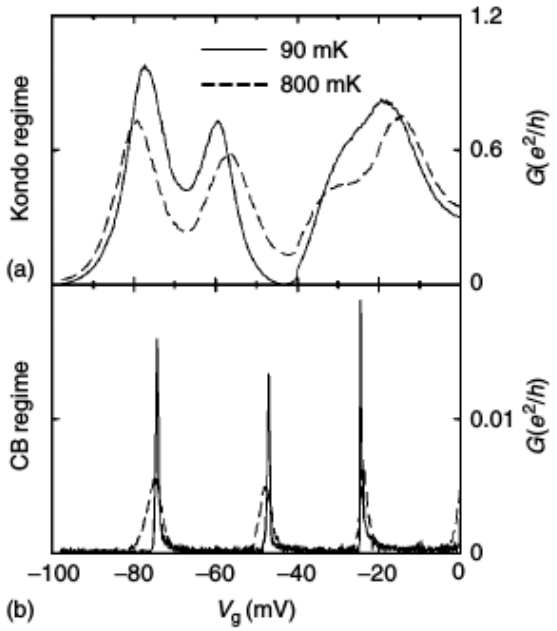

Figure 5 – Linear conductance of a QD coupled to metallic leads as function of the gate potential V_g. (a) In the Kondo regime ($T < T_K$), the Kondo resonance opens a large conductance window. (b) At temperatures $T > T_K$ the system is in the Coulomb blockage regime and the conduction occurs only for specific degenerated points. Figure extract from Goldhaber-Gordon et all., Phys. Rev. Lett., 81, 5225–5228 (1998).

2.2.3 Connection between the Anderson and the Kondo model

In the previous sections we saw two fundamental models for magnetic impurities coupled to a metallic host, the SIAM, whose Hamiltonian is given by the equation (2.1) and the Kondo's model given by (2.25). Although both models deal with magnetic impurities coupled to a metallic bath, the SIAM is more complete. This occurs because in the latter the impurity spin is treated as just another electron site, whereas in the Kondo model the local spin is treat as a separated entity. Consequently, in the Kondo's model the interaction between the conduction electrons and the local spin is purely magnetic, without charge fluctuations.

In the SIAM, charge fluctuations are controlled by the hybridization Γ. For large hybridization the impurity is strongly hybridized to the metallic host and the local moment formation is not possible. When the local Coulomb repulsion U at the impurity is large relative to Γ, true charge fluctuations are inhibited and only virtual process are allowed. Furthermore, in this regime the impurity is magnetic and the interaction between the impurity and the conduction electrons is essentially magnetic mediated by the local spin and the conduction electrons spin as in the Kondo model.

Formally, the SIAM can be mapped in the Kondo model. The reason for this is the

fact that the Kondo Hamiltonian can be described by the single occupied subspace of the single level SIAM Hilbert space. The first connection between the two models was done by Schrieffer and Wolf (SCHRIEFFER; WOLFF, 1966), using a unitary transformation, nowadays called Schrieffer-Wolf transformation. Later, Hewson used a projection approach to obtain the same effective Kondo Hamiltonian from the SIAM (HEWSON, 1997). The details of this mapping are given in Appendix A. The resulting effective Kondo Hamiltonian obtained from the SIAM is

$$H_{\text{eff}} = \sum_{\mathbf{k}\mathbf{k}'} J_{\mathbf{k}\mathbf{k}'} \mathbf{s}_{\mathbf{k}\mathbf{k}'} \cdot S, \tag{2.27}$$

where

$$J_{\mathbf{k}\mathbf{k}'} = V_{\mathbf{k}} V_{\mathbf{k}'} \left(\frac{1}{\varepsilon_k - \varepsilon_d} + \frac{1}{\varepsilon_d + U - \varepsilon_{k'}} \right). \tag{2.28}$$

Note that now the coupling $J_{\mathbf{k}\mathbf{k}'}$ is dependent on the SIAM parameters. Many proprieties obtained from the Kondo model are obtained by the SIAM one, which still has more general physical effects that can be captured by the Kondo model. In this sense, the SIAM is not only more complete, but also more realistic. Yet, in regimes where only the spin degree of freedom is important, it is interesting look at the effective Kondo model to understand the involved process.

2.3 Renormalization Group

One of the most important concepts in physics is the concept of scale. Almost all the physical phenomena are ruled by characteristic scales of length, time, and energy. For this reason, for several physical systems the different scales do not contributes in the same way to their fundamental physical features, so it is important to keep the focus in the most relevant degrees of freedom. The formal way to do so is the main subject of the called renormalization group (RG). In the RG procedure a high energy (short wavelength) cutoff is imposed to the original system with a set of coupling constants and scales. Then, the high energy cutoff is systematically reduced. As consequence, the system acquire "renormalized" coupling constants, which depends on the systematic reduction of the original high energy cutoff.

There are two types of RG: the renormalization group in the real space, where the systematic reduction of the system scale is done using the called Kadanoff's block spin (KADANOFF et al., 1967; WILSON, 1971a; CAPPELLI; MUSSARDO, 2012). The principal playground for this method is in statistical physics. The second RG procedure is done in the momentum (energy) space and it was introduced by K.G.Wilson (WILSON, 1971b). This method has been applied from high energy physics to condensed matter physics. Here, we will use the method developed by Wilson. First, let us discuss the Wilson RG procedure from a heuristic approach. Let us take a generic field $\phi(x)$, that can be either a scalar or vector associated with a boson or a fermion (or even a classical particle),

and $\phi(x) \equiv \phi(\mathbf{x}, t)$[6]. The degrees of freedom of the field $\phi(x)$ may be spins (quantum or classical), fermions, gauge fields, etc. The Fourier transformation of the field $\phi(x)$ in a D-dimensional space is

$$\phi(x) = \int \frac{d^D k}{(2\pi)^D} e^{ik\cdot x}\phi(k), \tag{2.29}$$

where we define $\phi(\mathbf{k}, \omega) = \phi(k)(e^{ik\cdot x} = e^{i(\mathbf{k}\cdot\mathbf{x}-\omega t)})$. The partition function of a system with degrees of freedom described by ϕ is given by [7]

$$\mathcal{Z} = \int \mathcal{D}\phi e^{-S(\phi)}. \tag{2.30}$$

In the equation above

$$\mathcal{D}\phi = \prod_{|k|<\Lambda} d\phi(k),$$

and Λ is the high energy cutoff and $S(\phi)$ is the Euclidean action. The next steep is the rescale of the system by a parameter $b(b < 1)$. Then, the degrees of freedom can be written as

$$\phi = \phi_< + \phi_>, \tag{2.31}$$

where the $\phi_<$ are the degrees of freedom with $|k| < b\Lambda$ and $\phi_>$ are the degrees of freedom in the region $b\Lambda < |k| < \Lambda$. The degrees of freedom $\phi_<$ are called "slow-modes" and $\phi_>$ "fast-modes" (high energy), and the momentum region $b\Lambda < |k| < \Lambda$ is called momentum shell, see figure 6. In the RG procedure the fast-modes $\phi_>$ in the momentum shell are integrate out, rendering an effective action S_{eff}. Using the partition function (2.30) we have

$$\begin{aligned} \mathcal{Z} = \int \mathcal{D}\phi e^{-S(\phi)} &= \int \mathcal{D}\phi_< \mathcal{D}\phi_> e^{-S(\phi_< + \phi_>)} \\ &= \int \mathcal{D}\phi_< e^{-S_{\text{eff}}(\phi_<)}, \end{aligned} \tag{2.32}$$

where

$$e^{-S_{\text{eff}}(\phi_<)} = \int \mathcal{D}\phi_> e^{-S(\phi_< + \phi_>)}, \tag{2.33}$$

and

$$\mathcal{D}\phi_< = \prod_{|k|<b\Lambda} d\phi(k), \qquad \mathcal{D}\phi_> = \prod_{b\Lambda<|k|<\Lambda} d\phi(k).$$

Once the energy scale is reduced by the parameter b, all the other characteristic scale should to be rescale to keep their original dimensional consistency. Then we have

$$x' = \frac{x}{b}, \qquad k' = bk \quad (\omega' = b\omega), \tag{2.34}$$

the relations above can be verified by direct inspection. This is done showing that the dimensional analysis of the Fourier modes is unaltered under the rescale $(e^{ik'x'} = e^{ikx})$.

[6] In the present section we adopt the RG ideas using the quantum field theory concepts, an analogue procedure using the Hamiltonian formulation was done by Cardy (CARDY; GODDARD; YEOMANS, 1996).

[7] See Appendix D.

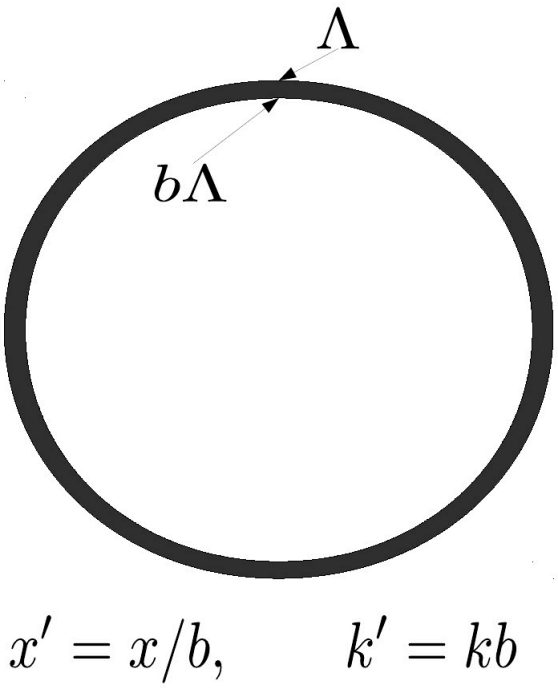

Figure 6 – The rescale of the momentum cutoff. The black area is called *momentum shell* and represents the degrees of freedom which will be integrate out in the RG procedure.

Suppose we find reach an action S^* that is *invariant* under the RG-transformations (rescale), in other words

$$S^*_{\text{eff}}(\phi_<) = S^*(\phi). \tag{2.35}$$

This is a *scale invariance* called the *fixed point* of the RG. Then, a system at the fixed point presents a scale invariance that can be interpreted as a new symmetry of the system.[8] To see what occurs with a system under the RG transformations is interesting look around the fixed point. To this end, let us consider a system close to the fixed point, whose action can be written as

$$S(\phi) = S^*(\phi) + \delta S(\phi). \tag{2.36}$$

In the above $\delta S(\phi)$ is a small deviation from the action at the fixed point, thus still linear in the fields. We can expand $\delta S(\phi)$ in the complete bases $\{\phi_n(x)\}$, with the correspondent eigenvalues g_n, associated with a system's fixed point. Then, the action (2.36) becomes

$$S(\phi) = S^*(\phi) + \int dx^D \sum_n g_n \phi_n(x). \tag{2.37}$$

We already saw that the RG transformation rescale the energy as $\Lambda \to b\Lambda$ (and the length as $x \to b^{-1}x$). Moreover, the fields $\phi_n(x)$ also transforms under the RG transformations.

[8] This is the origin of the term "group" in the Renormalization Group nomination. However, from the formal mathematical definition of group, the RG transformations do not represents a group. This occurs because the RG transformations do not have inversion. Even so, for historic reasons the denomination "Renormalization Group" was remained.

This transformation is given by

$$\phi_n(b^{-1}x) = b^{\Delta_n}\phi_n(x), \tag{2.38}$$

where Δ_n is called scale dimension of the operator $\phi_n(x)$. Operators that transform irreducibly (i.e. homogeneously) under rescaling are called primary (scaling) fields (CAPPELLI; MUSSARDO, 2012). Using this we obtain

$$\begin{aligned}\int dx^D \sum_n g_n\phi_n(x) &\rightarrow \int dx'^D \sum_n g_n\phi_n(x') \\ &\rightarrow \int d(b^{-1}x)^D \sum_n g_n b^{\Delta_n}\phi_n(x) \\ &\rightarrow \int dx^D \sum_n (g_n b^{(\Delta_n - D)})\phi_n(x).\end{aligned}$$

Notice from the equation above that all the RG transformation dependence can be associated with the transformation of the coupling constant as

$$g_n \rightarrow g_n b^{(\Delta_n - D)} \equiv g_n(b). \tag{2.39}$$

Now we can ask what occurs with the system under a infinitesimal rescale. The RG is applicable to systems where the different scales do not contributes in the same way for the physical phenomena. This naturally occurs in a logarithmic scale dependence. Note that from (2.39) the renormalized coupling constant $g_n(b)$ have a *logarithmic dependence* on the rescale parameter b. Therefore, a good way to written the rescale parameter b is $b = e^{-\delta\ell}$, where $\delta\ell \rightarrow 0$, which is consistent with $b^- \rightarrow 1$. The infinitesimal change of the coupling constant $g_n(b)$ can be encoded in $\frac{g_n(b)-g_n}{\delta \ln b} = \frac{dg_n}{d\ln b}$. However, note that $g_n b^{(\Delta_n - D)} = g_n e^{\ln b(\Delta_n - D)}$ and $\ln b = -\delta\ell$, which finally leads to the differential equation

$$\frac{dg_n}{d\ell} = (D - \Delta_n)g_n + \mathcal{O}(g_n^2). \tag{2.40}$$

Before extending the discussion for a more general point of view, let us understand the physical consequences of the RG transformations solving the equation (2.40). The differential equation

$$\frac{dg_n}{d\ell} = (D - \Delta_n)g_n,$$

can be solved by direct integration

$$\int_{g_n(0)}^{g_n(\ell)} \frac{dg_n}{g_n} = \int_0^\ell (\Delta_n - D)d\ell', \tag{2.41}$$

which leads to

$$g_n(\ell) = g_n(0)e^{(D-\Delta_n)\ell}. \tag{2.42}$$

Where $g_n(0) = g_n(\ell = 0)$ is the original coupling constant before the rescale, sometimes called bare coupling constant. Using the fact that the rescaled moment cutoff is $b\Lambda$ and $b = e^{-\delta\ell}$ we have the systematic rescale of the cutoff as b decreases (ℓ increases), which

corresponds to the system running for low-energies. From (2.42) we can see that dependence of the dimension system and the dimension scale have three different situation: when $D - \Delta_n > 0 (D > \Delta_n)$ the constant coupling grows under the momentum rescale, in this case the operator $\phi_n(x)$ is called *relevant*. The second case is when $D - \Delta_n = 0 (D = \Delta_n)$, so $\phi_n(x)$ is called *marginal*. In this case to determine how the operator behaves under the RG transformation high orders are necessary. The last case is when $D - \Delta_n < 0 (D < \Delta_n)$, then the coupling constant g_n decreases under the RG transformation, so $\phi_n(x)$ is called *irrelevant*.

The differential equation which rules the renormalization of the coupling constants under the RG transformations, for the example above, the equation (2.40), carries all the relevant information of the rescale dependence of the system. The general form of this RG differential equation is given by the called Gell-Mann-Low equation (GELL-MANN; LOW, 1954) [9]

$$\frac{dg}{d\ell} = \beta(g), \tag{2.43}$$

where $\beta(g)$ is called *β-function*. The equation (2.40) is called *three level β-function*. For the most physical problems the beta function may be expressed by the perturbative series

$$\beta(g) = \sum_n a_n g^n + \sum_{ab\cdots} \prod_{\alpha\beta\cdots} \alpha_{ab\cdots} g_\alpha g_\beta \cdots . \tag{2.44}$$

As we saw in the discussion above, the signal of the coefficients of the β-functions are fundamental to the understanding of the behavior of the renormalized coupling constants.

2.3.1 Renormalization Group

In the previous section we discussed the principal aspects of the renormalization group procedure, which consist of three fundamental steps:

1. **Subdivision of the field manifold:** The first step is the division of the integration manifold of the field $\{\phi\}$ in two submanifolds: The submanifold of the fast-modes $\{\phi_>\}$ which will be integrate out and the complementary submanifold of the slow-modes $\{\phi_<\}$. This can be done using the already mentioned Kadanoff block spin, or integrating out some momentum region, the called momentum shell, $b\Lambda < |k| < \Lambda$. The later is called *momentum shell integration*, see figure 6. There are other RG methods to make the manifold division of the field manifold used in some

[9] The Gell-Mann-Low equation also can be expressed in terms of the rescale parameter b as

$$\frac{dg}{d\ln b} = \beta(g).$$

In the present thesis we will also use the terminology RG equation to describe the Gell-Mann-Low equation.

physical fields, for example, dimension regulation and the operator product expansion, etc (CAPPELLI; MUSSARDO, 2012).

2. **RG step:** The second step is integrate out the fast-modes, which results in an effective action (or Hamiltonian). Generically, the effective action can be written as

$$S_{\text{eff}}(\phi_<) = \sum_n g_n \mathcal{O}'_n(\phi_<), \tag{2.45}$$

where $\{g_n\}$ are the altered coupling constants and $\mathcal{O}'$ describe some generic operator composed by the slow-modes. The effective action (or Hamiltonian) may be obtained using several methods, by direct integration, using projection operators, Feynman diagrams (loop expansion), etc (ALTLAND; SIMONS, 2010).

3. **Rescaling:** The last step is the rescale of the effective fields ϕ' to recover the original scale of the field ϕ, in the momentum/frequency space. This is done by

$$k' \to bk, \quad \omega' \to b^z \omega, \tag{2.46}$$

where z is the called *frequency renormalization exponent* or *dynamical exponent*, z can be one, two, three, or even a non-integer. The field renormalization under the rescaling is given by

$$\phi \to b^{\Delta_\phi} \phi, \tag{2.47}$$

where Δ_ϕ is the field scaling dimension. After returning to the original scales we obtain the generic effective action

$$S_{\text{eff}}(\phi) = \sum_n g'_n \mathcal{O}(\phi). \tag{2.48}$$

The functional structure of the effective action (Hamiltonian) *should* preserve the original action (Hamiltonian) structure. Sometimes, new terms not present in the original action can be generated in the effective action, if relevant (in the RG sense) they must be introduced in the original action since the beginning. All the information of the RG transformations is contained in the map

$$\mathbf{g}' = \tilde{\mathcal{R}}(\mathbf{g}), \tag{2.49}$$

where $\tilde{\mathcal{R}}$ maps the set $\mathbf{g} = \{g_n\}$ of bare coupling constants (before the RG procedure) into the renormalized set of coupling constants $\mathbf{g}' = \{g'_n\}$. Using the control parameter ℓ we can write

$$\lim_{\ell \to 0} \frac{\mathbf{g}' - \mathbf{g}}{\ell} = \lim_{\ell \to 0} \frac{\tilde{\mathcal{R}}(\mathbf{g}) - \mathbf{g}}{\ell},$$

and results in the generalized Gell-Mann-Low equation

$$\frac{d\mathbf{g}}{d\ell} = \mathcal{R}(\mathbf{g}), \tag{2.50}$$

with the generalized β-function

$$\mathcal{R}(\mathbf{g}) = \lim_{\ell \to 0} \left[\frac{\tilde{\mathcal{R}}(\mathbf{g}) - \mathbf{g}}{\ell} \right]. \tag{2.51}$$

2.3.2 The Renormalization Group flow

To analyze how the set of coupling constant $\mathbf{g}$ changes under the RG transformations, it is interesting to look to the submanifold composed by the *fixed points* $\mathbf{g}^*$. This submanifold is constituted by the points that are invariant under the scale, in other words, $\mathcal{R}(\mathbf{g}^*) = 0$. If we choose a manifold $\mathbf{g}$ close to the manifold $\mathbf{g}^*$, $\mathbf{g} = \mathbf{g}^* + \delta\mathbf{g}$ we can write

$$\mathbf{g}^* + \delta\mathbf{g}' \simeq \mathcal{R}(\mathbf{g}^* + \delta\mathbf{g}) = \mathcal{R}(\mathbf{g}^*) + \mathcal{K}\delta\mathbf{g}, \quad \mathcal{K}_{ab} = \left(\frac{\partial \mathcal{R}_a}{\partial g_b}\right)_{\mathbf{g}=\mathbf{g}^*},$$

and using that $\mathcal{R}(\mathbf{g}^*) = 0$ we obtain

$$\delta\mathbf{g}' \simeq \mathcal{K}\delta\mathbf{g} - g^*.$$

This results shows that close to the fixed points manifold the RG mapping is linear, then

$$\mathcal{R}(\mathbf{g}) \simeq \mathcal{K}(\mathbf{g} - \mathbf{g}^*). \tag{2.52}$$

The matrix $\mathcal{K}$ is general and may be not symmetric. Therefore, the left-eigenvalues can be different of the right-eigenvalues, denoting the left-eigenvalues by λ_α and the left-eigenvectors by ϕ_α^T, with $\alpha = 1, 2, \cdots N$ we have the equation

$$\phi_\alpha^T \mathcal{K} = \phi_\alpha^T \lambda_\alpha. \tag{2.53}$$

Now, let us take the vector $(\mathbf{g} - \mathbf{g}^*)$, the αth component of this vector in the basis $\{\phi\}$ can be written as

$$v_\alpha = \phi_\alpha^T(\mathbf{g} - \mathbf{g}^*). \tag{2.54}$$

With this we have that

$$\frac{dv_\alpha}{d\ell} = \phi_\alpha^T \frac{d}{d\ell}(\mathbf{g} - \mathbf{g}^*).$$

Using now the fact that $\mathcal{R}(\mathbf{g}) \simeq \mathcal{K}(\mathbf{g} - \mathbf{g}^*)$, together with the generalized β-function (2.50) we have

$$\frac{d}{d\ell}(\mathbf{g} - \mathbf{g}^*) = \mathcal{K}(\mathbf{g} - \mathbf{g}^*).$$

Then

$$\frac{dv_\alpha}{d\ell} = \phi_\alpha^T \mathcal{K}(\mathbf{g} - \mathbf{g}^*) = \lambda_\alpha \phi_\alpha^T \mathcal{K}(\mathbf{g} - \mathbf{g}^*) = \lambda_\alpha v_\alpha,$$

so the component v_α obey a simple RG equation that can be easily solved resulting in

$$v_\alpha(\ell) \sim e^{\lambda_\alpha \ell}. \tag{2.55}$$

The components $\{v_\alpha\}$ are called *scaling variables* in the RG language. We see that the components $\{v_\alpha\}$ are associated with the vector $(\mathbf{g} - \mathbf{g}^*)$, which shows the direction towards which the system *flows*. From (2.55) we have three possibilities: [10]:

[10] Note that when the RG equation is written in terms of the rescale parameter b, as $\frac{dg}{d\ln b} = \beta(g)$, the flow direction follows the opposite direction that when is expressed by ℓ. This occurs because $b = e^{-\delta\ell}$. In this case when $\lambda_\alpha > 0 (\lambda_\alpha < 0)$ corresponds to irrelevant(relevant) scaling variables.

- For $\lambda_\alpha < 0$ under the renormalization the flow goes towards the fixed points. In this case the scaling variable v_α is said to be *irrelevant*.
- For $\lambda_\alpha > 0$ the flow is in the opposite direction of the fixed points, in this case v_α is called *relevant*.
- The last case is when $\lambda_\alpha = 0$, in this case v_α is called *marginal*, and is necessary to look to the next order of the β-function to determine the flow direction. For example, consider the RG equation $v'_\alpha = \lambda_\alpha v_\alpha + x_\alpha v_\alpha^2$, if $\lambda_\alpha = 0$ the equation becomes $v'_\alpha = x_\alpha v_\alpha^2$. In this case v_α is marginal and the scaling flow will be determined by the higher order coefficient x_α. Following the definition above, for $x_\alpha < 0 (x_\alpha > 0)$ the scaling variable is *marginally irrelevant(relevant)*. Sometimes more higher orders are necessary to the flow analysis of determined scaling variable.

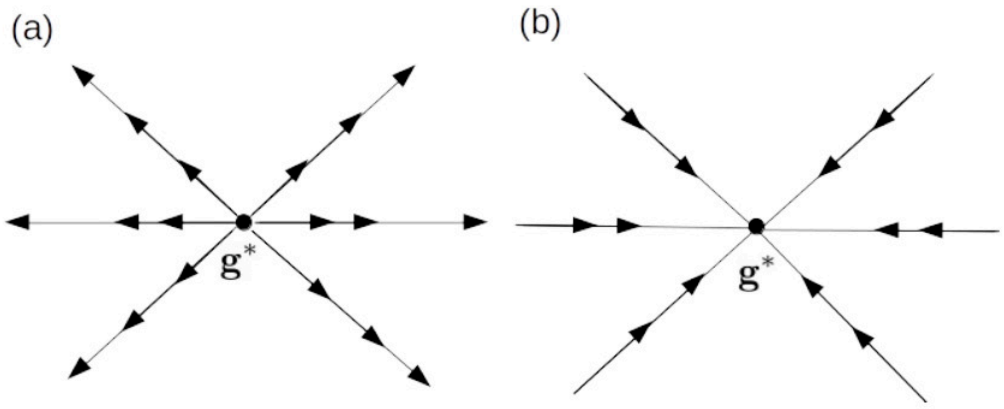

Figure 7 – Flow direction for (a) an repulsive fixed point manifold and (b) for an attractive fixed point manifold.

2.3.3 Few Simple Examples

2.3.3.1 Free scalar field

The simplest physical example is the massless free scalar fields in a D-dimensional space. In this example, the action is given by (ZEE, 2003)

$$S = \frac{1}{2}\int d^D x \left(\frac{\partial\phi(x)}{\partial \mathbf{x}}\right)^2 = \int^{\Lambda} \frac{d^D k}{(2\pi)^D}\frac{k^2}{2}|\phi(k)|^2. \tag{2.56}$$

The first step is the separation of the manifold by $\phi = \phi_< + \phi_>$ using the rescale parameter b. In the case of the free scalar field this division take the simple form

$$S(\phi_< + \phi_>) = S_< + S_> = \int^{b\Lambda} \frac{d^D k}{(2\pi)^D}\frac{k^2}{2}|\phi_<(k)|^2 + \int_{b\Lambda}^{\Lambda} \frac{d^D k}{(2\pi)^D}\frac{k^2}{2}|\phi_>(k)|^2. \tag{2.57}$$

The second step is the calculation of the effective action. We see that

$$e^{-S_{\text{eff}}(\phi_<)} = \int \mathcal{D}\phi_> e^{-S(\phi_< + S_{\phi_>})}.$$

With this, we can write

$$\begin{aligned} e^{-S_{\text{eff}}(\phi_<)} &= \int \mathcal{D}\phi_> e^{-\left(\int^{b\Lambda} \frac{d^D k}{(2\pi)^D}\frac{k^2}{2}|\phi_<(k)|^2 + \int_{b\Lambda}^{\Lambda} \frac{d^D k}{(2\pi)^D}\frac{k^2}{2}|\phi_>(k)|^2\right)} \\ &= e^{-\int^{b\Lambda} \frac{d^D k}{(2\pi)^D}\frac{k^2}{2}|\phi_<(k)|^2} \int \mathcal{D}\phi_> e^{-\int_{b\Lambda}^{\Lambda} \frac{d^D k}{(2\pi)^D}\frac{k^2}{2}|\phi_>(k)|^2}. \end{aligned}$$

Note that the path integral above is quadratic in the field, then results in a constant (see Appendix D)

$$\int \mathcal{D}\phi_> e^{-\int_{b\Lambda}^{\Lambda} \frac{d^D k}{(2\pi)^D}\frac{k^2}{2}|\phi_>(k)|^2} = \text{constant}.$$

Therefore,

$$e^{-S_{\text{eff}}(\phi_<)} = \text{constant} \times e^{-\int^{b\Lambda} \frac{d^D k}{(2\pi)^D}\frac{k^2}{2}|\phi_<(k)|^2}, \tag{2.58}$$

from which we can identify the effective action

$$S_{\text{eff}}(\phi_<) = \int^{b\Lambda} \frac{d^D k}{(2\pi)^D}\frac{k^2}{2}|\phi_<(k)|^2. \tag{2.59}$$

In the real space the effective action becomes

$$S_{\text{eff}}(\phi') = \frac{1}{2}\int d^D x' \left(\frac{\partial \phi'(x')}{\partial \mathbf{x}'}\right)^2. \tag{2.60}$$

The last step is the rescale of the system into the original scales. We saw that this can be done by $x' \to b^{-1}x$, and $\phi'(x') \to b^{\Delta}\phi(x)$, leading to

$$\begin{aligned} S_{\text{eff}}(\phi') = \frac{1}{2}\int d^D x' \left(\frac{\partial \phi'(x')}{\partial \mathbf{x}'}\right)^2 \quad &\to \quad S_{\text{eff}}(\phi) = \int d^D x b^{-D} \left(\frac{\partial (b^{\Delta}\phi(x))}{\partial (b^{-1}\mathbf{x})}\right)^2 \\ &\to \quad S_{\text{eff}}(\phi) = \int d^D x b^{(2\Delta+2-D)} \left(\frac{\partial \phi(x)}{\partial \mathbf{x}}\right)^2. \end{aligned}$$

Then, the effective action is invariant under scale if the scaling dimension is $\Delta = (D-2)/2$. In other words, the free scalar field is rescaled as

$$\phi'(x') \to b^{(D-2)/2}\phi(x). \tag{2.61}$$

Notice that the case $D = 2$ is special and corresponds to a situation in which the scale dimension is zero.

2.3.3.2 The Gaussian model

Many systems have interactions with quadratic dependence at the scalar quantum fields, for example the celebrated harmonic oscillator. The generic action that describes these system is

$$S(\phi) = \frac{1}{2}\int dx^D \left[\left(\frac{\partial \phi(x)}{\partial \mathbf{x}}\right)^2 + g\phi(x)^2\right], \tag{2.62}$$

where g is the coupling constant associated with the interaction. In the reciprocal space we have

$$S(\phi) = \frac{1}{2}\int^{\Lambda} \frac{d^D k}{(2\pi)^D}(k^2+g)|\phi(k)|^2. \tag{2.63}$$

We can now apply the RG ideas. First, the division between fast-mods and slow-modes, $\phi = \phi_< + \phi_>$, which leads to

$$S(\phi_< + \phi_>) = S_< + S_> = \frac{1}{2}\int^{b\Lambda} \frac{d^D k}{(2\pi)^D}(k^2+g)|\phi_<(k)|^2 + \frac{1}{2}\int_{b\Lambda}^{\Lambda} \frac{d^D k}{(2\pi)^D}(k^2+g)|\phi_>(k)|^2. \tag{2.64}$$

Next, we compute the effective action

$$e^{-S_{\text{eff}}(\phi_<)} = \int \mathcal{D}\phi_> e^{-S(\phi_< + S_{\phi_>})}.$$

With this we obtain

$$\begin{aligned} e^{-S_{\text{eff}}(\phi_<)} &= \int \mathcal{D}\phi_> e^{-\left(\frac{1}{2}\int^{b\Lambda} \frac{d^D k}{(2\pi)^D}(k^2+g)|\phi_<(k)|^2 + \frac{1}{2}\int_{b\Lambda}^{\Lambda} \frac{d^D k}{(2\pi)^D}(k^2+g)|\phi_>(k)|^2\right)} \\ &= e^{-\frac{1}{2}\int^{b\Lambda} \frac{d^D k}{(2\pi)^D}(k^2+g)|\phi_<(k)|^2} \int \mathcal{D}\phi_> e^{-\frac{1}{2}\int_{b\Lambda}^{\Lambda} \frac{d^D k}{(2\pi)^D}(k^2+g)|\phi_>(k)|^2}. \end{aligned}$$

Again, we have a Gaussian path integral

$$\int \mathcal{D}\phi_> e^{-\frac{1}{2}\int_{b\Lambda}^{\Lambda} \frac{d^D k}{(2\pi)^D}(k^2+g)|\phi_>(k)|^2} = \text{constant}.$$

Using this fact the exponential of the effective action becomes

$$e^{-S_{\text{eff}}(\phi_<)} = \text{constant} \times e^{-\frac{1}{2}\int^{b\Lambda} \frac{d^D k}{(2\pi)^D}(k^2+g)|\phi_<(k)|^2},$$

which allows us to identify the effective action

$$S_{\text{eff}}(\phi_<) = \frac{1}{2}\int^{b\Lambda} \frac{d^D k}{(2\pi)^D}(k^2+g)|\phi_<(k)|^2. \tag{2.65}$$

In the real space we have

$$S_{\text{eff}}(\phi') = \frac{1}{2}\int d^D x' \left[\left(\frac{\partial\phi'(x')}{\partial \mathbf{x}'}\right)^2 + g\phi'^2(x')\right]. \tag{2.66}$$

The last step is the restore of the original scales using $x' \to b^{-1}x$, $\phi' \to b^{\Delta}\phi$. Then, the effective action becomes

$$\begin{aligned} S_{\text{eff}}(\phi) &= \frac{1}{2}\int d^D x b^{-D}\left[\left(\frac{\partial(b^{\Delta}\phi(x)}{\partial(b^{-1}\mathbf{x})}\right)^2 + g(b^{\Delta}\phi)^2(x)\right] \\ &= \int d^D x b^{-D}\left[b^{2\Delta}b^2\left(\frac{\partial\phi(x)}{\partial\mathbf{x}}\right)^2 + gb^{2\Delta}\phi^2(x)\right] \\ &= \int d^D x b^{(2\Delta+2-D)}\left[\left(\frac{\partial\phi(x)}{\partial\mathbf{x}}\right)^2 + (b^{-2}g)\phi^2(x)\right]. \end{aligned}$$

Note that the effective action have the same original structure if $b^{2\Delta+2-D} = 1$, which results in the scaling dimension $\Delta = (D-2)/2$. However, now we have the renormalized coupling constant $g' = b^{-2}g$. So,

$$\phi' \rightarrow b^{(D-2)/2}\phi, \tag{2.67}$$

$$g' \rightarrow b^{-2}g. \tag{2.68}$$

Using now that the rescale parameter b can be written as $b = e^{-\ell}$ in the transformation above we have the RG equation

$$\frac{dg}{d\ell} = 2g. \tag{2.69}$$

Obviously, $g = 0$ is one fixed point of the Gaussian model. Another one is obtained when $g \rightarrow \infty$. The fixed point $g = 0$ is called *Gaussian fixed point* (SACHDEV, 2001). The sign of the coefficient of the RG equation above shows that the coupling constant g is a relevant scaling variable. In the two examples presented, the calculation of the effective action is easy (and exactly) due the Gaussian nature of the original action. However, for more complex actions the path integral can be hard to compute. Even so, the path integral still useful and is the base of many (non)perturbative methods (SHANKAR, 1994; SACHDEV, 2001; ALTLAND; SIMONS, 2010; CAPPELLI; MUSSARDO, 2012).

2.4 Poor Man's Scaling

The original solution for the minimum of the resistance, using traditional second order perturbation theory, has reveled the break down of the perturbative approach for the low-energy regime, also called infra-red limit (IR) (ALTLAND; SIMONS, 2010). Later on, the successful perturbative diagrammatic approach for many-body interacting systems, borrowed from high-energy physics, was applied to the Kondo model as well (ANDERSON; YUVAL; HAMANN, 1970; MATTUCK, 2012). The diagrammatic calculations of the renormalized vertex correction for the Kondo model has lead to logarithmic divergences for the IR-limit. This results showed that even more sophisticated perturbative methods break down in the IR-regime, an intrinsic nonperturbative signature of the model which has been called *Kondo problem* (HEWSON, 1997).

The diagrammatic approach for the Kondo problem is complicated and extensive. Part of this results from the fact that the spins operators do not obey the usual canonical algebra of the fermionic and bosonic fields, fundamental for the Wick's theorem application (MAHAN, 2013). This difficulty can be solved by mean of different methods. The most traditional one is the use of a pseudo-fermion representation for the spin operators, which allows the use of the usual diagrammatic techniques (COLEMAN, 2015). By the end of 1960s, Anderson has used the elegant renormalization group (RG) approach for the Kondo model for the first time (ANDERSON, 1970). Few years later, Anderson's ideas has inspired

K.G.Wilson to develops the numerical renormalization group (NRG), a nonperturbative approach that provided the best solution for the Kondo problem (WILSON, 1975).

We saw in the previous section that the physical idea behind the RG is the fact that for some physical phenomena different energy scales do not have the same contribution for the physics of the phenomena. In other words, the high-energy scales do not contribute in the same way for the problem how the low-energy scales do. To address this energy scale behavior the RG procedure consists of three steps [11]:

1. Rescale of the energy cutoff as $\Lambda \to \Lambda' = b\Lambda$, with $b < 1$ and Λ is the high-energy cutoff. The region $b\Lambda < |\mathbf{p}| < \Lambda$ is called *momentum shell*.
2. The degrees of freedom in the momentum shell $[b\Lambda, \Lambda]$ are integrate out, leading to a renormalized Hamiltonian $H(\Lambda) \to H'$.
3. Rescaling back to the original energy scale, $\omega = b\omega'$ and the new Hamiltonian by $H(b\Lambda) = bH'$.

Anderson showed that the third step is unnecessary in the RG application for Kondo model, since that this simplified rescale give the qualitative correct results for the Kondo model(ANDERSON; YUVAL; HAMANN, 1970). For this reason Anderson gave it the name *Poor Man's Scaling* (PMS)(ANDERSON, 1970). The points that are invariant under the RG procedure are called *fixed points*, see section 2.3. These special points are invariant under scale transformations, an important concept in phase transitions theory (SACHDEV, 2001).

In the RG approach to the Kondo problem, the Poor Man's scaling, Anderson do not used field theory techniques, as traditionally done in the high-energy physics and statistical physics. Instead, he used the traditional scattering theory, more intuitive and accessible to the Kondo model. A generic Hamiltonian for particles in the presence of a scattering potential is given by

$$H = H_0 + V, \tag{2.70}$$

where H_0 is the unperturbed system and V is the scattering potential. The single particle propagator in the presence of the scattering potential is

$$G(\omega) = G_0(\omega) + G_0(\omega)TG_0(\omega), \qquad G_0(\omega) = (\omega - H_0)^{-1}, \tag{2.71}$$

where $G_0(\omega)$ is the free propagator and T is the scattering matrix (T-Matrix) that obeys the Dyson equation

$$T(\omega) = V + VG_0(\omega)T(\omega). \tag{2.72}$$

All information about the interactions are contained in the Dyson equation for the T-Matrix.

[11] For the Kondo problem the Hamiltonian formalism is most useful than the Lagrangian formalism, for this reason we will use the former in this section.

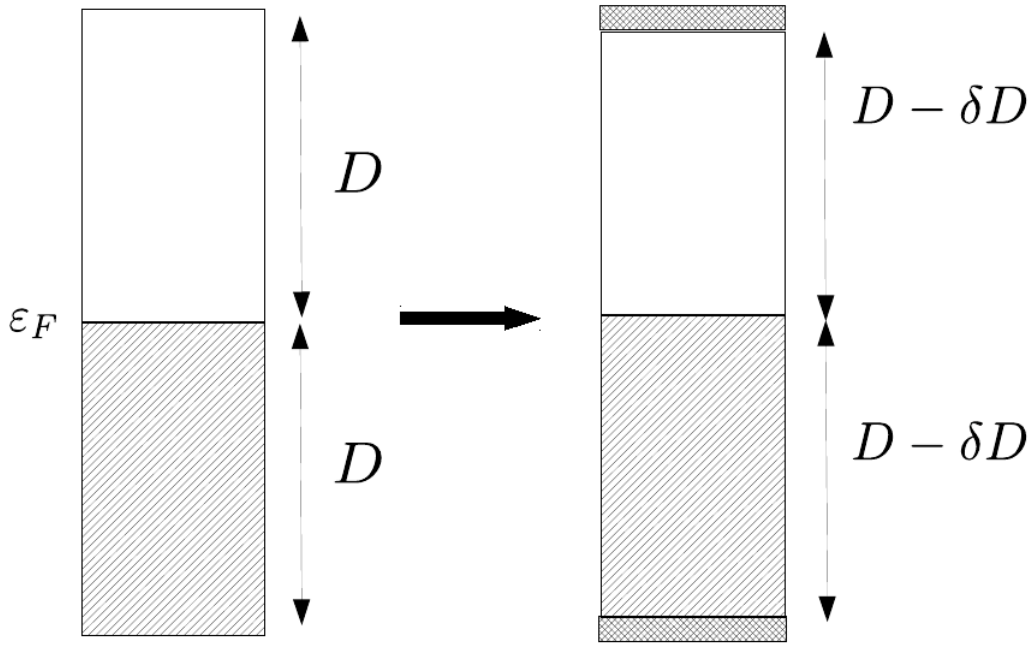

Figure 8 – Reduction of the conduction bandwidth in the RG procedure. The High-energy states in the top $(D - |\delta D| < \varepsilon_k < D)$ and bottom $(-D + |\delta D| > \varepsilon_k > -D)$ are integrate out which leads to renormalized interactions.

Consider a conduction band of bandwidth $2D$ in which all the energy states in the range $[-D, \varepsilon_{\rm F}]$ are filled, and the energy states in the range $[\varepsilon_{\rm F}, D]$ are empty. For simplicity, let us set $\varepsilon_{\rm F} = 0$. In the first step of the RG procedure the high-energy cutoff is rescaled as $D \to \tilde{D} = D - |\delta D|$ and $-D \to -\tilde{D} = -D + |\delta D|$, see figure 8. In the second step we integrate out the high-energy states. For this, we need account all the scattering process allowed in the range $[D - |\delta D|, D]$ for electron-like scattering, and $[-D, -D + |\delta D|]$ for hole-like scattering. This can be done by introducing the projection operator P which projects on scattering process in the energy ranges that will be integrate out. Then, the equation (2.72) becomes

$$T = V + V(1 - P)G_0(\omega)T + VPG_0(\omega)T. \tag{2.73}$$

The Dyson equation can be solved iteratively as

$$\begin{aligned} T &= V + V(1-P)G_0[V + V(1-P)G_0T + VPG_0T] \\ &\quad + VPG_0[V + V(1-P)G_0T + VPG_0T] \\ &= [V + VPG_0V] + [V + VPG_0V](1-P)G_0T \\ &\quad + V(1-P)[G_0V(1-P)G_0T + G_0VPG_0T] + VPG_0VPG_0T \\ &= [V + VPG_0V] + [V + VPG_0V](1-P)G_0T + VPG_0VPG_0T. \end{aligned}$$

Thus,

$$T = [V + VPG_0V + \cdots] + [V + VPG_0V + \cdots](1-P)G_0T + VPG_0VPG_0V \cdots PG_0T. \tag{2.74}$$

Defining $T' = (1-P)T(1-P)$ as the T-Matrix for the reduced conduction band in the (2.74) we obtain the invariant form of the Dyson equation for the reduced T-Matrix

$$T'(\omega) = V' + V'G_0(\omega)T'(\omega). \tag{2.75}$$

In the above

$$V' = (1-P)[V + VPG_0(\omega)V + VPG_0(\omega)VPG_0(\omega)V + \cdots](1-P). \tag{2.76}$$

From (2.76) we can see that as a result of the bandwidth reduction the original interaction V has changed as

$$V \to V + \Delta V, \quad \text{with} \quad \Delta V = VPG_0(\omega)V + VPG_0(\omega)VPG_0(\omega)V + \cdots \tag{2.77}$$

Here ΔV is the interaction correction raised in the energy sector of the reduced conduction band. Moreover, from ΔV we can see that interaction correction is expressed by a perturbative series. The series contains all the the high-energy scattering process that will be integrate out in the RG procedure.

2.4.1 Poor Man's scaling applied to the Kondo's model

The Kondo's model can be written in terms of fermionic operators as

$$H_0 = \sum_{\mathbf{k}\sigma} \varepsilon_k c^\dagger_{\mathbf{k}\sigma} c_{\mathbf{k}\sigma} \tag{2.78}$$

which describes the conduction electrons and

$$V = \sum_{\mathbf{k}\mathbf{k}'} [J_z S^z (c^\dagger_{\mathbf{k}'\uparrow} c_{\mathbf{k}\uparrow} - c^\dagger_{\mathbf{k}'\downarrow} c_{\mathbf{k}\downarrow}) + J_+ S^+ c^\dagger_{\mathbf{k}'\downarrow} c_{\mathbf{k}\uparrow} + J_- S^- c^\dagger_{\mathbf{k}'\uparrow} c_{\mathbf{k}\downarrow}] \tag{2.79}$$

describes the Kondo scattering potential. Note that the Kondo scattering potential can change both spin and momentum of an incident electron on the magnetic impurity. The T-matrix correction to the Kondo model to second order is

$$\begin{aligned} \Delta V^{(2)} &= VPG_0(\omega)V = \sum_{\mathbf{k}_1\mathbf{k}_2} [J_z S^z (c^\dagger_{\mathbf{k}_1\uparrow} c_{\mathbf{k}_2\uparrow} - c^\dagger_{\mathbf{k}_1\downarrow} c_{\mathbf{k}_2\downarrow}) + J_+ S^+ c^\dagger_{\mathbf{k}_1\downarrow} c_{\mathbf{k}_2\uparrow} + J_- S^- c^\dagger_{\mathbf{k}_1\uparrow} c_{\mathbf{k}_2\downarrow}] \\ &\quad \times P \frac{1}{\omega - H_0} \sum_{\mathbf{k}_3\mathbf{k}_4} [J_z S^z (c^\dagger_{\mathbf{k}_3\uparrow} c_{\mathbf{k}_4\uparrow} - c^\dagger_{\mathbf{k}_3\downarrow} c_{\mathbf{k}_4\downarrow}) + J_+ S^+ c^\dagger_{\mathbf{k}_3\downarrow} c_{\mathbf{k}_4\uparrow} + J_- S^- c^\dagger_{\mathbf{k}_3\uparrow} c_{\mathbf{k}_4\downarrow}]. \end{aligned} \tag{2.80}$$

There are two distinct intermediary virtual processes involved in the expression above. The first one is the creation of an electron ($c^\dagger_{\mathbf{k}_3\sigma}$) within the top layer of the conduction band and then annihilated ($c_{\mathbf{k}_{2\sigma'}}$). This kind of virtual process is called *electron-type*. The second process within the lowest layer of the conduction band, a hole is created ($c_{\mathbf{k}_4\sigma}$) and

annihilated subsequently ($c^{\dagger}_{\mathbf{k}_1\sigma'}$). As such, this corresponds to a *hole-type* process. Taking care of this two distinct processes and applying the momentum conservation we obtain

$$\begin{aligned}\Delta V^{(2)} &= \sum_{\mathbf{k}_1\mathbf{k}_2\mathbf{k}_4}[J_zS^z(c^{\dagger}_{\mathbf{k}_1\uparrow}c_{\mathbf{k}_2\uparrow}-c^{\dagger}_{\mathbf{k}_1\downarrow}c_{\mathbf{k}_2\downarrow})+J_+S^+c^{\dagger}_{\mathbf{k}_1\downarrow}c_{\mathbf{k}_2\uparrow}+J_-S^-c^{\dagger}_{\mathbf{k}_1\uparrow}c_{\mathbf{k}_2\downarrow}]\\ &\times P\frac{1}{\omega-\varepsilon_{\mathbf{k}_2}+\varepsilon_{\mathbf{k}_4}}[J_zS^z(c^{\dagger}_{\mathbf{k}_2\uparrow}c_{\mathbf{k}_4\uparrow}-c^{\dagger}_{\mathbf{k}_2\downarrow}c_{\mathbf{k}_4\downarrow})+J_+S^+c^{\dagger}_{\mathbf{k}_2\downarrow}c_{\mathbf{k}_4\uparrow}+J_-S^-c^{\dagger}_{\mathbf{k}_2\uparrow}c_{\mathbf{k}_4\downarrow}]\\ &+\sum_{\mathbf{k}_1\mathbf{k}_2\mathbf{k}_3}[J_zS^z(c^{\dagger}_{\mathbf{k}_1\uparrow}c_{\mathbf{k}_2\uparrow}-c^{\dagger}_{\mathbf{k}_1\downarrow}c_{\mathbf{k}_2\downarrow})+J_+S^+c^{\dagger}_{\mathbf{k}_1\downarrow}c_{\mathbf{k}_2\uparrow}+J_-S^-c^{\dagger}_{\mathbf{k}_1\uparrow}c_{\mathbf{k}_2\downarrow}]\\ &\times P\frac{1}{\omega-\varepsilon_{\mathbf{k}_3}+\varepsilon_{\mathbf{k}_1}}[J_zS^z(c^{\dagger}_{\mathbf{k}_3\uparrow}c_{\mathbf{k}_1\uparrow}-c^{\dagger}_{\mathbf{k}_3\downarrow}c_{\mathbf{k}_1\downarrow})+J_+S^+c^{\dagger}_{\mathbf{k}_3\downarrow}c_{\mathbf{k}_1\uparrow}+J_-S^-c^{\dagger}_{\mathbf{k}_3\uparrow}c_{\mathbf{k}_1\downarrow}].\end{aligned} \tag{2.81}$$

The projection operator P will select process in the top of the conduction band for electron-type process and in the bottom for hole-like process. Notice that for process in the top of the conduction bandwidth we have $c_{\mathbf{k}_2}c^{\dagger}_{\mathbf{k}_2}=(1-n_{\mathbf{k}_2})\approx 1$ and for process in the bottom $c^{\dagger}_{\mathbf{k}_1}c_{\mathbf{k}_1}=n_{\mathbf{k}_1}\approx 1$, also at the edges $\varepsilon_{\mathbf{k}_2}\approx D$ and $\varepsilon_{\mathbf{k}_1}\approx -D$. Besides, the energies summation for the virtual processes integrate out in the PMS are given by

$$\sum_{\mathbf{k}_2}=\sum^{D>|\varepsilon_{\mathbf{k}_2}|<D-\delta D},\quad \sum_{\mathbf{k}_1}=\sum^{-D<|\varepsilon_{\mathbf{k}_1}|<-D+\delta D}.$$

The summations above can be transformed in energy integrals as

$$\sum^{D>|\varepsilon_{\mathbf{k}_2}|<D-\delta D}\to\int_{D-\delta D}^{D}\rho d\varepsilon,\qquad \sum^{-D<|\varepsilon_{\mathbf{k}_1}|<-D+\delta D}\to\int_{-D}^{-D+\delta D}\rho d\varepsilon,$$

where ρ is the density of states (DOS). After some cumbersome algebra we obtain

$$\begin{aligned}V' &= V+\Delta V^{(2)}\\ &= \sum_{\mathbf{k}\mathbf{k}'}[(J_z+\delta J_z)S^z(c^{\dagger}_{\mathbf{k}'\uparrow}c_{\mathbf{k}\uparrow}-c^{\dagger}_{\mathbf{k}'\downarrow}c_{\mathbf{k}\downarrow})+(J_++\delta J_+)S^+c^{\dagger}_{\mathbf{k}'\downarrow}c_{\mathbf{k}\uparrow}+(J_-+\delta J_-)S^-c^{\dagger}_{\mathbf{k}'\uparrow}c_{\mathbf{k}\downarrow}],\end{aligned} \tag{2.82}$$

in which the couplings constant renormalization are

$$\delta J_z = -J_{\pm}^2\rho|\delta D|\left[\frac{1}{\omega-D+\varepsilon_k}+\frac{1}{\omega-D-\varepsilon_{k'}}\right] \tag{2.83}$$

$$\delta J_{\pm} = -J_zJ_{\pm}\rho|\delta D|\left[\frac{1}{\omega-D+\varepsilon_k}+\frac{1}{\omega-D-\varepsilon_{k'}}\right]. \tag{2.84}$$

The RG equations can be written in their traditional Gell-Mann-Low (RG) equation form (2.50). To this end, notice that for low-energy excitations the frequency dependence in the denominator can be neglected in comparison with the high energy cutoff D. Thus,

$$\frac{|\delta D|}{(\omega-D)}=-\frac{|\delta D|}{D}.$$

Recalling that the bandwidth is reduced of -$|\delta D|$, then

$$\delta J = -\frac{dJ}{dD}|\delta D|,$$

which gives

$$\frac{dJ_z}{d\ln D} = -2\rho J_\pm^2 + \mathcal{O}(\rho^2 J^3), \tag{2.85}$$

$$\frac{dJ_\pm}{d\ln D} = -2\rho J_z J_\pm + + \mathcal{O}(\rho^2 J^3). \tag{2.86}$$

The Gell-Mann-Low equation is traditionally written as function of dimensionless couplings. For the Kondo model we can define the dimensionless coupling $g_\alpha = \rho J_\alpha$ ($\alpha = z, \pm$). With this we obtain

$$\frac{dg_z}{d\ln D} = -2g_\pm^2 + \mathcal{O}(g^3) \equiv \beta_z(g_\alpha), \tag{2.87}$$

$$\frac{dg_\pm}{d\ln D} = -2g_z g_\pm + \mathcal{O}(g^3) \equiv \beta_\pm(g_\alpha). \tag{2.88}$$

Let us look to the isotropic Kondo model $J_z = J_\pm$, in which case we obtain the simple RG equation

$$\frac{dJ}{d\ln D} = -2\rho J^2 + \mathcal{O}(\rho^2 J^3). \tag{2.89}$$

Note that after integrating out the high-energy states, the coupling constant is a function of the reduction of the bandwidth, for this reason is now called *running coupling constant*. The solution of the RG equation leads to

$$J(\tilde{D}) = \frac{J_0}{1 - 2J_0\rho\ln(D/\tilde{D})}, \tag{2.90}$$

where D is the original bandwidth, $\tilde{D}$ is the reduced bandwidth and J_0 is the original (bare) Kondo coupling (before the bandwidth reduction). The behavior of the coupling constant for low-energies is quite different for the ferromagnetic and anti-ferromagnetic interaction:

- **Ferromagnetic interaction**: For a ferromagnetic interaction between the magnetic impurity and the conduction electron we can write the bare coupling as $J_0 = -|J_0|$, the running coupling constant becomes

$$J(\tilde{D}) = -\frac{|J_0|}{1 + 2|J_0|\rho\ln(D/\tilde{D})}. \tag{2.91}$$

  When we run to the low-energies (systematic reduction of D), the module of $\ln(D/\tilde{D})$ increases and the renormalized coupling constant $J(\tilde{D})$ decreases as $\tilde{D}$ approaches to zero. In this case the coupling $J(\tilde{D})$ is called marginally irrelevant. Physically this mean that for a ferromagnetic interaction between the magnetic impurity and the conduction electrons at low energies (temperatures) the magnetic impurity decouples from the conduction electrons resulting in a *free local fixed point*, $J \to 0$, see figure [9].

- **Anti-ferromagnetic interaction**: In the anti-ferromagnetic case the bare coupling J_0 is positive and

$$J(\tilde{D}) = \frac{J_0}{1 - 2J_0\rho\ln(D/\tilde{D})}. \tag{2.92}$$

The behavior in the low-energy regime is different from the ferromagnetic case. When we run towards low-energies, the renormalized interaction $J(\tilde{D})$ increases meaning that at low-temperatures the impurity and the conduction electrons become strongly correlated. The impurity and the conduction electrons form a many-body singlet ground state called *Kondo singlet*. The consequence of this strongly correlation is the increase of the resistivity for low temperatures in metallic compounds and the conductance in quantum dot systems, both originating from the same mechanism. Thus, the Kondo effect can only manifests in systems where the interaction between the magnetic impurity and the conduction electrons is anti-ferromagnetic. When the coupling constant runs to $J \to \infty$ we have the *strong coupling fixed point* to the Kondo model showed in the figure [9].

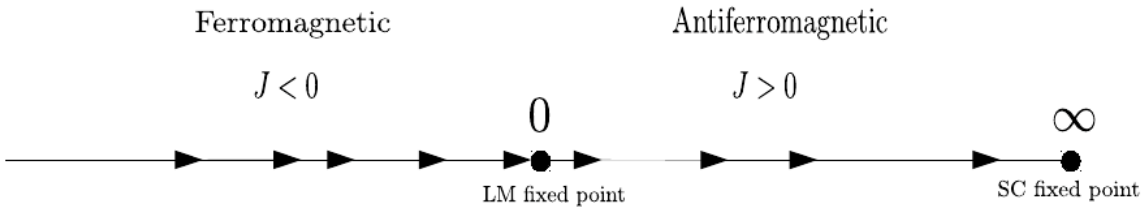

Figure 9 – RG flow for the Kondo coupling constant J. In the ferromagnetic case the coupling constant running to a free local moment fixed point, and the magnetic impurity is decoupled from the metallic bath. For the antiferromagnetic case the coupling constant increases and running to a strong coupling fixed point which corresponds to the the "Kondo-singlet" formation.

The energy scale that marks the crossover between the weakly interacting regime and strongly (kondo) interacting regime is the Kondo temperature. From the RG procedure this energy scale is defined when the running coupling constant diverges, from (2.92) we obtain

$$T_K = D\exp\left(-\frac{1}{2\rho J_0}\right). \tag{2.93}$$

Using the Kondo temperature definition above the running coupling constant can be written as

$$J(\tilde{D}) = \frac{1}{2\rho\ln(\tilde{D}/T_K)}. \tag{2.94}$$

From the result above we realize that there is no dependence of the high-energy cutoff D. This means that the high-energy details are not important to describe the low-energy behavior. The only relevant energy scale in this regime is the Kondo temperature T_K.

2.4.1.1 Kondo temperature from the PMS analysis

A more accurate calculation of the Kondo temperature from the PMS can be done if we compute the third order correction of the T-matrix for the coupling constant g. A cumbersome calculation results in

$$\frac{dg}{d\ln D} = -2g^2 + 2g^3 + \mathcal{O}(g^4). \tag{2.95}$$

Now the RG equation is integrated from the original bandwidth D to a reduced bandwidth D^* which renormalizes the bare coupling constant g_0 to g^*

$$\int_D^{D^*} \ln D' dD' = -\frac{1}{2}\int_{g_0}^{g^*} \frac{dg'}{g'^2 - g'^3}.$$

The left hand of the equation above can be solved using

$$-\frac{1}{2}\int \frac{dg'}{g'^2 - g'^3} = \frac{1}{2g} + \frac{1}{2}\ln\left|\frac{1}{g} - 1\right| + \text{constant}.$$

With this we have

$$\ln\left(\frac{D^*}{D}\right) = \frac{1}{2g^*} + \frac{1}{2}\ln\left|\frac{1}{g^*} - 1\right| - \frac{1}{2g_0} + \frac{1}{2}\ln\left|\frac{1}{g_0} - 1\right|.$$

Again, the Kondo temperature is defined when the coupling constant running to the strong coupling fixed point, $g^* \to \infty$ ($1/g^* \to 0$), see figure [9]. The energy scale D^* corresponds to the Kondo temperature T_K. Applying this in the equation above results in

$$D^* \sim D\frac{\sqrt{g_0}}{\sqrt{1-g_0}}\exp\left(-\frac{1}{2g_0}\right).$$

Using now that $g_0 = \rho J_0 \sim J_0/D \ll 1$, $\sqrt{1-g_0} \approx 1$ and $D^* \equiv T_K$, we finally obtain

$$T_K \sim \sqrt{\rho J_0} D \exp\left(-\frac{1}{2\rho J_0}\right). \tag{2.96}$$

The expression above was obtained using the third order correction of the T-matrix. However, notice that it differs only in the prefatory as compared to (2.93) obtained with the T-matrix second order correction. For this reason, many times for more complicated problems the second order correction can give a good estimative of the Kondo temperature and high order corrections are not necessary. The Kondo temperature obtained by the PMS is not quantitative exact because for temperatures bellow T_K perturbative calculations are no longer valid. Even so, surprisingly, the qualitative behavior of the Kondo temperature

can be captured by the PMS. The effective Kondo Hamiltonian obtained from the SIAM has coupling given by [12]

$$J_{\mathbf{k}\mathbf{k}'} = V_{\mathbf{k}} V_{\mathbf{k}'} \left(\frac{1}{\varepsilon_k - \varepsilon_d} + \frac{1}{\varepsilon_d + U - \varepsilon_{k'}} \right).$$

For scattering processes occurring at energies close to the Fermi level we can take $\varepsilon_k = \varepsilon'_k \approx 0$, also $V_{\mathbf{k}} = V_{\mathbf{k}'} = V$. With these we have the bare Kondo coupling

$$J_0 = V^2 \left(\frac{1}{\varepsilon_d + U} - \frac{1}{\varepsilon_d} \right).$$

In the SIAM for energies above $U/2$ the mix valence regime is dominant, so the Kondo physics manifests only in lower energies. Therefore, we can take as the high-energy cutoff $D = U/2$ to write equation (2.96) as

$$T_K \sim \sqrt{\frac{\Gamma U}{\pi}} \exp\left(\frac{\varepsilon_d(\varepsilon_d + U)\pi}{2\Gamma U} \right), \tag{2.97}$$

where we have defined $\Gamma = \pi \rho V^2$. This is the celebrated Haldane's formula for the Kondo temperature (HALDANE, 1978). In the PHS limit we have that $\varepsilon_d = -U/2$, which results in

$$T_K \sim \sqrt{\frac{U\Gamma}{\pi}} \exp\left(-\frac{U\pi}{8\Gamma} \right). \tag{2.98}$$

In current experiments in quantum dots, quantities as the impurity energy level, Coulomb repulsion, coupling with the metallic bath can be controlled with great accuracy (GOLDHABER-GORDON et al., 1998). Therefore, the Kondo temperature expressed in terms of these parameters is extremely useful.

2.5 Numerical Renormalization Group

In the previous section we applied a perturbative renormalization group method to the Kondo model it results in the RG equations for the Kondo bare coupling J (2.85). From the perturbative RG results, we saw that for the Kondo problem the energy integrals are the kind

$$\int_{k_B T}^{D} \frac{dD'}{D'} \sim \ln\left(\frac{D}{k_B T} \right). \tag{2.99}$$

For low temperatures, $k_B T \ll D$, the integral above leads to divergences

$$\int_{k_B T}^{D} \frac{dD'}{D'} \sim \ln\left(\frac{D}{k_B T} \right) \to \infty \qquad (k_B T \ll D).$$

This suggests that the low-energy states contributes more significantly to the problem as compared to the high-energy states. Indeed, for $k_B T \ll D$ the perturbative approach breaks

[12] See Appendix A.

down and a nonperturbative method is necessary. As already said, to solve this problem K. G. Wilson proposed an approach, called numerical renormalization group (NRG)(WILSON, 1975). Here we will briefly resume the principal ideas underlying the Wilson NRG. For further information see (HEWSON, 1997).

The heart of the Wilson's idea is the logarithmic discretization of the conduction band to solve the divergences in the energy integrals. The discretization proposed by Wilson is given by

$$D\Lambda^{-(n+1)} < |\varepsilon_{\mathbf{k}} - \varepsilon_F| < D\Lambda^{-n}, \quad \text{with} \quad n \in \mathbb{N} \quad \text{and} \quad \Lambda > 1. \tag{2.100}$$

An important simplification of the problem can be made by considering a expansion of $\varepsilon_{\mathbf{k}}$ in power series of $k - k_F$. In this case we have

$$\varepsilon_k = \varepsilon_F + (k - k_F)\frac{d\varepsilon_k}{dk}\bigg|_{k=k_F} + \mathcal{O}((k - k_F)^2), \tag{2.101}$$

where we use $\varepsilon_{\mathbf{k}} = \varepsilon_k$. The next step is the transformation of the conduction Hamiltonian

$$H_0 = \sum_{\mathbf{k}} \varepsilon_k c^\dagger_{\mathbf{k}\sigma} c_{\mathbf{k}\sigma}$$

into a semi-infinite linear chain. This can be formally done by the Lanczos tridiagonalization method (GOLUB et al., 1996). The result is the tight-binding linear chain

$$H_0 = \sum_{n\sigma} \varepsilon_{n\sigma} c^\dagger_{n\sigma} c_{n\sigma} + \sum_{n\sigma} (\gamma_n c^\dagger_{n\sigma} c^\dagger_{n+1\sigma} + \gamma^*_n c^\dagger_{n+1\sigma} c_{n\sigma}), \tag{2.102}$$

where ε_n and γ_n are given by

$$\varepsilon_n = 0, \qquad \gamma_n = \frac{D(1 + \Lambda^{-1})\epsilon_n}{2\Lambda^{n/2}}, \tag{2.103}$$

with

$$\epsilon_n = (1 - \Lambda^{-(n+1)})(1 - \Lambda^{-2n+1})^{1/2}(1 - \Lambda^{-(2n+1)})^{1/2}. \tag{2.104}$$

The next step is the coupling of an impurity to the first site of the discrete chain. For a magnetic impurity described by the Kondo's model we obtain the discrete Hamiltonian chain with N sites

$$H_N = D' \sum_{n=0,\sigma}^{N-1} (\gamma_n c^\dagger_{n\sigma} c^\dagger_{n+1\sigma} + \gamma^*_n c^\dagger_{n+1\sigma} c_{n\sigma}) + J \sum_{n\sigma\sigma'} \mathbf{S} \cdot c^\dagger_{0\sigma}(\mathbf{s}_0)_{\sigma\sigma'} c_{0\sigma'}, \tag{2.105}$$

with $D' = D(1 + \Lambda^{-1})/2$. For the SIAM the discrete Hamiltonian becomes

$$\begin{aligned} H_N \;=\; & D' \sum_{n=0,\sigma}^{N-1} (\gamma_n c^\dagger_{n\sigma} c^\dagger_{n+1\sigma} + \gamma^*_n c^\dagger_{n+1\sigma} c_{n\sigma}) \\ & + \sum_{\sigma} \varepsilon_d d^\dagger_\sigma d_\sigma + U n_{d\uparrow} n_{d\downarrow} + \sum_{\sigma} (V c^\dagger_{0\sigma} d_\sigma + V^* d^\dagger_\sigma c_{0\sigma}). \end{aligned} \tag{2.106}$$

More complicated impurity models can be described by the discrete Hamiltonian with proper considerations. The next stage is the addition of a new site in the chain resulting in

$$H_{N+1} = H_N + D' \sum_\sigma \Lambda^{N/2} (c^\dagger_{N\sigma} c_{N+1\sigma} + c^\dagger_{N+1\sigma} c_{N\sigma}). \tag{2.107}$$

The Hamiltonian H_N is numerically diagonalized, for this reason the choice of the many-body basis $|\mathbf{m}\rangle$ is important. Using the symmetries of the system the Hamiltonian can be written in a block-diagonal form, which reduces numerical effort. Due the $U(1)$ and $SU(N)$ symmetries of the Kondo and the SIAM a good choice is $|\mathbf{m}\rangle = |n_e, S, S_z, m\rangle$, where n_e is the total number of electrons, S is the total spin, S_z is the z-component of the total spin and m is a generic index associated with the specific Hamiltonian block. For other impurity models the symmetries identification is fundamental for the construction of the appropriated basis. Upon the addition of the extra site we must multiply the many-body eigenstate by $\{|0,0\rangle, |\uparrow,0\rangle, |0,\downarrow\rangle, |\uparrow,\downarrow\rangle\}$. We can see that this procedure increase the Hilbert space exponentially with N leading to a numerically intractable diagonalization. It is therefore mandatory to set N_{st} as the maximum number of states at each stage. To keep the energy scale comparable with the previous stage in the iterative diagonalization as $N \to \infty$ is defined the sequence of Hamiltonians $\bar{H}_N$ by

$$\bar{H}_N = \frac{\Lambda^{(N-1)/2}}{D'}, \qquad N = 0, 1, 2, 3, \cdots \tag{2.108}$$

These Hamiltonians obey the recurrence relation

$$\bar{H}_{N+1} = \Lambda^{1/2} \bar{H}_N + \sum_\sigma (c^\dagger_{N\sigma} c_{N+1\sigma} + c^\dagger_{N+1\sigma} c_{N\sigma}). \tag{2.109}$$

Notice now that in the sequence $\bar{H}_N$ the coupling to the extra site is the same for each N. The original continuous Hamiltonian corresponds to the limit

$$H = \lim_{N\to\infty} (D' \Lambda^{-(N-1)/2} \bar{H}_N). \tag{2.110}$$

The recurrence relation (2.109) can be understand in the spirit of the renormalization group. A sequence of renormalization group transformations can be defined by the map

$$\bar{H}_{N+1} = R(\bar{H}_N). \tag{2.111}$$

The numerical diagonalization of H_N allow us to write

$$\bar{H}_N = \sum_{\mathbf{m}} E(\mathbf{m}) |\mathbf{m}\rangle\langle\mathbf{m}|. \tag{2.112}$$

The next Hamiltonian to be diagonalized is

$$\bar{H}_{N+1} = \sum_{\mathbf{m}}^{N_{\text{st}}} \bar{E}(\mathbf{m}) |\mathbf{m}\rangle\langle\mathbf{m}| + \sum_{\mathbf{m}\mathbf{m}'}^{N_{\text{st}}} (g_\sigma(\mathbf{m}, \mathbf{m}') |\mathbf{m}\rangle\langle\mathbf{m}'| + \text{H.c.}) \tag{2.113}$$

with $g_\sigma(\mathbf{m},\mathbf{m}') = \langle \mathbf{m}|c^\dagger_{n\sigma}c_{n+1\sigma}|\mathbf{m}'\rangle$ and $\bar{E}(\mathbf{m}) = \Lambda^{1/2}E(\mathbf{m})$. In the fixed number of states $N_{\rm st}$, at each iteration the RG relation (2.111) maps the Hamiltonian with the same form for each stage, but with the renormalized set of parameters $\{\bar{E}(\mathbf{m}), g_\sigma(\mathbf{m},\mathbf{m}')\}$. This is exactly the second step of the general RG procedure, described in the section 2.3.1. This is the reason why the method received the name numerical renormalization group. In the NRG approach the fixed points are associated with the energy flow as the chain is increased. In other words, if there is a fixed point the parameters of H_{N+1} and H_N are unchanged.

The NRG approach is a powerful method that allows the analysis of thermodynamic properties in a large energy range. Thermodynamic properties of magnetic impurities as the entropy $S_{\rm imp}(T)$, magnetic susceptibility $\chi_{\rm imp}(T)$ and the specific heat $C_{\rm imp}(T)$ are nicely calculated for low and high-temperatures regimes using the NRG due the nonperturbative nature of the method. Following the Wilson definition (KRISHNA-MURTHY; WILKINS; WILSON, 1980), the contribution of the impurity is calculated from the difference of the chain with the impurity coupled to the first site of the linear chain and the "clean", system without the impurity,

$$S_{\rm imp}(T) = S_{\rm total}(T) - S^{(0)}_{\rm total}(T), \tag{2.114}$$

$$\chi_{\rm imp}(T) = \chi_{\rm total}(T) - \chi^{(0)}_{\rm total}(T), \tag{2.115}$$

$$C_{\rm imp}(T) = C_{\rm total}(T) - C^{(0)}_{\rm total}(T). \tag{2.116}$$

In the above $O_{\rm total}$ is the thermodynamic quantity of the system with the impurity and $O^{(0)}_{\rm total}$ without it. The spectral properties of the system can also be extracted from the NRG by the numerical calculation of the interacting self-energy. This subject goes beyond the scope of the present thesis. For more information and technical details about the extraction of thermodynamic and spectral properties see the complete review by Bulla *et al.* (BULLA; COSTI; PRUSCHKE, 2008).

2.6 Majorana zero modes

2.6.1 Majorana fermions in relativistic quantum theory

For relativistic phenomena, the dynamics of quantum systems was formulated by Dirac to solve the evident Lorentz invariance violation of the original Schrödinger equation (DIRAC, 1926). Dirac proposed that a relativistic quantum system is governed by the equation (later on called Dirac equation) (SAKURAI, 2006)

$$i\frac{\partial}{\partial t}\Psi(\mathbf{r},t) = H_{\rm Dirac}\Psi(\mathbf{r},t), \tag{2.117}$$

where H_{Dirac} is the Dirac Hamiltonian given by[13]

$$H_{\text{Dirac}} = \boldsymbol{\alpha} \cdot \mathbf{p} + \boldsymbol{\beta} m. \tag{2.118}$$

In the above α_i are the so-called Dirac matrices, which are 4×4 matrices defined as

$$\alpha_i = \begin{pmatrix} 0 & \sigma_i \\ \sigma_i & 0 \end{pmatrix}, \tag{2.119}$$

with $i = 1, 2, 3$, σ_i denotes the Pauli matrices

$$\sigma_1 = \begin{pmatrix} 0 & 1 \\ 1 & 0 \end{pmatrix}, \quad \sigma_2 = \begin{pmatrix} 0 & -i \\ i & 0 \end{pmatrix}, \quad \sigma_3 = \begin{pmatrix} 1 & 0 \\ 0 & -1 \end{pmatrix}, \tag{2.120}$$

and $\boldsymbol{\beta}$ is the matrix

$$\boldsymbol{\beta} = \begin{pmatrix} \mathbb{1}_{2\times2} & 0 \\ 0 & -\mathbb{1}_{2\times2} \end{pmatrix}. \tag{2.121}$$

Because of its relativistic nature, the Dirac equation (2.117) is usually written in its covariant form by the introduction of the Gamma matrices $\gamma^\mu = (\beta, \beta\alpha_i)$. With this, the Dirac equation becomes

$$(i\gamma^\mu \partial_\mu - m)\Psi = 0, \tag{2.122}$$

where $\partial_\mu = \partial/\partial x_\mu$. The Gamma matrices must obey the following algebra

$$\gamma^\mu \gamma^\nu + \gamma^\nu \gamma^\mu = 2\delta_{\mu\nu}. \tag{2.123}$$

The Gamma matrices definition is arbitrary provided the condition above is satisfied. This algebra frequently appears in mathematics and physics and is called Clifford algebra (GARLING, 2011).

One of the most common representations for the Gamma matrices is

$$\gamma^0 = \begin{pmatrix} 0 & 1 \\ 1 & 0 \end{pmatrix}, \qquad \gamma^i = \begin{pmatrix} 0 & \sigma^i \\ -\sigma^i & 0 \end{pmatrix}. \tag{2.124}$$

This representation is called chiral (or Weyl) representation (WEINBERG, 1995). In this basis, the four-component spinor Ψ can be decomposed into two-component spinors (called Weyl spinors)

$$\Psi = \begin{pmatrix} \psi_1 \\ \psi_2 \\ \psi_3 \\ \psi_4 \end{pmatrix} \equiv \begin{pmatrix} \psi_R \\ \psi_L \end{pmatrix}. \tag{2.125}$$

In the chiral representation, the Dirac equation (2.122) reduces to a set of coupled equations

$$(i\partial_t + \boldsymbol{\sigma} \cdot \mathbf{p})\psi_L - m_D \psi_R = 0, \tag{2.126}$$

$$(i\partial_t - \boldsymbol{\sigma} \cdot \mathbf{p})\psi_R - m_D \psi_L = 0, \tag{2.127}$$

[13] Here $\hbar = c = 1$.

where the subindex D in m_D stands for Dirac mass. When $m_D = 0$ the equation above are decoupled and we get the so-called Weyl equations

$$(i\partial_t + \boldsymbol{\sigma}\cdot\mathbf{p})\psi_L = 0, \tag{2.128a}$$
$$(i\partial_t - \boldsymbol{\sigma}\cdot\mathbf{p})\psi_R = 0. \tag{2.128b}$$

In this case, the particle has a well-defined chirality (PESKIN, 2018). The Dirac spinor Ψ is a complex object. However, in the search for a purely real solution of the Dirac equation, in 1937, Etore Majorana (MAJORANA, 1937) proposed the following gamma matrices

$$\tilde{\gamma}^0 = i\begin{pmatrix} 0 & -\sigma^1 \\ \sigma^1 & 0 \end{pmatrix}, \tilde{\gamma}^1 = i\begin{pmatrix} 0 & \sigma^0 \\ \sigma^0 & 0 \end{pmatrix}, \tilde{\gamma}^2 = i\begin{pmatrix} \sigma^0 & 0 \\ 0 & -\sigma^0 \end{pmatrix}, \tilde{\gamma}^3 = \begin{pmatrix} 0 & \sigma^2 \\ -\sigma^2 & 0 \end{pmatrix}. \tag{2.129}$$

In this representation, latter on dubbed Majorana representation, the Gamma matrices are purely imaginary, $(\gamma^\mu)^* = -\gamma^\mu$, then

$$\begin{aligned} (i\tilde{\gamma}^\mu\partial_\mu - m)\Psi = 0 &\Rightarrow (-i(\tilde{\gamma}^\mu)^*\partial_\mu - m)\Psi^* = 0 \\ &\Rightarrow (i\tilde{\gamma}^\mu\partial_\mu - m)\Psi^* = 0. \end{aligned}$$

Therefore in the Majorana representation

$$\Psi = \Psi^*. \tag{2.130}$$

In the general case, we have the so-called charge conjugated of the spinor Ψ given by

$$\Psi^{(c)} = C\Psi^*, \tag{2.131}$$

where C is called charge conjugation operator, with the properties

$$C^\dagger C = 1, \qquad C^\dagger\gamma^\mu C = -(\gamma^\mu)^*. \tag{2.132}$$

Using the properties above, it's easy to show that if Ψ is a solution of the Dirac equation, $\Psi^{(c)}$ is also a solution. This follows from

$$\begin{aligned} (i\gamma^\mu\partial_\mu - m)\Psi = 0 &\Rightarrow (-i(\gamma^\mu)^*\partial_\mu - m)\Psi^* = 0 \\ &\Rightarrow C(-i(\gamma^\mu)^*\partial_\mu - m)\Psi^* = 0 \\ &= (-iC(\gamma^\mu)^*\partial_\mu - Cm)\Psi^* = 0 \\ &= (i\gamma^\mu\partial_\mu - m)\Psi^{(c)} = 0. \end{aligned}$$

In the last line we use the properties (2.132) to obtain $C(\gamma^\mu)^* = -\gamma^\mu C$. In the Majorana representation it is clear from the calculations above that $C_{\text{Maj}} = \mathbb{1}$, which results in $\Psi^{(c)} = \Psi^*$. Together with the fact that in the Majorana representation $\Psi = \Psi^*$, we have

$$\Psi^{(c)} = \Psi. \tag{2.133}$$

This is called Majorana condition. On the other hand, in the chiral representation only the γ^2 is imaginary, wherefore a good choice for the charge conjugation operator is

$$C_{\text{ch}} = i\gamma^2 = \begin{pmatrix} 0 & i\sigma^2 \\ -i\sigma^2 & 0 \end{pmatrix}.$$

Therefore, in the Weyl representation we have that the charge conjugated Dirac spinor is

$$\Psi^{(c)} = C\Psi^* = i\gamma^2 = \begin{pmatrix} 0 & i\sigma^2 \\ -i\sigma^2 & 0 \end{pmatrix} \begin{pmatrix} \psi_R^* \\ \psi_L^* \end{pmatrix} = \begin{pmatrix} i\sigma^2\psi_L^* \\ -i\sigma^2\psi_R^* \end{pmatrix}.$$

The relation between the Weyl representation and the Majorana representation can be established using the Majorana condition $\Psi^{(c)} = \Psi$ above resulting in

$$\begin{pmatrix} \psi_R \\ \psi_L \end{pmatrix} = \begin{pmatrix} i\sigma^2\psi_L^* \\ -i\sigma^2\psi_R^* \end{pmatrix}. \tag{2.134}$$

This is the Majorana spinor in terms of the Weyl spinors, in which case, a set of equations (2.128) becomes

$$(i\partial_t + \boldsymbol{\sigma}\cdot\mathbf{p})\psi_L - i\sigma^2 m_L \psi_L^* = 0, \tag{2.135a}$$
$$(i\partial_t - \boldsymbol{\sigma}\cdot\mathbf{p})\psi_R - i\sigma^2 m_R \psi_R^* = 0. \tag{2.135b}$$

Here, the distinct subindex m_L and m_R denotes the fact that the mass for the different chiral modes, now decoupled, are not necessarily equal. The four-component Majorana spinor in terms of the Weyl spinors can be expressed as

$$\Psi_L = \begin{pmatrix} -i\sigma^2\psi_L^* \\ \psi_L \end{pmatrix}, \qquad \Psi_R = \begin{pmatrix} \psi_R \\ i\sigma^2\psi_R^* \end{pmatrix}. \tag{2.136}$$

The equivalence between the Majorana spinor and Dirac spinor is obtained when $m_L = m_R$ and $\psi_L = i\sigma^2\psi_R^*$. The Majorana condition can be expressed in an arbitrary representation by

$$i\gamma^\mu\partial_\mu\Psi^{(c)} - m\Psi = 0, \tag{2.137}$$

known as Majorana equation.

One of the most important properties of the Dirac equation is its global gauge invariance, which means that the Dirac spinor is invariant under the gauge transformation

$$\Psi \to e^{i\theta}\Psi.$$

This exposes the $U(1)$ symmetry of the Dirac equation associated with the charge conservation. Note, however, that for the Majorana equation (2.137) there is no gauge invariance. Therefore, particles described by the Majorana equation cannot couple to the electromagnetic field, they must be neutral. The general solution for the Dirac equation

can be expressed by the plane wave $\Psi(\mathbf{r},t) = e^{-iEt}\Phi(\mathbf{r})$, with conjugated Dirac spinor $\Psi^{(c)}(\mathbf{r},t) = e^{iEt}\Phi^{(c)}(\mathbf{r})$, where $\Phi^{(c)} = C\Phi^*$. The physical relation of the pair of solutions is that for each particle of energy E described by Ψ there is a conjugated solution with energy $-E$ and opposite charge, described by $\Psi^{(c)}$ known as anti-particle. Note that for $E \neq 0$ the Majorana condition (2.133) is not satisfied, because $\Psi(\mathbf{r},t) \neq \Psi^{(c)}(\mathbf{r},t)$. However, the scenario is different for $E = 0$, in this case the Majorana condition is satisfied by the stationary state as

$$\Phi^{(c)}(\mathbf{r}) = \Phi(\mathbf{r}), \qquad E = 0. \tag{2.138}$$

These states received the special name *Majorana zero modes* and play a fundamental role in condensed matter physics (see the next sections).

The physical implications of the Dirac and Majorana representations is better understood within the second quantization language for the Dirac and Majorana fields. The quantization of the Dirac field is given by

$$\hat{\Psi}(\mathbf{r},t) = \sum_{E>0} a_E e^{-iEt}\Phi_E(\mathbf{r}) + \sum_{E<0} b^\dagger_{-E} e^{-iEt}\Phi^{(c)}_E(\mathbf{r}), \tag{2.139}$$

where $a^\dagger_E$ and $b^\dagger_{-E}$ are the creation operators which create a particle with energy E and an anti-particle with energy $-E$, respectively. The Dirac field can be written as

$$\begin{aligned}
\hat{\Psi}(\mathbf{r},t) &= \sum_{E>0} a_E e^{-iEt}\Phi_E(\mathbf{r}) + \sum_{E<0} b^\dagger_{-E} e^{-iEt}\Phi^{(c)}_E(\mathbf{r}) && (2.140)\\
&= \sum_{E>0} \left[a_E e^{-iEt}\Phi_E(\mathbf{r}) + b^\dagger_E e^{iEt}\Phi^{(c)}_E(\mathbf{r}) \right] && (2.141)\\
&= \sum_{E>0} \left[a_E e^{-iEt}\Phi_E(\mathbf{r}) + b^\dagger_E e^{iEt} C\Phi^*_E(\mathbf{r}) \right]. && (2.142)
\end{aligned}$$

From the equation above it is easy to see that $\hat{\Psi}(\mathbf{r},t) \neq \hat{\Psi}^\dagger(\mathbf{r},t)$, and that the Dirac field obey the canonical Fermi commutation for equal-time

$$\{\hat{\Psi}_\sigma(\mathbf{r},t), \hat{\Psi}^\dagger_{\sigma'}(\mathbf{r}',t)\} = \delta_{\sigma\sigma'}\delta(\mathbf{r}-\mathbf{r}'), \qquad \{\hat{\Psi}_\sigma(\mathbf{r},t), \hat{\Psi}_{\sigma'}(\mathbf{r}',t)\} = \{\hat{\Psi}^\dagger_\sigma(\mathbf{r},t), \hat{\Psi}^\dagger_\sigma(\mathbf{r}',t)\} = 0. \tag{2.143}$$

The second quantization form of the Dirac Hamiltonian is

$$\mathcal{H}_D = \int d^3r \hat{\Psi}^\dagger(\mathbf{r},t)(\boldsymbol{\alpha}\cdot\mathbf{p} + \boldsymbol{\beta} m_D)\hat{\Psi}(\mathbf{r},t). \tag{2.144}$$

Using (2.139) and the orthogonality properties, we obtain

$$\mathcal{H}_D = \sum_{E>0} E(a^\dagger_E a_E + b^\dagger_E b_E). \tag{2.145}$$

The quantization of the Majorana field is analogous, but with the Majorana condition (2.133), which can be imposed by taking $a_E = b_E$ resulting in

$$\hat{\Psi}(\mathbf{r},t) = \sum_{E>0} \left[a_E e^{-iEt}\Phi_E(\mathbf{r}) + a^\dagger_E e^{iEt} C\Phi^*_E(\mathbf{r}) \right]. \tag{2.146}$$

From this result, it is straightforward to see that

$$\hat{\Psi}(\mathbf{r},t) = \Psi^{\dagger}(\mathbf{r},t) \tag{2.147}$$

with the canonical relation

$$\{\hat{\Psi}_{\sigma}(\mathbf{r},t), \hat{\Psi}_{\sigma'}(\mathbf{r}',t)\} = \delta_{\sigma\sigma'}\delta(\mathbf{r}-\mathbf{r}'). \tag{2.148}$$

Equation (2.147) reflects the exceptional fact that a Majorana particle is indistinguishable from its own antiparticle. The second quantized Majorana Hamiltonian is given by

$$\mathcal{H}_M = \sum_{E>0} E a_E^{\dagger} a_E, \tag{2.149}$$

which contains only half of independent solutions in comparison with H_D. In high-energy physics the search for Majorana particles is an old issue which stands from particle physics to the dark matter nature (ELLIOTT; FRANZ, 2015). Despite the lack of experimental evidence of fundamental particles which behave as Majorana particles, some condensed matter systems may present excitations with properties analogous to those of Majorana particles, which is the subject of the following sections.

2.6.2 Majorana fermions in condensed matter systems

In second quantization, fermionic fields are described by fermionic operators. For example $c_j^{\dagger}(c_j)$ creates (annihilates) a fermion with the generic quantum number j. Fermion operators are complex objects that obey the canonical algebra

$$[c_i, c_j^{\dagger}]_+ = \delta_{ij}. \tag{2.150}$$

Analogously to complex numbers, that can be written as a combination of real numbers $z = a + ib$, with $[a,b] \in \mathbb{Z}$, fermionic operators can be written as a combination of fermionic real operators as

$$c_j = \frac{1}{2}(\gamma_{j1} + i\gamma_{j2}), \qquad c_j^{\dagger} = \frac{1}{2}(\gamma_{j1} - i\gamma_{j2}), \tag{2.151}$$

where the real fermionic operators have the properties

$$\gamma_{i\alpha}^{\dagger} = \gamma_{i\alpha}, \qquad [\gamma_{i\alpha}, \gamma_{j\beta}]_+ = 2\delta_{ij}\delta_{\alpha\beta}. \tag{2.152}$$

We saw in the previous section that the real fermionic operators are associated with the Majorana fermions, for this reason $\gamma_{i\alpha}$ is called Majorana operator. Then, the fermionic operators can be mathematically written in terms of two Majorana operators.

The use of Majorana operators as a mathematical artifice is widely used in magnetic systems. This follows from the direct relation between the spin operators and the Majorana operators. Indeed, a spin operator can be expressed in terms of Majorana fermions as

$$S^a = \frac{i}{4}\epsilon_{abc}\gamma_b\gamma_c. \tag{2.153}$$

With this representation and the properties (2.152) we can recover the canonical Lie algebra for the magnetic operators

$$[S^a, S^b] = i\epsilon_{abc}S^c, \tag{2.154}$$

which shows the validation of the spin operator written in terms of Majorana operators. The use of Majorana operators to describe spin operators is widely used together with other theoretical tools, as quantum field methods and bosonization (AMBJøRN; SEMENOFF, 1989; GOGOLIN; NERSESYAN; TSVELIK, 2004). More discussion on Majorana fermions and important magnetic systems, as the Ising model, can be found in the Tsvelik's classical textbook (TSVELIK, 2007). In some especial cases, Majorana fermions are not only a mathematical artifice, but can be true excitations in condensed matter systems. This is the subject of the next section.

2.6.2.1 Majorana fermions in topological superconductors

Superconductivity is one of the most surprising phenomena in Condensed Matter. The effect was discovered by Onnes in the early years of the 20th century (ONNES, 1991). Onnes observed that at very low temperatures the resistivity of some metals goes to zero, becoming thus perfect conductors. Moreover, Onnes also observed that in this limit the metals also acquired perfect diamagnetism. These two properties were fundamental characteristics of a new property of matter, often called superconductivity. Later, many other metals and compounds with superconducting phases were discovered. However, only in 1957, almost five decades after their experimental discovery, the superconducting effect received appropriated theoretical explanation. Bardeen, Cooper and Schrieffer were responsible for the development of a microscopic model able to describe the superconducting mechanism (BARDEEN; COOPER; SCHRIEFFER, 1957). Nowadays, this celebrated theory is called BCS theory of superconductivity.

The heart of the microscopic mechanism underlying superconductivity is an effective attraction between electrons, mediated by phonons. This interaction gives rise to pairs of correlated electrons called Cooper pairs (COOPER, 1956), which behave as bosons. At low temperatures, in superconductor systems with a critical temperature T_c, all electrons form Cooper pairs and the system becomes a superconducting condensate. Another fundamental property of superconductors, perfect diamagnetism, was explained only few years latter by P.W. Anderson. Anderson showed that the spontaneous symmetry breaking of the gauge symmetry in superconductors gives rise to a gauge field whose interaction with the electromagnetic field results in massive photons (ANDERSON, 1963). The same mechanism was used by Higgs to explain the mass generation in the standard model for fundamental particles (HIGGS, 1964). Nowadays, this mechanism is called Anderson-Higgs mechanism (COLEMAN, 2015).

Here, we will give only a brief overview of the fundamental aspects of the BCS theory. A more complete description of the theory can be found in classical textbooks as (ABRIKOSOV et al., 2012; FETTER; WALECKA, 2012; MAHAN, 2013; COLEMAN, 2015). The minimal model for the microscopic mechanism behind superconductivity in d-dimensions is

$$\mathcal{H} = \int d^d r \Big[h_0^{\sigma\sigma'}(\mathbf{r}) c^\dagger_{\sigma\mathbf{r}} c_{\sigma'\mathbf{r}} - V n_{\uparrow\mathbf{r}} n_{\downarrow\mathbf{r}} \Big], \tag{2.155}$$

where $h_0^{\sigma\sigma'}(\mathbf{r}) = (\hbar^2\nabla^2/2m_{\text{eff}} - \mu)\delta_{\sigma\sigma'}$ is the kinetic term, m_{eff} is the effective mass, $n_{\sigma\mathbf{r}} = c^\dagger_{\sigma\mathbf{r}} c_{\sigma\mathbf{r}}$ is the number operator and $V > 0$ is the attractive interaction between the electrons, mediated by phonons. The next step in the BCS theory is the Bogoliubov mean-field decoupling of the interaction term

$$-n_\uparrow n_\downarrow = -c^\dagger_\uparrow c_\uparrow c^\dagger_\downarrow c_\downarrow = c^\dagger_\uparrow c^\dagger_\downarrow c_\uparrow c_\downarrow \simeq \langle c^\dagger_\uparrow c^\dagger_\downarrow \rangle c_\uparrow c_\downarrow + c^\dagger_\uparrow c^\dagger_\downarrow \langle c_\uparrow c_\downarrow \rangle - \langle c^\dagger_\uparrow c^\dagger_\downarrow \rangle \langle c_\uparrow c_\downarrow \rangle.$$

Now, let us define the superconducting order parameter

$$\Delta(\mathbf{r}) = V \langle c_{\uparrow\mathbf{r}} c_{\downarrow\mathbf{r}} \rangle, \tag{2.156}$$

with which the mean-field Hamiltonian becomes

$$\mathcal{H}_{\text{BCS}} = \int d^d r \Big[h_0^{\sigma\sigma'}(\mathbf{r}) c^\dagger_{\sigma\mathbf{r}} c_{\sigma'\mathbf{r}} + (\Delta(\mathbf{r}) c^\dagger_{\uparrow\mathbf{r}} c^\dagger_{\downarrow\mathbf{r}} + \Delta^*(\mathbf{r}) c_{\downarrow\mathbf{r}} c_{\uparrow\mathbf{r}}) + \frac{1}{V}|\Delta(\mathbf{r})|^2 \Big]. \tag{2.157}$$

The BCS Hamiltonian is better understood using the so-called Nambu spinors, defined as

$$\Psi_\mathbf{r} = \begin{pmatrix} c_{\uparrow\mathbf{r}} \\ c_{\downarrow\mathbf{r}} \\ c^\dagger_{\downarrow\mathbf{r}} \\ -c^\dagger_{\uparrow\mathbf{r}} \end{pmatrix} = \begin{pmatrix} \psi_\mathbf{r} \\ i\sigma^y \psi^*_\mathbf{r} \end{pmatrix}, \tag{2.158}$$

with $\psi_\mathbf{r} = (c_{\uparrow\mathbf{r}}, c_{\downarrow\mathbf{r}})^T$. Using the Nambu spinors in the BCS Hamiltonian (2.157) we obtain

$$\mathcal{H}_{\text{BCS}} = \int d^d r \Big[\Psi^\dagger_\mathbf{r} H_{\text{BdG}}(\mathbf{r}) \Psi_\mathbf{r} + \frac{1}{V}|\Delta(\mathbf{r})|^2 \Big], \tag{2.159}$$

in the equation above H_{BdG} is the called Bogoliubov-de Gennes Hamiltonian

$$H_{\text{BdG}}(\mathbf{r}) = \begin{pmatrix} h_0(\mathbf{r}) & \hat{\Delta}(\mathbf{r}) \\ \hat{\Delta}^*(\mathbf{r}) & -\sigma^y h_0^*(\mathbf{r}) \sigma^y \end{pmatrix}, \tag{2.160}$$

where the order parameter operator $\hat{\Delta}(\mathbf{r})$ is a 2×2 matrix. In the four-dimensional Nambu space it is necessary the definition of additional matrices. We define the four-dimensional matrices $\boldsymbol{\tau} = (\tau^x, \tau^y, \tau^z)$ which act directly on the Nambu space. We also have the traditional Pauli matrices $\boldsymbol{\sigma} = (\sigma^x, \sigma^y, \sigma^z)$ acting on the two dimensional spin space. Note that the Nambu spinor (2.158) has the property

$$C\Psi^*_\mathbf{r} = \Psi_\mathbf{r}, \tag{2.161}$$

where $\Psi^*_{\mathbf{r}} = (\Psi^\dagger_{\mathbf{r}})^T$ and $C = \tau^y\sigma^y$ is the charge conjugation operator. The Bogoliubov-de Gennes Hamiltonian can be diagonalized using the Bogoliubov eigenvector $\Phi_n(\mathbf{r}) = (u_{n\uparrow}(\mathbf{r}), u_{n\downarrow}(\mathbf{r}), v_{n\uparrow}(\mathbf{r}), v_{n\downarrow}(\mathbf{r}))^T$ with energy, E_n which satisfies the Bogoliubov-de Gennes equation

$$H_{\text{BdG}}(\mathbf{r})\Phi_n(\mathbf{r}) = E_n\Phi_n(\mathbf{r}). \tag{2.162}$$

On the Bogoliubov basis the BCS Hamiltonian has the diagonal form

$$\mathcal{H}_{\text{BCS}} = \sum_n E_n\alpha^\dagger_n\alpha_n + E_g, \tag{2.163}$$

where E_g is the ground state energy (superconductor condensate) and $\alpha^\dagger_n$ creates an excitation with energy E_n called *Bogoliubov quasiparticle*, expressed in the Nambu basis as

$$\alpha_n = \int d^d r \Phi^\dagger_n(\mathbf{r})\Psi_{\mathbf{r}}. \tag{2.164}$$

Moreover, notice that the diagonal form of the BCS Hamiltonian (2.163) has the same form of the Majorana Hamiltonian (2.149). The Bogoliubov-de Gennes states have an intrinsic particle-hole symmetry, i.e. for each eigenstate $\Phi_n(\mathbf{r})$ with energy E_n there is a conjugated eigenstate $\Phi^{(c)}_n(\mathbf{r}) = C\Phi^*_n(\mathbf{r})$ with energy $-E_n$. This can be verified using the Bogoliubov-de Gennes equation (2.162)

$$\begin{aligned} H_{\text{BdG}}(\mathbf{r})\Phi_n(\mathbf{r}) = E_n\Phi_n(\mathbf{r}) \quad &\Rightarrow \quad [CH_{\text{BdG}}(\mathbf{r})C^\dagger](C\Phi^*_n(\mathbf{r})) = CE_nC^\dagger(C\Phi^*_n(\mathbf{r})) \\ &\Rightarrow \quad -H_{\text{BdG}}(\mathbf{r})(C\Phi^*_n(\mathbf{r})) = CC^\dagger E_n(C\Phi^*_n(\mathbf{r})) \\ &\Rightarrow \quad H_{\text{BdG}}(\mathbf{r})(C\Phi^*_n(\mathbf{r})) = -E_n(C\Phi^*_n(\mathbf{r})). \end{aligned}$$

Above we have used $CC^\dagger = 1$ and

$$\begin{aligned} CH_{\text{BdG}}(\mathbf{r})C^\dagger &= \begin{pmatrix} 0 & -i\sigma^y \\ i\sigma^y & 0 \end{pmatrix}\begin{pmatrix} h_0(\mathbf{r}) & \hat{\Delta}(\mathbf{r}) \\ \hat{\Delta}^*(\mathbf{r}) & -\sigma^y h_0^*(\mathbf{r})\sigma^y \end{pmatrix}\begin{pmatrix} 0 & i\sigma^y \\ -i\sigma^y & 0 \end{pmatrix} \\ &= \begin{pmatrix} -h_0(\mathbf{r}) & -\hat{\Delta}(\mathbf{r}) \\ -\hat{\Delta}^*(\mathbf{r}) & \sigma^y h_0^*(\mathbf{r})\sigma^y \end{pmatrix} = -H_{\text{BdG}}(\mathbf{r}). \end{aligned} \tag{2.165}$$

Something very special occurs *if* we have a single zero energy state $E = 0$, in this case we have

$$H_{\text{BdG}}(\mathbf{r})\Phi_0(\mathbf{r}) = 0,$$

and for the charge conjugated zero energy state

$$H_{\text{BdG}}(\mathbf{r})(C\Phi^*_0(\mathbf{r})) = 0.$$

Therefore,

$$\Phi_0(\mathbf{r}) = C\Phi^*_0(\mathbf{r}). \tag{2.166}$$

Explicitly, we have

$$\Phi_0(\mathbf{r}) = \tau^y\sigma^y\Phi^*_0,$$

which implies

$$\begin{pmatrix} u_{0\uparrow}(\mathbf{r}) \\ u_{0\downarrow}(\mathbf{r}) \\ v_{0\uparrow}(\mathbf{r}) \\ v_{0\downarrow}(\mathbf{r}) \end{pmatrix} = \begin{pmatrix} -v^*_{0\downarrow}(\mathbf{r}) \\ v^*_{0\uparrow}(\mathbf{r}) \\ u^*_{0\downarrow}(\mathbf{r}) \\ -u^*_{0\uparrow}(\mathbf{r}) \end{pmatrix}. \tag{2.167}$$

The zero energy Bogoliubov quasiparticle α_0 can be written using (2.164) as

$$\alpha_0 = \int d^d r \Phi_0^\dagger(\mathbf{r})\Psi_{\mathbf{r}} = \int d^d r [u^*_{0\uparrow}(\mathbf{r})c_{\mathbf{r}\uparrow} + u^*_{0\downarrow}(\mathbf{r})c_{\mathbf{r}\downarrow} + v^*_{0\uparrow}(\mathbf{r})c^\dagger_{\mathbf{r}\downarrow} - v^*_{0\downarrow}(\mathbf{r})c^\dagger_{\mathbf{r}\uparrow}], \tag{2.168}$$

then

$$\alpha_0^\dagger = \int d^d r [u_{0\uparrow}(\mathbf{r})c^\dagger_{\mathbf{r}\uparrow} + u_{0\downarrow}(\mathbf{r})c^\dagger_{\mathbf{r}\downarrow} + v_{0\uparrow}(\mathbf{r})c_{\mathbf{r}\downarrow} - v_{0\downarrow}(\mathbf{r})c_{\mathbf{r}\uparrow}]. \tag{2.169}$$

Using relations (2.167) for the zero energy state in the equations above it is straightforward to see that

$$\alpha_0 = \alpha_0^\dagger. \tag{2.170}$$

then the zero energy Bogoliubov quasiparticle in a superconductor system behaves exactly as a true Majorana fermion[14]. This is why the zero energy Bogoliubov quasiparticle receives the name Majorana zero modes (MZMs).

Although the generic description above, the physical existence of a single zero energy state in superconductors, with the propriety (2.170), and consequently MZMs, is only possible in a special class of superconductors, they are the called topological superconductors (READ; GREEN, 2000)[15]. Here, the term 'topological' is associated with smooth deformations of the Hamiltonian parameters, usually in reciprocal space. Systems that belong to the same topological class can be mapped (smoothly deformed) into one another. However, systems with different topological phases cannot be connected by smooth deformations. A given topological class (phase) is characterized by a topological invariant analogous to an order parameter in conventional quantum phase transition theory. For an extensive discussion of topological phases in matter and topology in general physics, see (NAKAHARA, 2003; BERNEVIG; HUGHES, 2013).

In topological superconductors with non-trivial topological phases, a topological phase can sustain exotic phenomena in their surface, or edges for 1D systems. The vacuum topology is trivial, therefore the surface states of a topological superconductor cannot be smoothly deformed into trivial vacuum states, implying a topological phase transition. The transition is manifested by the closing of the superconducting gap, resulting in a zero energy state (MZM) at the surface of a topological superconductor. The natural candidates to be topological superconductors are the so-called p-wave superconductors (IVANOV, 2001; SARMA; NAYAK; TEWARI, 2006; KRAUS et al., 2009). However, p-wave superconducting pairing seems to be rare in nature (SIGRIST, 2005; KALLIN; BERLINSKY, 2009;

[14] Here we consider a neutral superconductor, for charged superconductors the neutrality condition of the Majorana fermions is not satisfied.

[15] A classical example of topological superconductor is the Kitaev model discussed in the Appendix B.

VOLOVIK, 2003). Alternatively, there are several proposals which combine conventional s-wave superconductors, magnetic fields and strong spin-orbit coupling to create effective p-wave paring (ALICEA, 2010; ALICEA, 2012). Magnetic chains have also been used to try experimental detection of MZMs (NADJ-PERGE et al., 2014). The first proposal of MZMs in a superconductor system was done by Kitaev in 2001 (KITAEV, 2001). Kitaev proposed a 1D superconducting chain with p-wave paring mechanism and showed that in the topological phase the chain presents MZMs in the chain ends, which results from a topological phase transition. The details of the Kitaev model are given in Appendix B.

3 The Kondo effect in the presence of polarized Majorana zero modes

In this chapter, we revisit the Majorana-Kondo problem in a QD coupled to a metallic lead and to a topological superconducting quantum wire (TSQW). The physical properties of an interacting QD coupled to a single MZM was previous studied in (RUIZ-TIJERINA et al., 2015). There, the authors used the Green's functions approach together with NRG to show the coexistence of the Kondo singlet and a local Majorana singlet, composed by the QD and the MZM. However, the microscopic mechanisms responsible for the physical phenomena obtained were not explored. To fill this gap, we present a detailed investigation focusing on the mechanisms that make the Kondo effect resilient to TRS breaking, and to the superconducting pairing induced by the TSQW. To this end, we consider a more general case, in comparison with the one studied by Tijerina et al (RUIZ-TIJERINA et al., 2015). Now, we consider a QD coupled not only to one MZN, but two. Moreover, we assume that the MZMs are spin polarized in opposite directions. This configuration can be obtained by coupling the QD to two spatially separated TSQWs, each of which is in the proximity of ferromagnets with opposite polarizations (HOFFMAN et al., 2017). In this configuration, the QD-MZM spin-dependent couplings arising from the wave-function overlap between dot orbitals. Then, the polarized MZM states (PRADA; AGUADO; SAN-JOSE, 2017) will couple with only the QD electronic states with the same spin direction, which we take to be "up" or "down." As a result, if the QD is symmetrically coupled to both MZMs, local TRS in the QD is restored.

Here, we consider an effective single-impurity Anderson model that describes the coupling of an "impurity" (QD and MZMs) with a metallic lead. The low-energy properties of this model are investigated using Wilson's numerical renormalization group (NRG) method as well as Anderson poor-man's scaling, discussed in the previous chapter. The NRG calculations allow for a quantitative description of local properties at the fixed points of the model, particularly the impurity contribution to the entropy at a given temperature $S_{\mathrm{imp}}(T)$.

To understand the relevance of Kondo correlations to the flow to the low-energy fixed point, we derive an effective Kondo-like Hamiltonian to investigate how the coupling to both MZMs modifies the Kondo physics of the model. This effective Kondo model is then studied within the traditional Anderson poor-man's scaling renormalization analysis, which allows us to identify the evolution of the effective parameters under the renormalization procedure. We obtain a set of differential equations (β function) for the effective coupling that is solved numerically.

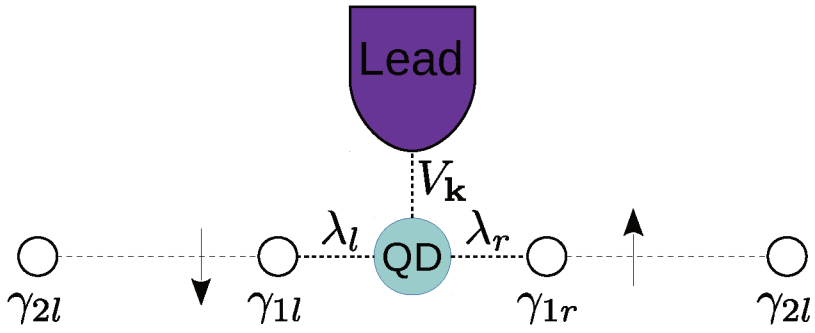

Figure 10 – Schematic representation of the model. The quantum dot (QD) couples to the lead via matrix element $V_{\mathbf{K}}$ and to left (l) and right (r) Majorana modes, assumed to present opposite polarization as denoted by the up and down arrows. Figure published in (SILVA; SILVA; VERNEK, 2020).

As one of the central results of this chapter, we show that the scaling equation for the effective coupling J associated with the Kondo effect appears fully decoupled from the other scaling equations, clearly indicating that the Kondo strong coupling fixed point remains intact in the presence of the TSQW. As a result, the Kondo temperature T_K extracted from the solution for J is insensitive to the parameters involving the TSQW. This result sheds light on *why* the T_K obtained by the thermodynamic properties of the system calculated with the numerical renormalization group depends weakly on the coupling between the QD and a single MZM, as studied previously. Moreover, the results show that the low-energy limit $S_{\rm imp}(T \to 0)$ assumes Fermi-liquid-like values of $k_B \ln 2$ (or $2k_B \ln 2$) if both (or none) MZMs are coupled to the QD. When only one of the MZMs is coupled, then $S_{\rm imp}(T \to 0) = (3/2)k_B \ln 2$, indicating a non-Fermi-liquid behavior marked by the presence of three free MZMs. More importantly, we establish that electron- electron interactions or the presence of Kondo correlations do not change this overall picture. Thus, the Kondo effect plays a "spectator role" in the process. The principal results of the present chapter were published in (SILVA; SILVA; VERNEK, 2020).

3.1 Description of the system

We consider an interacting quantum dot coupled to topological superconductors carrying Majorana zero modes at their edges with different spins polarizations. A schematic representation of the system is showed in Fig. 10. The quantum dot is also coupled to a normal metallic lead. The system is described by the following Anderson impurity Hamiltonian

$$H = H_{\rm dot} + H_{\rm lead} + H_{\rm dot-lead} + H_{\rm dot-M}. \tag{3.1}$$

In which

$$H_{\text{dot}} = \sum_{\sigma} \varepsilon_d d_\sigma^\dagger d_\sigma + U n_{d\uparrow} n_{d\downarrow} \tag{3.2}$$

describes the isolated quantum dot, where $d_\sigma^\dagger$ and d_σ are the operators that creates and annihilates an electron with energy ε_d and spin σ in the single level QD, $n_\sigma = d_\sigma^\dagger d_\sigma$ is the number operator and U represents the onsite Coulomb interaction at the dot.

$$H_{\text{lead}} = \sum_{\mathbf{k},\sigma} \varepsilon_{\mathbf{k},\sigma} c_{\mathbf{k},\sigma}^\dagger c_{\mathbf{k},\sigma} \tag{3.3}$$

describes the normal lead, with $c_{\mathbf{k}}^\dagger\sigma$ ($c_{\mathbf{k}\sigma}$) being the operator that creates (annihilates) an electrons with momentum $\mathbf{k}$, energy $\varepsilon_{\mathbf{k}}$ and spin σ in the normal metal.

$$H_{\text{dot-lead}} = \sum_{\mathbf{k},\sigma} \left(V_{\mathbf{k}} d_\sigma^\dagger c_{\mathbf{k},\sigma} + V_{\mathbf{k}}^* c_{\mathbf{k},\sigma}^\dagger d_\sigma \right) \tag{3.4}$$

connects the dot to the normal lead via matrix element $V_{\mathbf{k}}$. Finally,

$$H_{\text{dot-M}} = i\lambda_r (e^{-i\phi_r 2} d_\uparrow^\dagger + e^{i\phi_r/2} d_\uparrow)\gamma_r + \lambda_l (e^{i\phi_l 2} d_\downarrow^\dagger - e^{-i\phi_l/2} d_\downarrow)\gamma_l \tag{3.5}$$

describes the coupling between the QD and the Majorana zero modes in the topological superconductors edges. Here, the operators $\gamma_{l,r}$ are Majorana operators, with the property

$$\gamma_{i\sigma} = \gamma_{i\sigma}^\dagger, \tag{3.6}$$

and obeying the fermion anti-commutation relation $[\gamma_{i\sigma}, \gamma_{j,\sigma'}]_+ = \delta_{i,j}\delta_{\sigma,\sigma'}$ and $\phi_{r/l}$ represents the phase of the left/right topological superconductor. For convenience, we perform a gauge transformation $d_\sigma \to d_\sigma e^{-i\phi_l/2}$, with which the expression (3.4) can be rewritten as

$$H_{\text{dot-M}} = i\lambda_r (e^{-i\delta\phi/2} d_\uparrow^\dagger + e^{i\delta\phi/2} d_\uparrow)\gamma_r + \lambda_l (d_\downarrow^\dagger - d_\downarrow)\gamma_l, \tag{3.7}$$

where $\delta\phi = \phi_r - \phi_l$ is the phase difference between the two superconductors. We emphasize that the QD-MZM coupling strengths $\lambda_{l,r}$ in Eqs. (3.5) and (3.7) are, in general, spin-dependent and can couple to both dot spins depending on the respective "spin canting angle" $\theta_{l,r}$ as $\left(\lambda_{\uparrow(l,r)}, \lambda_{\downarrow(l,r)}\right) \equiv \lambda_{l,r} \left(\sin\frac{\theta_{l,r}}{2}, -\cos\frac{\theta_{l,r}}{2}\right)$ (PRADA; AGUADO; SAN-JOSE, 2017; HOFFMAN et al., 2017; DENG et al., 2018). Here, we take $\theta_r = \pi$ and $\theta_l = 2\pi$ such that only a single dot spin operator is coupled to each MZM, making $H_{\text{dot-M}}$ fully spin-conserving. This choice adds an extra symmetry [spin parity $P_\sigma = (-1)^{N_\sigma}$] to the full Hamiltonian, which is important for the NRG calculations presented in the next section.

3.2 Numerical Renormalization Group Analysis

The lack of particle conservation due the presence of the Majorana fermions is better understood when the Majorana operators is described using regular fermionic operators. To do so, we should write the Hamiltonian (3.7) in term of regular fermions as $f_\uparrow = (\gamma_{1r} + i\gamma_{2r})/\sqrt{2}$ and $f_\downarrow = (\gamma_{1l} + i\gamma_{2l})/\sqrt{2}$ we obtain

$$\begin{aligned} H_{\text{dot}-\text{M}} &= \frac{i\lambda_r}{\sqrt{2}}[e^{-i\delta\phi/2}(d_\uparrow^\dagger f_\uparrow + d_\uparrow^\dagger f_\uparrow^\dagger) + e^{i\delta\phi/2}(d_\uparrow f_\uparrow + d_\uparrow f_\uparrow^\dagger)] \\ &\quad + \frac{\lambda_l}{\sqrt{2}}(d_\downarrow^\dagger f_\downarrow + d_\downarrow^\dagger f_\downarrow^\dagger - d_\downarrow f_\downarrow - d_\downarrow f_\downarrow^\dagger). \end{aligned} \tag{3.8}$$

We can now construct a Fock space for the occupation numbers of the QD electrons and of the f-fermions as $\{|n_{d\sigma}\rangle \otimes |n_{f\sigma}\rangle\}$, where $n_{d\sigma} = d_\sigma^\dagger d_\sigma$ and $n_{f\sigma} = f_\sigma^\dagger f_\sigma$ with $\sigma = \uparrow, \downarrow$. From now on, we consider the wide-band limit for the (particle-hole symmetric) conduction band of the metallic lead. As such, the density of states of the metallic electrons is taken to be a constant, given by $\rho_0 = (2D)^{-1}$ for energies in the range $\omega \in [-D, D]$ and zero otherwise. In the following, we set the the Fermi energy at $\omega = 0$ and the half-bandwidth D as our energy unit.

The presence of Majorana modes breaks gauge invariance in the system and introduces some technical difficulties for the NRG implementation as the total charge $N_{\text{occ}} \equiv N_\uparrow + N_\downarrow$ with $N_\sigma = n_{d\sigma} + n_{f\sigma}$ is no longer a good quantum number (LEE; LIM; LÓPEZ, 2013; RUIZ-TIJERINA et al., 2015; CIFUENTES; SILVA, 2019). Nevertheless, the parities for each spin σ, defined as $P_\sigma \equiv (-1)^{N_\sigma}$, can be used as a good quantum numbers in our case, thereby reducing the block size of the Hamiltonians generated along the NRG procedure.

To get a better insight of the low-energy physics of the system, we use the NRG to calculate the contribution from the QD-Majorana system to the entropy. In the remainder of the section, we will refer to this quantity as the "impurity entropy" S_{imp}. In the following, we use the same parameters as those in Fig. 13 unless stated otherwise. To perform the NRG calculations we use the code developed by Prof. L.G.D. Silva, using $\Lambda = 2.5$, keeping a maximum number of states $N_s = 1000$ at each iteration and z-averaging $N_z = 9$ (YOSHIDA; WHITAKER; OLIVEIRA, 1990; ZITKO; PRUSCHKE, 2009).

Figure 11 shows the impurity entropy as a function of temperature $[S_{\text{imp}}(T)]$ for different values of λ_r and λ_l. The different plateaus correspond to the fixed points of the renormalization flow of the MZM-QD-leads system. The first plateau (large T) at $S_{\text{imp}} \sim 4k_B \ln(2)$ corresponds to the free orbital fixed point. As the temperature lowers, the system approaches the local moment fixed point, marked by a plateau at $S_{\text{imp}} \sim 3k_B \ln(2)$. Finally, for $T \to 0$, the system approaches the strong coupling fixed point. The value of S_{imp} in this fixed point depends strongly on how many MZMs are directly coupled to the QD.

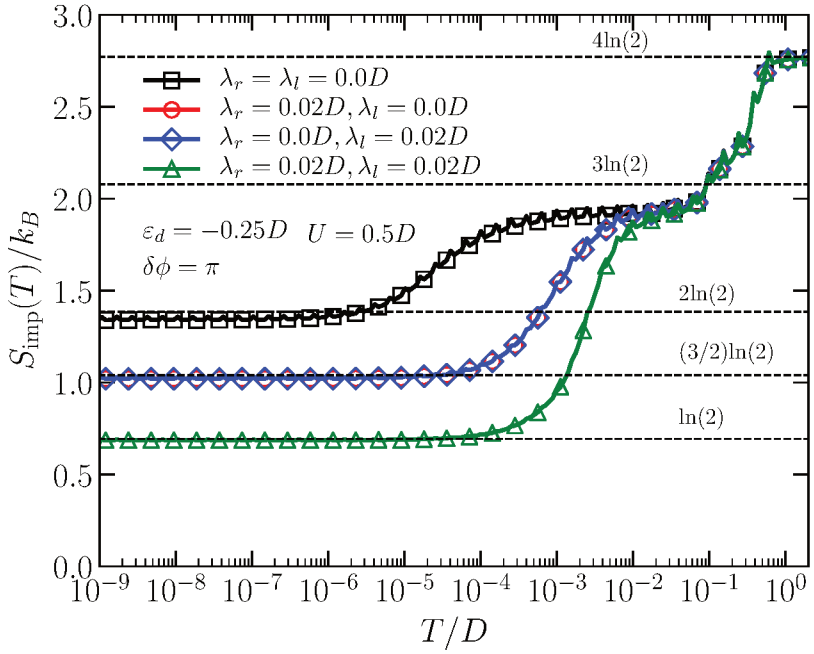

Figure 11 – Impurity entropy extracted using NRG. In the presence of one Majorana mode the Kondo singlet and the local Majorana singlet coexists and the entropy presents the peculiar value (3/2)ln(2) for $T = 0$. Figure published in (SILVA; SILVA; VERNEK, 2020).

For $\lambda_l = \lambda_r = 0$ (black curve), the results show that $S_{\rm imp}(T \to 0) \sim 2k_B \ln(2)$. One can understand this result qualitatively as follows: in the strong coupling fixed point, the QD is Kondo-screened in a singlet state, while the decoupled Majorana modes provide an additional double degeneracy to the ground state, yielding an $\ln(4)$ residual entropy. In fact, within the f-fermion representation, $f_\sigma^\dagger f_\sigma |n_{f,\sigma}\rangle = n_{f,\sigma}|n_{f,\sigma}\rangle$, we find four different possible zero-energy states which account for the four-fold ground state degeneracy.

As we turn on the couplings to the Majorana modes, some of these degeneracies are lifted and the entropy goes to a lower value as $T \to 0$. The most interesting case occurs when only a single Majorana mode is coupled to the QD, i.e., $\lambda_l = 0$, $\lambda_r \neq 0$ or vice-versa [circles (red) and diamond (blue) curves in Fig. 11]. Notice that, in this case, the strong coupling fixed point plateau behaves as $S_{\rm imp}(T \to 0) \sim (3/2)k_B \ln(2)$. This is consistent with the fact that there are now three decoupled MZMs at low energies and the MZM directly coupled to the QD does not contribute to the entropy.

When both couplings are nonzero (e.g., $\lambda_r = \lambda_l = 0.02$ corresponding to the green curve with triangle symbols in Fig. 11), the ground state exhibits a residual entropy $S_{\rm res} \equiv S_{\rm imp}(T \to 0) = k_B \ln(2)$, stemming from the two MZMs that remain decoupled from the rest of the system. From these results, we can see that the low-energy residual entropy $S_{\rm res}$ takes the form $S_{\rm res} = (N_0/2)k_B \ln(2)$, where N_0 is the number of uncoupled ("free") Majorana modes. In fact, this result can be rigorously proven in the case of free MZMs (see Appendix C). Note that if N_0 is odd, the entire system behaves as a non-Fermi

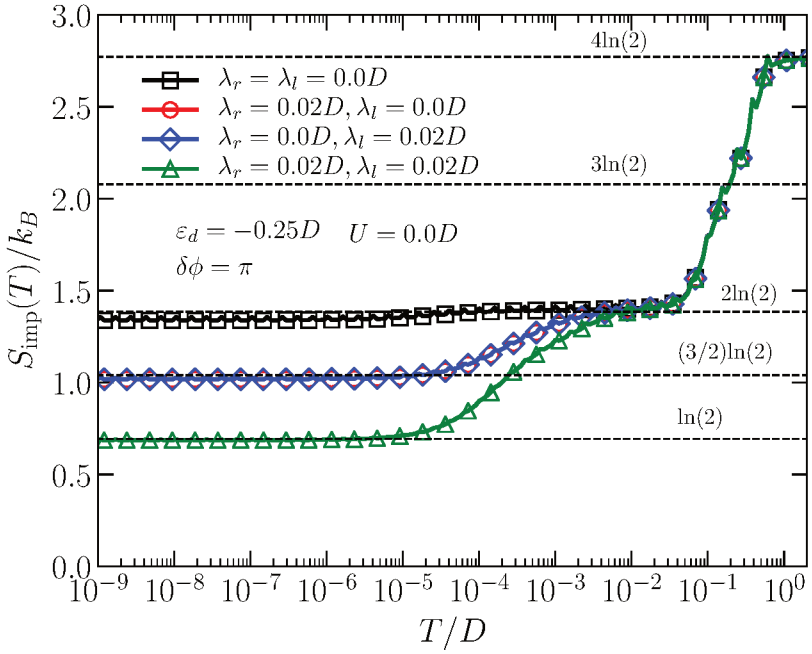

Figure 12 – Impurity entropy extracted using NRG for the non-interacting regime ($U = 0$). For $T \to 0$ the entropy behaves as in the interacting case giving the same results for $T = 0$ which confirms that the residual entropy behavior is due only the free Majorana modes. Figure published in (SILVA; SILVA; VERNEK, 2020).

liquid. This is quite similar to the results obtained in the (unstable) non-Fermi-liquid fixed point of the two-channel Kondo problem, where in the Majorana representation there is a free Majorana mode left as $T \to 0$ (EMERY; KIVELSON, 1992; COLEMAN; IOFFE; TSVELIK, 1995; COX; ZAWADOWSKI, 1998; ZHANG; HEWSON; BULLA, 1999). The fractional aspect of the entropy of a single MZM coupled to a quantum dot has also been subject of more recent studies (SMIRNOV, 2015; SELA et al., 2019).

To show that the residual entropy of the QD is dominated by the free Majorana modes of the system, and thereby is not affected by the Kondo singlet, it is interesting to consider the the noninteracting regime. This can be accomplished by taking $U=0$ in (3.2). In this regime, no Kondo effect takes place and the entropy features are entirely due the coupling of the QD with Majorana modes and the metallic leads. As before, we compute $S_{\rm imp}(T)$ with NRG. The results are shown in Fig 12 and the residual entropy follows precisely the behavior of the interacting case shown in Fig. 11. This result is also consistent with analytical calculations for $S_{\rm imp}(T \to 0)$ carried out for $U=0$ shown in section 3.3.3.

The impurity entropy in the noninteracting case (Fig. 12) displays a free orbital plateau ($S_{\rm imp} \sim 4k_B \ln(2)$) at large temperatures, but not the local moment plateau ($S_{\rm imp} \sim 3k_B \ln(2)$). This is expected as the local moment regime is not present for $U = 0$. The interesting region occurs for $T \to 0$. In this regime, we have $S_{\rm imp}(T \to 0)$ displaying

the same behavior as in the interacting case (Fig. 11). This indicates that, in the presence or absence of the Kondo singlet, the low-temperature behavior of the entropy is entirely determined by the free Majorana modes of the system. The absence of an additional contribution for the entropy in the interacting regime shows that the Kondo singlet is preserved even in the presence of the Majorana modes, indicating a disassociation of the processes leading to Kondo screening at low-energies from the QD-MZMs couplings at high-energies. In order to clarify the origin of this interesting behavior, in the following we derive an effective Hamiltonian that describes the low-energy regime of the system and perform an RG scaling analysis.

To close this section, let us briefly discuss the fractional residual entropy observed in the NRG results (Figs. 11 and 12). The situation here is closely related to the non-Fermi liquid regime of the two-channel Kondo problem. As showed by Emery and Kivelson (EMERY; KIVELSON, 1992), the bosonization (refermionalization) approach to the two-channel Kondo problem uses a Majorana representation to map the problem into a zero-energy resonant level coupled to metallic channels. In fact, only a "half fermion" (Majorana mode) in the resonant level is strongly coupled to the metallic electrons while the other "half" is free. This "free" Majorana mode sets the non-zero value of the residual entropy, resulting in the celebrated result $S_{\text{imp}}(T \to 0) = k_{\text{B}} \ln(2)/2$.

This result reveals a special *non-integer* ground state degeneracy, which is a characteristic of the non-Fermi liquid behavior of the two-channel Kondo problem (Nozières, Ph.; Blandin, A., 1980). In fact, Affleck and Ludwig, using a boundary conformal field approach, showed that some quantum critical systems (including the multichannel Kondo impurity problem), may display a non-integer ground state degeneracy g, whose specific value depends on the universality class of the boundary conditions (AFFLECK; LUDWIG, 1991b).

In the present context, the system (namely two topological quantum wires coupled to an interacting QD) is distinct from the two-channel Kondo problem. However, as it has already been pointed out previously (VERNEK et al., 2014; RUIZ-TIJERINA et al., 2015), a Majorana mode from the edge of a wire can "leak" into the QD once it is tunnel coupled to it. The scenario of MZMs coupled to the QD (and to a metallic lead) and their correspondent free partners in the other edge (see Fig.10) can be viewed as a formal analogue of the two-channel Kondo problem, but with a different physical origin. A detailed calculation of the impurity residual entropy promoted by a free MZM is shown in Appendix C.

We should also point out that such fractional character of the residual entropy may be used to distinguish MZMs from trivial zero-energy states in experiments. Indeed, a protocol based in entropy measurements to detect MZMs was recently proposed by Sela *et al.* (SELA et al., 2019). Their proposal consists of a MZM coupled to a metallic lead

close to a QD in the Coulomb blockage regime. The QD occupation can change from N to $N+1$ by changing the chemical potential μ of a reservoir coupled to the QD. This change can be monitored by a charge detector and it is related to the local entropy via the Maxwell's relation $(dS/d\mu)|_T = (dN/dT)|_\mu$. A careful measurement of the QD occupation as a function of temperature can, therefore, give experimental access to the change in entropy ΔS and thus allow for the detection of fractional entropy values (SELA et al., 2019).

3.3 Perturbative Renormalization Group Analysis

3.3.1 Effective Kondo-Majorana Hamiltonian

In this section we will use the projection method to obtain a Kondo-like Hamiltonian for the system described by the equation (3.1). To do so we follow the same procedures used for the traditional single impurity Anderson model, see Appendix A. For the present case the projection operators still are the same

$$P_0 = (1-n_{d\uparrow})(1-n_{d\downarrow}), \tag{3.9}$$

$$P_1 = n_{d\uparrow}+n_{d\downarrow}-2n_{d\uparrow}n_{d\downarrow}, \tag{3.10}$$

$$P_2 = n_{d\uparrow}n_{d\downarrow}, \tag{3.11}$$

with the effective Hamiltonian

$$[H_{11}+H_{01}(E-H_{00})^{-1}H_{10}+H_{21}(E-H_{22})^{-1}H_{12}]\Psi_1 = E\Psi_1, \tag{3.12}$$

where $H_{ij} = P_iHP_j$, with H given by (3.1). Again we use the fact $H_{02} = H_{20} = 0$. The same algebraic tricks for the quantum operators used in the Appendix A can be used to obtain

$$H_{01} = \sum_{\mathbf{k}\sigma} V^*_{\mathbf{k}}(1-n_{d\bar{\sigma}})c^\dagger_{\mathbf{k}\sigma}d_\sigma + i\lambda_r e^{i\delta\phi/2}(1-n_{d\downarrow})d_\uparrow\gamma_r - \lambda_l(1-n_{d\uparrow})d_\downarrow\gamma_l \tag{3.13}$$

and

$$H_{10} = \sum_{\mathbf{k}\sigma} V^*_{\mathbf{k}}(1-n_{d\bar{\sigma}})d^\dagger_\sigma c_{\mathbf{k}\sigma} - i\lambda_r e^{-i\delta\phi/2}(1-n_{d\downarrow})\gamma_r d^\dagger_\uparrow - \lambda_l(1-n_{d\uparrow})\gamma_l d^\dagger_\downarrow. \tag{3.14}$$

Proceeding likewise for H_{12}, and $H_{21} = H^\dagger_{12}$ we obtain

$$H_{12} = \sum_{\mathbf{k}\sigma} V^*_{\mathbf{k}} n_{d\bar{\sigma}}c^\dagger_{\mathbf{k}\sigma}d_\sigma + i\lambda_r e^{i\delta\phi/2}n_{d\downarrow}d_\uparrow\gamma_r - \lambda_l n_{d\uparrow}d_\downarrow\gamma_l, \tag{3.15}$$

$$H_{21} = \sum_{\mathbf{k}\sigma} V_{\mathbf{k}} n_{d\bar{\sigma}}d^\dagger_\sigma c_{\mathbf{k}\sigma} - i\lambda_r e^{-i\delta\phi/2}n_{d\downarrow}\gamma_r d^\dagger_\uparrow - \lambda_l n_{d\uparrow}\gamma_l d^\dagger_\downarrow. \tag{3.16}$$

Let us now define again the Hamiltonians $H_1 = H_{10}(E - H_{00})^{-1}H_{01}$ and $H_2 = H_{12}(E - H_{22})^{-1}H_{21}$. Using (3.13) and (3.14) in H_1 results in

$$\begin{aligned}
H_1 &= \sum_{\mathbf{k}\mathbf{k}',\sigma\sigma'} V_{\mathbf{k}} V^*_{\mathbf{k}'} (E - \varepsilon_k - H_0)^{-1}(1 - n_{d\bar{\sigma}}) d^\dagger_\sigma c_{\mathbf{k}\sigma}(1 - n_{d\bar{\sigma}'}) c_{\mathbf{k}'\sigma'} d_{\sigma'} \\
&+ \sum_{\mathbf{k}\sigma} i\lambda_r V_{\mathbf{k}} e^{i\delta\phi/2}(E - \varepsilon_k - H_0)^{-1}(1 - n_{d\bar{\sigma}}) d^\dagger_\sigma c_{\mathbf{k}\sigma}(1 - n_{d\downarrow}) d_\downarrow \gamma_r \\
&- \sum_{\mathbf{k}\sigma} i\lambda_r V^*_{\mathbf{k}} e^{-i\delta\phi/2}(E - \varepsilon_k - H_0)^{-1}(1 - n_{d\downarrow})\gamma_r d^\dagger_\downarrow (1 - n_{d\bar{\sigma}}) c^\dagger_{\mathbf{k}\sigma} d_\sigma \\
&+ \sum_{\mathbf{k}\sigma} i\lambda_l V^*_{\mathbf{k}} (E - \varepsilon_k - H_0)^{-1}(1 - n_{d\uparrow})\gamma_l d^\dagger_\downarrow (1 - n_{d\bar{\sigma}}) c^\dagger_{\mathbf{k}\sigma} d_\sigma \\
&- \sum_{\mathbf{k}\sigma} i\lambda_l V_{\mathbf{k}} (E - \varepsilon_k - H_0)^{-1}(1 - n_{d\bar{\sigma}}) d^\dagger_\sigma c_{\mathbf{k}\sigma}(1 - n_{d\uparrow}) d_\downarrow \gamma_l \\
&+ \lambda_r^2 (E - H_0)^{-1}(1 - n_{d\downarrow})\gamma_r d^\dagger_\uparrow (1 - n_{d\downarrow}) d_\uparrow \gamma_r \\
&+ \lambda_l^2 (E - H_0)^{-1}(1 - n_{d\uparrow})\gamma_l d^\dagger_\downarrow (1 - n_{d\uparrow}) d_\downarrow \gamma_l \\
&- \lambda_r\lambda_l e^{-i\delta\phi/2}(E - H_0)^{-1}(1 - n_{d\downarrow})\gamma_r d^\dagger_\uparrow (1 - n_{d\uparrow}) d_\downarrow \gamma_l \\
&- \lambda_l\lambda_r e^{i\delta\phi/2}(E - H_0)^{-1}(1 - n_{d\uparrow})\gamma_l d^\dagger_\downarrow (1 - n_{d\downarrow}) d_\uparrow \gamma_r .
\end{aligned}$$

Note that we can write

$$\begin{aligned}
(E - \varepsilon_k - H_0)^{-1} &= (E - \varepsilon_k - H_0 + \varepsilon_d - \varepsilon_d)^{-1} = \frac{1}{\varepsilon_d - \varepsilon_k}\left[1 - \frac{E - H_0 - \varepsilon_d}{\varepsilon_k - \varepsilon_d}\right]^{-1}, \\
(E - H_0)^{-1} &= (E - H_0 + \varepsilon_d - \varepsilon_d)^{-1} = \frac{1}{\varepsilon_d}\left[1 + \frac{E - H_0 - \varepsilon_d}{\varepsilon_d}\right]^{-1}.
\end{aligned}$$

For the single occupied state and for energies near to the Fermi energy we have $\varepsilon_k \ll \varepsilon_d$ and $E - H_0 - \varepsilon_d \ll \varepsilon_d$, therefore (see Appendix A for details)

$$\begin{aligned}
(E - \varepsilon_k - H_0)^{-1} &\approx \frac{1}{\varepsilon_d - \varepsilon_k}, \\
(E - H_0)^{-1} &\approx \frac{1}{\varepsilon_d}.
\end{aligned}$$

Using this in H_1 we obtain

$$\begin{aligned}
H_1 &= \sum_{\mathbf{k}\mathbf{k}',\sigma\sigma'} \frac{V_{\mathbf{k}}V^*_{\mathbf{k}'}}{\varepsilon_d-\varepsilon_k}(1-n_{d\bar{\sigma}})d^\dagger_\sigma c_{\mathbf{k}\sigma}(1-n_{d\bar{\sigma}'})c_{\mathbf{k}'\sigma'}d_{\sigma'} \\
&+\sum_{\mathbf{k}\sigma}\frac{i\lambda_r V_{\mathbf{k}}e^{i\delta\phi/2}}{\varepsilon_d-\varepsilon_k}(1-n_{d\bar{\sigma}})d^\dagger_\sigma c_{\mathbf{k}\sigma}(1-n_{d\downarrow})d_\downarrow\gamma_r \\
&-\sum_{\mathbf{k}\sigma}\frac{i\lambda_r V^*_{\mathbf{k}}e^{-i\delta\phi/2}}{\varepsilon_d-\varepsilon_k}(1-n_{d\downarrow})\gamma_r d^\dagger_\downarrow(1-n_{d\bar{\sigma}})c^\dagger_{\mathbf{k}\sigma}d_\sigma \\
&+\sum_{\mathbf{k}\sigma}\frac{i\lambda_l V^*_{\mathbf{k}}}{\varepsilon_d-\varepsilon_k}(1-n_{d\uparrow})\gamma_l d^\dagger_\downarrow(1-n_{d\bar{\sigma}})c^\dagger_{\mathbf{k}\sigma}d_\sigma \\
&-\sum_{\mathbf{k}\sigma}\frac{i\lambda_l V_{\mathbf{k}}}{\varepsilon_d-\varepsilon_k}(1-n_{d\bar{\sigma}})d^\dagger_\sigma c_{\mathbf{k}\sigma}(1-n_{d\uparrow})d_\downarrow\gamma_l \\
&+\frac{\lambda_r^2}{\varepsilon_d}(1-n_{d\downarrow})\gamma_r d^\dagger_\uparrow(1-n_{d\downarrow})d_\uparrow\gamma_r \\
&+\frac{\lambda_l^2}{\varepsilon_d}(1-n_{d\uparrow})\gamma_l d^\dagger_\downarrow(1-n_{d\uparrow})d_\downarrow\gamma_l \\
&-\frac{\lambda_r\lambda_l}{\varepsilon_d}e^{-i\delta\phi/2}(1-n_{d\downarrow})\gamma_r d^\dagger_\uparrow(1-n_{d\uparrow})d_\downarrow\gamma_l \\
&-\frac{\lambda_l\lambda_r}{\varepsilon_d}e^{i\delta\phi/2}(1-n_{d\uparrow})\gamma_l d^\dagger_\downarrow(1-n_{d\downarrow})d_\uparrow\gamma_r.
\end{aligned}$$

Now, for $H_2 = H_{12}(E-H_{22})^{-1}H_{21}$ we use (3.15) and (3.16) to write

$$\begin{aligned}
H_2 &= \sum_{\mathbf{k}\mathbf{k}',\sigma\sigma'} V_{\mathbf{k}}V^*_{\mathbf{k}'}n_{d\bar{\sigma}}c^\dagger_{\mathbf{k}\sigma}d_\sigma(E-H_{22})^{-1}n_{d\bar{\sigma}'}d^\dagger_{\sigma'}c_{\mathbf{k}'\sigma'} \\
&-\sum_{\mathbf{k}\sigma}V^*_{\mathbf{k}}i\lambda_r e^{-i\delta\phi/2}n_{d\bar{\sigma}}c^\dagger_{\mathbf{k}\sigma}d_\sigma(E-H_{22})^{-1}n_{d\downarrow}\gamma_r d^\dagger_\uparrow \\
&-\sum_{\mathbf{k}\sigma}V^*_{\mathbf{k}}\lambda_l n_{d\bar{\sigma}}c^\dagger_{\mathbf{k}\sigma}d_\sigma(E-H_{22})^{-1}n_{d\uparrow}\gamma_l d^\dagger_\downarrow \\
&+\sum_{\mathbf{k}\sigma}V_{\mathbf{k}}i\lambda_r e^{i\delta\phi/2}n_{d\downarrow}d_\uparrow\gamma_r(E-H_{22})^{-1}n_{d\bar{\sigma}}d^\dagger_\sigma c_{\mathbf{k}\sigma} \\
&-\sum_{\mathbf{k}\sigma}V_{\mathbf{k}}i\lambda_l n_{d\uparrow}d_\downarrow\gamma_l(E-H_{22})^{-1}n_{d\bar{\sigma}}d^\dagger_\sigma c_{\mathbf{k}\sigma} \\
&+\lambda_r\lambda_r e^{-i\delta\phi/2}n_{d\uparrow}d_\downarrow\gamma_l(E-H_{22})^{-1}n_{d\downarrow}\gamma_r d^\dagger_\uparrow-\lambda_r\lambda_r e^{i\delta\phi/2}n_{d\downarrow}d_\uparrow\gamma_r(E-H_{22})^{-1}n_{d\uparrow}\gamma_l d^\dagger_\downarrow \\
&+\lambda_l^2 n_{d\uparrow}d_\downarrow\gamma_l(E-H_{22})^{-1}n_{d\uparrow}\gamma_l d^\dagger_\downarrow+\lambda_r^2 n_{d\downarrow}d_\uparrow\gamma_r(E-H_{22})^{-1}n_{d\downarrow}\gamma_r d^\dagger_\uparrow.
\end{aligned}$$

Using the fact that $(E-H_{22})^{-1} = (E-2\varepsilon_d-U-H_0)^{-1}$ and the same tricks and approximations used in H_1 we find

$$\begin{aligned}
(E-2\varepsilon_d-U-H_0+\varepsilon_k)^{-1} &\approx -\frac{1}{\varepsilon_d+U-\varepsilon_k}, \\
(E-2\varepsilon_d-U-H_0)^{-1} &\approx \frac{1}{\varepsilon_d+U}.
\end{aligned}$$

Thus, H_2 acquires the form

$$\begin{aligned}
H_2 &= -\sum_{\mathbf{k}\mathbf{k}',\sigma\sigma'} \frac{V_{\mathbf{k}}V^*_{\mathbf{k}'}}{\varepsilon_d+U-\varepsilon_{k'}} n_{d\bar{\sigma}} c^\dagger_{\mathbf{k}\sigma} d_\sigma n_{d\bar{\sigma}'} d^\dagger_{\sigma'} c_{\mathbf{k}'\sigma'} \\
&+\sum_{\mathbf{k}\sigma} \frac{V^*_{\mathbf{k}} i\lambda_r e^{-i\delta\phi/2}}{\varepsilon_d+U-\varepsilon_{k'}} n_{d\bar{\sigma}} c^\dagger_{\mathbf{k}\sigma} d_\sigma n_{d\downarrow} \gamma_r d^\dagger_\uparrow \\
&+\sum_{\mathbf{k}\sigma} \frac{V^*_{\mathbf{k}} \lambda_l}{\varepsilon_d+U-\varepsilon_{k'}} n_{d\bar{\sigma}} c^\dagger_{\mathbf{k}\sigma} d_\sigma n_{d\uparrow} \gamma_l d^\dagger_\downarrow \\
&-\sum_{\mathbf{k}\sigma} \frac{V_{\mathbf{k}} i\lambda_r e^{i\delta\phi/2}}{\varepsilon_d+U-\varepsilon_{k'}} n_{d\downarrow} d_\uparrow \gamma_r n_{d\bar{\sigma}} d^\dagger_\sigma c_{\mathbf{k}\sigma} \\
&+\sum_{\mathbf{k}\sigma} \frac{V_{\mathbf{k}} \lambda_l}{\varepsilon_d+U-\varepsilon_{k'}} n_{d\uparrow} d_\downarrow \gamma_l n_{d\bar{\sigma}} d^\dagger_\sigma c_{\mathbf{k}\sigma} \\
&-\frac{\lambda_r\lambda_r e^{-i\delta\phi/2}}{\varepsilon_d+U} n_{d\uparrow} d_\downarrow \gamma_l n_{d\downarrow} \gamma_r d^\dagger_\uparrow + \frac{\lambda_r\lambda_r e^{i\delta\phi/2}}{\varepsilon_d+U} n_{d\downarrow} d_\uparrow \gamma_r n_{d\uparrow} \gamma_l d^\dagger_\downarrow \\
&-\frac{\lambda_l^2}{\varepsilon_d+U} n_{d\uparrow} d_\downarrow \gamma_l n_{d\uparrow} \gamma_l d^\dagger_\downarrow - \frac{\lambda_r^2}{\varepsilon_d+U} n_{d\downarrow} d_\uparrow \gamma_r n_{d\downarrow} \gamma_r d^\dagger_\uparrow .
\end{aligned}$$

To obtain the effective Hamiltonian we need to show the explicit spin index in the momentum sums in H_1 and H_2. For H_1 we have

$$\sum_{\mathbf{k}\mathbf{k}',\sigma\sigma'} (1-n_{d\bar{\sigma}}) d^\dagger_\sigma c_{\mathbf{k}\sigma} (1-n_{d\bar{\sigma}'}) c^\dagger_{\mathbf{k}'\sigma} d_{\sigma'} = \sum_{\mathbf{k}\mathbf{k}'} (n_{d\uparrow} c^\dagger_{\mathbf{k}\uparrow} c_{\mathbf{k}'\uparrow} + n_{d\downarrow} c^\dagger_{\mathbf{k}\downarrow} c_{\mathbf{k}'\downarrow} + d^\dagger_\uparrow d_\downarrow c_{\mathbf{k}\uparrow} c^\dagger_{\mathbf{k}'\downarrow} + d^\dagger_\downarrow d_\uparrow c_{\mathbf{k}\downarrow} c^\dagger_{\mathbf{k}'\uparrow}),$$

$$\begin{aligned}
\sum_{\mathbf{k}\sigma} (1-n_{d\bar{\sigma}}) d^\dagger_\sigma c_{\mathbf{k}\sigma} (1-n_{d\downarrow}) d_\uparrow \gamma_r &= \sum_{\mathbf{k}} (n_{d\uparrow}\gamma_r c_{\mathbf{k}\uparrow} - d^\dagger_\downarrow d_\uparrow c_{\mathbf{k}\downarrow}\gamma_r), \\
\sum_{\mathbf{k}\sigma} (1-n_{d\bar{\sigma}}) d^\dagger_\sigma c_{\mathbf{k}\sigma} (1-n_{d\uparrow}) d_\downarrow \gamma_l &= \sum_{\mathbf{k}} (n_{d\downarrow}\gamma_l c_{\mathbf{k}\downarrow} - d^\dagger_\uparrow d_\downarrow c_{\mathbf{k}\uparrow}\gamma_l), \\
\sum_{\mathbf{k}\sigma} (1-n_{d\downarrow}) \gamma_r d^\dagger_\uparrow (1-n_{d\bar{\sigma}}) c^\dagger_{\mathbf{k}\sigma} d_\sigma &= \sum_{\mathbf{k}} (n_{d\uparrow} c^\dagger_{\mathbf{k}\uparrow}\gamma_r + d^\dagger_\uparrow d_\downarrow c_{\mathbf{k}\downarrow}\gamma_r), \\
\sum_{\mathbf{k}\sigma} (1-n_{d\uparrow}) \gamma_l d^\dagger_\downarrow (1-n_{d\bar{\sigma}}) c^\dagger_{\mathbf{k}\sigma} d_\sigma &= \sum_{\mathbf{k}} (n_{d\downarrow} c^\dagger_{\mathbf{k}\downarrow}\gamma_l + d^\dagger_\downarrow d_\uparrow c_{\mathbf{k}\uparrow}\gamma_l).
\end{aligned}$$

In addition, we can see that

$$\begin{aligned}
(1-n_{d\downarrow})\gamma_r d^\dagger_\uparrow (1-n_{d\downarrow}) d_\uparrow \gamma_r &= n_{d\uparrow}, \\
(1-n_{d\uparrow})\gamma_l d^\dagger_\downarrow (1-n_{d\uparrow}) d_\downarrow \gamma_l &= n_{d\downarrow}
\end{aligned}$$

and

$$(1-n_{d\downarrow})\gamma_r d^\dagger_\uparrow (1-n_{d\uparrow}) d_\downarrow \gamma_l = d^\dagger_\uparrow d_\downarrow \gamma_r \gamma_l,$$

where we use the fact that $\gamma_i^2 = 1$. Using the identities above we can rewrite H_1 as

$$\begin{aligned}
H_1 &= \sum_{\mathbf{k}\mathbf{k}'} \frac{V_{\mathbf{k}}V^*_{\mathbf{k}'}}{\varepsilon_d-\varepsilon_k} \left[n_{d\uparrow} c_{\mathbf{k}\uparrow} c^\dagger_{\mathbf{k}'\uparrow} + n_{d\downarrow} c_{\mathbf{k}\downarrow} c_{\mathbf{k}\downarrow} c^\dagger_{\mathbf{k}'\downarrow} + d^\dagger_\uparrow d_\downarrow c_{\mathbf{k}\uparrow} c_{\mathbf{k}'\downarrow} + d^\dagger_\downarrow d_\uparrow c_{\mathbf{k}\downarrow} c_{\mathbf{k}'\uparrow} \right] \\
&+\sum_{\mathbf{k}} \frac{i\lambda_r V_{\mathbf{k}} e^{i\delta\phi/2}}{\varepsilon_d-\varepsilon_k} \left[d^\dagger_\downarrow d_\uparrow \gamma_r c_{\mathbf{k}\downarrow} + n_{d\uparrow}\gamma_r c_{\mathbf{k}\uparrow} \right] - \sum_{\mathbf{k}} \frac{i\lambda_r V^*_{\mathbf{k}} e^{-i\delta\phi/2}}{\varepsilon_d-\varepsilon_k} \left[d^\dagger_\uparrow d_\downarrow c^\dagger_{\mathbf{k}\downarrow}\gamma_r + n_{d\uparrow} c^\dagger_{\mathbf{k}\uparrow}\gamma_r \right] \\
&-\sum_{\mathbf{k}} \frac{\lambda_l V^*_{\mathbf{k}}}{\varepsilon_d-\varepsilon_k} \left[d^\dagger_\downarrow d_\uparrow c^\dagger_{\mathbf{k}\uparrow}\gamma_l + n_{d\downarrow} c^\dagger_{\mathbf{k}\downarrow}\gamma_l \right] - \sum_{\mathbf{k}} \frac{\lambda_l V_{\mathbf{k}}}{\varepsilon_d-\varepsilon_k} \left[d^\dagger_\uparrow d_\downarrow \gamma_l c_{\mathbf{k}\uparrow} + n_{d\downarrow}\gamma_l c_{\mathbf{k}\downarrow} \right] \\
&+\frac{i\lambda_l\lambda_r}{\varepsilon_d} e^{-i\delta\phi/2} d^\dagger_\uparrow d_\downarrow \gamma_r\gamma_l - \frac{i\lambda_r\lambda_l}{\varepsilon_d} e^{i\delta\phi/2} d^\dagger_\downarrow d_\uparrow \gamma_l\gamma_r + \frac{\lambda_r^2}{\varepsilon_d} n_{d\uparrow} + \frac{\lambda_l^2}{\varepsilon_d} n_{d\downarrow}.
\end{aligned} \tag{3.17}$$

Likewise, for H_2 we have

$$\begin{aligned}
\sum_{\mathbf{k}\mathbf{k}',\sigma\sigma'} n_{d\bar{\sigma}} c^\dagger_{\mathbf{k}\sigma} d_\sigma n_{d\bar{\sigma}'} d^\dagger_{\sigma'} c_{\mathbf{k}'\sigma'} &= \sum_{\mathbf{k}\mathbf{k}'} (n_{d\downarrow} c^\dagger_{\mathbf{k}\uparrow} c_{\mathbf{k}'\uparrow} + n_{d\uparrow} c^\dagger_{\mathbf{k}\downarrow} c_{\mathbf{k}'\downarrow} + d_\uparrow d^\dagger_\downarrow c^\dagger_{\mathbf{k}\uparrow} c_{\mathbf{k}'\downarrow} + d_\downarrow d^\dagger_\uparrow c^\dagger_{\mathbf{k}\downarrow} c_{\mathbf{k}'\uparrow}), \\
\sum_{\mathbf{k}\sigma} n_{d\bar{\sigma}} c^\dagger_{\mathbf{k}\sigma} d_\sigma n_{d\downarrow} \gamma_r d^\dagger_\uparrow &= \sum_{\mathbf{k}} (c^\dagger_{\mathbf{k}\downarrow} d^\dagger_\uparrow d_\downarrow \gamma_r - c^\dagger_{\mathbf{k}\uparrow} n_{d\downarrow} \gamma_r), \\
\sum_{\mathbf{k}\sigma} n_{d\bar{\sigma}} c^\dagger_{\mathbf{k}\sigma} d_\sigma n_{d\uparrow} \gamma_l d^\dagger_\downarrow &= \sum_{\mathbf{k}} (c^\dagger_{\mathbf{k}\uparrow} d^\dagger_\downarrow d_\uparrow \gamma_l - c^\dagger_{\mathbf{k}\downarrow} n_{d\uparrow} \gamma_l), \\
\sum_{\mathbf{k}\sigma} n_{d\downarrow} d_\uparrow \gamma_r n_{d\bar{\sigma}} d^\dagger_\sigma c_{\mathbf{k}\sigma} &= \sum_{\mathbf{k}} (d^\dagger_\downarrow d_\uparrow \gamma_r c_{\mathbf{k}\downarrow} - n_{d\downarrow} \gamma_r c_{\mathbf{k}\uparrow}), \\
\sum_{\mathbf{k}\sigma} n_{d\uparrow} d_\downarrow \gamma_l n_{d\bar{\sigma}} d^\dagger_\sigma c_{\mathbf{k}\sigma} &= \sum_{\mathbf{k}} (d^\dagger_\uparrow d_\downarrow \gamma_l c_{\mathbf{k}\uparrow} - n_{d\uparrow} \gamma_l c_{\mathbf{k}\downarrow}).
\end{aligned}$$

Using the operator identities

$$\begin{aligned}
n_{d\downarrow} d_\uparrow \gamma_r n_{d\downarrow} \gamma_r d^\dagger_\uparrow &= n_{d\downarrow}, \\
n_{d\uparrow} d_\downarrow \gamma_l n_{d\uparrow} \gamma_l d^\dagger_\downarrow &= n_{d\uparrow}, \\
n_{d\downarrow} d_\uparrow \gamma_r n_{d\uparrow} \gamma_l d^\dagger_\downarrow &= d_\uparrow d^\dagger_\downarrow \gamma_r \gamma_l, \\
n_{d\uparrow} d_\downarrow \gamma_l n_{d\downarrow} \gamma_r d^\dagger_\uparrow &= d_\downarrow d^\dagger_\uparrow \gamma_l \gamma_r.
\end{aligned}$$

We can obtain

$$\begin{aligned}
H_2 = & -\sum_{\mathbf{k}\mathbf{k}'} \frac{V_{\mathbf{k}} V_{\mathbf{k}'}}{\varepsilon_d + U - \varepsilon_k} (n_{d\downarrow} c^\dagger_{\mathbf{k}\uparrow} c_{\mathbf{k}'\uparrow} + n_{d\uparrow} c^\dagger_{\mathbf{k}\downarrow} c_{\mathbf{k}'\downarrow} + d_\uparrow d^\dagger_\downarrow c^\dagger_{\mathbf{k}\uparrow} c_{\mathbf{k}'\downarrow} + d_\downarrow d^\dagger_\uparrow c^\dagger_{\mathbf{k}\downarrow} c_{\mathbf{k}'\uparrow}) \\
& + \sum_{\mathbf{k}} \frac{i\lambda_r V^*_{\mathbf{k}}}{\varepsilon_d + U - \varepsilon_k} e^{-i\delta\phi/2} (c^\dagger_{\mathbf{k}\downarrow} d^\dagger_\uparrow d_\downarrow \gamma_r - c^\dagger_{\mathbf{k}\uparrow} n_{d\downarrow} \gamma_r) + \sum_{\mathbf{k}} \frac{\lambda_l V^*_{\mathbf{k}}}{\varepsilon_d + U - \varepsilon_k} (c^\dagger_{\mathbf{k}\uparrow} d^\dagger_\downarrow d_\uparrow \gamma_l - c^\dagger_{\mathbf{k}\downarrow} n_{d\uparrow} \gamma_l) \\
& - \sum_{\mathbf{k}} \frac{i\lambda_r V_{\mathbf{k}}}{\varepsilon_d + U - \varepsilon_k} e^{i\delta\phi/2} (d^\dagger_\downarrow d_\uparrow \gamma_r c_{\mathbf{k}\downarrow} - n_{d\downarrow} \gamma_r c_{\mathbf{k}\uparrow}) + \sum_{\mathbf{k}} \frac{\lambda_l V_{\mathbf{k}}}{\varepsilon_d + U - \varepsilon_k} (d^\dagger_\uparrow d_\downarrow \gamma_l c_{\mathbf{k}\uparrow} - n_{d\uparrow} \gamma_l c_{\mathbf{k}\downarrow}) \\
& + \frac{i\lambda_l \lambda_r}{\varepsilon_d + U} e^{i\delta\phi/2} d_\uparrow d^\dagger_\downarrow \gamma_r \gamma_l - \frac{i\lambda_r \lambda_l}{\varepsilon_d + U} e^{-i\delta\phi/2} d_\downarrow d^\dagger_\uparrow \gamma_l \gamma_r - \frac{\lambda_r^2}{\varepsilon_d + U} n_{d\downarrow} - \frac{\lambda_l^2}{\varepsilon_d + U} n_{d\uparrow}. \qquad (3.18)
\end{aligned}$$

Now, it is very useful to rearrange the operators as

$$\begin{aligned}
n_{d\uparrow} c_{\mathbf{k}\uparrow} c^\dagger_{\mathbf{k}'\uparrow} + n_{d\downarrow} c_{\mathbf{k}\downarrow} c^\dagger_{\mathbf{k}'\downarrow} &= S_z (c_{\mathbf{k}\uparrow} c^\dagger_{\mathbf{k}'\uparrow} - c_{\mathbf{k}\downarrow} c^\dagger_{\mathbf{k}'\downarrow}) + \frac{1}{2} (n_{d\uparrow} + n_{d\downarrow}) (c_{\mathbf{k}\uparrow} c^\dagger_{\mathbf{k}'\uparrow} + c_{\mathbf{k}\downarrow} c^\dagger_{\mathbf{k}'\downarrow}) \\
n_{d\downarrow} c^\dagger_{\mathbf{k}'\uparrow} c_{\mathbf{k}\uparrow} + n_{d\uparrow} c^\dagger_{\mathbf{k}'\downarrow} c_{\mathbf{k}\downarrow} &= -S_z (c^\dagger_{\mathbf{k}'\uparrow} c_{\mathbf{k}\uparrow} - c^\dagger_{\mathbf{k}'\downarrow} c_{\mathbf{k}\downarrow}) + \frac{1}{2} (n_{d\uparrow} + n_{d\downarrow}) (c_{\mathbf{k}\uparrow} c^\dagger_{\mathbf{k}'\uparrow} + c_{\mathbf{k}\downarrow} c^\dagger_{\mathbf{k}'\downarrow}),
\end{aligned}$$

where $S_z = (n_{d\uparrow} - n_{d\downarrow})/2$. Putting together the two contributions H_1 and H_2 as $H_{\text{eff}} = H_1 + H_2$, we finally obtain

$$H_{\text{eff}} = H_0 + H_{\text{K}} + H_{\gamma_r} + H_{\gamma_l} + H_{\gamma_l r} + H_{\lambda_r^2} + H_{\lambda_l^2}. \qquad (3.19)$$

The explicit form of these terms are

$$H_0 = \sum_{\mathbf{k}\sigma} \varepsilon_{\mathbf{k}\sigma} c^\dagger_{\mathbf{k}\sigma} c_{\mathbf{k}\sigma}, \qquad (3.20)$$

$$H_{\text{K}} = \sum_{\mathbf{k}\mathbf{k}'} J_{\mathbf{k}\mathbf{k}'} [S_z (c^\dagger_{\mathbf{k}'\uparrow} c_{\mathbf{k}\uparrow} - c^\dagger_{\mathbf{k}'\downarrow} c_{\mathbf{k}\downarrow}) + S_+ c^\dagger_{\mathbf{k}'\downarrow} c_{\mathbf{k}\uparrow} + S_- c^\dagger_{\mathbf{k}'\uparrow} c_{\mathbf{k}\downarrow}], \qquad (3.21)$$

$$H_{\gamma_r} = \sum_{\mathbf{k}} (\Upsilon_{r\mathbf{k}} S_- \gamma_r c_{\mathbf{k}\downarrow} + \Upsilon^*_{r\mathbf{k}} S_+ c^\dagger_{\mathbf{k}\downarrow} \gamma_r) - \sum_{\mathbf{k}} (\hat{T}_{r\mathbf{k}} \gamma_r c_{\mathbf{k}\uparrow} + \hat{T}^*_{r\mathbf{k}} c^\dagger_{\mathbf{k}\uparrow} \gamma_r), \tag{3.22}$$

$$H_{\gamma_l} = \sum_{\mathbf{k}} (\Upsilon_{l\mathbf{k}} S_+ \gamma_l c_{\mathbf{k}\uparrow} + \Upsilon^*_{l\mathbf{k}} S_- c^\dagger_{\mathbf{k}\uparrow} \gamma_l) - \sum_{\mathbf{k}} (\hat{T}_{l\mathbf{k}} \gamma_l c_{\mathbf{k}\downarrow} + \hat{T}^*_{l\mathbf{k}} c^\dagger_{\mathbf{k}\downarrow} \gamma_l), \tag{3.23}$$

$$H_{\gamma_{lr}} = \Upsilon_{lr} S_- \gamma_l \gamma_r + \Upsilon^*_{lr} S_+ \gamma_r \gamma_l, \tag{3.24}$$

$$H_{\lambda_r^2} = \lambda_r^2 \left(\frac{n_{d\uparrow}}{\varepsilon_d} - \frac{n_{d\downarrow}}{\varepsilon_d + U} \right), \tag{3.25}$$

and

$$H_{\lambda_l^2} = \lambda_l^2 \left(\frac{n_{d\downarrow}}{\varepsilon_d} - \frac{n_{d\uparrow}}{\varepsilon_d + U} \right). \tag{3.26}$$

In the above we have used the relations $S_z = (n_{d\uparrow} - n_{d\downarrow})/2$, $S_+ = d^\dagger_\uparrow d_\downarrow$ and $S_- = d^\dagger_\downarrow d_\uparrow$. The effective couplings are given by

$$J_{\mathbf{k}\mathbf{k}'} = V_{\mathbf{k}} V^*_{\mathbf{k}'} \left(\frac{1}{\varepsilon_{\mathbf{k}} - \varepsilon_d} + \frac{1}{\varepsilon_d + U - \varepsilon_{\mathbf{k}'}} \right), \tag{3.27}$$

$$\Upsilon_{r\mathbf{k}} = -\lambda_r V_{\mathbf{k}} \left(\frac{1}{\varepsilon_{\mathbf{k}} - \varepsilon_d} + \frac{1}{\varepsilon_d + U - \varepsilon_{\mathbf{k}}} \right) e^{i\theta}, \tag{3.28}$$

$$\hat{T}_{r\mathbf{k}} = -\lambda_r V_{\mathbf{k}} \left(\frac{n_{d\uparrow}}{\varepsilon_d - \varepsilon_{\mathbf{k}}} + \frac{n_{d\downarrow}}{\varepsilon_d + U - \varepsilon_{\mathbf{k}}} \right) e^{i\theta}, \tag{3.29}$$

$$\Upsilon_{l\mathbf{k}} = \lambda_l V_{\mathbf{k}} \left(\frac{1}{\varepsilon_{\mathbf{k}} - \varepsilon_d} + \frac{1}{\varepsilon_d + U - \varepsilon_{\mathbf{k}}} \right), \tag{3.30}$$

$$\hat{T}_{l\mathbf{k}} = \lambda_r V_{\mathbf{k}} \left(\frac{n_{d\downarrow}}{\varepsilon_d - \varepsilon_{\mathbf{k}}} + \frac{n_{d\uparrow}}{\varepsilon_d + U - \varepsilon_{\mathbf{k}}} \right) \tag{3.31}$$

and

$$\Upsilon_{lr} = \lambda_r \lambda_l e^{i\theta} \left(\frac{1}{U + \varepsilon_d} - \frac{1}{\varepsilon_d} \right), \tag{3.32}$$

with $\theta = \delta\phi/2 + \pi/2$. Now, assuming that the QD coupling with the metallic leads is isotropic (therefore, $\mathbf{k}$-independent), we have $V_{\mathbf{k}} = V$. Moreover, for scattering processes near to the Fermi surface, $\varepsilon_{\mathbf{k}} = \varepsilon_{\mathbf{k}'} \approx 0$. Thus, we obtain

$$J = |V|^2 \left(\frac{1}{\varepsilon_d + U} - \frac{1}{\varepsilon_d} \right), \tag{3.33}$$

$$\Upsilon_r = -\lambda_r V \left(\frac{1}{\varepsilon_d + U} - \frac{1}{\varepsilon_d} \right) e^{i\theta}, \tag{3.34}$$

$$\hat{T}_r = -\lambda_r V \left(\frac{n_{d\uparrow}}{\varepsilon_d} + \frac{n_{d\downarrow}}{\varepsilon_d + U} \right) e^{i\theta}, \tag{3.35}$$

$$\Upsilon_l = \lambda_l V \left(\frac{1}{\varepsilon_d + U} - \frac{1}{\varepsilon_d} \right), \tag{3.36}$$

$$\hat{T}_l = \lambda_r V \left(\frac{n_{d\downarrow}}{\varepsilon_d} + \frac{n_{d\uparrow}}{\varepsilon_d + U} \right). \tag{3.37}$$

We need to be careful about the couplings $\hat{T}_{r,l}$ because, unlike the other couplings that are c-numbers, they are operators. Let us look for these couplings near to the particle-hole symmetry point. For this, we choose the quantum dot level as $\varepsilon_d = -U/2 + \delta\varepsilon$, with $\delta\varepsilon \ll U/2$. Then

$$\begin{aligned}
\hat{T}_r &= -\lambda_r V \left(\frac{n_{d\uparrow}}{\varepsilon_d} + \frac{n_{d\downarrow}}{U + \varepsilon_d} \right) e^{i\theta} \\
&= -\lambda_r V \left[n_{d\uparrow} (\delta\varepsilon - U/2)^{-1} + n_{d\downarrow} (\delta\varepsilon + U/2)^{-1} \right] e^{i\theta} \\
&= -\lambda_r V \left[-2\frac{n_{d\uparrow}}{U} \left(1 - \frac{2\delta\varepsilon}{U} \right)^{-1} + 2\frac{n_{d\downarrow}}{U} \left(1 + \frac{2\delta\varepsilon}{U} \right)^{-1} \right] e^{i\theta}.
\end{aligned}$$

Now, using $(1-x)^{-1} \approx 1 + x$, and $(1+x)^{-1} \approx 1 - x$, for $x << 1$, in our case $x = 2\delta\varepsilon/U$, so we have

$$\begin{aligned}
\hat{T}_r &= -\lambda_r V \left[-2\frac{n_{d\uparrow}}{U} \left(1 + \frac{2\delta\varepsilon}{U} \right) + 2\frac{n_{d\downarrow}}{U} \left(1 - \frac{2\delta\varepsilon}{U} \right) \right] e^{i\theta} \\
&= -\lambda_r V \left[-\frac{4}{U}\frac{1}{2}(n_{d\uparrow} - n_{d\downarrow}) - \frac{4\delta\varepsilon}{U^2}(n_{d\uparrow} + n_{d\downarrow}) \right] e^{i\theta} \\
&= -\lambda_r V \left[-\frac{4}{U} S_z - \frac{4\delta\varepsilon}{U^2} \right] e^{i\theta},
\end{aligned}$$

in the last line we use the relations $S_z = (n_{d\uparrow} - n_{d\downarrow})/2$ and $n_{d\uparrow} + n_{d\downarrow} = 1$. With the expression above we can write

$$\begin{aligned}
\sum_{\mathbf{k}} (\hat{T}_r \gamma_r c_{\mathbf{k}\uparrow} + \hat{T}_r^* c_{\mathbf{k}\uparrow}^\dagger \gamma_r) &= \sum_{\mathbf{k}} (T_r \gamma_r c_{\mathbf{k}\uparrow} + T_r^* c_{\mathbf{k}\uparrow}^\dagger \gamma_r) \\
&\quad - \sum_{\mathbf{k}} (T_{rz} S_z \gamma_r c_{\mathbf{k}\uparrow} + T_{rz}^* S_z c_{\mathbf{k}\uparrow}^\dagger \gamma_r), \\
&\equiv H_{T_r} + H_{T_{rz}}
\end{aligned} \tag{3.38}$$

and we define

$$T_r = \frac{4\delta\varepsilon}{U^2} \lambda_r V e^{i\theta}, \quad T_{rz} = -\frac{4}{U} \lambda_r V e^{i\theta}. \tag{3.39}$$

Similarly, we find

$$\hat{T}_l = \lambda_l V \left[\frac{4}{U} S_z - \frac{4\delta\varepsilon}{U^2} \right], \tag{3.40}$$

and

$$\begin{aligned}
\sum_{\mathbf{k}} (\hat{T}_l \gamma_r c_{\mathbf{k}\downarrow} + \hat{T}_l^* c_{\mathbf{k}\downarrow}^\dagger \gamma_l) &= \sum_{\mathbf{k}} (T_l \gamma_l c_{\mathbf{k}\downarrow} + T_l^* c_{\mathbf{k}\downarrow}^\dagger \gamma_l) \\
&\quad + \sum_{\mathbf{k}} (T_{lz} S_z \gamma_l c_{\mathbf{k}\downarrow} + T_{lz}^* S_z c_{\mathbf{k}\downarrow}^\dagger \gamma_l), \\
&\equiv H_{T_l} + H_{T_{lz}}
\end{aligned} \tag{3.41}$$

with

$$T_l = -\frac{4\delta\varepsilon}{U^2}\lambda_l V, \quad T_{lz} = \frac{4}{U}\lambda_l V. \tag{3.42}$$

3.3.2 Physical interpretation of the effective Hamiltonian

Let us look individually at each term of the effective Hamiltonian (3.19). The first term of (3.19)

$$H_{\mathrm{K}} = \sum_{\mathbf{k}\mathbf{k}'} J_{\mathbf{k}\mathbf{k}'}[S_z(c^\dagger_{\mathbf{k}'\uparrow}c_{\mathbf{k}\uparrow} - c^\dagger_{\mathbf{k}'\downarrow}c_{\mathbf{k}\downarrow}) + S_+c^\dagger_{\mathbf{k}'\downarrow}c_{\mathbf{k}\uparrow} + S_-c^\dagger_{\mathbf{k}'\uparrow}c_{\mathbf{k}\downarrow}]$$

is the usual Kondo Hamiltonian, and describes the magnetic interaction between the QD magnetic momentum and the spin of the conduction electrons of the metallic leads. The terms in (3.19)

$$H_{\gamma_r} = \sum_{\mathbf{k}}(\Upsilon_{r\mathbf{k}}S_-\gamma_r c_{\mathbf{k}\downarrow} + \Upsilon^*_{r\mathbf{k}}S_+c^\dagger_{\mathbf{k}\downarrow}\gamma_r) - \sum_{\mathbf{k}}(\hat{T}_{r\mathbf{k}}\gamma_r c_{\mathbf{k}\uparrow} + \hat{T}^*_{r\mathbf{k}}c^\dagger_{\mathbf{k}\uparrow}\gamma_r),$$

and

$$H_{\gamma_l} = \sum_{\mathbf{k}}(\Upsilon_{l\mathbf{k}}S_+\gamma_l c_{\mathbf{k}\uparrow} + \Upsilon^*_{l\mathbf{k}}S_-c^\dagger_{\mathbf{k}\uparrow}\gamma_l) - \sum_{\mathbf{k}}(\hat{T}_{l\mathbf{k}}\gamma_l c_{\mathbf{k}\downarrow} + \hat{T}^*_{l\mathbf{k}}c^\dagger_{\mathbf{k}\downarrow}\gamma_l)$$

are similar between them. The first term in the two Hamiltonians above are associated with a spin dynamic process which spin-flips the electron spin in the quantum dot (lead) mediated by the Majorana zero mode, which is polarized and carries a defined spin index, $\gamma_{\uparrow r}(\gamma_{\downarrow l}) \equiv \gamma_r(\gamma_l)$, see figure 10. The second ones are associated with interactions between the quantum dot electron and the conduction electrons in the metallic lead mediated by the Majorana zero mode, but without spin dynamics, see Eqs. (3.38)-(3.41), such process we will call "Majorana triple exchange interaction". The next term of the effective Hamiltonian (3.19) to be analyzed is

$$H_{\gamma_{lr}} = \Upsilon_{lr}S_-\gamma_l\gamma_r + \Upsilon^*_{lr}S_+\gamma_r\gamma_l.$$

This piece of the effective Hamiltonian describes a kind of exchange interaction between the Majorana zero modes and the quantum dot spin associated with the formation of a local singlet. [1] A more complete analysis of this process is given in the sections 3.3.5 and 3.4. The two last terms in (3.19) are

$$H_{\lambda_r^2} = \lambda_r^2\left(\frac{n_{d\uparrow}}{\varepsilon_d} - \frac{n_{d\downarrow}}{\varepsilon_d + U}\right),$$

and

$$H_{\lambda_l^2} = \lambda_l^2\left(\frac{n_{d\downarrow}}{\varepsilon_d} - \frac{n_{d\uparrow}}{\varepsilon_d + U}\right).$$

[1] In the present case the number of Majorana zero modes coupled to the system is $M = 2$, when we have $M \geq 3$ the Majorana bilinears $i\gamma_i\gamma_j$ reproduces the $SO_2(M)$ structure and the exchange interaction between the quantum dot (or a quantum island) and the Majorana modes can give rises to a "*topological Kondo effect*" (BÉRI; COOPER, 2012; ALTLAND et al., 2014).

These terms can be better understood near the particle-hole symmetry point. In this case we can write $\varepsilon_d = -U/2 + \delta\varepsilon$ and perform the same approximations used to obtain $T_{r(l)}(T_{rz(lz)})$ in the previous section. A direct calculation leads to

$$\begin{aligned} H_{\lambda_r^2} &\approx \lambda_r^2\left(-\frac{2}{U} - \frac{8\delta\varepsilon}{U^2}S_z\right), \\ H_{\lambda_l^2} &\approx \lambda_l^2\left(-\frac{2}{U} + \frac{8\delta\varepsilon}{U^2}S_z\right). \end{aligned}$$

From the equations above we can see that the terms $H_{\lambda_r^2}$ and $H_{\lambda_l^2}$ are responsible for the effective Zeeman fields $B^r_{\text{eff}} = -8\lambda_r^2\delta\varepsilon/U^2$ and $B^l_{\text{eff}} = 8\lambda_l^2\delta\varepsilon/U^2$, respectively. Then $|B^r_{\text{eff}}| = -|B^l_{\text{eff}}|$ which is a consequence of the opposite polarizations of the Majorana zero modes.

3.3.3 The non-interacting limit of the effective Kondo-Majorana Hamiltonian

In the non-interacting limit ($U = 0$) we have, from (3.19), (3.33)-(3.37), $J = \Upsilon_{lr} = \Upsilon_r = \Upsilon_l = 0$ and the effective Kondo-Majorana Hamiltonian becomes

$$\begin{aligned} H_{\text{eff}} &= \sum_{\mathbf{k}\sigma}\varepsilon_{\mathbf{k}\sigma}c^\dagger_{\mathbf{k}\sigma}c_{\mathbf{k}\sigma} + \sum_{\mathbf{k}}(T_r\gamma_r c_{\mathbf{k}\uparrow} + T_r^* c^\dagger_{\mathbf{k}\uparrow}\gamma_r) \\ &\quad + \sum_{\mathbf{k}}(T_l\gamma_l c_{\mathbf{k}\downarrow} + T_l^* c^\dagger_{\mathbf{k}\downarrow}\gamma_l), \end{aligned} \tag{3.43}$$

with

$$T_r = 2\lambda_r\left(\frac{V}{\varepsilon_d}\right)e^{i\theta}, \quad T_r = -2\lambda_l\left(\frac{V}{\varepsilon_d}\right). \tag{3.44}$$

Notice that the effective Hamiltonian (3.43) has the same form of the Hamiltonian (C.1). The main difference is that now we have an additional degree of freedom associated with the spin. As we have seen before, the connection between the regular fermions and the Majorana Fermions can be describe as

$$f_\uparrow = \frac{1}{\sqrt{2}}(\gamma_{1r} + i\gamma_{2r}), \qquad f_\downarrow = \frac{1}{\sqrt{2}}(\gamma_{1l} + i\gamma_{2l}). \tag{3.45}$$

The number of free MZMs is determined by the couplings T_r and T_l. Let us look at each possible configurations and their respective residual entropies.

3.3.3.1 $T_r = T_l = 0$

When $T_r = T_l = 0$, from Eqs. (3.43) and (3.45) we see four free Majorana modes and, as shown in Appendix C each free Majorana mode contributes to the density of states with $\delta(\omega)/2$. As a result,

$$\rho_f(\omega) = 2\delta(\omega), \tag{3.46}$$

rendering the entropy

$$S_f(T) = 2k_{\text{B}}\ln(2) = S_{\text{res}}. \tag{3.47}$$

3.3.3.2 $T_r \neq 0$ or $T_l \neq 0$

In this situation, we have three free Majorana modes and one coupled to the metallic lead which results in the density of states

$$\rho_f(\omega) = \frac{3}{2}\delta(\omega) + \frac{1}{2\pi}\frac{\Gamma}{\omega^2 + \Gamma^2}. \tag{3.48}$$

Using the results from Sec. C we obtain the following entropy

$$S_f(T) \approx \frac{3k_\mathrm{B}}{2}\ln(2) + \frac{\mathrm{k_B}}{2}\frac{\pi}{6}\left(\frac{\mathrm{k_B T}}{\Gamma}\right). \tag{3.49}$$

At zero temperature the residual entropy

$$S_\mathrm{res} = \frac{3k_\mathrm{B}}{2}\ln(2), \tag{3.50}$$

from which the NFL behavior of the system is explicit.

3.3.3.3 $T_r \neq 0$ and $T_l \neq 0$

This is the last possible situation. We now have two free Majorana modes and two coupled Majorana modes, which provides us with the density of states

$$\rho_f = \delta(\omega) + \frac{1}{\pi}\frac{\Gamma}{\omega^2 + \Gamma^2}, \tag{3.51}$$

and entropy

$$S_f(T) \approx k_\mathrm{B}\ln(2) + \mathrm{k_B}\frac{\pi}{6}\left(\frac{\mathrm{k_B T}}{\Gamma}\right). \tag{3.52}$$

For $T = 0$ we then obtain

$$S_\mathrm{res} = k_\mathrm{B}\ln(2). \tag{3.53}$$

In summary, the residual entropy in the three cases can be written as

$$S_\mathrm{res} = \begin{cases} 2k_\mathrm{B}\ln(2), & \text{if } T_r = T_l = 0. \\ \frac{3}{2}k_\mathrm{B}\ln(2), & \text{if } T_r \neq 0 \quad \text{or} \quad T_r \neq 0. \\ k_\mathrm{B}\ln(2), & \text{if } T_r \neq 0 \quad \text{and} \quad T_l \neq 0. \end{cases} \tag{3.54}$$

It can be observed that the results in (3.54) corroborate the results obtained by NRG shown in figure 12. Moreover, in general the residual entropy can be associated to the number of free Majorana modes (N_0) of the system as

$$S_\mathrm{res} = \frac{N_0}{2}k_\mathrm{B}\ln(2). \tag{3.55}$$

3.3.4 Renormalization Group equations

Since the effective Hamiltonian (3.19) obtained in the previous section has a Kondo-like structure we can apply the Renormalization group (RG) ideas to study the behavior of the effective couplings. Here we will perform a poor man's scaling on the effective Kondo-Majorana Hamiltonian (for details of the method see section 2.3). In the RG procedure, the conduction bandwidth is reduced from D to $D-\delta D$ and the high-energy states at the edges of the conduction band are integrate out which leads to the renormalized interaction Hamiltonian (up to second order)

$$V \to V + \Delta V^{(2)}, \qquad \Delta V^{(2)} = VP(\omega - H_0)^{-1}V, \tag{3.56}$$

where the operator P selects the states which will be integrate out in the range $[D, D-|\delta D|]$ for electron-like process, and $[-D, -D+|\delta D|]$ for hole-like process. In our case

$$V = H_K + H_{\gamma_r} + H_{\gamma_l} + H_{\gamma_{lr}} + H_{\lambda_r^2} + H_{\lambda_l^2}. \tag{3.57}$$

The explicit form of the components of (3.56) is[2]

$$\Delta V^{(2)e}_{\mathbf{kk'}} = \sum_{\mathbf{q}}^{D-|\delta D|<\varepsilon_q<D} V_{\mathbf{k'q}}(\omega - H_0)^{-1}V_{\mathbf{qk}} \quad \text{(electron-like process)}, \tag{3.58}$$

$$\Delta V^{(2)h}_{\mathbf{kk'}} = \sum_{\mathbf{q}}^{-D<\varepsilon_q<-D+|\delta D|} V_{\mathbf{qk'}}(\omega - H_0)^{-1}V_{\mathbf{kq}} \quad \text{(hole-like process)}. \tag{3.59}$$

Obviously, the total contribution is

$$\Delta V^{(2)}_{\mathbf{kk'}} = \Delta V^{(2)e}_{\mathbf{kk'}} + \Delta V^{(2)h}_{\mathbf{kk'}}. \tag{3.60}$$

From (3.57) and (3.56) the RG correction ($\Delta V^{(2)}$) is

$$\begin{aligned} \Delta V^{(2)} &= [H_K + H_{\gamma_r} + H_{\gamma_l} + H_{\gamma_{lr}} + H_{\lambda_r^2} + H_{\lambda_l^2}] \\ &\quad \times P(\omega - H_0)^{-1}[H_K + H_{\gamma_r} + H_{\gamma_l} + H_{\gamma_{lr}} + H_{\lambda_r^2} + H_{\lambda_l^2}]. \end{aligned} \tag{3.61}$$

To perform the spin operator products contained in the renormalized interaction, the following relations are useful

$$S_zS_+ = \frac{S_+}{2}, \qquad S_+S_z = -\frac{S_+}{2}, \tag{3.62}$$

$$S_zS_- = -\frac{S_-}{2}, \qquad S_-S_z = \frac{S_-}{2}, \tag{3.63}$$

$$S_+S_- = \frac{1}{2} + S_z, \qquad S_-S_+ = \frac{1}{2} - S_z. \tag{3.64}$$

[2] Notice that the projector operator P already has selected the states which will be integrate out.

The calculation of the renormalized interaction is lengthy, but straightforward. Let us look carefully at one of the products which arise in $\Delta V^{(2)}$ (3.61). For example, let us take the product of H_{Υ_r} with H_K in (3.61). From (3.58) for an electron-like process we have

$$
\begin{aligned}
H_{\Upsilon_r} \times H_K \xrightarrow[\text{process}]{\text{electron-like}} & \\
& \sum_{\mathbf{q}}^{D-|\delta D|<\varepsilon_q<D} (\Upsilon_r S_- \gamma_r c_{\mathbf{q}\downarrow} + \Upsilon_r^* S_+ c_{\mathbf{q}\downarrow}^\dagger \gamma_r)(\omega - H_0)^{-1} \\
& \quad \times J[S_z(c_{\mathbf{q}\uparrow}^\dagger c_{\mathbf{k}\uparrow} - c_{\mathbf{q}\downarrow}^\dagger c_{\mathbf{k}\downarrow}) + S_+ c_{\mathbf{q}\downarrow}^\dagger c_{\mathbf{k}\uparrow} + S_- c_{\mathbf{q}\uparrow}^\dagger c_{\mathbf{k}\downarrow}] \\
= & \sum_{\mathbf{q}}^{D-|\delta D|<\varepsilon_q<D} \{-J\Upsilon_r(S_- S_z)[\gamma_r c_{\mathbf{q}\downarrow}(\omega - H_0)^{-1} c_{\mathbf{q}\downarrow}^\dagger c_{\mathbf{k}\downarrow}] \\
& \quad + J\Upsilon_r(S_- S_+)[\gamma_r c_{\mathbf{q}\downarrow}(\omega - H_0)^{-1} c_{\mathbf{q}\downarrow}^\dagger c_{\mathbf{k}\uparrow}]\} \\
= & \sum_{\mathbf{q}}^{D-|\delta D|<\varepsilon_q<D} \{-J\Upsilon_r(S_- S_z)[(\omega - \varepsilon_q - H_0)^{-1} \gamma_r c_{\mathbf{q}\downarrow} c_{\mathbf{q}\downarrow}^\dagger c_{\mathbf{k}\downarrow}] \\
& \quad + J\Upsilon_r(S_- S_+)[(\omega - \varepsilon_q - H_0)^{-1} \gamma_r c_{\mathbf{q}\downarrow} c_{\mathbf{q}\downarrow}^\dagger c_{\mathbf{k}\uparrow}]\}.
\end{aligned}
$$

In the last line it was used $c_{\mathbf{k}\downarrow}\gamma_r(E - H_0)^{-1} = (\omega - \varepsilon_q - H_0)^{-1} c_{\mathbf{k}\downarrow}\gamma_r$. The energy ε_q is closer to the energy at the top of the conduction band , so $\varepsilon_q \approx D$ and $c_{\mathbf{q}\sigma} c_{\mathbf{q}\sigma}^\dagger = (1 - n_{\mathbf{q}\sigma}) \approx 1$, since the states at the top of the conduction band are empty[3], using these facts we obtain

$$
\begin{aligned}
& \sum_{\mathbf{q}}^{D-|\delta D|<\varepsilon_q<D} \{-J\Upsilon_r(S_- S_z)[(\omega - \varepsilon_q - H_0)^{-1} \gamma_r c_{\mathbf{q}\downarrow} c_{\mathbf{q}\downarrow}^\dagger c_{\mathbf{k}\downarrow}] \\
& \quad + J\Upsilon_r(S_- S_+)[(\omega - \varepsilon_q - H_0)^{-1} \gamma_r c_{\mathbf{q}\downarrow} c_{\mathbf{q}\downarrow}^\dagger c_{\mathbf{k}\uparrow}]\} \\
= & \sum_{\mathbf{q}}^{D-|\delta D|<\varepsilon_q<D} [-J\Upsilon_r \left(\frac{S_-}{2}\right) \gamma_r c_{\mathbf{k}\downarrow}(\omega - D)^{-1} + J\Upsilon_r \left(\frac{1}{2} - S_z\right) \gamma_r c_{\mathbf{k}\uparrow}(\omega - D)^{-1}].
\end{aligned}
$$

In the above we use the relations (3.62) and $H_0 = 0$ as the ground-state energy referential. The summation in energy can be replaced by an integral as

$$
\sum_{\mathbf{q}}^{D-|\delta D|<\varepsilon_q<D} \to \int_{D-|\delta D|}^{D} \rho(\varepsilon) d\varepsilon,
$$

where $\rho(\varepsilon)$ is the density of states (DOS) of the conduction electrons. In the present case

[3] All the calculations is this section are done at $T = 0$.

$\rho(\varepsilon)=\rho$ is constant. Finally,

$$
\begin{aligned}
H_{\Upsilon_r}\times H_K \xrightarrow[\text{process}]{\text{electron-like}} & \\
&\sum_{\mathbf{q}}^{D-|\delta D|<\varepsilon_q<D}(\Upsilon_r S_-\gamma_r c_{\mathbf{q}\downarrow}+\Upsilon_r^* S_+ c_{\mathbf{q}\downarrow}^\dagger\gamma_r)(\omega-H_0)^{-1}\\
&\times J[S_z(c_{\mathbf{q}\uparrow}^\dagger c_{\mathbf{k}\uparrow}-c_{\mathbf{q}\downarrow}^\dagger c_{\mathbf{k}\downarrow})+S_+c_{\mathbf{q}\downarrow}^\dagger c_{\mathbf{k}\uparrow}+S_-c_{\mathbf{q}\uparrow}^\dagger c_{\mathbf{k}\downarrow}]\\
&=-\frac{\rho}{2}\frac{|\delta D|}{(\omega-D)}J\Upsilon_r S_-\gamma_r c_{\mathbf{k}\downarrow}-\rho\frac{|\delta D|}{(\omega-D)}J\Upsilon_r S_z\gamma_r c_{\mathbf{k}\uparrow}\\
&\quad+\frac{\rho}{2}\frac{|\delta D|}{(\omega-D)}J\Upsilon_r\gamma_r c_{\mathbf{k}\uparrow}.
\end{aligned}
\tag{3.65}
$$

For a hole-like process, using (3.59), we follow the same procedure

$$
\begin{aligned}
H_{\Upsilon_r}\times H_K \xrightarrow[\text{process}]{\text{hole-like}} & \\
&\sum_{\mathbf{q}}^{-D<\varepsilon_q<-D+|\delta D|}(\Upsilon_r S_-\gamma_r c_{\mathbf{q}\downarrow}+\Upsilon_r^* S_+ c_{\mathbf{q}\downarrow}^\dagger\gamma_r)(\omega-H_0)^{-1}\\
&\times J[S_z(c_{\mathbf{q}\uparrow}^\dagger c_{\mathbf{k}\uparrow}-c_{\mathbf{q}\downarrow}^\dagger c_{\mathbf{k}\downarrow})+S_+c_{\mathbf{q}\downarrow}^\dagger c_{\mathbf{k}\uparrow}+S_-c_{\mathbf{q}\uparrow}^\dagger c_{\mathbf{k}\downarrow}]\\
&=\sum_{\mathbf{q}}^{-D<\varepsilon_q<-D+|\delta D|}\{-J\Upsilon_r^*(S_+S_z)[c_{\mathbf{q}\downarrow}^\dagger\gamma_r(\omega-H_0)^{-1}c_{\mathbf{k}\downarrow}^\dagger c_{\mathbf{q}\downarrow}]\\
&\quad+J\Upsilon_r^*(S_+S_-)[c_{\mathbf{q}\downarrow}^\dagger\gamma_r(\omega-H_0)^{-1}c_{\mathbf{k}\uparrow}^\dagger c_{\mathbf{q}\downarrow}]\}\\
&=\sum_{\mathbf{q}}^{-D<\varepsilon_q<-D+|\delta D|}\{-J\Upsilon_r^*(S_+S_z)[(\omega+\varepsilon_q-H_0)^{-1}c_{\mathbf{q}\downarrow}^\dagger\gamma_r c_{\mathbf{k}\downarrow}^\dagger c_{\mathbf{q}\downarrow}]\\
&\quad+J\Upsilon_r^*(S_+S_-)[(\omega+\varepsilon_q-H_0)^{-1}c_{\mathbf{q}\downarrow}^\dagger\gamma_r c_{\mathbf{k}\uparrow}^\dagger c_{\mathbf{q}\downarrow}]\},
\end{aligned}
$$

where we use $c_{\mathbf{q}\downarrow}^\dagger\gamma_r(\omega-H_0)^{-1}=(\omega+\varepsilon_q-H_0)^{-1}c_{\mathbf{q}\downarrow}^\dagger\gamma_r$. For energies near the bottom of the conduction band we can take $\varepsilon_q\approx -D$ and $c_{\mathbf{q}\sigma}^\dagger c_{\mathbf{q}\sigma}=n_{\mathbf{q}\sigma}\approx 1$, since the energy levels close to the bottom are always filled. The energy summation in this case becomes

$$
\sum_{\mathbf{q}}^{-D<\varepsilon_q<-D+|\delta D|}\rightarrow\int_{-D}^{-D+|\delta D|}\rho d\varepsilon.
$$

Then, for a hole-like process

$$
\begin{aligned}
H_{\Upsilon_r}\times H_K \xrightarrow[\text{process}]{\text{hole-like}} & \\
&\sum_{\mathbf{q}}^{-D<\varepsilon_q<-D+|\delta D|}(\Upsilon_r S_-\gamma_r c_{\mathbf{q}\downarrow}+\Upsilon_r^* S_+ c_{\mathbf{q}\downarrow}^\dagger\gamma_r)(\omega-H_0)^{-1}\\
&\times J[S_z(c_{\mathbf{q}\uparrow}^\dagger c_{\mathbf{k}\uparrow}-c_{\mathbf{q}\downarrow}^\dagger c_{\mathbf{k}\downarrow})+S_+c_{\mathbf{q}\downarrow}^\dagger c_{\mathbf{k}\uparrow}+S_-c_{\mathbf{q}\uparrow}^\dagger c_{\mathbf{k}\downarrow}]\\
&=-\frac{\rho}{2}\frac{|\delta D|}{(\omega-D)}J\Upsilon_r^* S_+c_{\mathbf{k}\downarrow}^\dagger\gamma_r-\rho\frac{|\delta D|}{(\omega-D)}J\Upsilon_r^* S_z c_{\mathbf{k}\uparrow}^\dagger\gamma_r\\
&\quad+\frac{\rho}{2}\frac{|\delta D|}{(\omega-D)}J\Upsilon_r^* c_{\mathbf{k}\uparrow}^\dagger\gamma_r.
\end{aligned}
\tag{3.66}
$$

Thus the product $H_{\Upsilon_r} \times H_K$ in (3.61), using eqs.(3.65) and (3.66), leads to the renormalized Hamiltonians

$$\sum_{\ell\mathbf{k}}(\Upsilon_r S^- \gamma_r c_{\ell\mathbf{k}\downarrow} + \Upsilon_r^* S^+ c^\dagger_{\ell\mathbf{k}\downarrow}\gamma_r) \to \sum_{\ell\mathbf{k}}\left[\left(\Upsilon_r - \frac{\rho}{2}\frac{|\delta D|}{(\omega - D)} J\Upsilon_r\right) S^-\gamma_r c_{\ell\mathbf{k}\downarrow} + \left(\Upsilon_r^* - \frac{\rho}{2}\frac{|\delta D|}{(\omega - D)} J\Upsilon_r^*\right) S^+ c^\dagger_{\ell\mathbf{k}\downarrow}\gamma_r\right], \tag{3.67}$$

$$-\sum_{\ell\mathbf{k}}(T_r \gamma_r c_{\ell\mathbf{k}\uparrow} + T_r^* c^\dagger_{\ell\mathbf{k}\uparrow}\gamma_r) \to -\sum_{\ell\mathbf{k}}\left[\left(T_r - \frac{\rho}{2}\frac{|\delta D|}{(\omega - D)} J\Upsilon_r\right) \gamma_r c_{\ell\mathbf{k}\uparrow} + \left(T_r^* - \frac{\rho}{2}\frac{|\delta D|}{(\omega - D)} J\Upsilon_r^*\right) c^\dagger_{\ell\mathbf{k}\uparrow}\gamma_r\right], \tag{3.68}$$

$$\sum_{\mathbf{k}}(T_{rz} S_z \gamma_r c_{\ell\mathbf{k}\uparrow} + T_{rz}^* S_z c^\dagger_{\ell\mathbf{k}\uparrow}\gamma_r) \to \sum_{\mathbf{k}}\left[\left(T_{rz} - \rho\frac{|\delta D|}{(\omega - D)} J\Upsilon_r\right) S_z\gamma_r c_{\ell\mathbf{k}\uparrow} + \left(T_{rz}^* - \rho\frac{|\delta D|}{(\omega - D)} J\Upsilon_r^*\right) S_z c^\dagger_{\ell\mathbf{k}\uparrow}\gamma_r\right]. \tag{3.69}$$

The renormalization of the Hamiltonians is encoded in the coupling constant g as $g \to g+\delta g$. Then, from $H_{\Upsilon_r} \times H_K$ with the equation above we recognize

$$\Upsilon_r \to \Upsilon_r + [\delta\Upsilon_r]_{H_{\Upsilon_r}\times H_K}, \quad \text{with} \quad [\delta\Upsilon_r]_{H_{\Upsilon_r}\times H_K} = -\frac{\rho}{2}\frac{|\delta D|}{(\omega - D)}\Upsilon_r J \tag{3.70}$$

$$T_r \to T_r + [\delta T_r]_{H_{\Upsilon_r}\times H_K}, \quad \text{with} \quad [\delta T_r]_{H_{\Upsilon_r}\times H_K} = -\frac{\rho}{2}\frac{|\delta D|}{(\omega - D)}\Upsilon_r J, \tag{3.71}$$

$$T_{rz} \to T_{rz} + [\delta T_{rz}]_{H_{\Upsilon_r}\times H_K}, \quad \text{with} \quad [\delta T_{rz}]_{H_{\Upsilon_r}\times H_K} = -\rho\frac{|\delta D|}{(\omega - D)}\Upsilon_r J. \tag{3.72}$$

For the conjugated couplings we have the same set of equations

$$\Upsilon_r^* \to \Upsilon_r^* + [\delta\Upsilon_r^*]_{H_{\Upsilon_r}\times H_K}, \quad \text{with} \quad [\delta\Upsilon_r]_{H_{\Upsilon_r}\times H_K} = -\frac{\rho}{2}\frac{|\delta D|}{(\omega - D)}\Upsilon_r^* J \tag{3.73}$$

$$T_r^* \to T_r^* + [\delta T_r^*]_{H_{\Upsilon_r}\times H_K}, \quad \text{with} \quad [\delta T_r]_{H_{\Upsilon_r}\times H_K} = -\frac{\rho}{2}\frac{|\delta D|}{(\omega - D)}\Upsilon_r^* J, \tag{3.74}$$

$$T_{rz}^* \to T_{rz}^* + [\delta T_{rz}^*]_{H_{\Upsilon_r}\times H_K}, \quad \text{with} \quad [\delta T_{rz}]_{H_{\Upsilon_r}\times H_K} = -\rho\frac{|\delta D|}{(\omega - D)}\Upsilon_r^* J. \tag{3.75}$$

To compute the total renormalized interaction we need to perform all the products in (3.61). The operator algebra which appears in the other terms is quite similar to the one presented above for $H_{\Upsilon_r} \times H_K$. The contributions of each product are summarized bellow $H_{Tr} \times H_K$:

$$[\delta\Upsilon_r]_{H_{Tr}\times H_K} = -\rho\frac{|\delta D|}{(\omega - D)}T_r J, \qquad [\delta T_{rz}]_{H_{Tr}\times H_K} = -\rho\frac{|\delta D|}{(\omega - D)}T_r J, \tag{3.76}$$

$H_{Trz} \times H_K$:

$$[\delta\Upsilon_r]_{H_{Trz}\times H_K} = -\frac{\rho}{2}\frac{|\delta D|}{(\omega - D)}T_{rz} J, \qquad [\delta T_r]_{H_{Trz}\times H_K} = -\frac{\rho}{4}\frac{|\delta D|}{(\omega - D)}T_{rz} J. \tag{3.77}$$

The similar structure of H_{Υ_l}, H_{Tl} and H_{Tlz} with H_{Υ_l}, H_{Tl} and H_{Tlz} leads to the same set of equations for their respective renormalized couplings when the products $H_{\Upsilon_l} \times H_K$, $H_{Tl} \times H_K$ and $H_{Tlz} \times H_K$ are computed. The other products which contributes to the renormalized Hamiltonian are

$H_{\Upsilon_r} \times H_{Tl}$:

$$[\delta\Upsilon_{lr}]_{H_{\Upsilon_r} \times H_{Tl}} = -\rho \frac{|\delta D|}{(\omega - D)} \Upsilon_r T_l, \tag{3.78}$$

$H_{\Upsilon_r} \times H_{Tlz}$:

$$[\delta\Upsilon_{lr}]_{H_{\Upsilon_r} \times H_{Tlz}} = -\frac{\rho}{2} \frac{|\delta D|}{(\omega - D)} \Upsilon_r T_{lz}, \tag{3.79}$$

$H_{Tr} \times H_{\Upsilon_l}$:

$$[\delta\Upsilon_{lr}]_{H_{Tr} \times H_{\Upsilon_l}} = -\rho \frac{|\delta D|}{(\omega - D)} T_r \Upsilon_l, \tag{3.80}$$

$H_{Trz} \times H_{\Upsilon_l}$:

$$[\delta\Upsilon_{lr}]_{H_{Trz} \times H_{\Upsilon_l}} = -\frac{\rho}{2} \frac{|\delta D|}{(\omega - D)} T_{rz} \Upsilon_l \tag{3.81}$$

and

$H_K \times H_K$:

$$\delta J = -2\rho \frac{|\delta D|}{(\omega - D)} J^2. \tag{3.82}$$

The last is the traditional Kondo coupling renormalization. The other products are zero or give rise to terms which do not contain the original Hamiltonian structure. The conjugated couplings are renormalized with the same set of RG equations by hole-like processes, as before. With the results above we obtain the full set of RG equations

$$\begin{aligned}
\delta\Upsilon_r &= -\frac{\rho}{2} \frac{|\delta D|}{(\omega - D)} \Upsilon_r J - \rho \frac{|\delta D|}{(\omega - D)} T_r J - \frac{\rho}{2} \frac{|\delta D|}{(\omega - D)} T_{rz} J, && (3.83)\\
\delta T_r &= -\frac{\rho}{2} \frac{|\delta D|}{(\omega - D)} \Upsilon_r J - \frac{\rho}{4} \frac{|\delta D|}{(\omega - D)} T_{rz} J, && (3.84)\\
\delta T_{rz} &= -\rho \frac{|\delta D|}{(\omega - D)} \Upsilon_r J - \rho \frac{|\delta D|}{(\omega - D)} T_r J, && (3.85)\\
\delta\Upsilon_{lr} &= -\rho \frac{|\delta D|}{(\omega - D)} \Upsilon_r T_l - \rho \frac{|\delta D|}{(\omega - D)} T_r \Upsilon_l - \frac{\rho}{2} \frac{|\delta D|}{(\omega - D)} \Upsilon_r T_{lz} - \frac{\rho}{2} \frac{|\delta D|}{(\omega - D)} T_{rz} \Upsilon_l, && \\
\delta\Upsilon_l &= -\frac{\rho}{2} \frac{|\delta D|}{(\omega - D)} \Upsilon_l J - \rho \frac{|\delta D|}{(\omega - D)} T_l J - \frac{\rho}{2} \frac{|\delta D|}{(\omega - D)} T_{lz} J, && (3.86)\\
\delta T_l &= -\frac{\rho}{2} \frac{|\delta D|}{(\omega - D)} \Upsilon_l J - \frac{\rho}{4} \frac{|\delta D|}{(\omega - D)} T_{lz} J, && (3.87)\\
\delta T_{lz} &= -\rho \frac{|\delta D|}{(\omega - D)} \Upsilon_l J - \rho \frac{|\delta D|}{(\omega - D)} T_l J, && (3.88)\\
\delta J &= -2\rho \frac{|\delta D|}{(\omega - D)} J^2. && (3.89)
\end{aligned}$$

For low-energy processes the energy dependence ω in $|\delta D|/(\omega - D)$ can be neglected from the high energy cutoff D. Then, the RG equations can be written in their traditional

Gell-Mann-Low equation form, (for details see section 2.4)

$$\frac{d\Upsilon_r}{d\ln D} = -\frac{\rho}{2}\Upsilon_r J - T_r J - \frac{\rho}{2}T_{rz}J, \tag{3.90a}$$

$$\frac{dT_r}{d\ln D} = -\frac{\rho}{2}\Upsilon_r J - \frac{\rho}{4}T_{rz}J, \tag{3.90b}$$

$$\frac{dT_{rz}}{d\ln D} = -\rho\Upsilon_r J - \rho T_r J, \tag{3.90c}$$

$$\frac{d\Upsilon_{lr}}{d\ln D} = -\rho\Upsilon_r T_l - \rho T_r \Upsilon_l - \frac{\rho}{2}\Upsilon_r T_{lz} - \frac{\rho}{2}T_{rz}\Upsilon_l, \tag{3.90d}$$

$$\frac{d\Upsilon_l}{d\ln D} = -\frac{\rho}{2}\Upsilon_l J - T_l J - \frac{\rho}{2}T_{lz}J, \tag{3.90e}$$

$$\frac{dT_l}{d\ln D} = -\frac{\rho}{2}\Upsilon_l J - \frac{\rho}{4}T_{lz}J, \tag{3.90f}$$

$$\frac{dT_{lz}}{d\ln D} = -\rho\Upsilon_l J - \rho T_l J, \tag{3.90g}$$

$$\frac{dJ}{d\ln D} = -2\rho J^2. \tag{3.90h}$$

The RG equations describe how the coupling constants evolve with the systematic reduction of the bandwidth in the RG procedure, where D is the high-energy cutoff. Due to the complexity of this set of equations a numerical solution is required.

3.3.5 Numerical solution for the PMS equations

To obtain the evolution of the couplings under the bandwidth reduction $\tilde{D} \equiv D - \delta D$, the system of coupled differential equations above has to be solved, given an initial condition for the couplings. Note that only the couplings with subindex r can have complex initial values. Since Eq. (3.90h) is fully decoupled from the others, given a real initial condition $J(0)$, the coupling J will remain real along renormalization flow. Notice also that Eqs. (3.90e)-(3.90h) are fully decoupled from the others and thus have pure real solutions. It is now easy to see that the real (imaginary) part of the solution of Eqs. (3.90a)-(3.90b) depends only on the real (imaginary) part of their initial conditions.

As there are several model parameters, which can be tuned, we will resort to a numerical solution of the system of differential equations (3.90) within a few specific situations of interest and look at the evolution of the renormalized parameters as a function of the band width cut-off running parameter $\tilde{D}$. As in Sec. 3.2, we set $D = 1$, $U = 0.5$, $\delta = 0$ (the particle-hole symmetric case) and $V = 0.1$. We also set $\delta\phi = \pi$, for which case the couplings are all real (different values of $\delta\phi$ lead to qualitatively equivalent results).

The results for the calculation are shown in figure 13(a), for $\lambda_l = \lambda_r = 0.02$ (symmetric), and figure 13(b) for $\lambda_l = 0$ and $\lambda_r = 0.02$ (asymmetric) cases. These choices correspond to the diamond (green) and circle (red) curves of figure 11, respectively.

Despite the complexity of the set of equations (3.90), we see from their numerical solution (Fig.13) that the Kondo coupling J (black curve) renormalizes more strongly

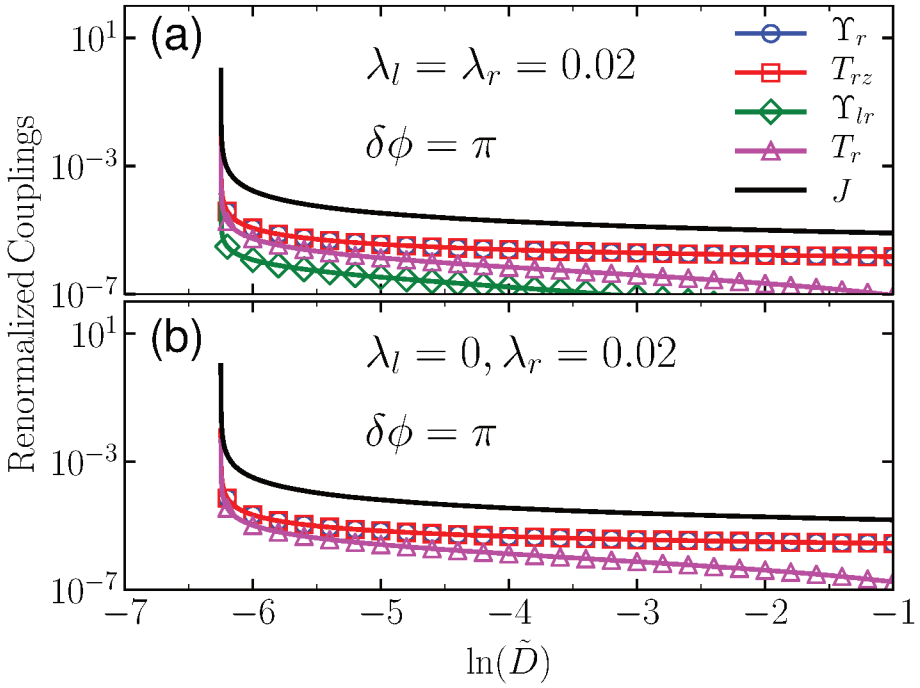

Figure 13 – Renormalized parameters as function of bandwidth cut-off $\tilde{D}$ for (a) symmetric case, $\lambda_l = \lambda_r = 0.02$ and (b) asymmetric case, $\lambda_r = 0.02$ and $\lambda_l = 0$. The other parameters are $\delta\phi = \pi$, $U = 0.5$, $V = 0.1$, $\delta = 0$. These parameters correspond to those of diamonds (green) and circles (red) curves, respectively, in Fig. 11. All couplings are normalized by the value of J right before the break down of the perturbative procedure. Figure published in (SILVA; SILVA; VERNEK, 2020).

than the other couplings under the bandwidth reduction. Thus, this fact reveals that the Kondo strong fixed point is not affected by the other fixed points associated with the additional couplings which appear in the effective Hamiltonian (3.19). This means that even in the presence of MZMs, the system always flows to the Kondo strong fixed point, where the impurity is screened by the conduction electrons and the many-body Kondo singlet takes place. Therefore, the Kondo singlet is robust against the local singlet composed by the MZMs and the impurity. These results are consistent with our NRG calculations of Sec. 3.2.

One can now ask how the couplings of the QD with the MZMs affects the Kondo temperature of the system. By extracting T_K from the value of $\tilde{D}$ for which $J \to \infty$, we can solve Eq. (3.90h) separately, obtaining exactly the same Kondo temperature for a single impurity Kondo model, $k_B T_{\rm K} = D \exp(-1/2\rho_0 J_0)$, with J_0 given by Eq. (3.33). Additionally, we could also choose to numerically extract $T_{\rm K}$ from the value of $\tilde{D}$ for which the renormalization flow of the entire system of equations (3.90) breaks down. By performing this procedure, we see no clear dependence of $T_{\rm K}$ with λ. We can see, however, that *all* couplings diverge at the same scale for which J diverges (see Fig. 13). Since

$\Upsilon \to \infty$ at the fixed point, this indicates that there is indeed a type of local strong interaction between the spins of the dot and the Majorana operators. Nevertheless, such effective coupling does not affect the Kondo screening.

More importantly, the fact that the renormalized couplings, $\Upsilon_{r(l)}$, Υ_{lr}, $T_{r(l)}$ and $T_{r(l)z}$ also diverge in the Kondo-screened fixed point ($J \to \infty$) suggests some sort of magnetic interaction between the Majorana modes and the QD. This interpretation relies solely on the form of the Hamiltonian H_{γ_r}, H_{γ_l} and $H_{\gamma_l r}$ of the effective model H_{eff} (3.19). From the RG perspective, the divergence of the renormalized couplings is associated with a marginally relevant local interaction between the Majorana modes and the QD spin.

3.4 Molecular Anderson Model Analysis

A complementary analysis of the results obtained from perturbative RG and NRG can be done using the so-called molecular Anderson model (MAM) (GROSSO; PARRAVICINI, 2000). This simplified model is similar to the SIAM, but with the difference that only one orbital of the metal (or metallic lead) is taken in account. In the MAM one metallic (extended) orbital ψ_0 is coupled to a localized impurity orbital ψ_d (a QD, for example), the Hamiltonian of this two-orbital molecule is given by

$$\begin{aligned} H_{\text{MAM}} &= \sum_{\sigma} \varepsilon_d d_\sigma^\dagger d_\sigma + U n_{d\uparrow} n_{d\downarrow} \\ &\quad + \sum_{\sigma} \varepsilon_0 c_{0\sigma}^\dagger c_{0\sigma} + V \sum_{\sigma} (c_{0\sigma}^\dagger d_\sigma + d_\sigma^\dagger c_{0\sigma}). \end{aligned} \tag{3.91}$$

The first two terms represent the impurity energy and Coulomb interaction U, the third is the metallic orbital energy and the last one is the coupling between the impurity and metallic orbital. The MAM has two important regimes, the *molecular regime*, where $U/\Gamma \ll 1$, and the *strong interacting regime*, with $U/\Gamma \gg 1$, where $\Gamma = \pi\rho V^2$ is the hybridization function and ρ is the density of states. In the molecular regime, the charge fluctuation between the metallic orbital and the impurity is dominant whereas in the strong interacting regime the spin fluctuations are responsible for the system features.

The microscopic origin of the Kondo effect is associated with spin fluctuations. Then, the MAM in the strong interacting regime can show, at least, qualitative aspects of the Kondo physics. The basis of the MAM is given by $|n_{0\sigma}\rangle \otimes |n_{d\sigma}\rangle$, which gives 16 states. The principal advantage of the MAM is that it can be described by a simple 16×16 matrix that can be exactly diagonalized without much computational effort.

The addition of two MZMs to the system can be done including the term $H_{\text{dot}-\text{M}}$ (3.8) to the MAM Hamiltonian (3.91)

$$H_{\text{M}} = H_{\text{MAM}} + H_{\text{dot}-\text{M}}. \tag{3.92}$$

The basis is now given by $|n_{0\sigma}\rangle \otimes |n_{f\sigma}\rangle \otimes |n_{d\sigma}\rangle$, resulting in 64 states. Using the parity symmetry, the Hamiltonian H_{M} can be written as a block-diagonal matrix with two blocks of size 32×32. The thermodynamic averages of the system can be computed by

$$\langle \hat{O} \rangle = Tr[\hat{\rho}\hat{O}], \tag{3.93}$$

were $Tr[\cdots]$ denotes the matrix trace, $\hat{O}$ is a generic operator and $\hat{\rho}$ is the system density matrix given by

$$\hat{\rho} = \frac{e^{-\beta H_{\mathrm{DM}}}}{Z}, \tag{3.94}$$

where

$$Z = \sum_n e^{-\beta \varepsilon_n} \tag{3.95}$$

is the Partition function. Here, $\beta = 1/k_B T$, where k_B is the Boltzmann constant, T is the temperature and H_{DM} is the diagonalized Hamiltonian $H_{\mathrm{DM}} = U^{\dagger} H_{\mathrm{M}} U$, the rotation matrix U is composed by the eigenstates set $\{|n\rangle\}$ which satisfies the eigenstate equation $H_{\mathrm{DM}}|n\rangle = \varepsilon_n |n\rangle$.

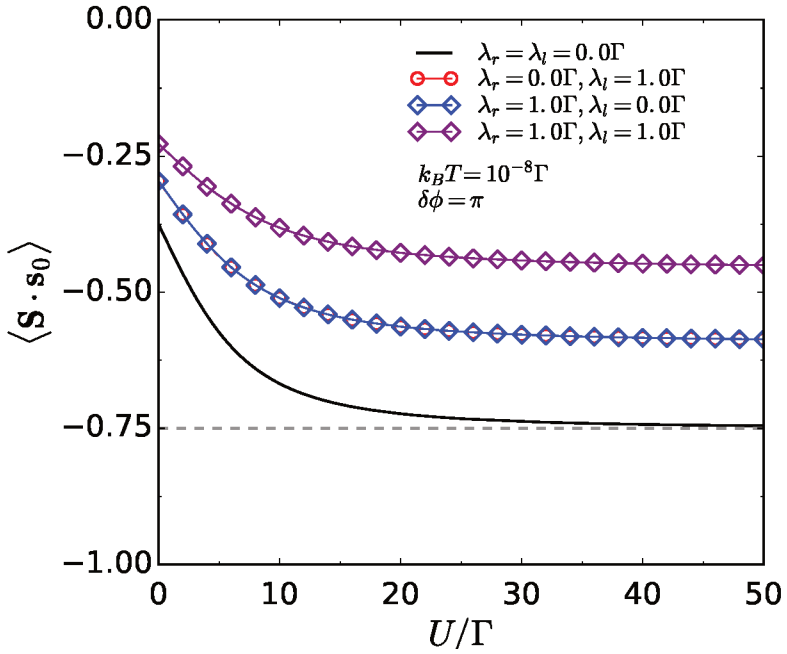

Figure 14 – Spin correlation of the the MAM as a function of the Coulomb interaction at low-temperature ($k_B T = 10^{-8}\Gamma$) for different Majorana couplings. Without MZMs in the strong interacting regime the molecule forms a full singlet which gives the traditional result $\langle \mathbf{S} \cdot \mathbf{s}_0 \rangle = -3/4$. In the presence of MZMs the spin impurity is screened by the metallic orbital which results in a decrease of the anti-ferromagnetic spin correlation between the impurity and the metallic orbital.

The spin correlation between the impurity and the metallic orbital can be computed as

$$\langle \mathbf{S} \cdot \mathbf{s}_0 \rangle = Tr[\hat{\rho}(\mathbf{S} \cdot \mathbf{s}_0)], \tag{3.96}$$

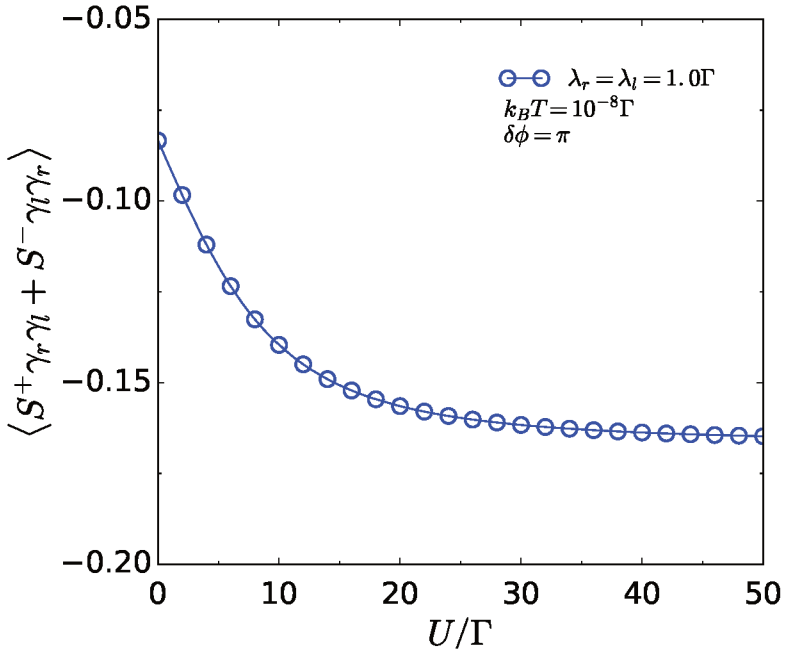

Figure 15 – Correlation between the MZMs and the impurity spin. In the strong interacting regime occurs the formation of a local singlet of the Majorana modes with the impurity.

in which the spin operator for the impurity and the orbital are given by

$$\mathbf{S} = \frac{1}{2}\Psi_d^\dagger \sigma \Psi_d \quad \text{and} \quad \mathbf{s}_0 = \frac{1}{2}\Psi_0^\dagger \sigma \Psi_0. \tag{3.97}$$

We define the spinors $\Psi_d = (d_\uparrow, d_\downarrow)^T$ and $\Psi_0 = (c_{0\uparrow}, c_{0\downarrow})^T$ and $\sigma = (\sigma_x, \sigma_y, \sigma_z)^T$, where σ_i are the Pauli matrices. In the above we used the fact that in the present case the spin of the impurity is 1/2. The spin correlation as a function of the Coulomb interaction, at low-temperature ($k_BT = 10^{-8}\Gamma$), is shown in figure 14, with and without MZMs. In the case where we do not have MZMs coupled to the impurity, black curve in figure 14, as the ratio U/Γ increases the system goes to the strong interacting regime and the correlation asymptotically tends to $-3/4$. This is the well-known result for a singlet composed by two 1/2-spin fermions, the singlet state is formed by the impurity and the metallic orbital. When one MZM is coupled to the impurity, the impurity spin is partially screened by the MZM, which results in a higher value of the spin correlation $\langle \mathbf{S} \cdot \mathbf{s}_0 \rangle$ (red and blue curves in figure 14). The screening is even more drastic when the impurity is coupled to two MZMs, as shown by the purple curve in figure 14.

To see how the presence of MZMs affects the impurity spin we need to analyze the correlation between them. From the effective Hamiltonian (3.24) we can see that the correlation between the MZMs and the impurity spin can be calculated as $\langle S^+\gamma_r\gamma_l + S^-\gamma_l\gamma_r\rangle$. In terms of regular fermions, the Majorana operators are described as $\gamma_r = (f_\uparrow + f_\uparrow^\dagger)/\sqrt{2}$

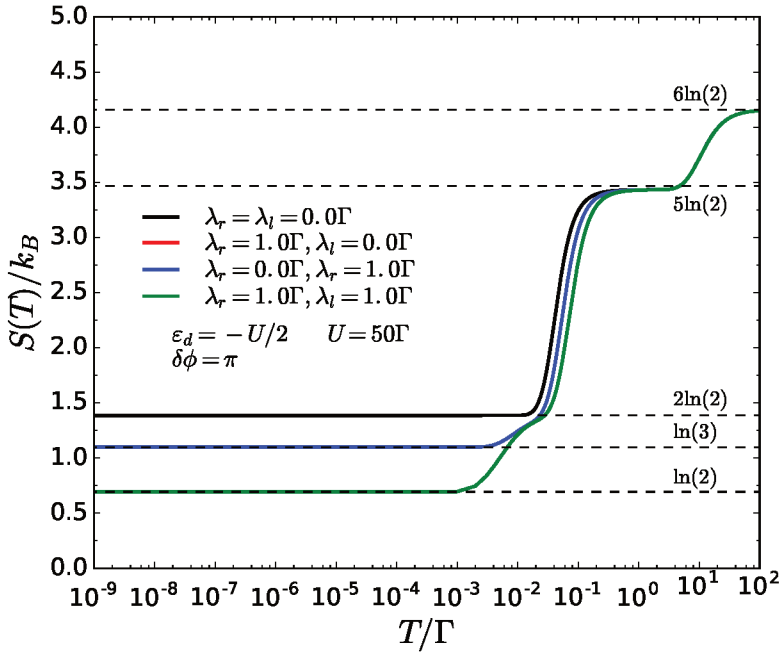

Figure 16 – The entropy of the MAM in the presence and absence of MZMs for the strong interacting regime ($U/\Gamma = 50$).

and $\gamma_l = (f_\downarrow + f_\downarrow^\dagger)/\sqrt{2}$, rendering the relation

$$\begin{aligned}\langle S^+\gamma_r\gamma_l + S^-\gamma_l\gamma_r\rangle &= \frac{1}{2}\langle S^+(f_\uparrow f_\downarrow + f_\uparrow f_\downarrow^\dagger + f_\uparrow^\dagger f_\downarrow + f_\uparrow^\dagger f_\downarrow^\dagger)\rangle \\ &+\frac{1}{2}\langle S^-(f_\downarrow f_\uparrow + f_\downarrow f_\uparrow^\dagger + f_\downarrow^\dagger f_\uparrow + f_\downarrow^\dagger f_\uparrow^\dagger)\rangle.\end{aligned} \tag{3.98}$$

The correlation between the MZMs and the impurity is shown in figure 15. In the strong interacting regime the correlation is negative which means a kind of anti-ferromagnetic coupling between the Majorana modes and the impurity. This local interaction is responsible for the impurity screening observed in figure 14.

Another interesting physical property that can be calculated using the density matrix is the entropy. The entropy of the MAM as a temperature function is

$$S(T) = \frac{\langle H_M\rangle}{T} + k_B\text{lnZ}. \tag{3.99}$$

The results for the MAM entropy are shown in figure 16. At high temperatures all the 64 states are statistically accessible and we always have the entropy $6k_B\ln(2)$. On the other hand, at low-temperatures the result is different in the presence or absence of MZMs. At $T = 0$, without any and in the presence of two MZMs, the residual entropy is $2k_B\ln(2)$ and $k_B\ln(2)$, respectively. These results are similar to the ones obtained from the SIAM by NRG (Fig. 11). However, when only one MZM is coupled to the impurity the residual entropy for the MAM is $k_B\ln(3)$. In this case, the residual entropy is quite different from $(3/2)k_B\ln(2)$, obtained from the SIAM in the presence of one MZM (Fig.11). This

occurs because the MAM does not have a continuum reservoir of electrons coupled to the impurity, but only the single orbital ψ_0 (see Appendix C). Despite the fact that the MAM cannot capture the non-Fermi liquid behavior of the system, it is useful to describe in a qualitative way how MZMs coupled to a magnetic impurity can affect the magnetic behavior of the system (Fig.14). Moreover, the MAM is also useful to the analyzes of possible magnetic interaction between MZMs with different polarization mediated by a magnetic impurity (Fig.15).

4 Conclusion and outlook

In this first part of the thesis we have studied the interplay between a localized magnetic moment and polarized MZMs. The proposed system was composed by a quantum magnetic impurity, which was simulated by an interacting QD, coupled to two topological superconducting quantum wires, with MZMs in their edges. The quantum wires have opposite polarization, resulting in opposite polarization of the MZMs coupled to the QD. The QD is also coupled to a normal metallic lead, providing the free electrons to screen the local magnetic moment. To tackle the system's low-energy physics we have employed both analytical and numerical methods. To access the Kondo regime, we derive an effective low-energy Kondo-like Hamiltonian, which we denominated Kondo-Majorana Hamiltonian. The effective Kondo-Majorana Hamiltonian reveals new spin-dependent mechanisms mediated by the magnetic impurity, beyond the traditional Kondo scatterings. Moreover, we have found an effective Kondo-like coupling between the MZMs and the conduction electrons of the metallic lead. The effective Kondo-Majorana Hamiltonian also revealed an indirect coupling between the MZMs with different polarization mediated by the impurity magnetic moment.

By performing a poor man scaling analysis we showed that the Kondo fixed point is robust, even in the presence of local Majorana operators. The robustness of the Kondo fixed point explains the coexistence of the many-body Kondo singlet and the local Majorana singlet. The full microscopic Hamiltonian was analyzed using the nonperturbative NRG whose results corroborate with Poor Man's scaling analysis. In addition, the NRG results for the impurity entropy reveals that the residual impurity entropy is dominated by the free MZMs of the system, even in the non-interacting limit. The contribution to the residual impurity entropy by the Majorana modes is given by $S_{\text{res}} = \frac{N_0}{2} k_B \ln(2)$, where N_0 is the number of free MZMs. For an odd number of free MZMs the system has a fractional impurity entropy, which can be associated with a local non-Fermi liquid behavior, analogous to the two-channel Kondo problem.

The analysis of the Kondo-Majorana fixed points, as the behavior of the residual impurity entropy, has practical application in the experimental pursuit of the MZMs. Recently, Sela *et al.* (SELA et al., 2019), proposed a experimental mechanism for the observation of MZMs, where the central MZMs signature is the fractional residual impurity entropy originated from free MZMs. We believe the present work provides important answers to the coexistence of MZMs and the Kondo effect. As well, the results presented have practical applications to the experimental determination of MZMs signatures.

Finally, a natural extension of the present work is the multi-impurity case, in this case the full microscopic Hamiltonian can be described by the periodic SIAM and the Kondo lattice. The investigation of how MZMs can affect multi-impurity systems will be the subject of possible future investigations.

Part II

RKKY interaction and spin-orbit coupling

5 Background

5.1 Indirect interaction between magnetic impurities: The Ruderman-Kittel-Kasuya-Yosida (RKKY) interaction

The so-called Ruderman-Kittel-Kasuya-Yosida (RKKY) interaction is the indirect interaction of magnetic impurities in metals mediated by the conduction electrons. The formal theory was addressing this phenomena developed by Kittel and Ruderman in the context of nuclear magnetic moments (RUDERMAN; KITTEL, 1954). Latter, Kasuya and Yosida discovered the same base mechanism in the context of electronic spins (KASUYA, 1956; YOSIDA, 1957). The RKKY interaction can be described by a Heinsenberg-type interaction between two magnetic impurities as

$$H_{\mathrm{RKKY}} = I_{\mathrm{RKKY}}(\mathbf{R})\boldsymbol{S_1} \cdot \boldsymbol{S_2}, \tag{5.1}$$

where $\boldsymbol{S_1}$ and $\boldsymbol{S_2}$ are the magnetic moment of the impurities, and $I_{\mathrm{RKKY}}(\mathbf{R})$ is the RKKY coupling, $\mathbf{R} = \mathbf{r_1} - \mathbf{r_1}$ is the distance between the impurities. The main feature of the RKKY coupling $I_{\mathrm{RKKY}}(\mathbf{R})$ is its oscillatory character. The origin of this behavior is the magnetic polarization of the conduction electrons around a magnetic impurity. This polarization can affect other magnetics impurities giving rise to the indirect coupling between them. As such, this resulting inter-impurity effective interaction is therefore mediated by the magnetic polarization of the conduction electrons. The magnetic polarization has a similar structure as the called Friedel oscillations caused by charged impurities (GROSSO; PARRAVICINI, 2000; PIRÓTH; SÓLYOM, 2008), exhibiting also the characteristic precession $2k_F R$, where k_F is the Fermi momentum. Another important feature of the RKKY coupling is its decay with the increase of the distance between the impurities, which reduces the effective RKKY interaction to nearly zero for arbitrary large distances.

It is well known that the RKKY interaction depends intrinsically on the dimension (Fermi surface) of the host material (COLEMAN, 2015), see section 5.1.1. Unlike most of physical problems, the dimension reduction increases the difficulty of theoretical treatment of the RKKY interaction. The one dimensional case is particularly peculiar (YAFET, 1987). Kittel himself was the first one to notice this fact (KITTEL, 1969). Latter, this problem was addressed in several studies (YAFET, 1987; IMAMURA; BRUNO; UTSUMI, 2004; VALIZADEH, 2016; RUSIN; ZAWADZKI, 2017). The kernel of the puzzle around the 1D RKKY interaction was concerned in its exotic asymptotic behavior. Differently from the higher dimensional cases, in 1D the interaction did not seem to decay with the impurities distance. This unphysical result is associated with the Cauchy integrals

that appear in the perturbative approach of the 1D version of the problem. A formal mathematical solution for this problem was presented only recently (RUSIN; ZAWADZKI, 2017).

5.1.1 Theoretical formulation of the RKKY interaction

In theoretical formulation of the mechanism underlying the RKKY, we have to consider the local interaction between the individual impurities and conduction electrons. This can be described by the Kondo-like Hamiltonian

$$H_{Ki} = \frac{J}{V}\sum_{\mathbf{k}\mathbf{k}'} e^{-i(\mathbf{k}-\mathbf{k}')\cdot\mathbf{r}_i}\left[S_i^z\left(c^\dagger_{\mathbf{k}'\uparrow}c_{\mathbf{k}\uparrow} - c^\dagger_{\mathbf{k}'\downarrow}c_{\mathbf{k}\downarrow}\right) + S_i^+ c^\dagger_{\mathbf{k}'\downarrow}c_{\mathbf{k}\uparrow} + S_i^- c^+_{\mathbf{k}'\uparrow}c_{\mathbf{k}\downarrow}\right], \tag{5.2}$$

where $\mathbf{r}_i$ is the position of the magnetic impurity i (with $i = 1, 2$), which, for simplicity is assumed to exhibit spin $S = 1/2$. Ruderman and Kittel showed that the indirect interaction between these magnetic impurities can be derived using second order perturbation, see Appendix E. The Hamiltonian (5.2) is considered as the perturbation, $V_i = H_{Ki}$, on the Fermi sea of the metallic system, which in turn is described by

$$H_0 = \sum_{\mathbf{k},s}\varepsilon_{k\sigma}c^\dagger_{\mathbf{k}\sigma}c_{\mathbf{k}s}. \tag{5.3}$$

Up to second order perturbation theory an effective interacting term can be written as[1]

$$\Delta E^{(2)} = \sum_{i=1,2}\sum_{\mathbf{k},\sigma}^{\text{occ.}}\sum_{\mathbf{k}',\sigma'}^{\text{empty}}\left[\frac{\langle\mathbf{k}\sigma,\sigma|H_i|\mathbf{k}'\sigma',\sigma'\rangle\langle\mathbf{k}'\sigma',\sigma'|H_i|\mathbf{k}\sigma,\sigma\rangle}{\varepsilon_{k\sigma}-\varepsilon_{k'\sigma'}}\right], \tag{5.4}$$

where $\varepsilon_{k\sigma} = \hbar^2k^2/2m$ is the energy of a conduction electron with momentum k, spin σ and mass m. In the absence of external magnetic field, the energy is spin independent, so we can set $\varepsilon_{k\sigma} = \varepsilon_k$. The indirect interaction between the magnetic impurities comes from spin exchange processes. Therefore, for the analysis of the RKKY interaction, only the mixed terms of (5.4) are necessary. Other terms will provide contributions to the ground state energy, not important in the present context. Then, the second order contribution from the mixed terms can be written as

$$\Delta E^{(2)}_{\text{mixed}} = \sum_{\mathbf{k},\sigma}^{\text{occ.}}\sum_{\mathbf{k}',\sigma'}^{\text{empty}}\left[\frac{\langle\mathbf{k}\sigma,\sigma|H_1|\mathbf{k}'\sigma',\sigma'\rangle\langle\mathbf{k}'\sigma',\sigma'|H_2|\mathbf{k}\sigma,\sigma\rangle}{\varepsilon_k-\varepsilon_{k'}}\right] + \text{C.C.} \tag{5.5}$$

Here, C.C denotes the complex conjugated of the proceeding term. The brakets in the equation (5.5) can be directly evaluated using the creation and annihilation operators. For

[1] The momentum summations can be also expressed as

$$\sum_{\mathbf{k}}^{\text{occ.}}\sum_{\mathbf{k}'}^{\text{empty}} = \sum_{\mathbf{k}<\mathbf{k}_F}\sum_{\mathbf{k}'>\mathbf{k}_F},$$

where $\mathbf{k}_F$ is the Fermi momentum vector.

example, one of the terms related with the impurity spin z-component can be calculated as $S_1^z c^\dagger_{\mathbf{k}'\uparrow} c_{\mathbf{k}\uparrow}|\mathbf{k}\uparrow,\uparrow\rangle = S_1^z|\mathbf{k}'\uparrow,\uparrow\rangle$. After all calculations we find

$$\Delta E^{(2)}_{\text{mixed}} = 2\frac{J^2}{V^2}\sum_\sigma \sum_{\mathbf{k}}^{\text{occ.}} \sum_{\mathbf{k}'}^{\text{empty}} \frac{e^{-i(\mathbf{k}-\mathbf{k}')\cdot(\mathbf{r}_1-\mathbf{r}_2)}}{\frac{\hbar^2}{2m}(k^2-k'^2)}\langle\sigma|\left[S_1^z S_2^z + \frac{1}{2}(S_1^+ S_2^- + S_1^- S_2^+)\right]|\sigma\rangle + \text{C.C.} \tag{5.6}$$

Now, using the fact that $S^\pm = S^x + \pm iS^y$ we can rewrite Eq.(5.6) as

$$\Delta E^{(2)}_{\text{mixed}} = \sum_\sigma \langle\sigma|H_{\text{RKKY}}|\sigma\rangle, \tag{5.7}$$

where we identify

$$H_{\text{RKKY}} = I^D_{\text{RKKY}}(\mathbf{R})(\mathbf{S_1}\cdot\mathbf{S_2}) \tag{5.8}$$

as the RKKY Hamiltonian, in which I^D_{RKKY} is the RKKY coupling given by

$$I^D_{\text{RKKY}}(\mathbf{R}) = \frac{4m}{\hbar^2}\frac{J^2}{V^2}\sum_{\mathbf{k}}^{\text{occ.}}\sum_{\mathbf{k}'}^{\text{empty}} \frac{e^{i(\mathbf{k}-\mathbf{k}')\cdot\mathbf{R}}}{k^2-k'^2} + \text{C.C.} \tag{5.9}$$

In the equation above, $\mathbf{R} = \mathbf{r}_1 - \mathbf{r}_2$ is the vector connecting the two impurities. The index D in the RKKY coupling (5.9) anticipates the dimension dependence of the RKKY coupling. In the next sections we will calculate the RKKY coupling in different dimensions.

5.1.1.1 RKKY interaction in 1D

In one dimension, the Fermi momentum is a scalar $\mathbf{k} = k$, and the volume is $V = N$. Also, the momentum summation can be transformed into an integral using $(1/N)\sum_k \to \int dk/2\pi$. With this prescription, the RKKY coupling (5.9) in 1D can be written as

$$I^{1D}_{\text{RKKY}}(x) = \frac{4m}{\hbar^2}J^2\int_{-k_F}^{k_F}\frac{dk}{2\pi}\left(\int_{-\infty}^{-k_F}\frac{dk'}{2\pi}\frac{e^{i(k-k')x}}{k^2-k'^2} + \int_{k_F}^{\infty}\frac{dk'}{2\pi}\frac{e^{i(k-k')x}}{k^2-k'^2} + \text{C.C}\right), \tag{5.10}$$

where $x = x_2 - x_1$ is the distance between the impurities. First, let us calculate the integral over "k". This can be done using complex integration to write

$$\int_{-\infty}^{-k_F} dk'\frac{e^{i(k-k')x}}{k^2-k'^2} + \int_{k_F}^{\infty} dk'\frac{e^{i(k-k')x}}{k^2-k'^2} = \mathcal{P}\int_{-\infty}^{\infty} dk'\frac{e^{i(k-k')x}}{k^2-k'^2}, \tag{5.11}$$

where

$$\mathcal{P}\int_{-\infty}^{\infty} dk'\frac{e^{i(k-k')x}}{k^2-k'^2} = \lim_{k_F\to 0}\left[\int_{-\infty}^{-k_F} dk'\frac{e^{i(k-k')x}}{k^2-k'^2} + \int_{k_F}^{\infty} dk'\frac{e^{i(k-k')x}}{k^2-k'^2}\right], \tag{5.12}$$

and $\mathcal{P}[\cdots]$ denotes the Cauchy principal value (see Appendix F). To compute the complex integral we perform an integration on the upper complex half-plane in the anti-clockwise direction resulting in

$$\mathcal{P}\int_{-\infty}^{\infty} dk'\frac{e^{i(k-k')x}}{k^2-k'^2} + \int_{C_k} dk'\frac{e^{i(k-k')x}}{k^2-k'^2} + \int_{C_{-k}} dk'\frac{e^{i(k-k')x}}{k^2-k'^2} = 0.$$

In the above, C_k represents the contour on the upper complex half-plane around $z = k$ in the clockwise direction, and C_{-k} denotes the contour around $z = -k$ in the anti-clockwise direction. The poles of the complex integral (5.11) are given by $k' = k$ and $k' = -k$, the residues in these poles can be determined using the methods presented in the Appendix F and results

$$\text{Res}(k' = k) = \lim_{k' \to k} (k' - k) \frac{e^{i(k-k')x}}{(k + k')(k - k')} = -\frac{1}{2k} \tag{5.13}$$

and

$$\text{Res}(k' = -k) = \lim_{k' \to -k} (k' + k) \frac{e^{i(k-k')x}}{(k + k')(k - k')} = \frac{e^{i2kx}}{2k}. \tag{5.14}$$

Hence

$$\begin{aligned} \int_{C_k} dk' \frac{e^{i(k-k')x}}{k^2 - k'^2} &= -\pi i \text{Res}(k' = k) = -\pi i \left(-\frac{1}{2k} \right), \\ \int_{C_{-k}} dk' \frac{e^{i(k-k')x}}{k^2 - k'^2} &= \pi i \text{Res}(k' = -k) = \pi i \left(\frac{e^{i2kx}}{2k} \right). \end{aligned}$$

With these results we finally obtain

$$\mathcal{P} \int_{-\infty}^{\infty} dk' \frac{e^{i(k-k')x}}{k^2 - k'^2} = \frac{\pi}{k} e^{ikx} \text{sin}(kx). \tag{5.15}$$

Therefore,

$$\mathcal{P} \left(\int_{-\infty}^{\infty} dk' \frac{e^{i(k-k')x}}{k^2 - k'^2} + \text{C.C} \right) = \frac{2\pi}{k} \cos(kx) \text{sin}(kx). \tag{5.16}$$

Inserting this result into Eq.(5.10) we obtain

$$\begin{aligned} I^{1D}_{\text{RKKY}}(x) &= J^2 \frac{4m}{\hbar^2} \frac{1}{(2\pi)^2} \pi \int_{-k_F}^{k_F} \frac{2 \cos(kx) \text{sin}(kx)}{k} dk \\ &= J^2 \frac{m}{\hbar^2 \pi^2} \pi \int_{-k_F}^{k_F} \frac{\sin(2kx)}{k} dk \\ &= 2J^2 \frac{m}{\hbar^2 \pi^2} \pi \int_{0}^{k_F} \frac{\sin(2kx)}{k} dk. \end{aligned}$$

In the calculation above we have used the identity $2 \cos(x) \text{sin}(x) = \text{sin}(2x)$. The resulting expression for the RKKY coupling can then be written as

$$I^{1D}_{\text{RKKY}}(x) = J^2 \frac{2m}{\hbar^2} \frac{1}{\pi^2} \pi \text{Si}(2k_F x), \tag{5.17}$$

where

$$\text{Si}(x) = \int_0^x \frac{\sin(\text{t})}{t} dt \tag{5.18}$$

is the called "sine integral function". In the asymptotic limit ($k_F x >> 1$) the result (5.17) reveals a very peculiar behavior. Let us use the asymptotic expansion for the sine function (GRADSHTEYN; RYZHIK, 1980)($x \gg 1$)

$$\text{Si}(x) \sim \frac{\pi}{2} + \frac{\cos(x)}{x} \sum_{n=0}^{\infty} (-1)^n \frac{2n!}{x^{2n}} - \frac{\sin(x)}{x} \sum_{n=0}^{\infty} (-1)^n \frac{(2n+1)!}{x^{2n+1}}. \tag{5.19}$$

Using this expression, we see from (5.17) that $I^{1D}_{\mathrm{RKKY}} \to \pi/2$ as $k_F x \to \infty$, which does not decay with the impurities distance, in contrast to the 2D and 3D cases. The first one to notice this fact was Kittel (KITTEL, 1969), but the rigorous mathematical reason for this counter intuitive result was given only recently (RUSIN; ZAWADZKI, 2017). The authors realized that in 1D the singularities of the integral (5.12) around $k = k' = 0$ give extra contributions that must be calculated apart to introduce a correction in the RKKY coupling (5.17). The same does not occurs in 2D and 3D (VALIZADEH, 2016). Following Zawadzky, we compute the integral in the interval $[-\epsilon, \epsilon]$ with $\epsilon \to 0$. For k and k' close to zero we have $e^{i(k-k')x} = e^{-i(k-k')x} \approx 1$. Then, the integral correction due the singularities is

$$I_\epsilon = -2\int_{-\epsilon}^{\epsilon} dk \int_{-\epsilon}^{\epsilon} \frac{dk'}{k'^2 - k^2}.$$

Using now that

$$\frac{1}{k'^2 - k^2} = \frac{1}{2k}\left[\frac{1}{k' - k} - \frac{1}{k + k'}\right]$$

and performing the integral over "k'" we obtain

$$I_\epsilon = \int_{-\epsilon}^{\epsilon} \left[\frac{\ln|\epsilon - k|}{k} - \frac{\ln|\epsilon + k|}{k}\right] dk.$$

This can also be written as

$$\begin{aligned} I_\epsilon &= \int_{-1}^{1} \left[\frac{\ln|1 - u|}{u} - \frac{\ln|1 + u|}{u}\right] du \\ &= -2\mathrm{Li}_2(1) + 2\mathrm{Li}_2(-1) = -\frac{\pi^2}{2}, \end{aligned} \tag{5.20}$$

where

$$\mathrm{Li}_2(x) = -\int_0^x dt \ln|1 - t|/t \tag{5.21}$$

is the dilogarithmic function. We have used $\mathrm{Li}_2(1) = \pi^2/6$ e $\mathrm{Li}_2(-1) = -\pi^2/12$ (GRADSHTEYN; RYZHIK, 1980). The correct result for the RKKY coupling (5.17) is obtained by the subtraction of the contribution (5.20) resulting in

$$I^{1D}_{\mathrm{RKKY}}(x) = J^2 \frac{2m}{\hbar^2}\frac{1}{\pi^2}\left[\pi\left(\mathrm{Si}(2k_F x) - \frac{\pi}{2}\right)\right]. \tag{5.22}$$

Now, using the expansion (5.19) we obtain the asymptotic RKKY coupling

$$I^{1D}_{\mathrm{RKKY}}(x) \sim \frac{2mJ^2}{\hbar^2\pi}\frac{\cos(2k_F x)}{x}, \qquad \text{for } k_F x \gg 1. \tag{5.23}$$

Therefore, the RKKY interaction have an oscillatory behavior and decay with $1/x$, thus $I^{1D}_{\mathrm{RKKY}}(x) \to 0$, as $k_F x \to \infty$.

The result above is obtained for a free Fermi sea, in the presence interactions, as the spin-orbit coupling, the RKKY interaction presents different behavior. This is the principal subject of the second part of the present thesis, see chapter 6.

5.1.1.2 RKKY in 2D

From equation (5.9), for 2D the RKKY coupling reads

$$I^{2D}_{\mathrm{RKKY}}(\mathbf{R}) = \frac{4m}{\hbar^2}\frac{J^2}{V^2}\sum_{\mathbf{k}<\mathbf{k}_F}\sum_{\mathbf{k}'>\mathbf{k}_F}\frac{e^{i(\mathbf{k}-\mathbf{k}')\cdot\mathbf{R}}}{k^2-k'^2} + \text{C.C.} \tag{5.24}$$

Let us define $\mathbf{q} = \mathbf{k} - \mathbf{k}'$, so that $q^2 = k'^2 - k^2 + 2(\mathbf{q}\cdot\mathbf{k})$, and $k^2 - k'^2 = -q(q - 2k\cos\theta)$. Performing this variable change in the summations (5.24) we obtain

$$\sum_{\mathbf{k}<\mathbf{k}_F}\sum_{\mathbf{k}'>\mathbf{k}_F}\frac{e^{i(\mathbf{k}-\mathbf{k}')\cdot\mathbf{R}}}{k^2-k'^2} = -\sum_{\mathbf{q}>0}\frac{e^{i\mathbf{q}\cdot\mathbf{R}}}{q}\sum_{\mathbf{k}}\frac{1}{q-2k\cos\theta}. \tag{5.25}$$

Again, the momentum summation can be transformed into an integral as $(1/V)\sum_{\mathbf{k}} \to \int d^2k/(2\pi)^2$, upon which we can write

$$\sum_{\mathbf{k}}\frac{1}{q-2k\cos\theta} = V\int\frac{d^2k}{(2\pi)^2}\frac{1}{q-2k\cos\theta} = \frac{V}{(2\pi)^2}\int_{k_F}^{\infty}kdk\int_0^{2\pi}\frac{1}{q-2k\cos\theta}d\theta.$$

The integral over θ can be calculated using complex integration. In the complex plane, $z = e^{i\theta}$, then $d\theta = dz/iz$. Now, using that $\cos\theta = (e^{i\theta} + e^{-i\theta})/2 = (z + 1/z)/2$ results in

$$\int_0^{2\pi}\frac{1}{q-2k\cos\theta}d\theta = \mathcal{P}\oint\frac{dz}{iz}\frac{1}{(qz-kz^2-k)} = -\frac{1}{i}\mathcal{P}\oint\frac{dz}{k[z^2-(q/k)z+1]}. \tag{5.26}$$

The denominator in the complex integral above can be write as

$$z^2 - (q/k)z + 1 = \frac{1}{k}(z-\alpha)(z-\beta),$$

with $\alpha = (q + \sqrt{q^2-4k^2})/2$ and $\beta = (q - \sqrt{q^2-4k^2})/2$. Performing the integral on the upper complex half-plane we have contribution only from the pole $z = \alpha$, thus

$$\oint\frac{dz}{(z-\alpha)(z-\beta)} = 2\pi i\mathrm{Res}[z=\alpha]. \tag{5.27}$$

Using the residue technique for a simple pole (see Appendix F) we have

$$\mathrm{Res}[z=\alpha] = \lim_{z\to\alpha}(z-\alpha)\frac{1}{(z-\alpha)(z-\beta)} = \frac{1}{(\alpha-\beta)} = \frac{1}{\sqrt{q^2-4k^2}}. \tag{5.28}$$

Now, inserting (5.27) and (5.28) in (5.26) finally results in

$$\int_0^{2\pi}\frac{1}{q-2k\cos\theta}d\theta = \begin{cases} -\frac{2\pi}{\sqrt{q^2-4k^2}}, & \text{if} \quad q > 2k \\ 0, & \text{if} \quad q < 2k \end{cases}. \tag{5.29}$$

Up to now we have that the sum in the $\mathbf{k}$-index is

$$\sum_{\mathbf{k}}\frac{1}{q-2k\cos\theta} = \begin{cases} -\frac{V}{(2\pi)^2}\int_{k_F}^{\infty}k\frac{2\pi}{\sqrt{q^2-4k^2}}dk, & \text{if} \quad q > 2k \\ 0, & \text{if} \quad q < 2k \end{cases}. \tag{5.30}$$

The other momentum summation that appear in (5.25) can be also turned into an integral as

$$\sum_{\mathbf{q}>0}\frac{e^{i\mathbf{q}\cdot\mathbf{R}}}{q}=\frac{V}{(2\pi)^2}\int_{k_F}^{\infty}qdq\int_0^{2\pi}\frac{e^{i\mathbf{q}\cdot\mathbf{R}}}{q}d\theta=\int_{k_F}^{\infty}dq\int_0^{2\pi}e^{iqR\cos\theta}d\theta. \tag{5.31}$$

Now, using the results (5.30) and (5.31) in (5.25) we have

$$\begin{aligned}\sum_{\mathbf{k}<\mathbf{k}_F}\sum_{\mathbf{k}'>\mathbf{k}_F}\frac{e^{i(\mathbf{k}-\mathbf{k}')\cdot\mathbf{R}}}{k^2-k'^2} &= \frac{V}{(2\pi)^2}\frac{V}{(2\pi)^2}2\pi\int_0^{k_F}\frac{kdk}{\sqrt{q^2-4k^2}}\int_{2k_F}^{\infty}dq\int_0^{2\pi}e^{iqR\cos\theta}d\theta\\ &= \frac{V^2}{(2\pi)^2}\int_0^{k_F}\frac{kdk}{\sqrt{q^2-4k^2}}\int_{2k_F}^{\infty}dq\left(\frac{1}{2\pi}\int_0^{2\pi}e^{iqR\cos\theta}d\theta\right).\end{aligned} \tag{5.32}$$

From the definition of the 0-th Bessel function (GRADSHTEYN; RYZHIK, 1980)

$$\frac{1}{2\pi}\int_0^{2\pi}e^{ix\cos y}dy=J_0(x) \tag{5.33}$$

we can write

$$\sum_{\mathbf{k}<\mathbf{k}_F}\sum_{\mathbf{k}'>\mathbf{k}_F}\frac{e^{i(\mathbf{k}-\mathbf{k}')\cdot\mathbf{R}}}{k^2-k'^2}=\frac{V^2}{(2\pi)^2}\int_0^{k_F}kdk\int_{2k_F}^{\infty}J_0(qR)\frac{1}{\sqrt{q^2-4k^2}}dq. \tag{5.34}$$

Let us now perform a change of variable as $q'=q/2k$ to write

$$\int_{2k_F}^{\infty}J_0(qR)\frac{1}{\sqrt{q^2-4k^2}}dq=\int_1^{\infty}dq'J_0(2kRq')\frac{1}{\sqrt{q'^2-1}}.$$

Since

$$\int_1^{\infty}J_0(xy)\frac{1}{\sqrt{y^2-1}}=\frac{\pi}{2}\left[J_0\left(\frac{x}{2}\right)N_0\left(\frac{x}{2}\right)\right],$$

where $N_p(x)$ is the Neumann function, we obtain

$$\sum_{\mathbf{k}<\mathbf{k}_F}\sum_{\mathbf{k}'>\mathbf{k}_F}\frac{e^{i(\mathbf{k}-\mathbf{k}')\cdot\mathbf{R}}}{k^2-k'^2}=\frac{V^2}{(2\pi)^2}\int_0^{k_F}dkk\frac{\pi}{2}\Big[J_0(kR)N_0(kR)\Big].$$

Setting $x=kR$ and using

$$\int x[J_0(x)N_0(x)]dx=\frac{x^2}{2}[J_0(x)N_0(x)+J_1(x)N_1(x)]+\text{constant},$$

we can write

$$\sum_{\mathbf{k}<\mathbf{k}_F}\sum_{\mathbf{k}'>\mathbf{k}_F}\frac{e^{i(\mathbf{k}-\mathbf{k}')\cdot\mathbf{R}}}{k^2-k'^2}=\frac{V^2\pi}{(2\pi)^2}\frac{1}{R^2}\frac{x_F^2}{2}[J_0(x_F)N_0(x_F)+J_1(x_F)N_1(x_F)],$$

where $x_F=k_FR$. Using this result the 2D RKKY coupling (5.24) acquires the form

$$I^{2D}_{\text{RKKY}}(\mathbf{R})=J^2\frac{m^2}{\hbar^2}\frac{x_F^2}{R^2}[J_0(x_F)N_0(x_F)+J_1(x_F)N_1(x_F)]. \tag{5.35}$$

We can now use the asymptotic expansions for the Bessel and Neumann functions given by (GRADSHTEYN; RYZHIK, 1980)

$$J_\nu(z)\sim\sqrt{\frac{2}{\pi z}}\left[\cos\omega\sum_{n=0}^{\infty}(-1)^n\frac{a_{2n}(\nu)}{z^{2n}}-\sin\omega\sum_{n=0}^{\infty}(-1)^n\frac{a_{2n+1}(\nu)}{z^{2n+1}}\right], \tag{5.36}$$

$$N_\nu(z)\sim\sqrt{\frac{2}{\pi z}}\left[\sin\omega\sum_{n=0}^{\infty}(-1)^n\frac{a_{2n}(\nu)}{z^{2n}}+\cos\omega\sum_{n=0}^{\infty}(-1)^n\frac{a_{2n+1}(\nu)}{z^{2n+1}}\right], \tag{5.37}$$

where $\omega = z - \frac{1}{2}\nu\pi - \frac{1}{4}\pi$ and

$$a_n(\nu) = \frac{(4\nu^2 - 1^2)(4\nu^2 - 3^2)\cdots(4\nu^2 - (2n-1)^2)}{n!8^n}, \tag{5.38}$$

to get the asymptotic behavior of the RKKY coupling in 2D (5.35)

$$I^{2D}_{\text{RKKY}}(\mathbf{R}) \sim J^2 \frac{m^2}{\hbar^2} \frac{\sin(2k_F R)}{R^2}, \qquad (k_F R \gg 1). \tag{5.39}$$

Similar to the 1D case, the asymptotic behavior of the RKKY coupling is oscillatory and has the characteristic wave vector $2k_F$. However, now the coupling decay as $1/R^2$ and not as $1/R$ as in the 1D case.

5.1.1.3 RKKY in 3D

In 3D, the momentum summations are transformed into integral as $(1/V)\sum_{\mathbf{k}} \to \int d^3k/(2\pi)^3$, and Eq.(5.9) becomes

$$I^{3D}_{\text{RKKY}}(\mathbf{R}) = \frac{4m}{\hbar^2} J^2 \int \frac{d^3k}{(2\pi)^3} \int \frac{d^3k'}{(2\pi)^3} \frac{e^{i(\mathbf{k}-\mathbf{k}')\cdot\mathbf{R}}}{k^2 - k'^2} + \text{C.C.} \tag{5.40}$$

Let us first look to the integral over k'

$$\begin{aligned}
\int \frac{d^3k'}{(2\pi)^3} \frac{e^{i(\mathbf{k}-\mathbf{k}')\cdot\mathbf{R}}}{k^2 - k'^2} &= \frac{e^{i\mathbf{k}\cdot\mathbf{R}}}{(2\pi)^3} \int \frac{d^3k'}{(2\pi)^2} \frac{e^{-i\mathbf{k}'\cdot\mathbf{R}}}{k^2 - k'^2} \\
&= \frac{e^{i\mathbf{k}\cdot\mathbf{R}}}{(2\pi)^3} \int_0^{2\pi} d\phi \int_0^{\pi} d\theta \int_{-\infty}^{\infty} \frac{e^{-ik'R\cos\theta}}{k^2 - k'^2} k'^2 \sin\theta dk' \\
&= \frac{e^{i\mathbf{k}\cdot\mathbf{R}}}{(2\pi)^2} \int_{-\infty}^{\infty} k'^2 dk' \int_{-1}^{-1} \frac{e^{ik'Ru}}{k^2 - k'^2} du \\
&= \frac{e^{i\mathbf{k}\cdot\mathbf{R}}}{(2\pi)^2} \frac{1}{iR} \int_{-\infty}^{\infty} \frac{e^{ik'R} - e^{-ik'R}}{k^2 - k'^2} dk'.
\end{aligned} \tag{5.41}$$

The integral in the last line can be compute by complex integration as

$$\int_{-\infty}^{\infty} \frac{e^{ik'R} - e^{-ik'R}}{k^2 - k'^2} dk' = \mathcal{P} \int_{-\infty}^{\infty} \frac{e^{ik'R} - e^{-ik'R}}{k^2 - k'^2} dk'. \tag{5.42}$$

We can perform the variable changes $\sigma = kR$ and $\rho = k'R$, so

$$\mathcal{P} \int_{-\infty}^{\infty} \frac{e^{ik'R} - e^{-ik'R}}{k^2 - k'^2} dk' = \mathcal{P} \int_{-\infty}^{\infty} d\rho \frac{e^{i\rho} - e^{-i\rho}}{\sigma^2 - \rho^2} \rho. \tag{5.43}$$

For the integral with positive exponential above, from the residue calculus (see Appendix F) we have

$$\mathcal{P} \int_{-\infty}^{\infty} \frac{\rho e^{i\rho}}{\sigma^2 - \rho^2} d\rho + \int_{C_\sigma} \frac{\rho e^{i\rho}}{\sigma^2 - \rho^2} d\rho + \int_{C_{-\sigma}} \frac{\rho e^{i\rho}}{\sigma^2 - \rho^2} d\rho = 0. \tag{5.44}$$

Performing the contour integrals above we obtain

$$\begin{aligned}
\int_{C_\sigma} \frac{\rho e^{i\rho}}{\sigma^2 - \rho^2} d\rho &= \int_{C_\sigma} \frac{\rho e^{i\rho}}{(\sigma + \rho)(\sigma - \rho)} d\rho = \pi i \lim_{\rho \to \sigma} (\rho - \sigma) \frac{\rho e^{i\rho}}{(\sigma + \rho)(\sigma - \rho)} = -\frac{1}{2} e^{i\sigma} \pi i, \\
\int_{C_{-\sigma}} \frac{\rho e^{i\rho}}{\sigma^2 - \rho^2} d\rho &= \int_{C_{-\sigma}} \frac{\rho e^{i\rho}}{(\sigma + \rho)(\sigma - \rho)} d\rho = -\pi i \lim_{\rho \to \sigma} (\rho - \sigma) \frac{\rho e^{i\rho}}{(\sigma + \rho)(\sigma - \rho)} = -\frac{1}{2} e^{-i\sigma} \pi i.
\end{aligned}$$

Using this in Eq.(5.44) we obtain

$$\mathcal{P}\int_{-\infty}^{\infty}\frac{\rho e^{i\rho}}{\sigma^2-\rho^2}d\rho=\pi i\cos(\sigma)=\pi i\cos(kR).$$

For the negative exponential similar calculations results in

$$\mathcal{P}\int_{-\infty}^{\infty}\frac{\rho e^{-i\rho}}{\sigma^2-\rho^2}d\rho=\pi i\cos(\sigma)=-\pi i\cos(kR).$$

Therefore, using the result above into Eq.(5.43) leads to

$$\int_{-\infty}^{\infty}\frac{e^{ik'R}-e^{-ik'R}}{k^2-k'^2}dk'=2\pi i\cos(kR).$$

With this, the integral (5.41) becomes

$$\int\frac{d^3k'}{(2\pi)^3}\frac{e^{i(\mathbf{k}-\mathbf{k}')\cdot\mathbf{R}}}{k^2-k'^2}=\frac{e^{i\mathbf{k}\cdot\mathbf{R}}}{2\pi}\frac{1}{R}\cos(kR),$$

which helps us to write the RKKY coupling (5.40) as

$$\begin{aligned}I^{3D}_{\mathrm{RKKY}}(\mathbf{R}) &= \frac{4m}{\hbar^2}J^2\int\frac{d^3k}{(2\pi)^3}\int\frac{d^3k'}{(2\pi)^3}\frac{e^{i(\mathbf{k}-\mathbf{k}')\cdot\mathbf{R}}}{k^2-k'^2}+\mathrm{C.C}\\ &= \frac{4m}{\hbar^2}J^2\frac{1}{R}\frac{1}{2\pi}\int\frac{d^3k}{(2\pi)^3}e^{i\mathbf{k}\cdot\mathbf{R}}\cos(kR)+\mathrm{C.C}\\ &= \frac{4m}{\hbar^2}J^2\frac{1}{R}\frac{1}{\pi}\int\frac{d^3k}{(2\pi)^3}\cos(kR)\cos(\mathbf{k}\cdot\mathbf{R}).\end{aligned}\tag{5.45}$$

Now, let us look at the triple integral

$$\begin{aligned}\int\frac{d^3k}{(2\pi)^3}\cos(kR)\cos(\mathbf{k}\cdot\mathbf{R}) &= \int_0^{2\pi}d\phi\int_0^{\pi}\int_0^{k_F}dkk^2\sin\theta\cos(kR)\cos(kR\cos\theta)\\ &= 2\pi\int_0^{k_F}dk\int_0^{\pi}d\theta k^2\sin\theta\cos(kR)\cos(kR\cos\theta)\\ &= 2\pi\int_0^{k_F}dkk^2\cos(kR)\int_0^{\pi}d\theta\sin\theta\cos(kR\cos\theta).\end{aligned}$$

In the above, the integration over θ gives

$$\int_0^{2\pi}d\theta\sin\theta\cos(kR\cos\theta)=\frac{2}{kR}\sin(kR).$$

Therefore, the RKKY coupling becomes

$$I^{3D}_{\mathrm{RKKY}}(\mathbf{R})=\frac{4m}{\hbar^2}J^2\frac{2}{(2\pi)^2}\frac{1}{R^2}\int_0^{k_F}k\sin(kR)\cos(kR)dk.\tag{5.46}$$

To perform the integral over k we define $x=kR$ and use

$$\int x\sin(x)\cos(x)dx=\frac{1}{8}[2x\cos(2x)-\sin(2x)]+\text{constant}.$$

Thus, we finally obtain

$$I^{3D}_{\mathrm{RKKY}}(\mathbf{R}) = \frac{4m}{\hbar^2} J^2 \frac{1}{4} \frac{k_F^4}{(2\pi)^2} F(2k_F R), \tag{5.47}$$

where

$$F(x) = \frac{x\cos(x) - \sin(x)}{x^4}. \tag{5.48}$$

From the result above is easy sse that in the asymptotic limit the RKKY coupling reduces to

$$I^{3D}_{\mathrm{RKKY}}(\mathbf{R}) \sim \frac{mJ^2}{8\hbar^2} \frac{k_F}{(2\pi)^2} \frac{\cos(2k_F R)}{R^3}, \qquad k_F R \gg 1. \tag{5.49}$$

Therefore, in 3D the RKKY interaction is oscillatory with precession $2k_F R$ and decay with $1/R^3$. From the equations (5.23), (5.39) and (5.49) we see that

$$I^{1D}_{\mathrm{RKKY}} \sim \frac{\cos(2k_F R)}{R}, \tag{5.50}$$

$$I^{2D}_{\mathrm{RKKY}} \sim \frac{\sin(2k_F R)}{R^2} \tag{5.51}$$

$$I^{3D}_{\mathrm{RKKY}} \sim \frac{\cos(2k_F R)}{R^3}. \tag{5.52}$$

The results obtained for one, two and three dimensions, reveal a pattern for the RKKY coupling is always oscillatory, with wave number $2k_F$ and decays with $1/R^D$. The physical meaning of this results it follows from the fact that the presence of the magnetic impurity generates a magnetic polarization of the conduction electrons which depends on the impurity position. The polarization effect decays as the distance from the impurity increases. We anticipate here that this scenario is drastically changed in 1D, when the electrons of the conduction sea presents spin-orbit coupling. Besides the characteristic Friedel oscillation $2k_F R$, another oscillation provide by the spin-orbit coupling is also present, and the RKKY coupling do not decay with the impurities distance anymore. Details of these results are given in the chapter 6.

5.2 Spin-orbit coupling

One of the most interesting effects in the quantum realm is the spin-orbit coupling (SOC) (THOMAS, 1926; SAKURAI, 2006). This effect arises from relativistic character of the electron moving around the atomic nuclei, where the electron "feels" an external electrostatic potential $V(r)$ (due the nuclei or some confining potential) and, as consequence, the momentum and spin of the electron are coupled. A general form for the spin-orbit Hamiltonian is given by

$$H_{SO} = -\frac{\hbar e}{4m^2c^2}(\boldsymbol{\sigma} \cdot \mathbf{p}) \times \nabla V(r), \tag{5.53}$$

where $\mathbf{p}$ is the electron momentum, m is the electron mass, c is the speed of light, e is the electron charge, $\hbar$ is the Planck's constant, and $\boldsymbol{\sigma}$ is the Pauli matrices vector $\boldsymbol{\sigma} = (\sigma^x, \sigma^y, \sigma^z)^T$. The SOC is important in atomic physics, for example, to explain specific lines in the atomic spectrum of some atoms (RADWANSKI et al., 2002).

The SOC plays also a fundamental role in the topological materials (QI; ZHANG, 2011; HASAN; KANE, 2010). This is the main reason why the influence of the SOC in solid state systems was object of extensively study in the last years. In solid state systems the two most important type of SOC are *Dresselhaus* and *Rashba*. The Hamiltonians for this SOC are

$$H_D = \beta(k_x\sigma_x - k_y\sigma_y), \qquad \text{(Dresselhaus)} \tag{5.54}$$

$$H_R = \alpha(k_x\sigma_y - k_y\sigma_x), \qquad \text{(Rashba)}. \tag{5.55}$$

The Dresselhaus SOC is present in materials with bulk inversion asymmetry, for example, ZnS, GaAs and Diamond (DRESSELHAUS, 1955; WINKLER, 2003). On the other hand, Rashba SOC appears in systems with structural inversion asymmetry. The principal example is a bi-dimensional electronic gas (2DEG) in the presence of a external electric field (WINKLER, 2003). Another example, where Rashba SOC is important, is one-dimensional systems as quantum wires (NADJ-PERGE et al., 2012). As we saw above, SOC is fundamental to the understanding of the many materials with a huge practical application. It is, therefore, important ask how SOC can modify the properties of magnetic systems and this is one of the main problem discussed in the next chapter.

6 Modified RKKY interaction in quantum nanowires with spin-orbit coupling

SOC coupling is fundamental in "spintronics", where the transport is realized by spins instead charge (Wolf; Chtchelkanova; Treger, 2006). The canonical example is the Datta-Das transistor, where is produced a highly spin-polarized current controlled via SOC by external electric field (DATTA; DAS, 1990). The addition of impurities in the theoretical calculations is essential, since it is difficult to obtain perfect clean experimental samples. The understanding of the long-range interactions between magnetic impurities in quantum wires with SOC obtained in the present work indicates how possible magnetic impurities can affect the dynamics of the systems with SOC, which is important for practical spintronics applications.

The first part of the present thesis was dedicated to the study of Majorana zero modes. MZMs can occurs in the non-trivial topological phase of topological superconducting quantum wires (QWs). A key ingredient to generates effective topological phases in QWs is the strong spin-orbit coupling of the QW electrons (ALICEA, 2012). The presence of impurities is almost inevitable in real samples. Form this perspective, it is clearly important to consider how the presence of impurities modifies the magnetic properties of QWs.

6.1 Description of the system

To address the question of how the presence of impurities can affect the properties of a QW with strong spin-orbit coupling we consider a system composed by a QW with Rashba spin-orbit coupling in the presence of two magnetic impurities [1], as depicted in figure17. The Hamiltonian of the system is given by

$$H = H_{\text{wire}} + H_1 + H_2, \tag{6.1}$$

where

$$H_{\text{wire}} = \sum_k \left(\varepsilon_k \delta_{ss'} - \alpha_R k \sigma^y_{ss'}\right) c^\dagger_{ks} c_{ks'} \tag{6.2}$$

describes the quantum wire in, which $d^\dagger_{ks}$ creates (annihilates) and electron with momentum k, spin s and energy ε_k. Here, $\varepsilon_k = \hbar^2 k^2 / 2m^*$, where m^* is the effective mass of the conduction electrons. The linear Rashba (WINKLER, 2003) spin-orbit coupling is described

[1] The authors showed in a previous work that the Dresselhaus and Rashba spin-orbit coupling can be treat in the same foot in a QW (SOUSA; SILVA; VERNEK, 2016). Thus, the consideration of only the Rashba spin-orbit interaction do not affect the generality of the results.

Figure 17 – Schematic representation of the system composed by two magnetic impurities coupled to a quantum wire with spin-orbit interaction. Blue arrows represents the magnetic moments of the impurities while green arrows represent the spins of the conduction electrons that precess due to the spin-orbit coupling. Figure published in (SILVA; VERNEK, 2019).

by the term proportional to α_{R}, with σ^{μ} representing the μ-th the Pauli matrix. Finally, the couplings between the impurities and the conduction band are described by a local Kondo-type interaction which is given by (NOLTING; RAMAKANTH, 2009)

$$H_i = \frac{J}{N}\sum_{kk'} e^{-i(k-k')x_i}\left[S_i^z\left(c_{k'\uparrow}^{\dagger}c_{k\uparrow} - c_{k'\downarrow}^{\dagger}c_{k\downarrow}\right) + S_i^{+}c_{k'\downarrow}^{\dagger}c_{k\uparrow} + S_i^{-}c_{k'\uparrow}^{+}c_{k\downarrow}\right], \tag{6.3}$$

where x_i (with $i = 1, 2$) is the position of the $i-$th impurity.

6.2 Effective inter-impurities Hamiltonian

To obtain the indirect interaction between the magnetic impurities, mediated by the QW conduction electrons, we will follow the original second order perturbative approach used by Ruderman and Kittel (RUDERMAN; KITTEL, 1954). The unperturbed Hamiltonian H_0 in this case is given by the QW wire Hamiltonian (6.2) and the magnetic impurities (6.3) acts as the system perturbation V. The traditional quantum perturbation theory is constructed using the unperturbed eigenstates and eigenenergies (see Appendix E). In the present case, spin-orbit interaction mixes the spin components $\{|k\uparrow\rangle, |k\downarrow\rangle\}$. Therefore, in the spin basis the QW Hamiltonian (6.2) is not diagonal which encumber the application of the quantum perturbation theory. This difficulty can be transposed performing a rotation which diagonalizes the QW Hamiltonian (6.2), this can be done using the transformation

$$\begin{pmatrix} c_{k\uparrow} \\ c_{k\downarrow} \end{pmatrix} = \mathcal{U}_k \begin{pmatrix} c_{k+} \\ c_{k-} \end{pmatrix}, \tag{6.4}$$

where

$$\mathcal{U}_k = \frac{1}{\sqrt{2}}\begin{pmatrix} 1 & 1 \\ -i & i \end{pmatrix}, \tag{6.5}$$

is an unitary rotation matrix. In other words, the transformation above corresponds to a momentum-dependent rotation in the spin space. In the new base H_{wire} acquires the diagonal form

$$\tilde{H}_{\mathrm{wire}} = \sum_{kh} \varepsilon_{kh} c_{kh}^{\dagger} c_{kh}, \tag{6.6}$$

in which $h = +, -$ is the helical quantum number and $\varepsilon_{kh} = \hbar k^2/2m^* + h\alpha_R k$ are the eigenvalues of H_{wire}. The eigenstates are then defined as $|k, h\rangle$ such that $H_{\text{wire}}|k, h\rangle = \varepsilon_{kh}|k, h\rangle$.

The perturbation Hamiltonian also should be given in the diagonal basis of the unperturbed Hamiltonian. For simplicity, here we assume impurities have spin 1/2, so that the spin operators can be easily written in terms of fermion operators as $S^z = (d^\dagger_\uparrow d_\uparrow - d^\dagger_\downarrow d_\downarrow)/2$, $S^+ = d^\dagger_\uparrow d_\downarrow$, and $S^- = d^\dagger_\downarrow d_\uparrow$, where $d^\dagger_s$ (d_s) corresponds to the creation (annihilation) spin-1/2 fermion operator. This is very useful because we can now perform the same rotation (6.4) for these fermion operators, after which we can rewrite (6.3) as

$$H_i = \frac{J}{N}\sum_{kk'} e^{-i(k-k')x_i}\left[\tilde{S}^z_i\left(c^\dagger_{k'+}c_{k+} - c^\dagger_{k'-}c_{k-}\right) + \tilde{S}^+_i c^\dagger_{k'-}c_{k+} + \tilde{S}^-_i c^\dagger_{k'+}c_{k-}\right]. \tag{6.7}$$

Here, the $\tilde{S}^z_i, \tilde{S}^\pm_i$ emphasizes that the impurity spin operators are written on the rotated spin basis. Having the eigenstates and eigenenrgies of the unperturbed Hamiltonian, the prescription to obtain the RKKY coupling is to compute the correction to the total energies up to the second order perturbation theory. To account for the degrees of freedom of the impurities, an eigenstate of H_{wire} can be written as $|kh\rangle$, where h is the helical quantum number. For the magnetic impurity we define the helical number $|h_d\rangle$ associated with the state $|h_d\rangle$. Then, the full eigenstate in the helical space will be denoted by $|kh, h_d\rangle$.

Using quantum perturbation theory, we can compute the eigenenergy correction created by the perturbation (6.7) until second order at temperature $T = 0$ (see Appendix E) by

$$\Delta E^{(2)} = \sum_{i=1,2}\sum_{h_d h'_d}\sum_{k,h}^{\text{occ.}}\sum_{k',h'}^{\text{empty}}\left[\frac{\langle kh, h_d|H_i|k'h', h'_d\rangle\langle k'h', h'_d|H_i|kh, h_d\rangle}{\varepsilon_{kh} - \varepsilon_{k'h'}}\right]. \tag{6.8}$$

The equation above can be written in a more explicit form as

$$\Delta E^{(2)} = \sum_{h_d h'_d}\sum_{k,h}^{\text{occ.}}\sum_{k',h'}^{\text{empty}}\left[\frac{\langle kh, h_d|(H_1+H_2)|k'h', h'_d\rangle\langle k'h', h'_d|(H_1+H_2)|kh, h_d\rangle}{\varepsilon_{kh} - \varepsilon_{k'h'}}\right].$$

The product $\langle kh, h_d|(H_1 + H_2)|k'h', h'_d\rangle\langle k'h', h'_d|(H_1 + H_2)|kh, h_d\rangle$ generates four different processes. Two of them, $\langle kh, h_d|H_{1(2)}|k'h', h'_d\rangle\langle k'h', h'_d|H_{1(2)}|kh, h_d\rangle$ are impurities self-interactions, the others two, $\langle kh, h_d|H_1|k'h', h'_d\rangle\langle k'h', h'_d|H_2|kh, h_d\rangle$, and their conjugated hermitian, corresponds to mutual inter-impurities interaction. All terms of ΔE are necessary to compute the new ground-state in the presence of the perturbation. However, only the mixed terms are directly associated with the interaction among the impurities. Therefore, the energy correction due the inter-impurities interaction is

$$\begin{aligned}\Delta E^{(2)}_{\text{mixed}} &= \sum_{h_d h'_d}\sum_{k,h}^{\text{occ.}}\sum_{k',h'}^{\text{empty}}\frac{\langle kh, h_d|H_1|k'h', h'_d\rangle\langle k'h', h'_d|H_2|kh, h_d\rangle}{\varepsilon_{kh} - \varepsilon_{k'h'}} \\ &+ \sum_{h_d h'_d}\sum_{k,h}^{\text{occ.}}\sum_{k',h'}^{\text{empty}}\frac{\langle kh, h_d|H_2|k'h', h'_d\rangle\langle k'h', h'_d|H_1|kh, h_d\rangle}{\varepsilon_{kh} - \varepsilon_{k'h'}}.\end{aligned} \tag{6.9}$$

To evaluated the non vanish term of ΔE_{mixed} we apply the creation and annihilation operator in the helical eigenstates. As example, let us take the term $\tilde{S}_z c^\dagger_{k'+} c_{k+}|k+,h_d\rangle = \tilde{S}_z|k'+,h_d\rangle$, $\tilde{S}_+ c^\dagger_{k'-} c_{k+}|k+,h_d\rangle = \tilde{S}_+|k'-,h_d\rangle$, $\tilde{S}_- c^\dagger_{k'+} c_{k-}|k-,h_d\rangle = \tilde{S}_-|k'+,h_d\rangle$. After perform some operator algebra, together with the orthogonality relation $\langle kh|k'h'\rangle = \delta_{kk'}\delta_{hh'}$, we obtain the non-vanishing terms of $\langle kh,h_d|H_1|k'h',h_d^{'}\rangle$

$$\begin{aligned}
\langle k+,h_d|H_1|k'+,h_d^{'}\rangle &= \frac{J}{N}\sum_{kk'} e^{i(k-k')x_1}\langle h_d|\tilde{S}_{1z}|h_d^{'}\rangle,\\
\langle k-,h_d|H_1|k'-,h_d^{'}\rangle &= -\frac{J}{N}\sum_{kk'} e^{i(k-k')x_1}\langle h_d|\tilde{S}_{1z}|h_d^{'}\rangle,\\
\langle k-,h_d|H_1|k'+,h_d^{'}\rangle &= \frac{J}{N}\sum_{kk'} e^{i(k-k')x_1}\langle h_d|\tilde{S}_{1+}|h_d^{'}\rangle,\\
\langle k+,h_d|H_1|k'-,h_d^{'}\rangle &= \frac{J}{N}\sum_{kk'} e^{i(k-k')x_1}\langle h_d|\tilde{S}_{1-}|h_d^{'}\rangle.
\end{aligned}$$

Similar calculations can be done for H_2. In the helical space the energy denominator $\varepsilon_{kh'} - \varepsilon_{kh}$ depends on the helical index, $h = \pm$. The possible energy denominators are

$$\begin{aligned}
\varepsilon_{k+} - \varepsilon_{k'+} &= \frac{\hbar^2}{2m^*}(k^2 - k'^2) + \alpha_R(k - k'),\\
\varepsilon_{k-} - \varepsilon_{k'-} &= \frac{\hbar^2}{2m^*}(k^2 - k'^2) - \alpha_R(k - k'),\\
\varepsilon_{k-} - \varepsilon_{k'+} &= \frac{\hbar^2}{2m^*}(k^2 - k'^2) - \alpha_R(k + k'),\\
\varepsilon_{k+} - \varepsilon_{k'-} &= \frac{\hbar^2}{2m^*}(k^2 - k'^2) + \alpha_R(k + k').
\end{aligned}$$

Then, the calculation of ΔE_{mixed} results

$$\begin{aligned}
\Delta E^{(2)}_{\text{mixed}} &= \sum_{h_d}\Big[(I_{++} + I^*_{++} + I_{--} + I^*_{--})\langle h_d|\tilde{S}^z_1\tilde{S}^z_2|h_d\rangle + (I_{-+} + I^*_{+-})\langle h_d|\tilde{S}^+_1\tilde{S}^-_2|h_d\rangle\\
&\quad + (I_{+-} + I^*_{-+})\langle h_d|\tilde{S}^-_1\tilde{S}^+_2|h_d\rangle\Big]\\
&= \sum_{h_d}\langle h_d|H_{\text{imp}}|h_d\rangle. \qquad (6.10)
\end{aligned}$$

Where

$$H_{\text{imp}} = (I_{++} + I^*_{++} + I_{--} + I^*_{--})\tilde{S}^z_1\tilde{S}^z_2 + (I_{-+} + I^*_{+-})\tilde{S}^+_1\tilde{S}^-_2 + (I_{+-} + I^*_{-+})\tilde{S}^-_1\tilde{S}^+_2, \quad (6.11)$$

describes the effective inter-impurities interaction Hamiltonian and

$$I_{\delta\nu} = \frac{J^2}{N^2}\sum_{k}^{\text{occupied}}\sum_{k'}^{\text{empty}}\frac{e^{i(k-k')x}}{\frac{\hbar^2}{2m^*}(k^2 - k'^2) + \delta\alpha_{\text{R}}(k - \delta\nu k')}, \quad (6.12)$$

in which $x = x_2 - x_1$ is the distance between the impurities. The effective Hamiltonian (6.11) can be written in a more compact form

$$\tilde{H}_{\text{imp}} = I_{\parallel}\tilde{S}^z_1\tilde{S}^z_2 + I_{\perp}\tilde{S}^+_1\tilde{S}^-_2 + I^*_{\perp}\tilde{S}^-_2\tilde{S}^+_1, \quad (6.13)$$

where we have defined $I_{\parallel} = 2\mathrm{Re}\,(I_{++} + I_{--})$ e $I_{\perp} = (I_{-+} + I^{*}_{+-})$. We now transform the summations into integrals using the usual prescription $(1/N)\sum_k \to (1/2\pi \int dk)$ in the limit $N \to \infty$, so that the Eq. (6.12) can now be written as

$$I_{\delta\nu} = J^2 \int_{-k_\delta}^{k_\delta} \frac{dk}{2\pi} \int_{|k'|>k_\delta} \frac{dk'}{2\pi} \frac{e^{i(k-k')x}}{\frac{\hbar^2}{2m^*}(k^2 - k'^2) + \delta\alpha_{\mathrm{R}}(k - \delta\nu k')}. \tag{6.14}$$

Here we also used the fact that, because of the SOC, the bands + and − have different Fermi momenta, namely $k_\delta = k_F + \delta k_{\mathrm{R}}$ (for $\delta = +, -$). In the helical basis, the Hamiltonian (6.13) has the form of a anisotropic Heisenberg Hamiltonian. The physical insight of the Hamiltonian (6.13) is better understood in the real spin space. To do so we perform the rotation

$$\begin{pmatrix} d_+ \\ d_- \end{pmatrix} = \frac{1}{\sqrt{2}} \begin{pmatrix} 1 & i \\ 1 & -i \end{pmatrix} \begin{pmatrix} d_\uparrow \\ d_\downarrow \end{pmatrix}, \tag{6.15}$$

in the helical spin operators $\tilde{S}^z = (n_{d+} - n_{d-})/2$, $\tilde{S}^+ = d^\dagger_+ d_-$, $\tilde{S}^- = d^\dagger_- d_+$, $\tilde{S}^+ = \tilde{S}^x + i\tilde{S}^y$, and $\tilde{S}^- = \tilde{S}^x - i\tilde{S}^y$ resulting the relations

$$\tilde{S}^+_1 \tilde{S}^-_2 = \mathbf{S}_1 \cdot \mathbf{S}_2 + i(\mathbf{S}_1 \times \mathbf{S}_2) \cdot \hat{y} - S^y_1 S^y_2, \tag{6.16}$$

$$\tilde{S}^-_1 \tilde{S}^+_2 = \mathbf{S}_1 \cdot \mathbf{S}_2 - i(\mathbf{S}_1 \times \mathbf{S}_2) \cdot \hat{y} - S^y_1 S^y_2 \tag{6.17}$$

and

$$\tilde{S}^z_1 \tilde{S}^z_2 = S^y_1 S^y_2, \tag{6.18}$$

which applied in (6.13) results in the Hamiltonian

$$\tilde{H}_{\mathrm{imp}} = I_{\mathrm{RKKY}} \mathbf{S}_1 \cdot \mathbf{S}_2 + I_{\mathrm{DM}}[(\mathbf{S}_1 \times \mathbf{S}_2) \cdot \hat{\mathbf{y}}] + I_{\mathrm{Ising}} S^y_1 S^y_2. \tag{6.19}$$

Where, $I_{\mathrm{RKKY}} = 2\mathrm{Re}\,[I_\perp]$, $I_{\mathrm{DM}} = -2\mathrm{Im}\,[I_\perp]$ and $I_{\mathrm{Ising}} = I_\parallel - 2\mathrm{Re}\,[I_\perp]$ are the known RKKY, Dzyaloshinskii-Moriya the Ising couplings (DZYALOSHINSKY, 1958; MORIYA, 1960; MROSS; JOHANNESSON, 2009).

6.2.1 Analytical calculation of the couplings

We now focus on the calculation of the couplings I_{RKKY}, I_{DM} and I_{Ising}. This requires performing the integrals (6.14). To simplify the notation we define the dimensionless variables $q = k/k_{\mathrm{F}}$, $q' = k'/k_{\mathrm{F}}$, together with $a = 2k_{\mathrm{R}}$, with $k_{\mathrm{R}} = m\alpha_{\mathrm{R}}/\hbar^2$, and $\tilde{a} = a/k_{\mathrm{F}}$. With these definitions the Eq. (6.14) acquires the form

$$I_{\delta\nu} = I_0 \int_{-q_\delta}^{q_\delta} dq \int_{|q'|>q_\delta} dq' \frac{e^{i(q-q')k_F x}}{(q^2 - q'^2) + \delta\tilde{a}(q - \delta\nu q')}, \tag{6.20}$$

where $I_0 = J^2 m/2\pi^2\hbar^2$, and $q_\delta = 1 + \delta\tilde{a}/2$. An important point here that should be highlighted is that the order of the integrations above should not be changed as discussed by Yafet (YAFET, 1987). Later, Valizedeh (VALIZADEH, 2016) revisited the problem

and noted that the problem is that the integrals (6.14) do not obey the Fubini's condition (FUBINI; ITALIANA, 1957), leading to different results depending on the order in which the integrations are performed. Here we keep the order of integrations as it is in Eq. (6.14), avoiding the aforementioned problem. To perform the integral over q using the residues theorem we need to extend it to the entire real axis. With this we can write

$$I^{r}_{\delta\nu} = I_0 \int_{-q_\delta}^{q_\delta} dq \int_{-\infty}^{\infty} dq' \frac{e^{i(q-q')k_F x}}{(q^2 - q'^2) + \delta\tilde{a}(q - \delta\nu q')}. \tag{6.21}$$

This deformation of the integral limits introduce undesirable contributions. If we are able to account for these extra contributions separately, we can subtract them from the final results to obtain the correct expression. In the absence of SOC, the integrand of (6.21) is antisymmetric under the exchange $q \longleftrightarrow q'$, thus the extra contributions added to the results are solely those coming from corresponds to the singularities occurring at $q = q'$. However, in the presence of the SOC ($\tilde{a} \neq 0$) the integrand is no longer antisymmetric. Therefore, there are contributions other than those arising from the singularities. Here we will assume that the only relevant additional contributions are those arising from the singularities of (6.21). Thus, withing this approximation, we can write $I_{\delta\nu} = I^{r}_{\delta\nu} - I^{\epsilon}_{\delta\nu}$, where and $I^{\epsilon}_{\delta\nu}$ corresponds to the undesirable singularities. We first integrate over q' and then over q. The Eq. (6.21) can be written as

$$I^{r}_{\delta\nu} = I_0 \int_{-q_\delta}^{q_\delta} dq I^{rq}_{\delta\nu}, \tag{6.22}$$

where we have defined

$$I^{rq}_{\delta\nu} = \mathcal{P} \oint dz \frac{e^{i(q-z)k_F x}}{(q^2 - z^2) + \delta\tilde{a}(q - \delta\nu z)}. \tag{6.23}$$

In the above $\mathcal{P}[\cdots]$ denote the Cauchy principal value (see Appendix F).

Let us start with by calculating I^{rq}_{++} that has the form

$$I^{rq}_{++} = \mathcal{P} \oint dz \frac{e^{i(q-z)k_F x}}{q^2 - z^2 + \tilde{a}(q - z)}, \tag{6.24}$$

Closing the contour on the lower half-plane and using the residues theorem we obtain

$$\mathcal{P}[I^{rq}_{++}] = \frac{2\pi}{2q + \tilde{a}} \sin[(q + \tilde{a}/2)k_F x] e^{i(q+\tilde{a}/2)k_F x}. \tag{6.25}$$

Noticing from 6.21 that we can obtain I^{rq}_{--} by doing $\tilde{a} \to -\tilde{a}$ in the Eq.(6.25). Therefore we immediately obtain

$$\mathcal{P}[I^{rq}_{--}] = \frac{2\pi}{2q - \tilde{a}} \sin[(q - \tilde{a}/2)k_F x] e^{i(q-\tilde{a}/2)k_F x}. \tag{6.26}$$

Proceeding in a similar way for the other two integrals we obtain

$$\mathcal{P}[I^{rq}_{+-}] = \frac{2\pi}{2q + \tilde{a}} \sin[(q + \tilde{a}/2)k_F x] e^{i(q-\tilde{a}/2)k_F x}, \tag{6.27}$$

and

$$\mathcal{P}[I^{rq}_{-+}] = \frac{2\pi}{2q-\tilde{a}}\sin[(q-\tilde{a}/2)k_Fx]e^{i(q+\tilde{a}/2)k_Fx}. \tag{6.28}$$

Collecting the results (6.25)-(6.28) and grouping then properly, we obtain

$$\begin{aligned} I^r_{\rm RKKY} = 2{\rm Re}\,(I^r_{-+}+I^r_{+-*}) &= 4\pi I_0\left[\int_{-q_+}^{q_+}dq\frac{\cos[(q-\tilde{a}/2)k_Fx]\sin[(q+\tilde{a}/2)k_Fx]}{2q+\tilde{a}}\right. \\ &\left.+\int_{-q_-}^{q_-}dq\frac{\cos[(q+\tilde{a}/2)k_Fx]\sin[(q-\tilde{a}/2)k_Fx]}{2q-\tilde{a}}\right], \end{aligned} \tag{6.29}$$

$$\begin{aligned} I^r_{\rm DM} = -2{\rm Im}\,(I^r_{-+}+I^r_{+-*}) &= -4\pi I_0\left[\int_{-q_-}^{q_-}dq\frac{\sin[(q+\tilde{a}/2)k_Fx]\sin[(q-\tilde{a}/2)k_Fx]}{2q-\tilde{a}}\right. \\ &\left.-\int_{-q_+}^{q_+}dq\frac{\sin[(q+\tilde{a}/2)k_Fx]\sin[(q-\tilde{a}/2)k_Fx]}{2q+\tilde{a}}\right], \end{aligned} \tag{6.30}$$

and

$$\begin{aligned} I^r_{\rm Ising} = 2{\rm Re}\,(I^r_{++}+I^r_{--}) - I^r_{\rm RKKY} &= 2\pi I_0\left[\int_{-q_+}^{q_+}dq\frac{\sin[(2q+\tilde{a})k_Fx]}{2q+\tilde{a}}\right. \\ &\left.+\int_{-q_-}^{q_-}dq\frac{\sin[(2q-\tilde{a})k_Fx]}{2q-\tilde{a}}\right] - I^r_{\rm RKKY}. \end{aligned} \tag{6.31}$$

The superindices "r" denotes the uncorrected results, i.e., before subtracting the extra contribution. The six integrals appearing in the expressions (6.29)-(6.31) above are rather complicated but can still be can be computed analytically. After a tiresome work, apart from additive constants, we obtain the expressions for the undefined integrals

$$\int dq\frac{\sin[(2q+\tilde{a})k_Fx]}{2q+\tilde{a}} = \frac{1}{2}{\rm Si}[(2q+\tilde{a})k_Fx], \tag{6.32}$$

$$\int dq\frac{\sin[(2q-\tilde{a})k_Fx]}{2q-\tilde{a}} = \frac{1}{2}{\rm Si}[(2q-\tilde{a})k_Fx], \tag{6.33}$$

$$\begin{aligned} \int dq\frac{\cos[(q-\tilde{a}/2)k_Fx]\sin[(q+\tilde{a}/2)k_Fx]}{2q+\tilde{a}} &= \frac{1}{4}\Big\{-\sin(\tilde{a}k_Fx){\rm Ci}[(2q+\tilde{a})k_Fx] \\ &+\cos(\tilde{a}k_Fx){\rm Si}[(2q+\tilde{a})k_Fx] \\ &+\sin(\tilde{a}k_Fx)\ln[2(2q+\tilde{a})]\Big\}, \end{aligned} \tag{6.34}$$

$$\begin{aligned} \int dq\frac{\cos[(q+\tilde{a}/2)k_Fx]\sin[(q-\tilde{a}/2)k_Fx]}{2q-\tilde{a}} &= \frac{1}{4}\Big\{\sin(\tilde{a}k_Fx){\rm Ci}[(2q-\tilde{a})k_Fx] \\ &-\cos(\tilde{a}k_Fx){\rm Si}[(\tilde{a}-2q)k_Fx] \\ &-\sin(\tilde{a}k_Fx)\ln[2(\tilde{a}-2q)]\Big\}, \end{aligned} \tag{6.35}$$

$$\int dq \frac{\sin[(q-\tilde{a}/2)k_F x]\sin[(q+\tilde{a}/2)k_F x]}{2q+\tilde{a}} = \frac{1}{4}\Big\{ -\cos(\tilde{a}k_F x)\mathrm{Ci}[(2q+\tilde{a})k_F x] - \sin(\tilde{a}k_F x)\mathrm{Si}[(2q+\tilde{a})k_F x] + \cos(\tilde{a}k_F x)\ln[2(2q+\tilde{a})]\Big\}, \quad (6.36)$$

and

$$\int dq \frac{\sin[(q+\tilde{a}/2)k_F x]\sin[(q-\tilde{a}/2)k_F x]}{2q-\tilde{a}} = \frac{1}{4}\Big\{ -\cos(\tilde{a}k_F x)\mathrm{Ci}[(2q-\tilde{a})k_F x] - \sin(\tilde{a}k_F x)\mathrm{Si}[(\tilde{a}-2q)k_F x] + \cos(\tilde{a}k_F x)\ln[2(\tilde{a}-2q)]\Big\}. \quad (6.37)$$

In the above we use the usual definitions

$$\mathrm{Ci}(x) = \int_0^x \frac{\cos(t)}{t}dt \qquad \text{and} \qquad \mathrm{Si}(x) = \int_0^x \frac{\sin(t)}{t}dt. \quad (6.38)$$

After imposing the proper limits to the results (6.32)-(6.37) and some algebraic manipulations we can write

$$I^r_{\mathrm{RKKY}} = \pi I_0\Big\{ \sin(\tilde{a}k_F x)\Big[\mathrm{Ci}\left[(1-\tilde{a})2k_F x\right] - \mathrm{Ci}\left[(1+\tilde{a})2k_F x\right]\Big] + \cos(\tilde{a}k_F x)\Big[\mathrm{Si}\left[(1+\tilde{a})2k_F x\right] - \mathrm{Si}\left[(\tilde{a}-1)2k_F x\right] + 2\mathrm{Si}(2k_F x)\Big] - \ln\left|\frac{1-\tilde{a}}{1+\tilde{a}}\right|\sin(\tilde{a}k_F x)\Big\}, \quad (6.39a)$$

$$I^r_{\mathrm{DM}} = -\pi I_0\Big\{ \cos(\tilde{a}k_F x)\Big[\mathrm{Ci}\left[(1+\tilde{a})2k_F x\right] - \mathrm{Ci}\left[(1-\tilde{a})2k_F x\right]\Big] + \sin(\tilde{a}k_F x)\Big[\mathrm{Si}\left[(1+\tilde{a})2k_F x\right] - \mathrm{Si}\left[(\tilde{a}-1)2k_F x\right] + 2\mathrm{Si}(2k_F x)\Big] + \ln\left|\frac{1-\tilde{a}}{1+\tilde{a}}\right|\cos(\tilde{a}k_F x)\Big\}, \quad (6.39b)$$

$$I^r_{\mathrm{Ising}} = 2\pi I_0\Big[\mathrm{Si}((1+\tilde{a})2k_F x) - \mathrm{Si}\left[(\tilde{a}-1)2k_F x\right]\Big] - I^r_{\mathrm{RKKY}}. \quad (6.39c)$$

To obtain the final results we still need to compute the contribution from the singularities of the integrals (6.21).

6.2.1.1 Contribution from the singularities

To compute the contributions from the singularities we use the same method applied to the traditional RKKY problem in 1D (VALIZADEH, 2016; RUSIN; ZAWADZKI, 2017). Let us start with the integral

$$I_{++} = I_0 \int_{-q_+}^{q_+} dq \int_{|q'|>q_+} dq' \frac{e^{i(q-q')k_F x}}{q^2 - q'^2 + \tilde{a}(q-q')}. \quad (6.40)$$

The singularities of this integral occur when $(q-q')=0$ and $(q+q+\tilde{a})=0$ or $q'=-\tilde{a}/2$ and $q=-\tilde{a}/2$. In the following we calculate the integral above around $q=q'=\tilde{a}/2$. At

this point we have $e^{i(q-q')k_F x} = e^{i(-\tilde{a}+\tilde{a})k_F x/2} = 1$. Therefore,

$$I^{\epsilon}_{++} = \int_{-\frac{\tilde{a}}{2}-\epsilon}^{-\frac{\tilde{a}}{2}+\epsilon} dq \int_{-\frac{\tilde{a}}{2}-\epsilon}^{-\frac{\tilde{a}}{2}+\epsilon} \frac{dq'}{(q-q')(q+q'+\tilde{a})}, \qquad (\text{for } \epsilon \to 0^+) \tag{6.41}$$

The integral over q' variable can be calculated analytically using

$$\int \frac{dx}{(y-x)(y+x+a)} = \frac{\ln(-a-x-y) - \ln(y-x)}{2y+a} + \text{constant}. \tag{6.42}$$

Imposing the limits, after some algebraic manipulation we obtain

$$I^{\epsilon}_{++} = \int_{-\frac{\tilde{a}}{2}-\epsilon}^{-\frac{\tilde{a}}{2}+\epsilon} dq \frac{\ln|(q+\tilde{a}/2)+\epsilon| - \ln|(q+\tilde{a}/2)-\epsilon|}{q+\tilde{a}/2} \tag{6.43}$$

Performing the variable change $x = q + \tilde{a}/2$ the above integral becomes

$$I^{\epsilon}_{++} = \int_{-\epsilon}^{\epsilon} dx \left[\frac{\ln|x+\epsilon|}{x} - \frac{\ln|x-\epsilon|}{x}\right]. \tag{6.44}$$

This expression can be solved as written as

$$I^{\epsilon}_{++} = \int_{-1}^{1} du \left[\frac{\ln|1+u|}{u} - \frac{\ln|1-u|}{x}\right] = 2\text{Li}_2(1) - 2\text{Li}_2(-1) = \frac{\pi^2}{2}, \tag{6.45}$$

where

$$\text{Li}_2(x) = -\int_0^x \frac{\ln|1-t|}{t} dt \tag{6.46}$$

is the Dilogarithmic function. In the last line passage in (6.45) we have used (GRADSHTEYN; RYZHIK, 1980) $\text{Li}_2(1) = \pi^2/6$ and $\text{Li}_2(-1) = -\pi^2/12$.

Likewise, we can show that

$$I^{\epsilon}_{--} = \frac{\pi^2}{2}. \tag{6.47}$$

The others two integrals render slightly different results. Let us look at the correction for

$$I_{+-} = I_0 \int_{-q_+}^{q_+} dq \int_{-\infty}^{\infty} dq' \frac{e^{i(q-q')k_F x}}{q^2 - q'^2 + \tilde{a}(q+q')}. \tag{6.48}$$

Here the contribution are accounted when $(q+q') = 0$ and $(q-q'+\tilde{a}) = 0$, from which we extract $q' = \tilde{a}/2$ and $q = -\tilde{a}/2$. At this point, $e^{i(q-q')k_F x} = e^{i(-\tilde{a}-\tilde{a})k_F x/2} = e^{-i\tilde{a}k_F x}$, so that

$$I^{\epsilon}_{+-} = e^{-i\tilde{a}k_F x} \int_{-\frac{\tilde{a}}{2}-\epsilon}^{-\frac{\tilde{a}}{2}+\epsilon} dq \int_{\frac{\tilde{a}}{2}-\epsilon}^{\frac{\tilde{a}}{2}+\epsilon} \frac{dq'}{(q+q')(q-q'+\tilde{a})}. \tag{6.49}$$

Using the indefinite integral

$$\int \frac{dx}{(y+x)(y-x+a)} = \frac{\ln(y+x) - \ln(-a+x-y)}{2y+a} + \text{constant}, \tag{6.50}$$

we obtain

$$I^{\epsilon}_{+-} = e^{-i\tilde{a}k_F x}\int_{-\frac{\tilde{a}}{2}-\epsilon}^{-\frac{\tilde{a}}{2}+\epsilon} dq \frac{\ln|(q+\tilde{a}/2)+\epsilon| - \ln|(q+\tilde{a}/2)-\epsilon|}{q+\tilde{a}/2}. \tag{6.51}$$

Apart from the prefactor $e^{-i\tilde{a}k_F x}$, this is the same as in (6.43), therefore,

$$I^{\epsilon}_{+-} = \frac{\pi^2}{2}e^{-i\tilde{a}k_F x}. \tag{6.52}$$

The last correction, for I^{r}_{-+}, can be obtained using same argument of changing $\tilde{a} \to -\tilde{a}$ in (6.52), leading to

$$I^{\epsilon}_{-+} = \frac{\pi^2}{2}e^{i\tilde{a}k_F x}. \tag{6.53}$$

Colecting the results of (6.45), (6.47), (6.52) and (6.53) we obtain the corrections for the couplings

$$I^{\epsilon}_{\text{RKKY}} = 2\text{Re}\left(I^{\epsilon}_{-+} + I^{\epsilon}_{+-*}\right) = 4\pi I_0\left[\frac{\pi}{2}\cos(\tilde{a}k_F x)\right], \tag{6.54a}$$

$$I^{\epsilon}_{\text{DM}} = -2\text{Im}\left(I^{\epsilon}_{-+} + I^{\epsilon}_{+-*}\right) = -4\pi I_0\left[\frac{\pi}{2}\sin(\tilde{a}k_F x)\right], \tag{6.54b}$$

$$I^{\epsilon}_{\text{Ising}} = 2\text{Re}\left(I^{\epsilon}_{++} + I^{\epsilon}_{--}\right) - I^{\epsilon}_{\text{RKKY}} = 4\pi I_0\left(\frac{\pi}{2}\right) - I^{\epsilon}_{\text{RKKY}}. \tag{6.54c}$$

We now subtract the results of the Eqs. (6.54) from those of Eqs. (6.39) to obtain our final analytical results for the indirect coupling

$$\begin{aligned} I_{\text{RKKY}} = {} & \pi I_0\Big\{\sin(\tilde{a}k_F x)\Big[\text{Ci}\left[(1-\tilde{a})2k_F x\right] - \text{Ci}\left[(1+\tilde{a})2k_F x\right]\Big] \\ & + \cos(\tilde{a}k_F x)\Big[\text{Si}\left[(1+\tilde{a})2k_F x\right] - \text{Si}\left[(\tilde{a}-1)2k_F x\right] + 2\text{Si}(2k_F x)\Big] \\ & - \ln\left|\frac{1-\tilde{a}}{1+\tilde{a}}\right|\sin(\tilde{a}k_F x)\Big\} - 4\pi I_0\left[\frac{\pi}{2}\cos(\tilde{a}k_F x)\right], \end{aligned} \tag{6.55a}$$

$$\begin{aligned} I_{\text{DM}} = {} & -\pi I_0\Big\{\cos(\tilde{a}k_F x)\Big[\text{Ci}\left[(1+\tilde{a})2k_F x\right] - \text{Ci}\left[(1-\tilde{a})2k_F x\right]\Big] \\ & + \sin(\tilde{a}k_F x)\Big[\text{Si}\left[(1+\tilde{a})2k_F x\right] - \text{Si}\left[(\tilde{a}-1)2k_F x\right] + 2\text{Si}(2k_F x)\Big] \\ & + \ln\left|\frac{1-\tilde{a}}{1+\tilde{a}}\right|\cos(\tilde{a}k_F x)\Big\} + 4\pi I_0\left[\frac{\pi}{2}\sin(\tilde{a}k_F x)\right], \end{aligned} \tag{6.55b}$$

$$I_{\text{Ising}} = 2\pi I_0\Big[\text{Si}\left[(1+\tilde{a})2k_F x\right] - \text{Si}\left[(\tilde{a}-1)2k_F x\right]\Big] - 4\pi I_0\left(\frac{\pi}{2}\right) - I_{\text{RKKY}}. \tag{6.55c}$$

Notice that if we take $\tilde{a} = 0$ the usual result $I_{\text{RKKY}} = 4\pi I_0\left[\text{Si}(2k_F x) - \pi/2\right]$ and $I_{\text{DM}} = I_{\text{Ising}} = 0$ is recovered, as expected. Interestingly, however, is the asymptotic behavior of these expressions, using the asymptotic expansion for the cosine and sine function (GRADSHTEYN; RYZHIK, 1980)

$$\text{Si}(x) \sim \frac{\pi}{2} + \frac{\cos(x)}{x}\sum_{n=0}^{\infty}(-1)^n\frac{2n!}{x^{2n}} - \frac{\sin(x)}{x}\sum_{n=0}^{\infty}(-1)^n\frac{(2n+1)!}{x^{2n+1}}, \tag{6.56}$$

$$\text{Ci}(x) \sim \frac{\sin(x)}{x}\sum_{n=0}^{\infty}(-1)^n\frac{2n!}{x^{2n}} - \frac{\cos(x)}{x}\sum_{n=0}^{\infty}(-1)^n\frac{(2n+1)!}{x^{2n+1}}, \tag{6.57}$$

we get the asymptotic couplings

$$I_{\mathrm{RKKY}} = -\pi I_0 \ln\left|\frac{k_{\mathrm{F}}-2k_{\mathrm{R}}}{k_{\mathrm{F}}+2k_{\mathrm{R}}}\right| \sin(2k_{\mathrm{R}}x), \tag{6.58a}$$

$$I_{\mathrm{DM}} = -\pi I_0 \ln\left|\frac{k_{\mathrm{F}}-2k_{\mathrm{R}}}{k_{\mathrm{F}}+2k_{\mathrm{R}}}\right| \cos(2k_{\mathrm{R}}x), \tag{6.58b}$$

$$I_{\mathrm{Ising}} = \pi I_0 \ln\left|\frac{k_{\mathrm{F}}-2k_{\mathrm{R}}}{k_{\mathrm{F}}+2k_{\mathrm{R}}}\right| \sin(2k_{\mathrm{R}}x). \tag{6.58c}$$

Where we use $\lim_{x\to\infty} \mathrm{Ci}(x) = 0$, and $\lim_{x\to\infty} \mathrm{Si}(x) = \pi/2$. These unsuppressed oscillations appearing in these asymptotic expressions is one of the principal result of the present thesis. In the next section we will discuss the physical meaning of the undamped oscillations.

6.2.2 Physical meaning of the asymptotic behavior

The unsuppressed oscillations obtained here can be understood as follows: after a given electron is scattered by the first impurity, it travels throughout the quantum wire while its spin precesses due to the SOC. Since the momentum and spin are coupled together, this precession continues coherent until it collides with the second impurity. Here, the momentum-spin lock produced by the time-reversal symmetry of the SOC in this 1D system provides a natural protection (not topological) that prevents the suppression of the couplings. To provide a better physical intuition, let us analyze the scattering processes involved in the second order perturbation theory. We already saw that if we write the Kondo Hamiltonian onto the Rashba basis we obtain

$$H_i = \frac{J}{N}\sum_{kk'} e^{-i(k-k')x_i}\left[\tilde{S}_i^z\left(c_{k'+}^\dagger c_{k-} - c_{k'-}^\dagger c_{k+}\right) + \tilde{S}_i^+ c_{k'}^\dagger c_{k+} + \tilde{S}_i^- c_{k'+}^+ c_{k-}\right]. \tag{6.59}$$

Again, the tilde on the spin operators emphasizes that they are also written on the Rashba basis, meaning that the "spin" scattering processes correspond to removing electrons from one band to another. Although the processes formally very much similar to those ones that occur in the absence of the SOC. Here, by virtue of the shift property $\varepsilon_+(k) = \varepsilon_-(k+Q)$ (where $Q = 2k_{\mathrm{R}}$), the spin-flip processes in the second order perturbation theory involve intermediate states whose momenta is separated from the initial states by $2k_{\mathrm{R}}$ (for forward scattering process) or $2k_{\mathrm{F}}$ (for backscattering processes), see figure 18. In this sense, at zero temperature, conserving momenta scatterings are prevented by the SOC, which inhibits the decay of the couplings in the system. This analysis also allows us to understand enhancement of the oscillation amplitudes of Eqs. (6.58). When $k_{\mathrm{F}} \longrightarrow 2k_{\mathrm{R}}$ the Fermi momenta matches precisely the distance (in the momentum space) between the two bands, providing a resonant forward scattering. In reality, similarly to all the traditional approach to RKKY interaction, our results are limited distances smaller than the coherent length of the material. For distances larger than this characteristic length, other scattering processes have to be taken into account in the conduction electron propagation.

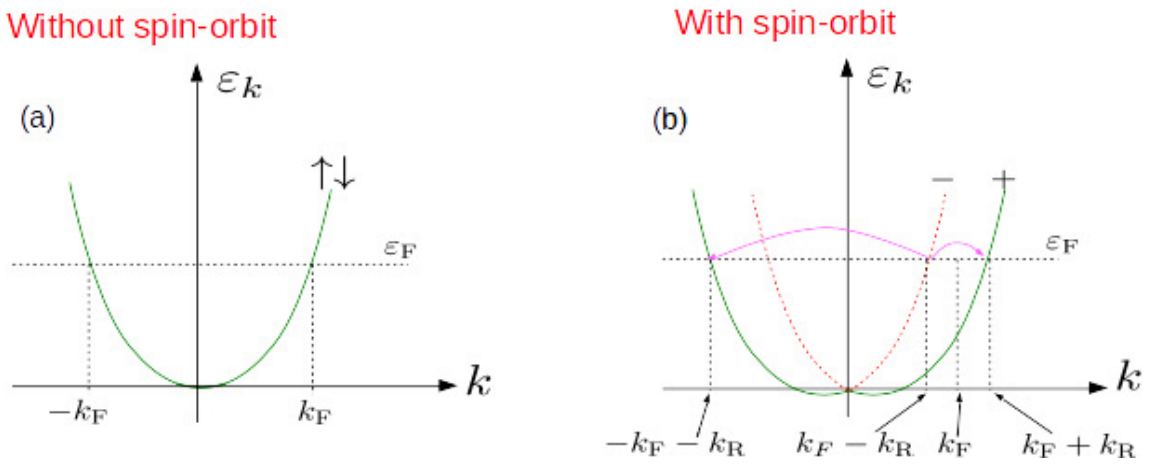

Figure 18 – (a) Dispersion relation in the absence of spin-orbit. (b) Dispersion relation in the presence of spin-orbit. The figure (b) shows the possible scattering process in the presence of magnetic impurities.

Somewhat similar to our results was found by J. Simonin (SIMONIN, 2006). He has found a spin-spin correlation between two magnetic moments induced by SOC that extends also to distances longer than those of the traditional RKKY interaction. Our results also resemble the persistent spin helix (BERNEVIG; ORENSTEIN; ZHANG, 2006) in which a "right" combination of Rashba and Dresselhaus SOCs produces a long lived spin excitation in the system. This contrasts with the traditional scattering in the absence of the SOC, in which there is a $Q = 0$ scattering processes is allowed since the $\varepsilon_\uparrow(k) = \varepsilon_\downarrow(k)$. Previous studies usually employ a very attractive expression based on real space Green's functions (IMAMURA; BRUNO; UTSUMI, 2004)

$$H_{\mathrm{RKKY}} = -\frac{1}{\pi}\mathrm{Im}J^2 \int_{-\infty}^{\varepsilon_F} d\varepsilon \mathrm{Tr}[(\mathbf{S}_1 \cdot \boldsymbol{\sigma})G(\mathbf{R}; \varepsilon + i0^+)(\mathbf{S}_2 \cdot \boldsymbol{\sigma})G(-\mathbf{R}; \varepsilon + i0^+)], \qquad (6.60)$$

where $\mathbf{S}_i (i = 1, 2)$ is the magnetic moment of impurity, $\boldsymbol{\sigma}$ is the Pauli matrices vector, $\mathbf{R} = \mathbf{r}_1 - \mathbf{r}_2$ is the impurities distance, and $G(\mathbf{R}; \varepsilon + i0^+)$ is the Green function for the conduction electrons. However, as thoroughly discussed by Valizadeh (VALIZADEH, 2016) this expression should be avoided in 1D systems. Essentially, the reason is because in the derivation of the Eq.(6.60) of Ref. (IMAMURA; BRUNO; UTSUMI, 2004) there is a change in the order of integration in double integral that should not performed in one-dimension. Here we avoid this problem by directly performing the integrals (6.14) both analytically and numerically. The detailed discussion of the limitation of the aforementioned expression will be discussed in the two next sections.

6.3 Analytical vs. numerical results

Despite the complexities involved in obtaining the analytical results, numerically it is rather straightforward. Basically, we need to calculate the integrals (6.14) numerically.

In fact, here we simply perform these integrals using a numerical subroutine built in `Julia` programming language (BEZANSON et al., 2017). To get convergence, as usual we add an infinitesimal imaginary to the denominator of (6.14) so that the integrals we indeed solve numerically are

$$I_{\delta\nu} = J^2 \int_{-k_\delta}^{k_\delta} \frac{dk}{2\pi} \int_{|k'|>k_\delta} \frac{dk'}{2\pi} \frac{e^{i(k-k')x}}{\frac{\hbar^2}{2m^*}(k^2 - k'^2) + \delta\alpha_{\mathrm{R}}(k - \delta\nu k') + i\eta}, \qquad \text{with } \eta = 0^+. \tag{6.61}$$

The expression above is exactly the same we obtain when we used scattering theory to obtain the indirect interaction via the Lippmann-Schwinger equation (SAKURAI; NAPOLITANO, 2017), having in mind that we need to account for the Fermi sea and the Pauli's exclusion principle. Having calculated the integrals numerically, we obtain the indirect coupling using the expressions (6.61), as well using the expressions for I_{RKKY}, I_{DM} and I_{Ising} obtained in the end of Sec. 6.2. The analytical (dashed red line) and the numerical (solid black line) results are compared in figure 19 in the absence of SOC ($a = 0$) and in Fig 20 for $k_R = 0.025k_{\mathrm{F}}$. Notice that, as expected, the oscillations are suppressed as $1/x$, as shown by the dashed blue line.

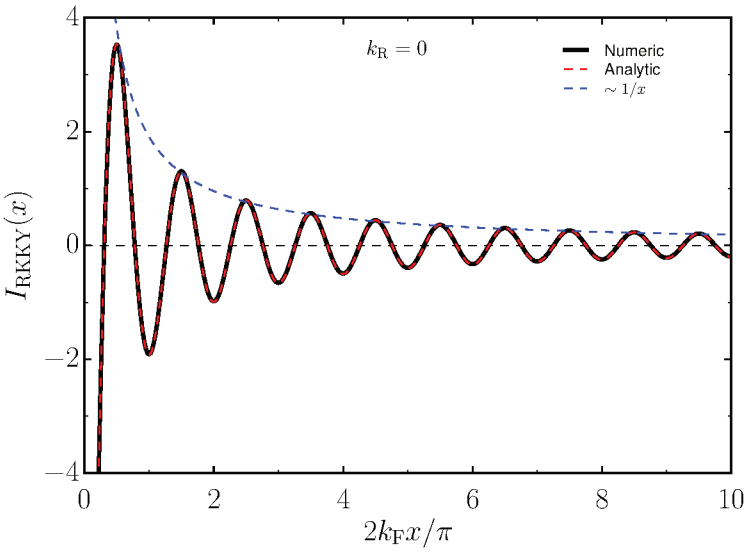

Figure 19 – Comparison between the analytical and the numerical results for the RKKY vs x in the absence of SOC ($a = 0$). Solid black line corresponds to the numerical results while dashed red line corresponds to the analytical results. The blue dashed line shows a function $\sim 1/x$ to show that in the absence of the SOC the RKKY coupling indeed decays as expected. Figure published in (SILVA; VERNEK, 2019).

The couplings showed in figure 20 presents different oscillations regimes, each of them is associated with distinct physical effects. When the impurities are closer there is a competition between the Ruderman-Kittel polarization, promoted by the spin polarization of conduction electrons around the impurities, and the QW conduction electrons precession

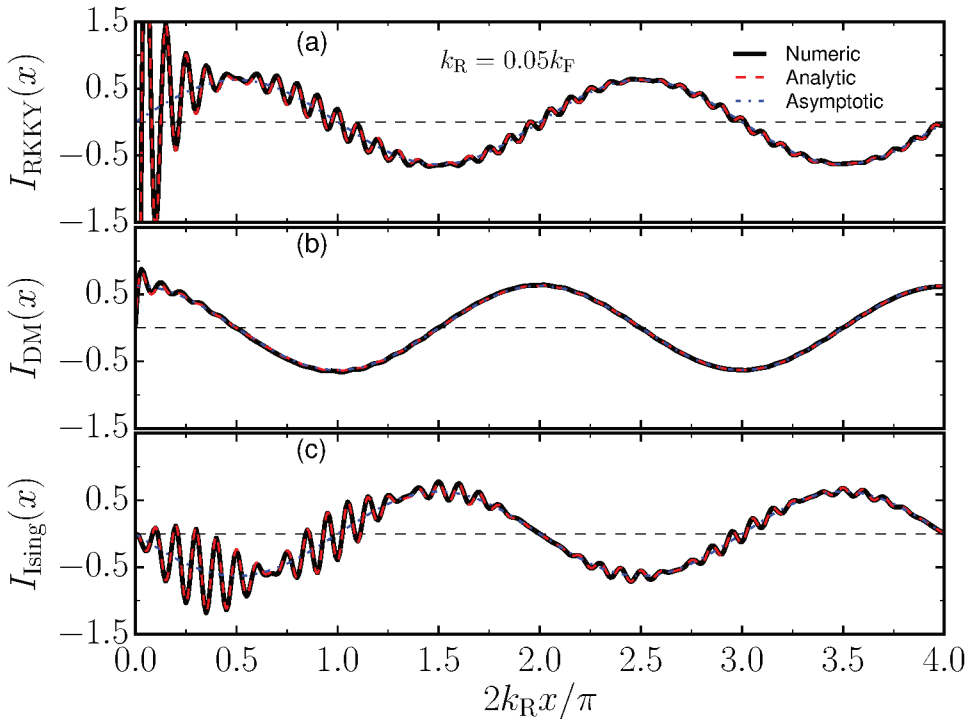

Figure 20 – Comparison between the analytical and the numerical results for the indirect couplings. RKKY (a) Dzaloshinskii-Moriya (b) and Ising (c) couplings as a function of x for $k_R = 0.05k_F$. Solid black lines corresponds to the numerical results, dashed red lines corresponds to the analytical results (Eqs.(6.55)) and dash-dot blue lines show the asymptotic behavior of the couplings (Eqs.(6.58)). Figure published in (SILVA; VERNEK, 2019).

coming from SOC. Their competition results in the fast oscillations presented in figure 20. In the opposite regime, the Ruderman-Kittel polarization precession decay with increase of impurity distance and only the slower oscillation provided by SOC survives at arbitrary large distances. For this reason, at large impurities distances the precession is entire dominated by the Rashba SOC precession, which corroborates with the asymptotic result (6.58) (dash-dot blue lines of figure 20).

6.4 Effective Hamiltonian in terms of Green's function

In this section we present a derivation of an expression for the effective Inter-impurity Hamiltonian in terms of Green's function in the position space for the 1D system in the presence of the spin-orbit interaction.

Let us start with the H_{eff} that can be written as

$$H_{\text{eff}} = \sum_{k,h}^{\text{occ.}} \sum_{k',h'}^{\text{empty}} \left[\frac{\langle k,h|H_1|k',h'\rangle\langle k',h'|H_2|k,h\rangle}{\varepsilon_{kh} - \varepsilon_{k'h'}} + \text{H.c} \right]. \tag{6.62}$$

Defining the retarded Green's function

$$\hat{G}_{k',h'}(\varepsilon_{kh}) = \frac{|k',h'\rangle\langle k',h'|}{\varepsilon_{kh} - \varepsilon_{k'h'}}, \tag{6.63}$$

in which $\varepsilon_{kh} \to \varepsilon_{kh} + 0^+$, the Eq. (6.62) can be written as

$$H_{\text{eff}} = \sum_{k,h}^{\text{occ.}} \sum_{k',h'}^{\text{empty}} \langle k,h|H_1 \hat{G}_{k',h'}(\varepsilon_{kh}) H_2|k,h\rangle + \text{H.c.} \tag{6.64}$$

Let us now introduce two closure relations in the position space, $\sum_{x,\sigma} |x,\sigma\rangle\langle x,\sigma|$, to obtain

$$H_{\text{eff}} = \sum_{k,h}^{\text{occ.}} \sum_{k',h'}^{\text{empty}} \sum_{xx'} \sum_{\sigma\sigma'} \langle k,h|H_1|x,\sigma\rangle\langle x,\sigma|\hat{G}_{k',h'}(\varepsilon_{kh})|x',\sigma'\rangle\langle x',\sigma'|H_2|k,h\rangle + \text{H.c.} \tag{6.65}$$

In the real position and spin space, the Hamiltonian H_i of Eq. (6.3) acquires the form

$$H_i = J\left[S_x^z(c_{x\uparrow}^\dagger c_{x\uparrow} - c_{x\downarrow}^\dagger c_{x\downarrow}) + S_x^+ c_{x\downarrow}^\dagger c_{x\uparrow} + S_x^- c_{x\uparrow}^\dagger c_{x\downarrow}\right]\delta(x - x_i) = H(x)\delta(x - x_i). \tag{6.66}$$

Inserting this into Eq. (6.65), after some straightforward algebra we obtain

$$H_{\text{eff}} = J^2 \sum_{hh'} \langle h|\left(\mathbf{S}_1 \cdot \mathbf{s}\right)|h'\rangle\langle h'|\left(\mathbf{S}_2 \cdot \mathbf{s}\right)|h\rangle \sum_{k}^{\text{occ.}} \sum_{k'}^{\text{empty}} G_{k',h'}(x_1,x_2,\varepsilon_{kh})\langle k|x_1\rangle\langle x_2|k\rangle + \text{H.c.} \tag{6.67}$$

Here we have defined the scalar retarded Green's function

$$G_{k',h'}(x_1,x_2,\varepsilon_{kh}) = \frac{\langle x_1|k'\rangle\langle k'|x_2\rangle}{\varepsilon_{kh} - \varepsilon_{k'h'}}. \tag{6.68}$$

We now use $\langle x_i|k\rangle = \frac{1}{\sqrt{N}} e^{ikx_i}$ and transform the summation into integrals we obtain

$$\begin{aligned} H_{\text{eff}} &= NJ^2 \sum_{hh'} \langle h|\left(\mathbf{S}_1 \cdot \mathbf{s}\right)|h'\rangle\langle h'|\left(\mathbf{S}_2 \cdot \mathbf{s}\right)|h\rangle \\ &\quad \times \int_{\text{occ.}} \frac{dk}{2\pi} e^{ik(x_2-x_1)} \int_{\text{empty}} \frac{dk'}{2\pi} G_{k',h'}(x_1,x_2,\varepsilon_{kh}) + \text{H.c.} \end{aligned} \tag{6.69}$$

As discussed in detail by Valizadeh (VALIZADEH, 2016), further simplification of Eq. (6.69) towards to a similar expression of Eq.(6.60) which requires changing in the order of the integrals over k and k', which cannot be performed in 1D case. Moreover, the integral over k' cannot be extended from $-\infty$ to ∞, since the extra contribution to the double integral does not vanish in the presence of spin-orbit coupling.

7 Conclusion and outlook

In second part of the thesis we have studied the indirect interaction between two quantum magnetic impurities mediated by the conduction electrons of a quantum wire with SOC. The coupling of the impurities with the quantum wire was described by a local Kondo-like interaction. To obtain the indirect interaction between the impurities we applied the original Ruderman-Kittel approach based on the usual quantum perturbation theory. Beyond the traditional RKKY interaction, the SOC in the quantum wire gives origin to two additional types of interactions between the impurities, the Dzyaloshinskii-Moriya and Ising interactions.

Once the effective interaction between the impurities was obtained, we computed the integral couplings analytically and numerically, with perfect agreement. Surprisingly, differently from the usual RKKY coupling, the asymptotic behavior of the couplings showed an undamped oscillatory behavior. These undamped oscillations are governed by the SOC characteristic wave number $2k_R$ and survive for long distances. The reason for such behavior is the momentum-spin lock caused by the SOC.

For future studies it is interesting to add more than two impurities, to create a finite impurity density and solve the system at finite temperature. Then, to analyze characteristic energy scales, and possible competitions between Kondo singlet formation and the RKKY interaction, as additional effects promoted by the SOC. This can be done in theoretical Kondo lattice models with SOC.

Appendix

APPENDIX A – The Kondo Model from the Single Impurity Anderson Model: The Projection Method

The Kondo Model can be obtained in the low-energy limit of the Single Impurity Anderson Model (SIAM) given by[1]

$$H = \sum_{\sigma} \varepsilon_d n_{d\sigma} + U n_{d\uparrow} n_{d\downarrow} + \sum_{\mathbf{k}\sigma} \varepsilon_{\mathbf{k}} c^{\dagger}_{\mathbf{k}\sigma} c_{\mathbf{k}\sigma} + \sum_{\mathbf{k}\sigma} V_{\mathbf{k}d} (c^{\dagger}_{\mathbf{k}\sigma} d_{\sigma} + d^{\dagger}_{\sigma} c_{\mathbf{k}\sigma}). \tag{A.1}$$

The first connection between the SIAM and the Kondo Hamiltonian was shown by Schrieffer and Wolf using an unitary transformation, nowadays known as Schrieffer-Wolf transformation (SCHRIEFFER; WOLFF, 1966). An equivalent method to obtain the Kondo model from the SIAM is using the projection method proposed by Hewson (HEWSON, 1997). Within this method the SIAM is projected onto the impurity occupation basis. For simplicity, we consider an impurity with a single energy level. In the impurity occupation basis we have the empty state (singly occupied state) labeled by Ψ_0 (non-magnetic), the state Ψ_1 with one electron in the impurity (magnetic state), and the state with two electrons in the impurity Ψ_2 (non-magnetic). The pictorial idea of the projection method is showed in the figure 21. In this basis, the Schrödinger equation for the SIAM in the matrix form is

$$\begin{pmatrix} H_{00} & H_{01} & H_{02} \\ H_{10} & H_{11} & H_{2} \\ H_{20} & H_{21} & H_{22} \end{pmatrix} \begin{pmatrix} \Psi_0 \\ \Psi_1 \\ \Psi_2 \end{pmatrix} = E \begin{pmatrix} \Psi_0 \\ \Psi_1 \\ \Psi_2 \end{pmatrix}, \tag{A.2}$$

where $H_{ij} = P_i H P_j$, P_i is the projection operator onto the subspace i. The Kondo Hamiltonian describe magnetic a magnetic impurity, so we perform a projection in the singly occupied state Ψ_1. From the matrix form of the SIAM (A.2) we obtain the equation for a state projected onto the singly occupied subspace

$$[H_{11} + H_{01}(E - H_{00})^{-1} H_{10} + H_{21}(E - H_{22})^{-1} H_{12}]\Psi_1 = E\Psi_1, \tag{A.3}$$

where we use the fact $H_{02} = H_{20} = 0$, since the empty and doubly occupied state cannot be directly connected by the Anderson Hamiltonian. Note that (A.3) is not a Schrödinger

[1] A detailed study of the SIAM is presented in the Section 2.1.

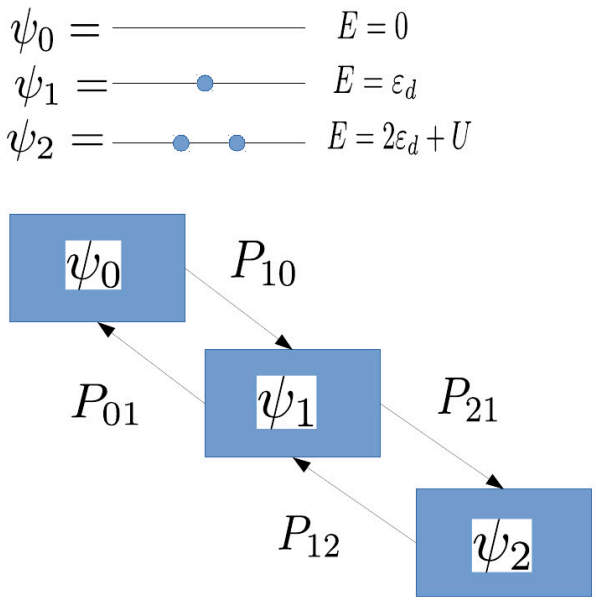

Figure 21 – The projection method applied to a single level impurity.

equation. In the SIAM the explicit form of the projection operators is

$$P_0 = (1 - n_{d\uparrow})(1 - n_{d\downarrow}), \tag{A.4}$$
$$P_1 = n_{d\uparrow} + n_{d\downarrow} - 2n_{d\uparrow}n_{d\downarrow}, \tag{A.5}$$
$$P_2 = n_{d\uparrow}n_{d\downarrow} \tag{A.6}$$
$$\tag{A.7}$$

First, let us compute the diagonal terms in the projection approach, H_{00}, H_{11} and H_{22}. For H_{00} we have $H_{00} = P_0 H P_0$, where H is given by (A.1), which gives

$$H_{00} = (1 - n_{d\uparrow})H(1 - n_{d\downarrow}).$$

For the spin up component of impurity energy $\varepsilon_d n_{d\uparrow}$ we obtain

$$\begin{aligned} P_0 n_{d\uparrow} P_0 = (1 - n_{d\uparrow})n_{d\uparrow}(1 - n_{d\downarrow}) &= (1 - n_{d\uparrow})(n_{d\uparrow} - n_{d\uparrow}n_{d\downarrow}) \\ &= n_{d\uparrow} - n_{d\uparrow}n_{d\downarrow} - (n_{d\uparrow})^2 + (n_{d\uparrow})^2 n_{d\downarrow} \\ &= 0. \end{aligned}$$

Here we use the fact that $(n_{d\sigma})^2 = n_{d\sigma}$. Similarly, we can show for the spin down component

$$(1 - n_{d\uparrow})n_{d\downarrow}(1 - n_{d\downarrow}) = 0.$$

Now, for the Coulomb term $U n_\uparrow n_\downarrow$ we have the expression

$$\begin{aligned} P_0(n_{d\uparrow}n_{d\downarrow})P_0 = (1 - n_{d\uparrow})n_{d\uparrow}n_{d\downarrow}(1 - n_{d\downarrow}) &= (1 - n_{d\uparrow})[n_{d\uparrow}n_{d\downarrow} - n_{d\uparrow}(n_{d\downarrow})^2] \\ &= 0. \end{aligned}$$

At last, for the kinetic term of the conduction electrons $\varepsilon_k c^\dagger_{\mathbf{k}\sigma} c_{\mathbf{k}\sigma} = \varepsilon_k n_{\mathbf{k}\sigma}$ we have

$$\begin{aligned}(1-n_{d\uparrow})n_{\mathbf{k}\sigma}(1-n_{d\downarrow}) &= n_{k\sigma}(1-n_{d\uparrow})(1-n_{d\downarrow}) \\ &= n_{\mathbf{k}\sigma}[1-(n_{d\uparrow}+n_{d\downarrow})+n_{d\uparrow}n_{d\downarrow}] \\ &= n_{\mathbf{k}\sigma},\end{aligned}$$

where we use $[n_{d\sigma}, n_{\mathbf{k}\sigma}] = 0$, in the single occupation subspace $n_{d\uparrow}+n_{d\downarrow} = 1$ and $n_{d\uparrow}n_{d\downarrow} = 0$, which leads to the result in the last line of the equation above. Using the same identities we obtain for the hybridization terms $V_{\mathbf{k}d}(c^\dagger_{\mathbf{k}\sigma}d_\sigma + d^\dagger_\sigma c_{\mathbf{k}\sigma})$

$$(1-n_{d\uparrow})c^\dagger_{\mathbf{k}\sigma}d_\sigma(1-n_{d\downarrow}) = 0,$$

$$(1-n_{d\uparrow})d^\dagger_\sigma c_{\mathbf{k}\sigma}(1-n_{d\downarrow}) = 0.$$

With these, for H_{00} the only term that remains is the kinetic energy of the conduction electrons

$$H_{00} = \sum_{\mathbf{k}\sigma}\varepsilon_k c^\dagger_{\mathbf{k}\sigma}c_{\mathbf{k}\sigma} \equiv H_0. \tag{A.8}$$

For the other diagonal terms, using similar tricks, we obtain

$$H_{11} = (\varepsilon_d + H_0)\sum_\sigma n_{d\sigma}(1-n_{d\bar{\sigma}}), \tag{A.9}$$

$$H_{22} = (2\varepsilon_d + U + H_0)n_{d\uparrow}n_{d\downarrow}. \tag{A.10}$$

Now, for H_{01} we have

$$\begin{aligned}H_{01} &= P_0 H P_1 \\ &= (1-n_{d\uparrow})(1-n_{d\downarrow})H(n_{d\uparrow}+n_{d\downarrow}-2n_{d\uparrow}n_{d\downarrow}).\end{aligned}$$

Performing the calculation explicitly we have

$$\begin{aligned}(1-n_{d\uparrow})(1-n_{d\downarrow})c^\dagger_{\mathbf{k}\uparrow}d_\uparrow(n_{d\uparrow}+n_{d\downarrow}-2n_{d\uparrow}n_{d\downarrow}) &= (1-n_{d\uparrow})(1-n_{d\downarrow})d_\uparrow(n_{d\uparrow}+n_{d\downarrow}-2n_{d\uparrow}n_{d\downarrow})c^\dagger_{\mathbf{k}\uparrow} \\ &= (d_\uparrow - n_{d\downarrow}d_\uparrow)c^\dagger_{\mathbf{k}\uparrow} = (1-n_{d\downarrow})d_\uparrow c^\dagger_{\mathbf{k}\uparrow},\end{aligned}$$

and

$$(1-n_{d\uparrow})(1-n_{d\downarrow})c^\dagger_{\mathbf{k}\downarrow}d_\downarrow(n_{d\uparrow}+n_{d\downarrow}-2n_{d\uparrow}n_{d\downarrow}) = (1-n_{d\uparrow})d_\downarrow c^\dagger_{\mathbf{k}\downarrow}.$$

Therefore,

$$H_{01} = \sum_{\mathbf{k}\sigma} V^*_{\mathbf{k}}(1-n_{d\bar{\sigma}})c^\dagger_{\mathbf{k}\sigma}d_\sigma, \tag{A.11}$$

$$H_{10} = \sum_{\mathbf{k}\sigma} V^*_{\mathbf{k}}(1-n_{d\bar{\sigma}})d^\dagger_\sigma c_{\mathbf{k}\sigma}. \tag{A.12}$$

To deduce the equations above we also use $d_\sigma n_\sigma = d_\sigma(1-d_\sigma d^\dagger_\sigma) = d_\sigma$ and $n_{d\sigma}d^\dagger_\sigma = d^\dagger_\sigma$. For H_{12} we have

$$H_{12} = P_1 H P_2 = (n_{d\uparrow}+n_{d\downarrow}-2n_{d\uparrow}n_{d\downarrow})H(n_{d\uparrow}n_{d\downarrow}).$$

After similar calculations performed for the previous terms we obtain

$$H_{12} = \sum_{\mathbf{k}\sigma} V_{\mathbf{k}}^{*} n_{d\bar{\sigma}} c_{\mathbf{k}\sigma}^{\dagger} d_{\sigma}, \tag{A.13}$$

$$H_{21} = \sum_{\mathbf{k}\sigma} V_{\mathbf{k}} n_{d\bar{\sigma}} d_{\sigma}^{\dagger} c_{\mathbf{k}\sigma}. \tag{A.14}$$

Let us now define the Hamiltonians $H_1 = H_{10}(E - H_{00})^{-1} H_{01}$ and $H_2 = H_{12}(E - H_{22})^{-1} H_{21}$. Using (A.11) and (A.12) we get

$$H_1 = \sum_{\mathbf{k}\mathbf{k}',\sigma\sigma'} V_{\mathbf{k}} V_{\mathbf{k}'}^{*} (E - \varepsilon_k - H_0)^{-1} (1 - n_{d\bar{\sigma}}) d_{\sigma}^{\dagger} c_{\mathbf{k}\sigma} (1 - n_{d\bar{\sigma}'}) c_{\mathbf{k}'\sigma'} d_{\sigma'}.$$

To obtain the equation above we used

$$\begin{aligned} c_{\mathbf{k}\sigma}(E - H_0)^{-1} &= \frac{c_{\mathbf{k}\sigma}}{E}\left(1 - \frac{H_0}{E}\right)^{-1} \\ &= \frac{1}{E}\sum_{n} \frac{1}{E^n} c_{\mathbf{k}\sigma} (H_0)^n. \end{aligned} \tag{A.15}$$

Now, note that

$$\begin{aligned} c_{\mathbf{k}\sigma} \sum_{\mathbf{k}'\sigma'} \varepsilon_{k'} c_{\mathbf{k}'\sigma'}^{\dagger} c_{\mathbf{k}'\sigma'} &= c_{\mathbf{k}\sigma} \left(\sum_{\mathbf{k}\neq\mathbf{k}',\sigma\neq\sigma'} \varepsilon_{k'} c_{\mathbf{k}'\sigma'}^{\dagger} c_{\mathbf{k}'\sigma} + \varepsilon_k c_{\mathbf{k}\sigma}^{\dagger} c_{\mathbf{k}\sigma} \right) \\ &= \left(\sum_{\mathbf{k}\neq\mathbf{k}',\sigma\neq\sigma'} \varepsilon_{k'} c_{\mathbf{k}'\sigma'}^{\dagger} c_{\mathbf{k}'\sigma} + \varepsilon_k \right) c_{\mathbf{k}\sigma} \\ &= (H_0 - \varepsilon_k c_{\mathbf{k}\sigma}^{\dagger} c_{\mathbf{k}\sigma} + \varepsilon_k) c_{\mathbf{k}\sigma} \\ &= (H_0 + \varepsilon_k) c_{\mathbf{k}\sigma}. \end{aligned}$$

Thus,

$$c_{\mathbf{k}\sigma} H_0 = (\varepsilon_k + H_0) c_{\mathbf{k}\sigma}.$$

Similar calculations leads to

$$H_0 c_{\mathbf{k}\sigma}^{\dagger} = c_{\mathbf{k}\sigma}^{\dagger} (\varepsilon_k + H_0).$$

So, using this results in the operator expansion (A.15) we obtain

$$c_{\mathbf{k}\sigma}(E - H_{00})^{-1} = \frac{1}{E}\sum_{n}\left(\frac{\varepsilon_k + H_0}{E}\right) = (E - \varepsilon_k - H_0)^{-1} c_{\mathbf{k}\sigma}.$$

The expression in the parenthesis above can be written as

$$(E - \varepsilon_k - H_0)^{-1} = (E - \varepsilon_k - H_0 + \varepsilon_d - \varepsilon_d)^{-1} = \frac{1}{\varepsilon_d - \varepsilon_k}\left[1 - \frac{E - H_0 - \varepsilon_d}{\varepsilon_k - \varepsilon_d}\right]^{-1}.$$

Moreover, for the single occupied state and for energies near of the Fermi energy we have $\varepsilon_k \ll \varepsilon_d$ and $E - H_0 - \varepsilon_d \ll \varepsilon_d$. These allow us to make the approximation

$$(E - \varepsilon_k - H_0)^{-1} \approx \frac{1}{\varepsilon_d - \varepsilon_k}.$$

Using this in H_1 we obtain

$$H_1 = \sum_{\mathbf{k}\mathbf{k}',\sigma\sigma'} \frac{V_{\mathbf{k}} V^*_{\mathbf{k}'}}{\varepsilon_d - \varepsilon_k} (1 - n_{d\bar{\sigma}}) d^\dagger_\sigma c_{\mathbf{k}\sigma} (1 - n_{d\bar{\sigma}'}) c_{\mathbf{k}'\sigma'} d_{\sigma'}.$$

For $H_2 = H_{12}(E - H_{22})^{-1} H_{21}$, using (A.13) and (A.14) we have

$$H_2 = \sum_{\mathbf{k}\mathbf{k}',\sigma\sigma'} V_{\mathbf{k}} V^*_{\mathbf{k}'} n_{d\bar{\sigma}} c^\dagger_{\mathbf{k}\sigma} d_\sigma (E - H_{22})^{-1} n_{d\bar{\sigma}'} d^\dagger_{\sigma'} c_{\mathbf{k}'\sigma'}.$$

Upon writing $(E - H_{22})^{-1} = (E - 2\varepsilon_d - U - H_0)^{-1}$, and applying the same tricks and approximations used in H_1 we obtain

$$(E - 2\varepsilon_d - U - H_0 + \varepsilon_k)^{-1} \approx -\frac{1}{\varepsilon_d + U - \varepsilon_k}.$$

Therefore, H_2 becomes

$$H_2 = -\sum_{\mathbf{k}\mathbf{k}',\sigma\sigma'} \frac{V_{\mathbf{k}} V^*_{\mathbf{k}'}}{\varepsilon_d + U - \varepsilon_{k'}} n_{d\bar{\sigma}} c^\dagger_{\mathbf{k}\sigma} d_\sigma n_{d\bar{\sigma}'} d^\dagger_{\sigma'} c_{\mathbf{k}'\sigma'}.$$

To obtain the effective Hamiltonian we need to perform explicitly the spin index summation in H_1 and H_2. For H_1, the momentum summation can be recast into the form

$$\sum_{\mathbf{k}\mathbf{k}',\sigma\sigma'} (1 - n_{d\bar{\sigma}}) d^\dagger_\sigma c_{\mathbf{k}\sigma} (1 - n_{d\bar{\sigma}'}) c^\dagger_{\mathbf{k}'\sigma} d_{\sigma'} = \sum_{\mathbf{k}\mathbf{k}'} (n_{d\uparrow} c^\dagger_{\mathbf{k}\uparrow} c_{\mathbf{k}'\uparrow} + n_{d\downarrow} c^\dagger_{\mathbf{k}\downarrow} c_{\mathbf{k}'\downarrow} + d^\dagger_\uparrow d_\downarrow c_{\mathbf{k}\uparrow} c^\dagger_{\mathbf{k}'\downarrow} + d^\dagger_\downarrow d_\uparrow c_{\mathbf{k}\downarrow} c^\dagger_{\mathbf{k}'\uparrow}).$$

Using the identity above we get for H_1

$$H_1 = \sum_{\mathbf{k}\mathbf{k}'} \frac{V_{\mathbf{k}} V^*_{\mathbf{k}'}}{\varepsilon_d - \varepsilon_k} \left[n_{d\uparrow} c_{\mathbf{k}\uparrow} c^\dagger_{\mathbf{k}'\uparrow} + n_{d\downarrow} c_{\mathbf{k}\downarrow} c^\dagger_{\mathbf{k}'\downarrow} + d^\dagger_\uparrow d_\downarrow c_{\mathbf{k}\uparrow} c_{\mathbf{k}'\downarrow} + d^\dagger_\downarrow d_\uparrow c_{\mathbf{k}\downarrow} c_{\mathbf{k}'\uparrow} \right]. \tag{A.16}$$

Now, for H_2 we have

$$\sum_{\mathbf{k}\mathbf{k}',\sigma\sigma'} n_{d\bar{\sigma}} c^\dagger_{\mathbf{k}\sigma} d_\sigma n_{d\bar{\sigma}'} d^\dagger_{\sigma'} c_{\mathbf{k}'\sigma'} = \sum_{\mathbf{k}\mathbf{k}'} (n_{d\downarrow} c^\dagger_{\mathbf{k}\uparrow} c_{\mathbf{k}'\uparrow} + n_{d\uparrow} c^\dagger_{\mathbf{k}\downarrow} c_{\mathbf{k}'\downarrow} + d_\uparrow d^\dagger_\downarrow c^\dagger_{\mathbf{k}\uparrow} c_{\mathbf{k}'\downarrow} + d_\downarrow d^\dagger_\uparrow c^\dagger_{\mathbf{k}\downarrow} c_{\mathbf{k}'\uparrow}),$$

which results

$$H_2 = -\sum_{\mathbf{k}\mathbf{k}'} \frac{V_{\mathbf{k}} V_{\mathbf{k}'}}{\varepsilon_d + U - \varepsilon_k} (n_{d\downarrow} c^\dagger_{\mathbf{k}\uparrow} c_{\mathbf{k}'\uparrow} + n_{d\uparrow} c^\dagger_{\mathbf{k}\downarrow} c_{\mathbf{k}'\downarrow} + d_\uparrow d^\dagger_\downarrow c^\dagger_{\mathbf{k}\uparrow} c_{\mathbf{k}'\downarrow} + d_\downarrow d^\dagger_\uparrow c^\dagger_{\mathbf{k}\downarrow} c_{\mathbf{k}'\uparrow}). \tag{A.17}$$

Using now the relations

$$\begin{aligned} n_{d\uparrow} c_{\mathbf{k}\uparrow} c^\dagger_{\mathbf{k}'\uparrow} + n_{d\downarrow} c_{\mathbf{k}\downarrow} c^\dagger_{\mathbf{k}'\downarrow} &= S_z (c_{\mathbf{k}\uparrow} c^\dagger_{\mathbf{k}'\uparrow} - c_{\mathbf{k}\downarrow} c^\dagger_{\mathbf{k}'\downarrow}) + \frac{1}{2} (n_{d\uparrow} + n_{d\downarrow}) (c_{\mathbf{k}\uparrow} c^\dagger_{\mathbf{k}'\uparrow} + c_{\mathbf{k}\downarrow} c^\dagger_{\mathbf{k}'\downarrow}), \\ n_{d\downarrow} c^\dagger_{\mathbf{k}'\uparrow} c_{\mathbf{k}\uparrow} + n_{d\uparrow} c^\dagger_{\mathbf{k}'\downarrow} c_{\mathbf{k}\downarrow} &= -S_z (c^\dagger_{\mathbf{k}'\uparrow} c_{\mathbf{k}\uparrow} - c^\dagger_{\mathbf{k}'\downarrow} c_{\mathbf{k}\downarrow}) + \frac{1}{2} (n_{d\uparrow} + n_{d\downarrow}) (c_{\mathbf{k}\uparrow} c^\dagger_{\mathbf{k}'\uparrow} + c_{\mathbf{k}\downarrow} c^\dagger_{\mathbf{k}'\downarrow}), \end{aligned}$$

where $S_z = (n_{d\uparrow} - n_{d\downarrow})/2$, we finally obtain the effective Hamiltonian

$$\begin{aligned} H_{\text{eff}} &= H_1 + H_2 \\ &= \sum_{\mathbf{k}\mathbf{k}'} K_{\mathbf{k}\mathbf{k}'}(c^\dagger_{\mathbf{k}'\uparrow}c_{\mathbf{k}\uparrow} + c^\dagger_{\mathbf{k}'\downarrow}c_{\mathbf{k}\downarrow}) + \sum_{\mathbf{k}\mathbf{k}'} J_{\mathbf{k}\mathbf{k}'}[S^z(c^\dagger_{\mathbf{k}'\uparrow}c_{\mathbf{k}\uparrow} - c^\dagger_{\mathbf{k}'\downarrow}c_{\mathbf{k}\downarrow}) + S^+c^\dagger_{\mathbf{k}'\downarrow}c_{\mathbf{k}\uparrow} + S^-c^\dagger_{\mathbf{k}'\uparrow}c_{\mathbf{k}\downarrow}], \end{aligned} \tag{A.18}$$

where we use the relations $S_z = (n_{d\uparrow} - n_{d\downarrow})/2$, $S_+ = d^\dagger_\uparrow d_\downarrow$ and $S_- = d^\dagger_\downarrow d_\uparrow$. The effective couplings of Hamiltonian (A.18) are

$$K_{\mathbf{k}\mathbf{k}'} = \frac{V_{\mathbf{k}}V^*_{\mathbf{k}'}}{2}\left(\frac{1}{\varepsilon_{\mathbf{k}} - \varepsilon_d} - \frac{1}{\varepsilon_d + U - \varepsilon_{\mathbf{k}'}}\right), \tag{A.19}$$

$$J_{\mathbf{k}\mathbf{k}'} = V_{\mathbf{k}}V^*_{\mathbf{k}'}\left(\frac{1}{\varepsilon_{\mathbf{k}} - \varepsilon_d} + \frac{1}{\varepsilon_d + U - \varepsilon_{\mathbf{k}'}}\right). \tag{A.20}$$

The first term in (A.18) corresponds to a spin-independent (scalar) scattering potential, and does not contributes for the Kondo physics. Considering only the spin-dependent process in the effective Hamiltonian and using $\mathbf{s}_{\mathbf{k}\mathbf{k}'} = \psi^\dagger_{\mathbf{k}}\boldsymbol{\sigma}\psi_{\mathbf{k}}$, where $\boldsymbol{\sigma} = (\sigma_x, \sigma_y, \sigma_z)^T$ and $\psi_{\mathbf{k}} = (c_{\mathbf{k}\uparrow}, c_{\mathbf{k}\downarrow})^T$, the effective Hamiltonian can be written as

$$H_{\text{eff}} = \sum_{\mathbf{k}\mathbf{k}'} J_{\mathbf{k}\mathbf{k}'}\left(\mathbf{s}_{\mathbf{k}\mathbf{k}'} \cdot \mathbf{S}\right), \tag{A.21}$$

which have the traditional Kondo Hamiltonian form. Note that now the effective coupling $J_{\mathbf{k}\mathbf{k}'}$ depends on the SIAM parameters and the moment of the conduction electrons.

APPENDIX B – Kitaev chain

Kitaev proposed a toy model of a superconducting spinless chain with p-wave pairing which presents non-trivial topological phases (KITAEV, 2001). The Kitaev Hamiltonian is given by

$$H_{\text{Kitaev}} = -\mu \sum_j c_j^\dagger c_j - \frac{1}{2} \sum_j \left(t c_j^\dagger c_{j+1} + \Delta e^{i\phi} c_j c_{j+1} + H.c. \right), \tag{B.1}$$

where μ is the chemical potential, t is the tight-binding hopping, $c_j^\dagger(c_j)$ creates(annihilates) a electron in the jth site, Δ is the superconductor order parameter and ϕ is the superconductor phase. The physical properties of the Kitaev chain is better understood in the reciprocal space. To do so, let us take the Fourier transformation

$$c_j = \frac{1}{\sqrt{N}} \sum_k e^{-ikx_j} c_k, \quad c_j^\dagger = \frac{1}{\sqrt{N}} \sum_k e^{ikx_j} c_k^\dagger.$$

After some algebraic manipulations, the Kitaev Hamiltonian in the k-space acquires the form

$$H_{\text{Kitaev}} = \frac{1}{2} \sum_k \{-2[\mu + t\cos(ka)] c_k^\dagger c_k + i\Delta e^{i\phi} \text{sen}(ka) c_k c_{-k} - i\Delta e^{-i\phi} \text{sen}(ka) c_{-k}^\dagger c_k^\dagger\}. \tag{B.2}$$

Using the Nambu spinor $\Psi_k = (c_k, c_{-k}^\dagger)^T$ the Kitaev Hamiltonian becomes

$$H_{\text{Kitaev}} = \frac{1}{2} \sum_k \Psi_k^\dagger \mathcal{H}_k(k) \Psi_k, \tag{B.3}$$

with

$$\mathcal{H}_k(k) = \begin{bmatrix} -[\mu + t\cos(ka)] & i\Delta e^{i\phi} sen(ka) \\ -i\Delta e^{-i\phi} sen(ka) & \mu + t\cos(ka) \end{bmatrix}. \tag{B.4}$$

The eigenenergies of the Kitaev chain is given by

$$E_k = \pm\sqrt{\varepsilon_k^2 + |\tilde{\Delta}_k|^2}.$$

From (B.4) we have

$$\varepsilon_k = -[\mu + t\cos(ka)], \tag{B.5}$$

$$\tilde{\Delta}_k = i\Delta e^{i\phi} \text{sen}(ka). \tag{B.6}$$

Then, explicitly we obtain the dispersion

$$\begin{aligned} E_k &= \pm\sqrt{[\mu + t\cos(ka)]^2 + \Delta^2 sen^2(ka)} \\ &= \pm\sqrt{(t - \Delta^2)\cos^2(ka) + 2\mu t\cos(ka) + \mu^2 + \Delta^2}. \end{aligned} \tag{B.7}$$

Looking at the equation above we see that the zero energy modes, $E_k = 0$, associated with the MZMs, are obtained by the condition

$$(t - \Delta^2)\cos^2(ka) + 2\mu t\cos(ka) + \mu^2 + \Delta^2 = 0.$$

The condition above must be satisfied for an arbitrary Δ, so we demand the mutual cancellation of $-\Delta^2\cos^2(ka)$ and Δ^2. This occurs for $\cos(ka) = \pm 1$. Thus, we obtain the relation

$$\begin{cases} (t+\mu)^2 = 0, & \text{if} \quad \cos(ka) = 1 \\ (t-\mu)^2 = 0, & \text{if} \quad \cos(ka) = -1. \end{cases} \tag{B.8}$$

Therefore, the zero energy modes are obtained when $\mu = \pm t$. Looking at the Brillouin zone, $k \in [0, \pi/a]$, we have that the point $k = 0$, corresponds to zero energy mode for $\mu = -t$ and the point $k = \pi/a$ corresponds to the zero energy mode for $\mu = t$.

B.1 Topological phases of the Kitaev chain

The analysis of the topological phases of the Kitaev chain in the k-space is performed by mapping the Brillouin zone on a unitary sphere. For this, notice that the Hamiltonian (B.4) can be written as

$$\mathcal{H}_k = \begin{bmatrix} \varepsilon_k & \tilde{\Delta}_k \\ \tilde{\Delta}_k^* & -\varepsilon_k \end{bmatrix} = \varepsilon_k \begin{bmatrix} 1 & 0 \\ 0 & -1 \end{bmatrix} + Re[\tilde{\Delta}_k] \begin{bmatrix} 0 & 1 \\ 1 & 0 \end{bmatrix} + Im[\tilde{\Delta}_k] \begin{bmatrix} 0 & -i \\ i & 0 \end{bmatrix}.$$

Using again the Pauli matrices

$$\sigma^x = \begin{bmatrix} 0 & 1 \\ 1 & 0 \end{bmatrix}; \quad \sigma^y = \begin{bmatrix} 0 & -i \\ i & 0 \end{bmatrix}; \quad \sigma^z = \begin{bmatrix} 1 & 0 \\ 0 & -1 \end{bmatrix},$$

we have

$$\mathcal{H}_k = \vec{h}(k) \cdot \vec{\sigma}, \tag{B.9}$$

with

$$\vec{h}(k) = h_x(k)\hat{x} + h_y(k)\hat{y} + h_z(k)\hat{z},$$

$$\vec{\sigma} = \sigma^x\hat{x} + \sigma^y\hat{y} + \sigma^z\hat{z},$$

$$h_x(k) = Re[\tilde{\Delta}_k], \quad h_y(k) = Im[\tilde{\Delta}_k], \quad h_z = \varepsilon_k.$$

From eqs.(B.5) and (B.6) we obtain the following properties

$$h_{x,y}(k) = -h_{x,y}(-k), \tag{B.10}$$

$$h_z(k) = h_z(-k). \tag{B.11}$$

These properties are consequence of the p-wave pairing of the Kitaev chain. Let us define the unitary vector

$$\hat{h}(k) = \frac{\vec{h}(k)}{|\vec{h}(k)|}, \tag{B.12}$$

which is the responsible for the map of the Brillouin zone onto the surface of an unitary sphere (Brillouin sphere). The particular points of the Brillouin zone ($k = 0$ and $k = \pi/a$) correspond to opposite poles of the unitary sphere. Moreover, from the relations above we have $h_{x,y}(0) = h_{x,y}(\pi) = 0$. Then, in the poles the unitary vector becomes

$$\widehat{h}(0) = s_0\hat{z}, \tag{B.13}$$

and

$$\widehat{h}(\pi) = s_\pi\hat{z}. \tag{B.14}$$

Where $s_{0,\pi}$ are the signs of the unitary vector in the poles. Notice that[1]

$$h_z(k) = -\mu + t\cos(k), \tag{B.15}$$

so the sign of the poles $s_{0,\pi}$ represents only the relative kinetic energy in the pole, that is ± 1. A more interesting quantity is the product $s_0 s_\pi$. There are two distinct ways of connection between the two poles ($k = 0$ to $k = \pi$). The first way is using closed trajectories that can be smoothly deformed to a single dot in the Brillouin sphere. In this case, the the sign of s_0 and s_π are always the same. Thus, $s_0 s_\pi = 1$ for all the distinct trajectories. The second way is using open trajectories, in which the signs s_0 and s_π are always opposites, resulting in $s_0 s_\pi = -1$. Therefore, the product

$$\nu = s_0 s_\pi \tag{B.16}$$

is a good topological invariant for the system. If $\nu = 1$, the phase is called topologically trivial (os simply trivial), while if $\nu = -1$ the phase is called topological. For the Kitaev chain, using (B.15) we obtain

$$s_0 = \frac{h_z(0)}{|h_z(0)|} = \frac{t-\mu}{|t-\mu|} = \begin{cases} +1, & \text{if} \quad \mu < t \\ -1, & \text{if} \quad \mu > t \end{cases} \tag{B.17}$$

and

$$s_\pi = \frac{h_z(\pi)}{|h_z(\pi)|} = \frac{-t-\mu}{|t-\mu|} = \begin{cases} +1, & \text{if} \quad \mu > -t \\ -1, & \text{if} \quad \mu < -t \end{cases}. \tag{B.18}$$

Then, the topological invariant for the Kitaev chain is

$$\nu = s_0 s_\pi = -\frac{t^2-\mu^2}{|t-\mu|^2} = \begin{cases} -1, & \text{if} \quad |\mu| < t \\ +1, & \text{if} \quad |\mu| > t \end{cases}. \tag{B.19}$$

The topological phase transition occurs when the gap is closed and corresponds exactly to the zero energy state. To see that, let us remember that for the Kitaev chain

$$E_k = \sqrt{\varepsilon_k^2 + |\tilde{\Delta}_k|^2},$$

[1] For simplicity we take $a = 1$.

with

$$\varepsilon_k = -[\mu + t\cos(k)], \qquad \tilde{\Delta}_k = i\Delta e^{i\phi} sen(k).$$

Then, in the Brillouin zone limits we have $\varepsilon_{0,\pi} = -[\mu \pm t]$ and $\tilde{\Delta}_k = 0$. Moreover, from the topological invariant (B.19) we see that the topological transition occurs for $\mu = \pm t$, which results

$$E_{0,\pi} = 0, \qquad \text{for} \quad \mu = \pm t. \tag{B.20}$$

Therefore, the zero energy states of the Kitaev chain occurs exactly at the topological transition point.

B.2 Majorana zero modes at the edges of the Kitaev chain

In the topological phase, the edges of the Kitaev sustain topological protected zero energy states which behaves as Majorana fermions. For a better understanding of this phenomena, let us write the conventional fermion operators c_j in terms of Majorana operators γ_{Aj} and γ_{Bj} as

$$c_j = \frac{e^{-i\phi/2}}{2}(\gamma_{B,j} + i\gamma_{A,j}). \tag{B.21}$$

The Majorana operators follows the canonical relations

$$\gamma_{\alpha,j} = \gamma^\dagger_{\alpha,j}, \tag{B.22}$$

$$[\gamma_{\alpha,j}, \gamma_{\alpha',j'}]_+ = 2\delta_{\alpha\alpha'}\delta_{jj'}. \tag{B.23}$$

The Kitaev model (B.1), on Majorana basis, can be written as

$$\begin{aligned}
H &= -\mu \sum_{j=1}^{N} \frac{e^{i\phi/2}}{2}(\gamma^\dagger_{B,j} - i\gamma^\dagger_{A,j})\frac{e^{-i\phi/2}}{2}(\gamma_{B,j} + i\gamma_{A,j}) \\
&\quad -\frac{t}{2}\sum_{j=1}^{N-1}\left[\frac{e^{i\phi/2}}{2}(\gamma^\dagger_{B,j} - i\gamma^\dagger_{A,j})\frac{e^{-i\phi/2}}{2}(\gamma_{B,j+1} + i\gamma_{A,j+1})\right] \\
&\quad -\frac{t}{2}\sum_{j=1}^{N-1}\left[\frac{e^{i\phi/2}}{2}(\gamma^\dagger_{B,j+1} - i\gamma^\dagger_{A,j+1})\frac{e^{-i\phi/2}}{2}(\gamma_{B,j} + i\gamma_{A,j})\right] \\
&\quad -\frac{\Delta}{2}\sum_{j=1}^{N-1} e^{i\phi}\frac{e^{-i\phi/2}}{2}\frac{e^{-i\phi/2}}{2}(\gamma^\dagger_{B,j} + i\gamma^\dagger_{A,j})(\gamma_{B,j+1} + i\gamma_{A,j+1}) \\
&\quad -\frac{\Delta}{2}\sum_{j=1}^{N-1} e^{-i\phi}\frac{e^{i\phi/2}}{2}\frac{e^{i\phi/2}}{2}(\gamma^\dagger_{B,j+1} + i\gamma^\dagger_{A,j+1})(\gamma_{B,j} + i\gamma_{A,j}).
\end{aligned} \tag{B.24}$$

After some algebraic manipulations and using the properties (B.22) and (B.23) we obtain

$$H = -\frac{\mu}{2}\sum_{j=1}^{N}(1 + i\gamma_{B,j}\gamma_{A,j}) - \frac{i}{4}\sum_{j=1}^{N-1}\left[(\Delta + t)\gamma_{B,j}\gamma_{A,j+1} + (\Delta - t)\gamma_{A,j}\gamma_{B,j+1}\right]. \tag{B.25}$$

This Hamiltonian has a rich topological phase. However, in some particular limits it is easy to understand the fundamental topological aspects of the system. First, let us take $\mu \neq 0$, $t = \Delta = 0$. From equation (B.19) we have $\nu = 1$, which corresponds to the trivial phase. In this limit, the Hamiltonian (B.25) acquires the simple form

$$H = -\frac{\mu}{2}\sum_{j=1}^{N}(1 + i\gamma_{B,j}\gamma_{A,j}). \tag{B.26}$$

There is no interesting physics in this limit, the Kitaev chain reduces to N isolated sites. On the other hand, when $\mu = 0$ and $t = \Delta$, where $\nu = -1$, corresponding to the topological phase, the Hamiltonian (B.25) becomes

$$H = -\frac{i}{2}t\sum_{j=1}^{N-1}\gamma_{B,j}\gamma_{A,j+1}. \tag{B.27}$$

This limit is better understood within the ordinary fermionic basis. This can be done by the definition of a new ordinary fermion operator

$$d_j = \frac{1}{2}(\gamma_{A,j+1} + i\gamma_{B,j}). \tag{B.28}$$

Then, the Hamiltonian (B.27) in terms of regular fermion operators can be written as

$$H = t\sum_{j=1}^{N-1}\left(d_j^\dagger d_j - \frac{1}{2}\right). \tag{B.29}$$

The important fact of this limit is that we can see from the Hamiltonian above (B.28) the presence of a pair os Majorana zero modes, $\gamma_{A,1}$ and $\gamma_{B,N}$, which not appears in (B.27). This occurs because they are decoupled from the chain and have zero energy. The pair of MZMs are protected by topology and corresponds to true Majorana excitations and not only a mathematical artifact. The question whether they have been observed or not in experiment is a long and interesting history (WILCZEK, 2009; ALICEA, 2012; ELLIOTT; FRANZ, 2015).

APPENDIX C – Residual entropy for a resonant level coupled to a Majorana zero mode

C.1 Free Majorana mode entropy

Let us consider a system composed of two Majorana modes, and a metallic lead. Let us assume that only one of them is coupled to the lead, while the other one remains free. The Hamiltonian of this toy model is given by

$$H = \sum_{\mathbf{k}} \varepsilon_k c^\dagger_{\mathbf{k}} c_{\mathbf{k}} + \sum_{\mathbf{k}} (V c_{\mathbf{k}} \gamma_1 + V^* \gamma_1 c^\dagger_{\mathbf{k}}), \tag{C.1}$$

where V is the hybridization matrix element of the coupled of the Majorana mode with the metallic lead. We introduce the Green's function of the level

$$G_f(\omega) \equiv \langle\langle f; f^\dagger \rangle\rangle_\omega, \tag{C.2}$$

where, the fermion operators are defined in terms of the Majorana operators as $f = (\gamma_1 + i\gamma_2)/\sqrt{2}$. To tell apart the contribution of the Majorana modes to the entropy, it is convenient to rewrite the Green's function in terms of the Majorana operators which results

$$G_f(\omega) = \frac{1}{2}\left[M_{11}(\omega) - iM_{12}(\omega) + iM_{21}(\omega) + M_{22}(\omega)\right]. \tag{C.3}$$

Here we have define the Majorana Green functions

$$M_{ij}(\omega) \equiv \langle\langle \gamma_i; \gamma_j \rangle\rangle_\omega. \tag{C.4}$$

The free energy of the level can be written as

$$F_f(T) = -k_{\mathrm{B}} T \int_{-\infty}^{\infty} \rho_f(\omega) \ln(1 + e^{-\beta\omega}) d\omega \tag{C.5}$$

in which $\beta = 1/k_{\mathrm{B}}T$ with k_B being the Boltzmann constant and T the temperature and

$$\rho_f(\omega) = -\frac{1}{\pi}\mathrm{Im}\{G_f(\omega)\}. \tag{C.6}$$

We can now compute the entropy using the relation

$$S_f(T) = -\frac{\partial F_f(T)}{\partial T}. \tag{C.7}$$

analytical expression for the the Majorana Green functions can be calculated using the equation of motion (EOM) in the energy domain (ZUBAREV, 1960)

$$\omega\langle\langle\gamma_i;\gamma_j\rangle\rangle_\omega = \delta_{i,j} + \langle\langle[\gamma_i, H]_-;\gamma_j\rangle\rangle_\omega. \tag{C.8}$$

There are two distinct regimes for the toy model (C.1), $V = 0$ and $V \neq 0$, let us take a closer look in them.

C.1.1 Decoupled regime (V=0)

In the decoupled regime the Hamiltonian (C.1) describes a free regular fermion, so using the EOM (C.8) we obtain

$$G_f(\omega) = \frac{1}{2}\left[\frac{1}{\omega + i\eta} + \frac{1}{\omega + i\eta}\right], \tag{C.9}$$

where $\eta \to 0^+$, which results from (C.6) the density of states

$$\rho_f(\omega) = \frac{1}{2}\left[\delta(\omega) + \delta(\omega)\right], \tag{C.10}$$

where the first term is the contribution of the Majorana mode γ_1 and the second from γ_2. Notice that in this case both Majorana modes are free. Inserting (C.10) into Eqs. (C.5) and using (C.7) we find

$$F_f(T) = -k_\mathrm{B}T\ln(2) \tag{C.11}$$

and

$$S_f(T) = k_\mathrm{B}\ln(2). \tag{C.12}$$

This is the entropy expected for the single zero-energy level for spinless fermion.

C.1.2 Coupled regime ($V \neq 0$)

In the coupled regime, using Eqs. (C.1), (C.3) and (C.8) we obtain the following Green function

$$G_f(\omega) = \frac{1}{2}\left(\frac{1}{\omega + i\Gamma} + \frac{1}{\omega + i\eta}\right). \tag{C.13}$$

Here, $\Gamma = 2\pi\rho_0|V|^2$, ρ_0 is the density of states of the metallic lead. Equation (C.13) render the density of states

$$\rho_f(\omega) = \frac{1}{2}\left[\frac{1}{\pi}\frac{\Gamma}{\omega^2 + \Gamma^2} + \delta(\omega)\right]. \tag{C.14}$$

This density of state is similar to that derived in Ref. (SELA et al., 2019). The Lorentzian form of the first term is due the Majorana coupled to the metallic lead, whereas the

δ-function in second term results from the free Majorana mode. Now, free energy acquires the form

$$\begin{aligned} F_f(T) &= F_1(T) + F_2(T) \\ &= -\frac{k_B T}{2}\int_{-\infty}^{\infty}\frac{1}{\pi}\frac{\Gamma}{\omega^2+\Gamma^2}\ln(1+e^{-\beta\omega})d\omega \\ &\quad -\frac{k_B T}{2}\ln(2). \end{aligned} \tag{C.15}$$

With this, using Eq. (C.7) we find

$$\begin{aligned} S_f(T) &= S_1(T) + S_2(T) \\ &= \frac{k_B}{2}\int_{-\infty}^{\infty}\frac{1}{\pi}\frac{\Gamma}{\omega^2+\Gamma^2}\frac{\partial}{\partial T}\left[T\ln(1+e^{-\beta\omega})\right]d\omega \\ &\quad +\frac{k_B}{2}\ln(2). \end{aligned} \tag{C.16}$$

In the above, $S_2(T) = (1/2)k_B\ln(2)$ corresponds to the contribution from the free Majorana mode, γ_2. The contribution $S_1(T)$ (given by the second line of the equation above) from the Majorana mode, γ_1, coupled to the metallic lead, requires more attention. Performing the temperature derivative we obtain

$$\begin{aligned} S_1(T) &= \frac{k_B}{2}\int_{-\infty}^{\infty}\frac{1}{\pi}\frac{\Gamma}{\omega^2+\Gamma^2}\frac{\partial}{\partial T}\left[T\ln(1+e^{-\beta\omega})\right]d\omega \\ &= \frac{k_B}{2}\int_{-\infty}^{\infty}\frac{1}{\pi}\frac{\Gamma}{\omega^2+\Gamma^2}\ln(1+e^{-\beta\omega})d\omega \\ &\quad +\frac{1}{2T}\int_{-\infty}^{\infty}\frac{1}{\pi}\frac{\Gamma}{\omega^2+\Gamma^2}\frac{\omega}{(e^{\beta\omega}+1)}d\omega. \end{aligned} \tag{C.17}$$

The integrals of Eq. (C.17) are rather complicated. Yet, approximated analytical expressions can be obtained in the low-temperature limit. First, note that since $\ln(1+e^{-\beta\omega}) \to 0$ for and $\Gamma \gg k_B T$ as $T \to 0$. With this we can see that

$$\int_{-\infty}^{\infty}\frac{1}{\pi}\frac{\Gamma}{\omega^2+\Gamma^2}\ln(1+e^{-\beta\omega})d\omega \to 0, \qquad (T\to 0).$$

Moreover, using the fact that $f(\omega) = (e^{\beta\omega}+1)^{-1}$ we can write

$$S_1(T\to 0) = \int_{-\infty}^{\infty} h(\omega)f(\omega)d\omega, \tag{C.18}$$

with

$$h(\omega) = \frac{1}{2\pi T}\frac{\omega\Gamma}{\omega^2+\Gamma^2} \tag{C.19}$$

For small T this class of integrals can be written in within the so called Sommerfeld expansion as

$$S_1(T) \approx g(0) + \frac{\pi^2}{6}\frac{d^2 g(\omega)}{d\omega^2}\Big|_{\omega=0}(k_B T)^2 + \mathcal{O}[(k_B T)^4], \tag{C.20}$$

in which

$$g(\omega) = \int_0^{\omega} h(\omega')d\omega'. \tag{C.21}$$

Upon performing the integration with the integrand (C.19) we obtain

$$g(\omega) = \frac{\Gamma}{4\pi T}\ln\left[\frac{\omega^2+\Gamma^2}{\Gamma^2}\right]. \tag{C.22}$$

Using this expression in (C.20), up to $\mathcal{O}[(k_{\mathrm{B}}T)^3]$ we find

$$S_1(T) \approx \frac{k_{\mathrm{B}}}{2}\frac{\pi}{6}\left(\frac{k_{\mathrm{B}}T}{\Gamma}\right). \tag{C.23}$$

The total entropy in the coupled case is then given by

$$S_f(T) \approx \frac{k_{\mathrm{B}}}{2}\ln(2) + \frac{\mathrm{k_B}}{2}\frac{\pi}{6}\left(\frac{\mathrm{k_B T}}{\Gamma}\right), \qquad (\mathrm{T}\to 0). \tag{C.24}$$

Strictly at $T = 0$ we obtain the interesting result

$$S_{\mathrm{res}} = \frac{k_{\mathrm{B}}}{2}\ln(2), \tag{C.25}$$

where $S_{\mathrm{res}} \equiv S_f(0)$. This result shows that only the free Majorana mode contributes to the residual entropy at $T = 0$. Furthermore the residual entropy is half of $k_B\ln(2)$, revealing the non-Fermi liquid (NFL) characteristic of the system. This is the analogue of what happens in the two channel Kondo effect (TSVELICK, 1985; AFFLECK; LUDWIG, 1991a; AFFLECK; LUDWIG, 1991b; AFFLECK; LUDWIG, 1993; EMERY; KIVELSON, 1992; GAN; ANDREI; COLEMAN, 1993; FABRIZIO; GOGOLIN, 1994; COLEMAN; IOFFE; TSVELIK, 1995; COX; ZAWADOWSKI, 1998).

APPENDIX D – Path integral formalism

One of the most useful formulation of quantum mechanics is using the called *path integrals*. This formalism is more natural for physical systems that deals with several degrees of freedom, as in statistical physics and high-energy physics (KLEINERT, 2009). For this reason, the path integral formalism is the basis of the quantum field theory (QFT) formulation. The renormalization group ideas was originally expressed in terms of path integral (WILSON, 1971a; WILSON, 1971b; WILSON, 1975). In this appendix we will give a brief review of the subject. Further information about path integrals and QFT can be found in (WEINBERG, 1995; TSVELIK, 2007; ALTLAND; SIMONS, 2010; ZEE, 2003).

D.1 Particle propagator as a path integral

Let us start with the propagation of a particle from the initial state $|q_i\rangle$ at the initial time $t_i = 0$ that propagate to the final state $|q_f\rangle$ in the time $t_f = t$. We know from the usual formulation of the quantum mechanics that this propagations is given by[1]

$$\langle q_f|e^{-i\hat{H}t}|q_i\rangle, \tag{D.1}$$

where $\hat{H}$ is the Hamiltonian. The propagation can be performed in N steps as

$$\langle q_f|e^{-i\hat{H}t}|q_i\rangle = \langle q_f|e^{-i\hat{H}\delta t}e^{-i\hat{H}\delta t}\cdots e^{-i\hat{H}\delta t}|q_i\rangle \tag{D.2}$$

In the above we define the differential time-step $\delta t = t/N$, with $N \to \infty$. Using now the closure relation $\int dq|q\rangle\langle q| = 1$ we can write

$$\begin{aligned}
\langle q_f|e^{-i\hat{H}\delta t}e^{-i\hat{H}\delta t}\cdots e^{-i\hat{H}\delta t}|q_i\rangle &= \langle q_f|e^{-i\hat{H}\delta t}\int dq_{N-1}|q_{N-1}\rangle\langle q_{N-1}|e^{-i\hat{H}\delta t} \\
&\quad\times\int dq_{N-2}|q_{N-2}\rangle\langle q_{N-2}|e^{-i\hat{H}\delta t}\int dq_{N-3}|q_{N-3}\rangle\langle q_{N-3}| \\
&\quad\cdots\times\langle q_2|e^{-i\hat{H}\delta t}\int dq_1|q_1\rangle\langle q_1|e^{-i\hat{H}\delta t}|q_i\rangle \\
&= \int\prod_{j=1}^{N-1}dq_j\langle q_f|e^{-i\hat{H}\delta t}|q_{N-1}\rangle\langle q_{N-1}|e^{-i\hat{H}\delta t}|q_{N-2}\rangle \\
&\quad\times\cdots\langle q_2|e^{-i\hat{H}\delta t}|q_1\rangle\langle q_1|e^{-i\hat{H}\delta t}|q_i\rangle.
\end{aligned} \tag{D.3}$$

Now, consider the Hamiltonian $\hat{H} = \hat{T} + \hat{V}$, where $\hat{T}$ denotes the kinetic term and $\hat{V}$ is the potential term. Let us look to the state evolution of $|q_j\rangle$ to $|q_{j+1}\rangle$ promoted by this

[1] Notice that $\hbar = 1$.

Hamiltonian[2]

$$\langle q_{j+1}|e^{-i\hat{H}\delta t}|q_j\rangle = \langle q_{j+1}|e^{-i(\hat{T}+\hat{V})\delta t}|q_j\rangle = \langle q_{j+1}|e^{-i\hat{T}(p_j)\delta t}|q_j\rangle e^{-i\hat{V}(q_j,t_j)\delta t}.$$

Using now the closure relation in the momentum space $\int \frac{dp}{2\pi}|p\rangle\langle p| = 1$ we have

$$\begin{aligned}\langle q_{j+1}|e^{-i\hat{T}(p_j)\delta t}|q_j\rangle e^{-i\hat{V}(q_j,t_j)\delta t} &= \int \frac{dp}{2\pi}\langle q_{j+1}|e^{-i\hat{T}(p_j)\delta t}|p\rangle\langle p|q_j\rangle e^{-i\hat{V}(q_j,t_j)\delta t} \\ &= \int \frac{dp}{2\pi}\langle q_{j+1}|p\rangle\langle p|q_j\rangle e^{-i[\hat{T}(p_j)+\hat{V}(q_j,t_j)]\delta t}. \end{aligned} \tag{D.4}$$

Recalling that $\langle q|p\rangle = e^{iqx}$ denotes the plane wave we obtain

$$\begin{aligned}\langle q_{j+1}|e^{-i\hat{T}(p_j)\delta t}|q_j\rangle e^{-i\hat{V}(q_j,t_j)\delta t} &= \int \frac{dp}{2\pi}\langle q_{j+1}|p\rangle\langle p|q_j\rangle e^{-i[\hat{T}(p_j)+\hat{V}(q_j,t_j)]\delta t} \\ &\quad \int \frac{dp}{2\pi} e^{ipq_{j+1}} e^{-ipq_j} e^{-i[\hat{T}(p_j)+\hat{V}(q_j,t_j)]\delta t} \\ &= \int \frac{dp}{2\pi} e^{\,i\left[p\left(\frac{q_{j+1}-q_j}{\delta t}\right)-\hat{T}(p_j)-\hat{V}(q_j,t_j)\right]\delta t}. \end{aligned} \tag{D.5}$$

In the thermodynamic limit, $N \to \infty$, so $\delta t \to 0$. Thus, $\frac{q_{j+1}-q_j}{\delta t} = \frac{\partial}{\partial t}q_j = \dot{q}_j$, resulting in

$$\langle q_{j+1}|e^{-i\hat{H}\delta t}|q_j\rangle = \int \frac{dp}{2\pi} e^{i\left[p\dot{q}_j-\hat{T}(p_j)-\hat{V}(q_j,t_j)\right]\delta t} = \int \frac{dp}{2\pi} e^{i\left[p\dot{q}_j-\hat{H}(p_j,q_j,t_j)\right]\delta t}. \tag{D.6}$$

Using this result in $\langle q_f|e^{-i\hat{H}t}|q_i\rangle = \langle q_f|e^{-i\hat{H}\delta t}e^{-i\hat{H}\delta t}\cdots e^{-i\hat{H}\delta t}|q_i\rangle$ leads to

$$\langle q_f|e^{-iHt}|q_i\rangle = \lim_{N\to\infty}\int \prod_{k=1}^{N-1} dq_k \prod_{j=1}^{N-1}\frac{dp_j}{2\pi} e^{i\delta t\sum_{j=0}^{N-1}[p_j\dot{q}_j-\hat{H}(p_j,q_j,t_j)]}. \tag{D.7}$$

Now, in the continuous time limit we have $\delta t\sum_{j=0}^{N-1} \to \int_0^t dt'$, which finally results

$$\langle q_f|e^{-i\hat{H}t}|q_i\rangle = \int \mathcal{D}q\mathcal{D}p e^{i\int_0^t[p\dot{q}-\hat{H}(p,q,t')]dt'}, \tag{D.8}$$

where

$$\mathcal{D}q\mathcal{D}p = \lim_{N\to\infty}\prod_{k=1}^{N-1} dq_k \prod_{j=1}^{N-1}\frac{dp_j}{2\pi}. \tag{D.9}$$

The quantity $\int \mathcal{D}q\mathcal{D}pF[q,p]$ is called *path integral* of the functional $F[p,q]$. Note that in the exponential above appears the general Lagrangian definition [3]

$$L = p\dot{q} - H(p,q,t'). \tag{D.10}$$

Defining now the *action* S

$$S[p,q,t] = \int_0^t L(p,q,t')dt', \tag{D.11}$$

the propagator can be written as

$$\langle q_f|e^{-i\hat{H}t}|q_i\rangle = \int \mathcal{D}q\mathcal{D}p e^{iS[p,q,t]}. \tag{D.12}$$

[2] In the general case $e^{i(\hat{H}+\hat{T})t} \neq e^{i\hat{T}t}e^{i\hat{V}t}$ but for a short-time δt the equality $e^{i(\hat{T}+\hat{V})\delta t} = e^{i\hat{T}\delta t}e^{i\hat{V}\delta t}$ can be safely taken.

[3] In the most usual cases the Lagrangian takes the usual form $L = T - V$.

D.2 Partition Function as a Path Integral

In statistical physics, the partition function is given by

$$Z = \mathrm{Tr} e^{-\beta \hat{H}} = \int dq \langle q | e^{-\beta \hat{H}} | q \rangle. \tag{D.13}$$

Note that the quantum propagator (D.1) can be connected with the partition function above by

$$\langle q | e^{-\beta \hat{H}} | q \rangle = \langle q_f | e^{-i\beta \hat{H} t} | q_i \rangle_{q_f = q_i, t = -i\beta}. \tag{D.14}$$

Then, inserting this result in (D.13) and using (D.12) we can written the partition function as a path integral

$$Z = \int \mathcal{D}q \mathcal{D}p e^{-S_E[p,q,\beta]}, \tag{D.15}$$

where

$$S_E[p,q,\beta] = -i \int_0^{-i\beta} dt' \left(p \frac{\partial}{\partial t'} q - H(p,q,t') \right). \tag{D.16}$$

If we define the imaginary time $\tau' = it'$ we have

$$\begin{aligned} S_E[p,q,\beta] &= -i \int_0^{-i\beta} dt' \left(p \frac{\partial}{\partial t'} q - H(p,q,t') \right) \\ &= \int_0^{-i\beta} (i dt') \left(-p \frac{\partial}{\partial t'} q + H(p,q,t') \right) \\ &= \int_0^{-i\beta} (i dt') \left(-ip \frac{\partial}{\partial (it')} q + H(p,q,t') \right) \\ &= \int_0^{\beta} d\tau' \left(-ip \frac{\partial}{\partial \tau'} q + H(p,q,\tau') \right), \end{aligned}$$

where in the last line we use $t = -i\beta = -i\tau = \beta$. Using the shorthand notation $\frac{\partial}{\partial \tau} = \partial_\tau$ we finally obtain [4]

$$S_E[p,q,\beta] = \int_0^{\beta} d\tau [-ip\partial_\tau q + H(p,q,\tau)]. \tag{D.17}$$

This action is known as "*Euclidean action*".

In general way, for an arbitrary quantum field ϕ, we can construct the partition function as the path integral

$$Z = \int \mathcal{D}\phi e^{-S_E[\phi]}, \tag{D.18}$$

where ϕ can be represented by a set of Grasmann, scalar, or vectorial fields which obey the Bose or Fermi statistics (NEGELE; ORLAND, 1988).

[4] Notice that in the imaginary time the usual Lagrangian becomes $L_E = T + V$ and not $L = T - V$.

D.3 Gaussian Path Integral

Consider the generic action

$$S = \int [\alpha\phi(x)\partial_x\phi(x) + J(x)\phi(x)]d^D x, \tag{D.19}$$

where α is a constant and the last term is a "source" term. To compute the partition function for this action we need of path integral of the kind

$$I = \int \mathcal{D}\phi e^{-\int [\phi(x)\partial_x\phi(x)+J(x)\phi(x)]d^D x}. \tag{D.20}$$

In the continuum form the action above is hard to be computed. However, in the discrete form it can be easily solved. The discrete form of this action can be taken using that $\partial\phi(x) \to \lim_{a\to 0}(1/a)(\phi_{i+1} - \phi_i) \equiv \sum_j M_{ij}\phi_j$, with the appropriated M matrix. The last terms transforms as $\int d^D x J(x)\phi(x) \to \lim_{a\to 0}(1/a^D)\sum_j J_i\phi(x)$. Therefore, the action in the discrete form becomes

$$S = \alpha \sum_{ij} \phi_i M_{ij}\phi_j + \sum_j J_i\phi_i. \tag{D.21}$$

With this, we have

$$I = \int \mathcal{D}\phi e^{-\left(\alpha\sum_{ij}\phi_i M_{ij}\phi_j + \sum_j J_i\phi_i\right)}, \tag{D.22}$$

where $\mathcal{D}\phi = \prod_{i=k}^N d\phi_k$. If we define a vector $\phi = (\phi_1, \phi_2, \cdots \phi_N)^T$ the integral above can be written as

$$I = \int \mathcal{D}\phi e^{-(\alpha(\phi\cdot M\cdot\phi) - J\cdot\phi)}, \tag{D.23}$$

where M is as symmetric matrix. Performing the rotation $\phi = Oy$ which diagonalizes the matrix M we have

$$\phi \cdot M \cdot \phi = (yO^{-1}) \cdot M \cdot Oy, \quad \text{with} \quad O^{-1}_{\lambda i} M_{ij} O_{j\lambda'} = m_\lambda \delta_{\lambda\lambda'}, \tag{D.24}$$

with m_λ denoting the λth eigenvalue of M. In terms of the components we have

$$\sum_{ij} \phi_i M_{ij}\phi_j = \sum_{ij} y_i O_{ji} M_{ij} O_{ij} y_j = \mathbf{y}\cdot M_D \cdot \mathbf{y},$$

where M_D is the matrix composed by the eigenvalues of M. Using this, and the fact that $d\phi_i = dy_i$,[5] we have explicitly

$$I = \int_{-\infty}^{\infty} dy_1 \int_{-\infty}^{\infty} dy_1 \cdots \int_{-\infty}^{\infty} dy_N e^{-\left(\alpha\sum_i y_i m_i y_i + (OJ)_i y_i\right)}. \tag{D.25}$$

Let us look to the integral

$$I_i = \int_{-\infty}^{\infty} dy_i e^{-\alpha y_i m_i y_i + (OJ)_i y_i} = \int_{-\infty}^{\infty} dy_i e^{-\alpha m_i y_i^2 + (OJ)_i y_i}.$$

[5] To see that the Jacobian in the present case is unitary notice that $O^{-1}O = 1$.

Now, note that exponential argument above can be written as

$$\alpha m_i y_i^2 + (OJ)_i y_i = \left((\alpha m_i)^{1/2} y_i + \frac{(OJ)_i}{2(\alpha m_i)^{1/2}} \right)^2 - \frac{(OJ)_i^2}{4\alpha m_i},$$

so

$$I_i = e^{-\frac{(OJ)_i^2}{4\alpha m_i}} \int_{-\infty}^{\infty} dy_i e^{-\left((\alpha m_i)^{1/2} y_i + \frac{(OJ)_i}{2(\alpha m_i)^{1/2}} \right)^2}.$$

Now, performing the variable change $u_i = (\alpha m_i)^{1/2} y_i + \frac{(OJ)_i}{2(\alpha m_i)^{1/2}}$ we get

$$I_i = \frac{e^{-\frac{(OJ)_i^2}{4\alpha m_i}}}{(\alpha m_i)^{1/2}} \int_{-\infty}^{\infty} du_i e^{-u_i^2}.$$

In integral above we recognize $\int_{-\infty}^{\infty} du_i e^{-u_i^2}$ as the usual Gaussian integral which well-known result $\sqrt{2\pi}$. Then, finally

$$I_i = \left(\frac{2\pi}{\alpha m_i} \right)^{1/2} e^{-\frac{1}{4\alpha} \left[(OJ) \frac{1}{m_i} (OJ) \right]}.$$

At last, using that $I = \prod_{i=1}^{N} I_i$ we obtain

$$\begin{aligned} I &= \left(\frac{2\pi}{\alpha} \right)^{N/2} e^{-\frac{1}{4\alpha} \sum_i \left[(OJ) \frac{1}{m_i} (OJ) \right]} \frac{1}{\prod_{i=1}^{N} m_i^{1/2}} \\ &= \left(\frac{2\pi}{\alpha} \right)^{N/2} e^{-\frac{1}{4\alpha} (OJ) M_D^{-1} (OJ)} \frac{1}{\prod_{i=1}^{N} m_i^{1/2}} \\ &= \left(\frac{2\pi}{\alpha} \right)^{N/2} e^{-\frac{1}{4\alpha} J (O^{-1} M_D^{-1} O) J)} \frac{1}{\prod_{i=1}^{N} m_i^{1/2}} \\ &= \left(\frac{2\pi}{\alpha} \right)^{N/2} e^{-\frac{1}{4\alpha} J M^{-1} J} \frac{1}{\prod_{i=1}^{N} m_i^{1/2}}. \end{aligned} \tag{D.26}$$

In the above we notice that $\det[M] = \prod_{i=1}^{N} m_i$, resulting in

$$I(J) = \left(\frac{2\pi}{\alpha \det[M]} \right)^{N/2} e^{-\frac{1}{4\alpha} J M^{-1} J}. \tag{D.27}$$

The integral $I(J)$ appears quite often in quantum field theory and it is called *Gaussian path integral* (ZEE, 2003). An important feature of the Gaussian path integral occurs when $J = 0$. In this case, from the result above we obtain

$$I(0) = \left(\frac{2\pi}{\alpha \det[M]} \right)^{N/2} = \text{constant}. \tag{D.28}$$

APPENDIX E – Quantum Perturbation Theory

A generic perturbed system can be described by the generic Hamiltonian

$$H = H_0 + \lambda V. \tag{E.1}$$

Where H_0 describes the unperturbed system and V corresponds to the perturbation. The parameter λ controls the strength of the perturbation on the unperturbed system. Suppose the eigenenergies and eigenstates of the unperturbed system are known. Then, from the Schrödinger equation we have

$$H_0|\psi_k^{(0)}\rangle = E_k^{(0)}|\psi_k^{(0)}\rangle, \tag{E.2}$$

where $E_k^{(0)}$ is an eigenenergy of the unperturbed system with correspondent eigenstate $|\psi^{(0)}\rangle$. The full eigenenergies and eigenstates of the perturbed system, described by the equation (E.1), are given by E_k and $|\psi_k\rangle$ which can be expressed in terms of a power series of the perturbation strength λ as

$$|\psi_k\rangle = |\psi_k^{(0)}\rangle + \lambda|\psi^{(1)}\rangle + \lambda^2|\psi_k^{(2)}\rangle + \cdots \tag{E.3}$$

$$E_k = E_k^{(0)} + \lambda E_k^{(1)} + \lambda^2 E_k^{(2)} + \cdots \tag{E.4}$$

Following this, we have the Schrödinger equation for the perturbed system

$$H|\psi_k\rangle = E_k|\psi_k\rangle, \tag{E.5}$$

which leads to

$$\begin{aligned}(H_0 + \lambda V)(|\psi_k^{(0)}\rangle + \lambda|\psi^{(1)}\rangle + \lambda^2|\psi_k^{(2)}\rangle + \cdots) = (E_k^{(0)} + \lambda E_k^{(1)} \\ +\lambda^2 E_k^{(2)} + \cdots)(|\psi_k^{(0)}\rangle + \lambda|\psi^{(1)}\rangle + \lambda^2|\psi_k^{(2)}\rangle + \cdots).\end{aligned} \tag{E.6}$$

The identity above can be written for each power of λ. For $\lambda^0 = 1$ we recovery the Schrödinger equation for the unperturbed system

$$H_0|\psi_k^{(0)}\rangle = E_k^{(0)}|\psi_k^{(0)}\rangle,$$

as expected. For the terms proportional to λ we have

$$H_0|\psi_k^{(1)}\rangle + V|\psi_k^{(0)}\rangle = E_k^{(0)}|\psi_k^{(1)}\rangle + E_k^{(1)}|\psi_k^{(0)}\rangle. \tag{E.7}$$

If we multiply by $\langle\psi_k^0|$ we get

$$\langle\psi_k^{(0)}|H_0|\psi_k^{(1)}\rangle + \langle\psi_k^{(0)}|V|\psi_k^{(0)}\rangle = E_k^{(0)}\langle\psi_k^{(0)}|\psi_k^{(1)}\rangle + E_k^{(1)}\langle\psi_k^{(0)}|\psi_k^{(0)}\rangle. \tag{E.8}$$

Using now that $\langle\psi_k^{(0)}|H_0 = \langle\psi_k^{(0)}|E_k^0$ and $\langle\psi_k^{(0)}|\psi_k^{(0)}\rangle = 1$ we obtain

$$E_k^{(1)} = \langle\psi_k^0|V|\psi_k^{(0)}\rangle, \tag{E.9}$$

which is the energy correction due to the perturbation at first-order in λ. To compute the first order correction of the eigenstate ($|\psi_k^1\rangle$) note that

$$\begin{aligned} V|\psi_k^{(0)}\rangle &= \sum_{k'} |\psi_{k'}^{(0)}\rangle\langle\psi_{k'}^{(0)}|V|\psi_{k'}^{(0)}\rangle \\ &= \sum_{k'\neq k} |\psi_{k'}^{(0)}\rangle\langle\psi_{k'}^{(0)}|V|\psi_k^{(0)}\rangle + |\psi_k^{(0)}\rangle\langle\psi_k^{(0)}|V|\psi_k^{(0)}\rangle \\ &= \sum_{k\neq k'} |\psi_{k'}^{(0)}\rangle\langle\psi_{k'}^{(0)}|V|\psi_k^{(0)}\rangle + E_k^{(1)}|\psi_k^{(0)}\rangle. \end{aligned} \tag{E.10}$$

In the above, to obtain the result above we use the completeness $\sum_{k'} |\psi_{k'}^{(0)}\rangle\langle\psi_{k'}^{(0)}| = \mathbf{1}$. Using this equation in (E.7) we get

$$(E_k^{(0)} - H_0)|\psi_k^{(1)}\rangle = \sum_{k'\neq k} \langle\psi_{k'}^{(0)}|V|\psi_k^{(0)}\rangle|\psi_{k'}^{(0)}\rangle. \tag{E.11}$$

Multiplying by $\langle\psi_{k'}^{(0)}|$ results in

$$\langle\psi_{k'}^{(0)}|\psi_k^{(1)}\rangle = \frac{\langle\psi_{k'}^{(0)}|V|\psi_k^{(0)}\rangle}{E_k^{(0)} - E_{k'}^{(0)}}.$$

Finally,

$$|\psi_k^{(1)}\rangle = \sum_{k'\neq k} \frac{\langle\psi_{k'}^{(0)}|V|\psi_k^{(0)}\rangle}{E_k^{(0)} - E_{k'}^{(0)}}|\psi_{k'}^{(0)}\rangle, \tag{E.12}$$

which is the eigenstate correction at first order. Obviously, this result is only true for non-degenerated systems ($E_{k'} \neq E_k$). For this reason the approach presented is sometimes called perturbation theory for non-degenerated systems.

For terms of second order in λ, the equation (E.6) results in

$$H_0|\psi_k^{(2)}\rangle + V|\psi_k^{(1)}\rangle = E_k^{(0)}|\psi_k^{(2)}\rangle + E_k^{(1)}|\psi_k^{(1)}\rangle + E_k^{(2)}|\psi_k^{(0)}\rangle. \tag{E.13}$$

Then,

$$\langle\psi_k^{(0)}|H_0|\psi_k^{(2)}\rangle + \langle\psi_k^{(0)}|V|\psi_k^{(1)}\rangle = E_k^{(0)}\langle\psi_k^{(0)}|\psi_k^{(2)}\rangle + E_k^{(1)}\langle\psi_k^{(0)}|\psi_k^{(1)}\rangle + E_k^{(2)}\langle\psi_k^{(0)}|\psi_k^{(0)}\rangle,$$

which gives

$$\langle\psi_k^{(0)}|V|\psi_k^{(1)}\rangle = E_k^{(2)} + E_k^{(1)}\langle\psi_k^{(0)}|\psi_k^{(1)}\rangle. \tag{E.14}$$

The term in the left side of the equation above can be written as

$$\begin{aligned}
\langle\psi_k^{(0)}|V|\psi_k^{(1)}\rangle &= \sum_{k'k''}\langle\psi_k^{(0)}|\psi_{k''}^{(0)}\rangle\langle\psi_{k''}^{(0)}|V|\psi_{k'}^{(0)}\rangle\langle\psi_{k'}^{(0)}|\psi_k^{(1)}\rangle \\
&= \sum_{k'k''}\delta_{k,k''}\langle\psi_{k''}^{(0)}|V|\psi_{k'}^{(0)}\rangle\langle\psi_{k'}^{(0)}|\psi_k^{(1)}\rangle \\
&= \sum_{k'}\langle\psi_k^{(0)}|V|\psi_{k'}^{(0)}\rangle\langle\psi_{k'}^{(0)}|\psi_k^{(1)}\rangle \\
&= \sum_{k'\neq k}\langle\psi_k^{(0)}|V|\psi_{k'}^{(0)}\rangle\langle\psi_{k'}^{(0)}|\psi_k^{(1)}\rangle + \langle\psi_k^{(0)}|V|\psi_k^{(0)}\rangle\langle\psi_k^{(0)}|\psi_k^{(1)}\rangle \\
&= \sum_{k'\neq k}\langle\psi_k^{(0)}|V|\psi_{k'}^{(0)}\rangle\langle\psi_{k'}^{(0)}|\psi_k^{(1)}\rangle + E_k^{(1)}\langle\psi_k^{(0)}|\psi_k^{(1)}\rangle \\
&= \sum_{k'\neq k}\frac{\langle\psi_k^{(0)}|V|\psi_{k'}^{(0)}\rangle\langle\psi_{k'}^{(0)}|V|\psi_k^{(0)}\rangle}{E_k^{(0)}-E_{k'}^{(0)}} + E_k^{(1)}\langle\psi_k^{(0)}|\psi_k^{(1)}\rangle. \qquad \text{(E.15)}
\end{aligned}$$

In the last line of the equation above we use

$$\langle\psi_{k'}^{(0)}|\psi_k^{(1)}\rangle = \frac{\langle\psi_{k'}^{(0)}|V|\psi_k^{(0)}\rangle}{E_k^{(0)}-E_{k'}^{(0)}}.$$

Inserting equation (E.15) in equation (E.14) leads to

$$E_k^{(2)} = \sum_{k'\neq k}\frac{\langle\psi_k^{(0)}|V|\psi_{k'}^{(0)}\rangle\langle\psi_{k'}^{(0)}|V|\psi_k^{(0)}\rangle}{E_k^{(0)}-E_{k'}^{(0)}}. \qquad \text{(E.16)}$$

This is the second order correction in the energy promoted by the perturbation on the system. The total contribution to the energy at second order from all the states E_k can be computed by

$$\Delta E^{(2)} = \sum_k\sum_{k'\neq k}\frac{\langle\psi_k^{(0)}|V|\psi_{k'}^{(0)}\rangle\langle\psi_{k'}^{(0)}|V|\psi_k^{(0)}\rangle}{E_k^{(0)}-E_{k'}^{(0)}}. \qquad \text{(E.17)}$$

The expression above is used in section 6.2 to obtain the effective interaction between two magnetic impurities.

APPENDIX F – Complex Integrals

F.1 Residue Theorem

Let the complex function $f(z)$ which can be expanded in the Laurent expansion as

$$f(z) = \sum_i \sum_{n=-\infty}^{\infty} a_{nz_i}(z - z_i)^n, \tag{F.1}$$

where z_i are isolated singular points (poles). The closed integral in the contour C, that contains all the poles $z = z_i$, can be performed using the called *residue theorem* (WHITTAKER; WATSON, 1996):

$$\oint_C f(z)dz = 2\pi i \sum_i a_{-1z_i}, \tag{F.2}$$

where the constant a_{-1z_i} in the Laurent expansion term $a_{-1z_i} = (z - z_i)^{-1}$ is called the residue of $f(z)$ at $z = z_i$. Sometimes, the residue is also denoted by

$$a_{-1z_i} = \text{Res}[f(z_i)]. \tag{F.3}$$

The contour integration depends on the integration direction, for example consider the integration in a semicircle contour, with a pole in $z = x_0$. Then, the integration over the semicircle pole with a infinitesimal radius δ gives

$$\begin{aligned}
\oint_C \frac{dz}{z - x_0} &= i\int_{\pi}^{2\pi} d\phi = i\pi \rightarrow i\pi\text{Res}[f(x_0)], \quad \text{for counterclockwise integration.} \\
\oint_C \frac{dz}{z - x_0} &= i\int_{\pi}^{0} d\phi = -i\pi \rightarrow -i\pi\text{Res}[f(x_0)], \quad \text{for clockwise integration.}
\end{aligned}$$

Where we use $z - x_0 = \delta e^{i\phi}$. There is several methods to compute the residue of the function $f(z)$, the most used are (BUTKOV, 2013)

1. **First method**. Using the definition, for a pole in $z = a$ we have

$$\text{Res}f(a) = \frac{1}{2\pi i}\oint_C f(z)dz. \tag{F.4}$$

2. **Second method**. For a simple pole in $z = a$ we can compute the residue using

$$\text{Res}f(a) = \lim_{z\to a}(z - a)f(z). \tag{F.5}$$

   This method is widely used, including in the present thesis.

3. **Third method**. For a pole of order m in $z = a$ we use

$$\text{Res}f(a) = \frac{1}{(m-1)!}\lim_{z\to a}\frac{d^{m-1}}{dz^{m-1}}[(z - a)^m f(z)]. \tag{F.6}$$

4. **Fourth method**. When $f(z)$ has the form

$$f(z) = \frac{\varphi(z)}{\psi(z)},$$

then, in this case we use

$$\text{Res}f(a) = \frac{\varphi(a)}{\psi'(a)}, \tag{F.7}$$

with $\varphi(a) \neq 0$ and $\psi(z)$ with a simple pole at $z = a$.

F.2 Cauchy Principal Value

Let us suppose that $f(z)$ has a simple pole in the real axis at $z = x_0$. Then, performing an integral in a closed contour C in the entire upper half-plane we obtain

$$\begin{aligned}\oint_C f(z)dz &= \int_{-\infty}^{x_0+\delta} f(x)dx + \int_{C_{x_0}} f(z)dz \\ &\quad + \int_{x_0+\delta}^{\infty} f(x)dx + \int_{C_D} f(z)dz = 2\pi i \sum \text{enclosed residues.}\end{aligned}$$

Above C_{x_0} is the contour around an infinitesimal circle centered at $x = x_0$ and radius $\delta \to 0$, and C_D is the contour in an infinite semicircle composed by the real axis and the imaginary axis, but which contours the pole. The integral along the real axis can be jointed as

$$\lim_{\delta\to 0}\left[\int_{-\infty}^{x_0+\delta} f(x)dx + \int_{x_0+\delta}^{\infty} f(x)dx\right] = \mathcal{P}\int_{-\infty}^{\infty} f(x)dx, \tag{F.8}$$

where $\mathcal{P}$ denotes the called *Cauchy principal value*. The Cauchy principal value can be defined using the contour integral. Suppose that the contour C is deformed in the contour $C(\delta)$ which is the same contour C but with an infinitesimal disk around the pole removed, then the Cauchy principal value is defined by

$$\mathcal{P}\int_C f(z)dz = \lim_{\delta\to 0^+}\int_{C(\delta)} f(z)dz. \tag{F.9}$$

We can use the Cauchy principal value with the residue theorem to write

$$\begin{aligned}\oint_C f(z)dz &= \mathcal{P}\int_{-\infty}^{\infty} f(x)dx + \int_{C_{x_0}} f(z)dz \\ &\quad + \int_{C_D} f(z)dz = 2\pi i \sum \text{enclosed residues.}\end{aligned}$$

The last integral in second line $\int_{C_D} f(z)dz$ is zero if $f(z)$ obey to conditions

- $f(z)$ is analytic in the upper half-plane except for a finite number of poles.
- $\lim_{|z|\to\infty} f(z) = 0$, for $0 \leq \arg z \leq \pi$.

this useful result is called *Jordan's lemma* (BROWN; CHURCHILL, 2009). Then, we have

$$\oint_C f(z)dz = \mathcal{P}\int_{-\infty}^{\infty} f(x)dx + \int_{C_{x_0}} f(z)dz = 2\pi i \sum \text{enclosed residues.} \tag{F.10}$$

The result above is one of the most powerful applications of the residue theorem and has been widely used in the present thesis. More details about complex calculus can be find in the excellent Butkov's mathematical physics book (BUTKOV, 2013).

Bibliography

ABRIKOSOV, A. et al. *Methods of Quantum Field Theory in Statistical Physics*. Dover Publications, 2012. (Dover Books on Physics). ISBN 9780486140155. Disponível em: <https://books.google.com.br/books?id=JYTCAgAAQBAJ>. Citado na página 70.

ABRIKOSOV, A. A. Electron scattering on magnetic impurities in metals and anomalous resistivity effects. *Physics Physique Fizika*, American Physical Society, v. 2, p. 5–20, Sep 1965. Disponível em: <https://link.aps.org/doi/10.1103/PhysicsPhysiqueFizika.2.5>. Citado na página 40.

AFFLECK, I.; LUDWIG, A. W. Critical theory of overscreened kondo fixed points. *Nuclear Physics B*, v. 360, n. 2, p. 641 – 696, 1991. ISSN 0550-3213. Disponível em: <http://www.sciencedirect.com/science/article/pii/055032139190419X>. Citado na página 156.

AFFLECK, I.; LUDWIG, A. W. W. Universal noninteger "ground-state degeneracy" in critical quantum systems. *Phys. Rev. Lett.*, American Physical Society, v. 67, p. 161–164, Jul 1991. Disponível em: <https://link.aps.org/doi/10.1103/PhysRevLett.67.161>. Citado 2 vezes nas páginas 81 and 156.

AFFLECK, I.; LUDWIG, A. W. W. Exact conformal-field-theory results on the multichannel kondo effect: Single-fermion green's function, self-energy, and resistivity. *Phys. Rev. B*, American Physical Society, v. 48, p. 7297–7321, Sep 1993. Disponível em: <https://link.aps.org/doi/10.1103/PhysRevB.48.7297>. Citado na página 156.

ALICEA, J. Majorana fermions in a tunable semiconductor device. *Phys. Rev. B*, American Physical Society, v. 81, p. 125318, Mar 2010. Disponível em: <https://link.aps.org/doi/10.1103/PhysRevB.81.125318>. Citado na página 73.

ALICEA, J. New directions in the pursuit of majorana fermions in solid state systems. *Reports on Progress in Physics*, v. 75, n. 7, p. 076501, 2012. Disponível em: <http://stacks.iop.org/0034-4885/75/i=7/a=076501>. Citado 4 vezes nas páginas 28, 73, 121, and 151.

ALTLAND, A. et al. Bethe ansatz solution of the topological kondo model. *Journal of Physics A: Mathematical and Theoretical*, IOP Publishing, v. 47, n. 26, p. 265001, jun 2014. Disponível em: <https://doi.org/10.1088%2F1751-8113%2F47%2F26%2F265001>. Citado na página 89.

ALTLAND, A.; SIMONS, B. *Condensed Matter Field Theory*. Cambridge University Press, 2010. (Cambridge books online). ISBN 9780521769754. Disponível em: <https://books.google.com.br/books?id=GpF0Pgo8CqAC>. Citado 3 vezes nas páginas 47, 52, and 157.

AMBJøRN, J.; SEMENOFF, G. Fermionized spin systems and the boson-fermion mapping in (2+1)-dimensional gauge theory. *Physics Letters B*, v. 226, n. 1, p. 107 – 112, 1989. ISSN 0370-2693. Disponível em: <http://www.sciencedirect.com/science/article/pii/0370269389902967>. Citado na página 69.

ANDERSON, P. W. Localized magnetic states in metals. *Phys. Rev.*, American Physical Society, v. 124, p. 41–53, Oct 1961. Disponível em: <https://link.aps.org/doi/10.1103/PhysRev.124.41>. Citado 2 vezes nas páginas 25 and 31.

ANDERSON, P. W. Plasmons, gauge invariance, and mass. *Phys. Rev.*, American Physical Society, v. 130, p. 439–442, Apr 1963. Disponível em: <https://link.aps.org/doi/10.1103/PhysRev.130.439>. Citado na página 69.

ANDERSON, P. W. A poor man's derivation of scaling laws for the kondo problem. *Journal of Physics C: Solid State Physics*, v. 3, n. 12, p. 2436, 1970. Disponível em: <http://stacks.iop.org/0022-3719/3/i=12/a=008>. Citado 3 vezes nas páginas 39, 52, and 53.

ANDERSON, P. W.; YUVAL, G. Some numerical results on the kondo problem and the inverse square one-dimensional ising model. *Journal of Physics C: Solid State Physics*, IOP Publishing, v. 4, n. 5, p. 607–620, apr 1971. Disponível em: <https://doi.org/10.1088%2F0022-3719%2F4%2F5%2F011>. Citado na página 39.

ANDERSON, P. W.; YUVAL, G.; HAMANN, D. R. Exact results in the kondo problem. ii. scaling theory, qualitatively correct solution, and some new results on one-dimensional classical statistical models. *Phys. Rev. B*, American Physical Society, v. 1, p. 4464–4473, Jun 1970. Disponível em: <https://link.aps.org/doi/10.1103/PhysRevB.1.4464>. Citado 3 vezes nas páginas 39, 52, and 53.

ANDREI, N. Diagonalization of the kondo hamiltonian. *Phys. Rev. Lett.*, American Physical Society, v. 45, p. 379–382, Aug 1980. Disponível em: <https://link.aps.org/doi/10.1103/PhysRevLett.45.379>. Citado na página 39.

ANDREI, N.; FURUYA, K.; LOWENSTEIN, J. H. Solution of the kondo problem. *Rev. Mod. Phys.*, American Physical Society, v. 55, p. 331–402, Apr 1983. Disponível em: <https://link.aps.org/doi/10.1103/RevModPhys.55.331>. Citado na página 39.

AUERBACH, A. *Interacting Electrons and Quantum Magnetism*. Springer New York, 2012. (Graduate Texts in Contemporary Physics). ISBN 9781461208693. Disponível em: <https://books.google.com.br/books?id=d-sHCAAAQBAJ>. Citado na página 25.

BAND, Y. B.; AVISHAI, Y. 13 - low-dimensional quantum systems. In: BAND, Y. B.; AVISHAI, Y. (Ed.). *Quantum Mechanics with Applications to Nanotechnology and Information Science*. Amsterdam: Academic Press, 2013. p. 749 – 823. ISBN 978-0-444-53786-7. Disponível em: <http://www.sciencedirect.com/science/article/pii/B9780444537867000137>. Citado 2 vezes nas páginas 27 and 28.

BARDEEN, J.; COOPER, L. N.; SCHRIEFFER, J. R. Theory of superconductivity. *Phys. Rev.*, American Physical Society, v. 108, p. 1175–1204, Dec 1957. Disponível em: <http://link.aps.org/doi/10.1103/PhysRev.108.1175>. Citado na página 69.

BERA, D. et al. Quantum dots and their multimodal applications: A review. *Materials*, Molecular Diversity Preservation International, v. 3, n. 4, p. 2260–2345, Mar 2010. ISSN 1996-1944. PMC5445848[pmcid]. Disponível em: <https://www.ncbi.nlm.nih.gov/pmc/articles/PMC5445848/>. Citado na página 27.

BÉRI, B.; COOPER, N. R. Topological kondo effect with majorana fermions. *Phys. Rev. Lett.*, American Physical Society, v. 109, p. 156803, Oct 2012. Disponível em: <https://link.aps.org/doi/10.1103/PhysRevLett.109.156803>. Citado na página 89.

BERNEVIG, B.; HUGHES, T. *Topological Insulators and Topological Superconductors*. Princeton University Press, 2013. ISBN 9781400846733. Disponível em: <http://books.google.com.br/books?id=_7r_UqFN0IEC>. Citado na página 72.

BERNEVIG, B. A.; ORENSTEIN, J.; ZHANG, S.-C. Exact su(2) symmetry and persistent spin helix in a spin-orbit coupled system. *Phys. Rev. Lett.*, American Physical Society, v. 97, p. 236601, Dec 2006. Disponível em: <https://link.aps.org/doi/10.1103/PhysRevLett.97.236601>. Citado na página 132.

BEZANSON, J. et al. Julia: A fresh approach to numerical computing. *SIAM Review*, v. 59, n. 1, p. 65–98, 2017. Disponível em: <https://doi.org/10.1137/141000671>. Citado na página 133.

BROWN, J.; CHURCHILL, R. *Complex Variables and Applications*. McGraw-Hill Education, 2009. (Brown and Churchill series). ISBN 9780073051949. Disponível em: <https://books.google.com.br/books?id=ytJFAQAAIAAJ>. Citado na página 169.

BULLA, R.; COSTI, T. A.; PRUSCHKE, T. Numerical renormalization group method for quantum impurity systems. *Rev. Mod. Phys.*, American Physical Society, v. 80, p. 395–450, Apr 2008. Disponível em: <https://link.aps.org/doi/10.1103/RevModPhys.80.395>. Citado na página 63.

BUTKOV, E. *Mathematical Physics*. Addison-Wesley, 2013. Disponível em: <https://books.google.com.br/books?id=_4sgygEACAAJ>. Citado 2 vezes nas páginas 167 and 169.

CAPPELLI, A.; MUSSARDO, G. *Statistical Field Theories*. Springer Netherlands, 2012. (Nato Science Series II:). ISBN 9789401005142. Disponível em: <https://books.google.com.br/books?id=vYtqCQAAQBAJ>. Citado 4 vezes nas páginas 42, 45, 47, and 52.

CARDY, J.; GODDARD, P.; YEOMANS, J. *Scaling and Renormalization in Statistical Physics*. Cambridge University Press, 1996. (Cambridge Lecture Notes in Physics). ISBN 9780521499590. Disponível em: <https://books.google.com.br/books?id=Wt804S9FjyAC>. Citado na página 43.

CHURCHILL, H. O. H. et al. Superconductor-nanowire devices from tunneling to the multichannel regime: Zero-bias oscillations and magnetoconductance crossover. *Phys. Rev. B*, American Physical Society, v. 87, p. 241401, Jun 2013. Disponível em: <https://link.aps.org/doi/10.1103/PhysRevB.87.241401>. Citado na página 26.

CIFUENTES, J. D.; SILVA, L. G. G. V. D. da. Manipulating majorana zero modes in double quantum dots. *Phys. Rev. B*, American Physical Society, v. 100, p. 085429, Aug 2019. Disponível em: <https://link.aps.org/doi/10.1103/PhysRevB.100.085429>. Citado na página 78.

CLOGSTON, A. M. et al. Local magnetic moment associated with an iron atom dissolved in various transition metal alloys. *Phys. Rev.*, American Physical Society, v. 125, p.

541–552, Jan 1962. Disponível em: <https://link.aps.org/doi/10.1103/PhysRev.125.541>. Citado na página 36.

COLEMAN, P. *Introduction to Many-Body Physics*. Cambridge University Press, 2015. ISBN 9780521864886. Disponível em: <https://books.google.com.br/books?id=kcrZCgAAQBAJ>. Citado 5 vezes nas páginas 25, 52, 69, 70, and 109.

COLEMAN, P.; IOFFE, L. B.; TSVELIK, A. M. Simple formulation of the two-channel kondo model. *Phys. Rev. B*, American Physical Society, v. 52, p. 6611–6627, Sep 1995. Disponível em: <https://link.aps.org/doi/10.1103/PhysRevB.52.6611>. Citado 2 vezes nas páginas 80 and 156.

COOPER, L. Bound electron pairs in a degenerate fermi gas. *Physical Review*, v. 104, p. 1189–1190, nov 1956. Disponível em: <http://adsabs.harvard.edu/abs/1956PhRv..104.1189C>. Citado na página 69.

COX, D. L.; ZAWADOWSKI, A. Exotic kondo effects in metals: Magnetic ions in a crystalline electric field and tunnelling centres. *Advances in Physics*, v. 47, n. 5, p. 599–942, 1998. Citado 2 vezes nas páginas 80 and 156.

DAS, A. et al. Zero-bias peaks and splitting in an al–inas nanowire topological superconductor as a signature of majorana fermions. *Nature Physics*, v. 8, n. 12, p. 887–895, Dec 2012. ISSN 1745-2481. Disponível em: <https://doi.org/10.1038/nphys2479>. Citado na página 26.

DATTA, S.; DAS, B. Electronic analog of the electrooptic modulator. *Applied Physics Letters*, v. 56, n. 7, p. 665–667, 1990. Disponível em: <https://doi.org/10.1063/1.102730>. Citado na página 121.

DAVIES, J. H. *The Physics of Low-dimensional Semiconductors: An Introduction*. [S.l.]: Cambridge University Press, 1997. Citado na página 27.

de Haas, W.; de Boer, J.; van dën Berg, G. The electrical resistance of gold, copper and lead at low temperatures. *Physica*, v. 1, n. 7, p. 1115 – 1124, 1934. ISSN 0031-8914. Disponível em: <http://www.sciencedirect.com/science/article/pii/S0031891434803102>. Citado 2 vezes nas páginas 25 and 37.

DENG, M.-T. et al. Nonlocality of majorana modes in hybrid nanowires. *Phys. Rev. B*, American Physical Society, v. 98, p. 085125, Aug 2018. Disponível em: <https://link.aps.org/doi/10.1103/PhysRevB.98.085125>. Citado na página 77.

DENG, M. T. et al. Anomalous zero-bias conductance peak in a nb–insb nanowire–nb hybrid device. *Nano Letters*, American Chemical Society, v. 12, n. 12, p. 6414–6419, Dec 2012. ISSN 1530-6984. Disponível em: <https://doi.org/10.1021/nl303758w>. Citado na página 26.

DIRAC, P. A. M. On the theory of quantum mechanics. *Proceedings of the Royal Society of London. Series A*, v. 112, n. 762, p. 661–677, out. 1926. Disponível em: <http://dx.doi.org/10.1098/rspa.1926.0133>. Citado na página 63.

DRESSELHAUS, G. Spin-orbit coupling effects in zinc blende structures. *Phys. Rev.*, American Physical Society, v. 100, p. 580–586, Oct 1955. Disponível em: <https://link.aps.org/doi/10.1103/PhysRev.100.580>. Citado na página 119.

DZYALOSHINSKY, I. A thermodynamic theory of "weak" ferromagnetism of antiferromagnetics. *Journal of Physics and Chemistry of Solids*, v. 4, n. 4, p. 241 – 255, 1958. ISSN 0022-3697. Disponível em: <http://www.sciencedirect.com/science/article/pii/0022369758900763>. Citado na página 125.

ELLIOTT, S. R.; FRANZ, M. Colloquium: Majorana fermions in nuclear, particle, and solid-state physics. *Rev. Mod. Phys.*, American Physical Society, v. 87, p. 137–163, Feb 2015. Disponível em: <https://link.aps.org/doi/10.1103/RevModPhys.87.137>. Citado 2 vezes nas páginas 68 and 151.

EMERY, V. J.; KIVELSON, S. Mapping of the two-channel kondo problem to a resonant-level model. *Phys. Rev. B*, American Physical Society, v. 46, p. 10812–10817, Nov 1992. Disponível em: <https://link.aps.org/doi/10.1103/PhysRevB.46.10812>. Citado 3 vezes nas páginas 80, 81, and 156.

FABRIZIO, M.; GOGOLIN, A. O. Toulouse limit for the overscreened four-channel kondo problem. *Phys. Rev. B*, American Physical Society, v. 50, p. 17732–17735, Dec 1994. Disponível em: <https://link.aps.org/doi/10.1103/PhysRevB.50.17732>. Citado na página 156.

FANO, U. Effects of configuration interaction on intensities and phase shifts. *Phys. Rev.*, American Physical Society, v. 124, p. 1866–1878, Dec 1961. Disponível em: <https://link.aps.org/doi/10.1103/PhysRev.124.1866>. Citado na página 40.

FETTER, A.; WALECKA, J. *Quantum Theory of Many-Particle Systems*. Dover Publications, 2012. (Dover Books on Physics). ISBN 9780486134758. Disponível em: <https://books.google.com.br/books?id=t5_DAgAAQBAJ>. Citado na página 70.

FÖLSCH, S. et al. Quantum dots with single-atom precision. *Nature Nanotechnology*, v. 9, n. 7, p. 505–508, Jul 2014. ISSN 1748-3395. Disponível em: <https://doi.org/10.1038/nnano.2014.129>. Citado na página 26.

FOWLER, M.; ZAWADOWSKI, A. Scaling and the renormalization group in the kondo effect. *Solid State Communications*, v. 9, n. 8, p. 471 – 476, 1971. ISSN 0038-1098. Disponível em: <http://www.sciencedirect.com/science/article/pii/0038109871903243>. Citado na página 39.

FRANZ, M. Majorana's wires. *Nature Nanotechnology*, v. 8, n. 3, p. 149–152, Mar 2013. ISSN 1748-3395. Disponível em: <https://doi.org/10.1038/nnano.2013.33>. Citado na página 26.

FRIEDEL, J. Metallic alloys. *Il Nuovo Cimento (1955-1965)*, v. 7, n. 2, p. 287–311, Sep 1958. ISSN 1827-6121. Disponível em: <https://doi.org/10.1007/BF02751483>. Citado na página 31.

FUBINI, G.; ITALIANA, U. matematica. *Opere scelte*. Edizioni cremonese, 1957. (Opere grandi matematici italiani). ISBN 9788870835045. Disponível em: <https://books.google.hn/books?id=vX0_AQAAIAAJ>. Citado na página 126.

GAN, J.; ANDREI, N.; COLEMAN, P. Perturbative approach to the non-fermi-liquid fixed point of the overscreened kondo problem. *Phys. Rev. Lett.*, American Physical Society, v. 70, p. 686–689, Feb 1993. Disponível em: <https://link.aps.org/doi/10.1103/PhysRevLett.70.686>. Citado na página 156.

GARLING, D. *Clifford Algebras: An Introduction*. Cambridge University Press, 2011. (London Mathematical Society Student Texts, 78). ISBN 9781139081245. Disponível em: <https://books.google.com.br/books?id=cIfctAEACAAJ>. Citado na página 64.

GELL-MANN, M.; LOW, F. E. Quantum electrodynamics at small distances. *Phys. Rev.*, American Physical Society, v. 95, p. 1300–1312, Sep 1954. Disponível em: <https://link.aps.org/doi/10.1103/PhysRev.95.1300>. Citado na página 46.

GOGOLIN, A.; NERSESYAN, A.; TSVELIK, A. *Bosonization and Strongly Correlated Systems*. Cambridge University Press, 2004. ISBN 9780521617192. Disponível em: <https://books.google.com.br/books?id=BZDfFIpCoaAC>. Citado na página 69.

GOLDHABER-GORDON, D. et al. Kondo effect in a single-electron transistor. *Nature*, v. 391, n. 6663, p. 156–159, Jan 1998. ISSN 1476-4687. Disponível em: <https://doi.org/10.1038/34373>. Citado 3 vezes nas páginas 25, 39, and 60.

GOLUB, G. et al. *Matrix Computations*. Johns Hopkins University Press, 1996. (Johns Hopkins Studies in the Mathematical Sciences). ISBN 9780801854149. Disponível em: <https://books.google.com.br/books?id=mlOa7wPX6OYC>. Citado na página 61.

GRADSHTEYN, I.; RYZHIK, I. *Table of Integrals, Series, and Products*. Academic Press, 1980. ISBN 9780122947605. Disponível em: <https://books.google.gm/books?id=9piquwEACAAJ>. Citado 5 vezes nas páginas 112, 113, 115, 129, and 130.

GROSSO, G.; PARRAVICINI, G. *Solid State Physics*. Elsevier Science, 2000. ISBN 9780080481029. Disponível em: <https://books.google.com.br/books?id=L5RrQbbvWn8C>. Citado 3 vezes nas páginas 27, 99, and 109.

HALDANE, F. D. M. Scaling theory of the asymmetric anderson model. *Phys. Rev. Lett.*, American Physical Society, v. 40, p. 416–419, Feb 1978. Disponível em: <https://link.aps.org/doi/10.1103/PhysRevLett.40.416>. Citado na página 60.

HASAN, M. Z.; KANE, C. L. *Colloquium* : Topological insulators. *Rev. Mod. Phys.*, American Physical Society, v. 82, p. 3045–3067, Nov 2010. Disponível em: <http://link.aps.org/doi/10.1103/RevModPhys.82.3045>. Citado na página 119.

Heisenberg, W. Zur Theorie des Ferromagnetismus. *Zeitschrift fur Physik*, v. 49, n. 9-10, p. 619–636, set. 1928. Citado na página 25.

HEWSON, A. *The Kondo Problem to Heavy Fermions*. Cambridge University Press, 1997. (Cambridge Studies in Magnetism). ISBN 9780521599474. Disponível em: <https://books.google.com.br/books?id=fPzgHneNFDAC>. Citado 8 vezes nas páginas 25, 31, 37, 39, 42, 52, 61, and 141.

HIGGS, P. W. Broken symmetries and the masses of gauge bosons. *Phys. Rev. Lett.*, American Physical Society, v. 13, p. 508–509, Oct 1964. Disponível em: <https://link.aps.org/doi/10.1103/PhysRevLett.13.508>. Citado na página 69.

HOFFMAN, S. et al. Spin-dependent coupling between quantum dots and topological quantum wires. *Phys. Rev. B*, American Physical Society, v. 96, p. 045440, Jul 2017. Disponível em: <https://link.aps.org/doi/10.1103/PhysRevB.96.045440>. Citado 2 vezes nas páginas 75 and 77.

IMAMURA, H.; BRUNO, P.; UTSUMI, Y. Twisted exchange interaction between localized spins embedded in a one- or two-dimensional electron gas with rashba spin-orbit coupling. *Phys. Rev. B*, American Physical Society, v. 69, p. 121303, Mar 2004. Disponível em: <https://link.aps.org/doi/10.1103/PhysRevB.69.121303>. Citado 2 vezes nas páginas 109 and 132.

INOSHITA, T. Kondo effect in quantum dots. *Science*, American Association for the Advancement of Science, v. 281, n. 5376, p. 526–527, 1998. ISSN 0036-8075. Disponível em: <https://science.sciencemag.org/content/281/5376/526>. Citado na página 25.

IVANOV, D. A. Non-abelian statistics of half-quantum vortices in p-wave superconductors. *Phys. Rev. Lett.*, American Physical Society, v. 86, p. 268–271, Jan 2001. Disponível em: <http://link.aps.org/doi/10.1103/PhysRevLett.86.268>. Citado na página 72.

KADANOFF, L. P. et al. Static phenomena near critical points: Theory and experiment. *Rev. Mod. Phys.*, American Physical Society, v. 39, p. 395–431, Apr 1967. Disponível em: <https://link.aps.org/doi/10.1103/RevModPhys.39.395>. Citado na página 42.

KALLIN, C.; BERLINSKY, A. J. Is sr2ruo4a chiral p-wave superconductor? *Journal of Physics: Condensed Matter*, IOP Publishing, v. 21, n. 16, p. 164210, mar 2009. Disponível em: <https://doi.org/10.1088%2F0953-8984%2F21%2F16%2F164210>. Citado 2 vezes nas páginas 72 and 73.

KASUYA, T. A Theory of Metallic Ferro- and Antiferromagnetism on Zener's Model. *Progress of Theoretical Physics*, v. 16, n. 1, p. 45–57, 07 1956. ISSN 0033-068X. Disponível em: <https://doi.org/10.1143/PTP.16.45>. Citado 2 vezes nas páginas 27 and 109.

KITAEV, A. Y. Unpaired Majorana fermions in quantum wires. *Physics-Uspekhi*, v. 44, n. 10S, p. 131–136, oct 2001. ISSN 1468-4780. Disponível em: <http://stacks.iop.org/1063-7869/44/i=10S/a=S29?key=crossref.8adaeb1befda6574f9e1617c47e8ae35>. Citado 2 vezes nas páginas 73 and 147.

KITTEL, C. Indirect exchange interactions in metals**supported by the national science foundation. In: SEITZ, F.; TURNBULL, D.; EHRENREICH, H. (Ed.). Academic Press, 1969, (Solid State Physics, v. 22). p. 1 – 26. Disponível em: <http://www.sciencedirect.com/science/article/pii/S0081194708600302>. Citado 2 vezes nas páginas 109 and 113.

KITTEL, C. *Introduction to Solid State Physics*. Wiley, 2004. ISBN 9780471415268. Disponível em: <https://books.google.com.br/books?id=kym4QgAACAAJ>. Citado na página 25.

KLEINERT, H. *Path Integrals in Quantum Mechanics, Statistics, Polymer Physics, and Financial Markets*. World Scientific, 2009. (EBL-Schweitzer). ISBN 9789814273572. Disponível em: <https://books.google.com.br/books?id=VJ1qNz5xYzkC>. Citado na página 157.

KNORR, N. et al. Kondo effect of single co adatoms on cu surfaces. *Phys. Rev. Lett.*, American Physical Society, v. 88, p. 096804, Feb 2002. Disponível em: <https://link.aps.org/doi/10.1103/PhysRevLett.88.096804>. Citado na página 40.

KONDO, J. Resistance minimum in dilute magnetic alloys. *Progress of Theoretical Physics*, v. 32, n. 1, p. 37–49, 1964. Disponível em: <+http://dx.doi.org/10.1143/PTP.32.37>. Citado na página 37.

KONDO, J. Theory of dilute magnetic alloys. In: SEITZ, F.; TURNBULL, D.; EHRENREICH, H. (Ed.). Academic Press, 1970, (Solid State Physics, v. 23). p. 183 – 281. Disponível em: <http://www.sciencedirect.com/science/article/pii/S0081194708606165>. Citado na página 37.

KOUWENHOVEN, L.; MARCUS, C. Quantum dots. *Physics World*, IOP Publishing, v. 11, n. 6, p. 35, 1998. Citado na página 36.

KRAUS, Y. E. et al. Majorana fermions of a two-dimensional $p_x + ip_y$ superconductor. *Phys. Rev. B*, American Physical Society, v. 79, p. 134515, Apr 2009. Disponível em: <http://link.aps.org/doi/10.1103/PhysRevB.79.134515>. Citado na página 72.

KRISHNA-MURTHY, H. R.; WILKINS, J. W.; WILSON, K. G. Renormalization-group approach to the anderson model of dilute magnetic alloys. i. static properties for the symmetric case. *Phys. Rev. B*, American Physical Society, v. 21, p. 1003–1043, Feb 1980. Disponível em: <https://link.aps.org/doi/10.1103/PhysRevB.21.1003>. Citado na página 63.

KRONMÜLLER, H.; PARKIN, S. *Handbook of Magnetism and Advanced Magnetic Materials: Spintronics and magnetoelectronics*. John Wiley & Sons, 2007. (Handbook of Magnetism and Advanced Magnetic Materials). ISBN 9780470022177. Disponível em: <https://books.google.com.br/books?id=N-rXAAAAMAAJ>. Citado na página 25.

LAW, K. T.; LEE, P. A.; NG, T. K. Majorana fermion induced resonant andreev reflection. *Phys. Rev. Lett.*, American Physical Society, v. 103, p. 237001, Dec 2009. Disponível em: <https://link.aps.org/doi/10.1103/PhysRevLett.103.237001>. Citado na página 26.

LEE, M.; LIM, J. S.; LÓPEZ, R. Kondo effect in a quantum dot side-coupled to a topological superconductor. *Phys. Rev. B*, American Physical Society, v. 87, p. 241402, Jun 2013. Disponível em: <https://link.aps.org/doi/10.1103/PhysRevB.87.241402>. Citado na página 78.

LIU, P.; WILLIAMS, J. R.; CHA, J. J. Topological nanomaterials. *Nature Reviews Materials*, v. 4, n. 7, p. 479–496, Jul 2019. ISSN 2058-8437. Disponível em: <https://doi.org/10.1038/s41578-019-0113-4>. Citado na página 25.

MACDONALD, D. K. C.; MENDELSSOHN, K.; SIMON, F. E. Resistivity of pure metals at low temperatures. i. the alkali metals. *Proceedings of the Royal Society of London. Series A. Mathematical and Physical Sciences*, v. 202, n. 1068, p. 103–126, 1950. Disponível em: <https://royalsocietypublishing.org/doi/abs/10.1098/rspa.1950.0088>. Citado na página 37.

MAHAN, G. *Many-Particle Physics*. Springer US, 2013. (Physics of Solids and Liquids). ISBN 9781475757149. Disponível em: <https://books.google.com.br/books?id=TFDUBwAAQBAJ>. Citado 2 vezes nas páginas 52 and 70.

MAJORANA, E. Teoria simmetrica dell'elettrone e del positrone. *Nuovo Cimento*, 1937. Citado 2 vezes nas páginas 26 and 65.

MARCOVICH, A.; SHINN, T. *Toward a New Dimension: Exploring the Nanoscale*. OUP Oxford, 2014. ISBN 9780191024009. Disponível em: <https://books.google.com.br/books?id=U-78AwAAQBAJ>. Citado na página 36.

MATTUCK, R. *A Guide to Feynman Diagrams in the Many-Body Problem: Second Edition*. Dover Publications, 2012. (Dover Books on Physics). ISBN 9780486131641. Disponível em: <https://books.google.com.br/books?id=1P_DAgAAQBAJ>. Citado na página 52.

MEYER, H. *A History of Electricity and Magnetism*. MIT Press, 1971. (Burndy Library publications). ISBN 9780262130707. Disponível em: <https://books.google.com.br/books?id=1stwQgAACAAJ>. Citado na página 25.

MORIYA, T. New mechanism of anisotropic superexchange interaction. *Phys. Rev. Lett.*, American Physical Society, v. 4, p. 228–230, Mar 1960. Disponível em: <https://link.aps.org/doi/10.1103/PhysRevLett.4.228>. Citado na página 125.

MOURIK, V. et al. Signatures of Majorana fermions in hybrid superconductor-semiconductor nanowire devices. *Science (New York, N.Y.)*, v. 336, n. 6084, p. 1003–7, may 2012. ISSN 1095-9203. Disponível em: <http://www.ncbi.nlm.nih.gov/pubmed/22499805>. Citado na página 26.

MROSS, D. F.; JOHANNESSON, H. Two-impurity kondo model with spin-orbit interactions. *Phys. Rev. B*, American Physical Society, v. 80, p. 155302, Oct 2009. Disponível em: <https://link.aps.org/doi/10.1103/PhysRevB.80.155302>. Citado na página 125.

MöCKLI, D.; HAIM, M.; KHODAS, M. Magnetic impurities in thin films and 2d ising superconductors. *Journal of Applied Physics*, v. 128, n. 5, p. 053903, 2020. Disponível em: <https://doi.org/10.1063/5.0010773>. Citado na página 28.

NADJ-PERGE, S. et al. Observation of majorana fermions in ferromagnetic atomic chains on a superconductor. *Science*, American Association for the Advancement of Science, v. 346, n. 6209, p. 602–607, 2014. ISSN 0036-8075. Disponível em: <https://science.sciencemag.org/content/346/6209/602>. Citado 2 vezes nas páginas 26 and 73.

NADJ-PERGE, S. et al. Spectroscopy of spin-orbit quantum bits in indium antimonide nanowires. *Phys. Rev. Lett.*, American Physical Society, v. 108, p. 166801, Apr 2012. Disponível em: <https://link.aps.org/doi/10.1103/PhysRevLett.108.166801>. Citado na página 119.

NAKAHARA, M. *Geometry, Topology and Physics*. 2. ed. Taylor & Francis, 2003. Paperback. ISBN 0750306068. Disponível em: <http://www.amazon.com/exec/obidos/redirect?tag=citeulike07-20&path=ASIN/0750306068>. Citado na página 72.

NÉEL, L. *Influence des fluctuations des champs moléculaires sur les propriétés magnétiques des corps*. Tese (Theses) — Universite, mar. 1932. Disponível em: <https://tel.archives-ouvertes.fr/tel-00278201>. Citado na página 25.

NEGELE, J.; ORLAND, H. *Quantum Many-particle Systems*. Basic Books, 1988. (Advanced Book Classics). ISBN 9780201125931. Disponível em: <https://books.google.com.br/books?id=EV8sAAAAYAAJ>. Citado na página 159.

NOLTING, W.; RAMAKANTH, A. *Quantum Theory of Magnetism*. Springer Berlin Heidelberg, 2009. ISBN 9783540854166. Disponível em: <https://books.google.com.br/books?id=vrcHC9XoHbsC>. Citado na página 122.

Nozières, Ph.; Blandin, A. Kondo effect in real metals. *J. Phys. France*, v. 41, n. 3, p. 193–211, 1980. Disponível em: <https://doi.org/10.1051/jphys:01980004103019300>. Citado na página 81.

ODASHIMA, M. M.; PRADO, B. G.; VERNEK, E. Pedagogical introduction to equilibrium Green's functions: condensed-matter examples with numerical implementations. *Revista Brasileira de Ensino de FÃsica*, scielo, v. 39, 00 2017. ISSN 1806-1117. Disponível em: <http://www.scielo.br/scielo.php?script=sci_arttext&pid=S1806-11172017000100402&nrm=iso>. Citado na página 32.

ONNES, H. Further experiments with liquid helium. c. on the change of electric resistance of pure metals at very low temperatures etc. iv. the resistance of pure mercury at helium temperatures. In: GAVROGLU, K.; GOUDAROULIS, Y. (Ed.). *Through Measurement to Knowledge*. Springer Netherlands, 1991, (Boston Studies in the Philosophy of Science, v. 124). p. 261–263. ISBN 978-94-010-7433-9. Disponível em: <http://dx.doi.org/10.1007/978-94-009-2079-8_15>. Citado 2 vezes nas páginas 37 and 69.

PAN, H. et al. *Quantized and unquantized zero-bias tunneling conductance peaks in Majorana nanowires: Conductance below and above* $2e^2/h$. 2021. Citado na página 26.

PESKIN, M. *An Introduction To Quantum Field Theory*. CRC Press, 2018. ISBN 9780429983184. Disponível em: <https://books.google.com.br/books?id=9EpnDwAAQBAJ>. Citado na página 65.

PIRÓTH, A.; SÓLYOM, J. *Fundamentals of the Physics of Solids: Volume II: Electronic Properties*. Springer Berlin Heidelberg, 2008. (Fundamentals of the Physics of Solids). ISBN 9783540853152. Disponível em: <https://books.google.com.br/books?id=XSo-a2n43xEC>. Citado na página 109.

PRADA, E.; AGUADO, R.; SAN-JOSE, P. Measuring majorana nonlocality and spin structure with a quantum dot. *Phys. Rev. B*, American Physical Society, v. 96, p. 085418, Aug 2017. Disponível em: <https://link.aps.org/doi/10.1103/PhysRevB.96.085418>. Citado 2 vezes nas páginas 75 and 77.

QI, X.-L.; ZHANG, S.-C. Topological insulators and superconductors. *Rev. Mod. Phys.*, American Physical Society, v. 83, p. 1057–1110, Oct 2011. Disponível em: <http://link.aps.org/doi/10.1103/RevModPhys.83.1057>. Citado na página 119.

RADWANSKI, R. et al. Crystal-field interactions and magnetism in rare-earth transition-metal intermetallic compounds. *Physica B: Condensed Matter*, v. 319, n. 1, p. 78 – 89, 2002. ISSN 0921-4526. Disponível em: <http://www.sciencedirect.com/science/article/pii/S0921452602011109>. Citado na página 119.

READ, N.; GREEN, D. Paired states of fermions in two dimensions with breaking of parity and time-reversal symmetries and the fractional quantum Hall effect. *Physical Review B*, American Physical Society, v. 61, n. 15, p. 10267–10297, apr 2000. ISSN 0163-1829. Disponível em: <http://link.aps.org/doi/10.1103/PhysRevB.61.10267https://link.aps.org/doi/10.1103/PhysRevB.61.10267>. Citado na página 72.

Ii. the doctor's dissertation (text and translation)**[see introduction, sect. 2.]. In: ROSENFELD, L.; NIELSEN, J. R. (Ed.). *EARLY WORK (1905–1911)*. Elsevier, 1972, (Niels Bohr Collected Works, v. 1). p. 163 – 393. Disponível em: <http://www.sciencedirect.com/science/article/pii/S187605030870015X>. Citado na página 25.

RUDERMAN, M. A.; KITTEL, C. Indirect exchange coupling of nuclear magnetic moments by conduction electrons. *Phys. Rev.*, American Physical Society, v. 96, p. 99–102, Oct 1954. Disponível em: <https://link.aps.org/doi/10.1103/PhysRev.96.99>. Citado 3 vezes nas páginas 27, 109, and 122.

RUIZ-TIJERINA, D. A. et al. Interaction effects on a majorana zero mode leaking into a quantum dot. *Phys. Rev. B*, American Physical Society, v. 91, p. 115435, Mar 2015. Disponível em: <https://link.aps.org/doi/10.1103/PhysRevB.91.115435>. Citado 4 vezes nas páginas 27, 75, 78, and 81.

RUSIN, T. M.; ZAWADZKI, W. On calculation of rkky range function in one dimension. *Journal of Magnetism and Magnetic Materials*, v. 441, p. 387 – 391, 2017. ISSN 0304-8853. Disponível em: <http://www.sciencedirect.com/science/article/pii/S0304885317307710>. Citado 4 vezes nas páginas 109, 110, 113, and 128.

SACHDEV, S. *Quantum Phase Transitions*. Cambridge University Press, 2001. ISBN 9780521004541. Disponível em: <https://books.google.com.br/books?id=Ih_E05N5TZQC>. Citado 2 vezes nas páginas 52 and 53.

SAKURAI, J. *Advanced Quantum Mechanics*. Pearson Education, Incorporated, 2006. ISBN 9788177589160. Disponível em: <https://books.google.com.br/books?id=lvmSZkzDFt0C>. Citado 2 vezes nas páginas 63 and 118.

SAKURAI, J.; NAPOLITANO, J. *Modern Quantum Mechanics*. Cambridge University Press, 2017. ISBN 9781108422413. Disponível em: <https://books.google.com.br/books?id=010yDwAAQBAJ>. Citado na página 133.

SARMA, S. D.; FREEDMAN, M.; NAYAK, C. Majorana zero modes and topological quantum computation. *npj Quantum Information*, v. 1, n. 1, p. 15001, Oct 2015. ISSN 2056-6387. Disponível em: <https://doi.org/10.1038/npjqi.2015.1>. Citado na página 26.

SARMA, S. D.; NAYAK, C.; TEWARI, S. Proposal to stabilize and detect half-quantum vortices in strontium ruthenate thin films: Non-abelian braiding statistics of vortices in a $p_x + ip_y$ superconductor. *Phys. Rev. B*, American Physical Society, v. 73, p. 220502, Jun 2006. Disponível em: <http://link.aps.org/doi/10.1103/PhysRevB.73.220502>. Citado na página 72.

SCHRIEFFER, J. R.; WOLFF, P. A. Relation between the anderson and kondo hamiltonians. *Phys. Rev.*, American Physical Society, v. 149, p. 491–492, Sep 1966. Disponível em: <https://link.aps.org/doi/10.1103/PhysRev.149.491>. Citado 2 vezes nas páginas 42 and 141.

SCHROER, M. D.; PETTA, J. R. Quantum dots: time to get the nukes out. *Nature Physics*, Nature Publishing Group, v. 4, n. 7, p. 516–518, 2008. Citado na página 36.

SELA, E. et al. Detecting the universal fractional entropy of majorana zero modes. *Phys. Rev. Lett.*, American Physical Society, v. 123, p. 147702, Oct 2019. Disponível em: <https://link.aps.org/doi/10.1103/PhysRevLett.123.147702>. Citado 5 vezes nas páginas 80, 81, 82, 105, and 154.

SHANKAR, R. Renormalization-group approach to interacting fermions. *Rev. Mod. Phys.*, American Physical Society, v. 66, p. 129–192, Jan 1994. Disponível em: <https://link.aps.org/doi/10.1103/RevModPhys.66.129>. Citado na página 52.

SIGRIST, M. Review on the Chiral p-Wave Phase of Sr2RuO4. *Progress of Theoretical Physics Supplement*, v. 160, p. 1–14, 06 2005. ISSN 0375-9687. Disponível em: <https://doi.org/10.1143/PTPS.160.1>. Citado 2 vezes nas páginas 72 and 73.

SILVA, J. F.; SILVA, L. G. G. V. D. da; VERNEK, E. Robustness of the kondo effect in a quantum dot coupled to majorana zero modes. *Phys. Rev. B*, American Physical Society, v. 101, p. 075428, Feb 2020. Disponível em: <https://link.aps.org/doi/10.1103/PhysRevB.101.075428>. Citado 6 vezes nas páginas 16, 27, 76, 79, 80, and 98.

SILVA, J. F.; VERNEK, E. Andreev and majorana bound states in single and double quantum dot structures. *Journal of Physics: Condensed Matter*, IOP Publishing, v. 28, n. 43, p. 435702, sep 2016. Disponível em: <https://doi.org/10.1088%2F0953-8984%2F28%2F43%2F435702>. Citado na página 26.

SILVA, J. F.; VERNEK, E. Modified exchange interaction between magnetic impurities in spin–orbit coupled quantum wires. *Journal of Physics: Condensed Matter*, IOP Publishing, v. 31, n. 13, p. 135802, feb 2019. Disponível em: <https://doi.org/10.1088%2F1361-648x%2Fab0076>. Citado 5 vezes nas páginas 17, 28, 122, 133, and 134.

SIMONIN, J. Kondo quantum dots and the novel kondo-doublet interaction. *Phys. Rev. Lett.*, American Physical Society, v. 97, p. 266804, Dec 2006. Disponível em: <https://link.aps.org/doi/10.1103/PhysRevLett.97.266804>. Citado na página 132.

SMIRNOV, S. Majorana tunneling entropy. *Phys. Rev. B*, American Physical Society, v. 92, p. 195312, Nov 2015. Disponível em: <https://link.aps.org/doi/10.1103/PhysRevB.92.195312>. Citado na página 80.

SMITH, J.; KMETKO, E. Magnetism or bonding: A nearly periodic table of transition elements. *Journal of the Less Common Metals*, v. 90, n. 1, p. 83 – 88, 1983. ISSN 0022-5088. Disponível em: <http://www.sciencedirect.com/science/article/pii/0022508883901194>. Citado na página 31.

SOUSA, G. R. de; SILVA, J. F.; VERNEK, E. Kondo effect in a quantum wire with spin-orbit coupling. *Phys. Rev. B*, American Physical Society, v. 94, p. 125115, Sep 2016. Disponível em: <https://link.aps.org/doi/10.1103/PhysRevB.94.125115>. Citado na página 121.

SUHL, H. Dispersion theory of the kondo effect. *Phys. Rev.*, American Physical Society, v. 138, p. A515–A523, Apr 1965. Disponível em: <https://link.aps.org/doi/10.1103/PhysRev.138.A515>. Citado na página 40.

THOMAS, L. H. The motion of the spinning electron. *Nature*, Nature Publishing Group SN -, v. 117, p. 514 EP –, Apr 1926. Disponível em: <https://doi.org/10.1038/117514a0>. Citado na página 118.

TSVELICK, A. M. The thermodynamics of multichannel kondo problem. *Journal of Physics C: Solid State Physics*, IOP Publishing, v. 18, n. 1, p. 159–170, jan 1985. Disponível em: <https://doi.org/10.1088%2F0022-3719%2F18%2F1%2F020>. Citado na página 156.

TSVELIK, A. *Quantum Field Theory in Condensed Matter Physics*. Cambridge University Press, 2007. ISBN 9780521529808. Disponível em: <https://books.google.com.br/books?id=78t7iDTth2YC>. Citado 2 vezes nas páginas 69 and 157.

ÚJSÁGHY, O. et al. Theory of the fano resonance in the stm tunneling density of states due to a single kondo impurity. *Phys. Rev. Lett.*, American Physical Society, v. 85, p. 2557–2560, Sep 2000. Disponível em: <https://link.aps.org/doi/10.1103/PhysRevLett.85.2557>. Citado na página 40.

VALIZADEH, M. M. Anisotropic heisenberg form of rkky interaction in the one-dimensional spin-polarized electron gas. *International Journal of Modern Physics B*, v. 30, n. 32, p. 1650234, 2016. Disponível em: <https://doi.org/10.1142/S0217979216502349>. Citado 6 vezes nas páginas 109, 113, 125, 128, 132, and 135.

VERNEK, E. et al. Subtle leakage of a Majorana mode into a quantum dot. *Physical Review B*, American Physical Society, v. 89, n. 16, p. 165314, apr 2014. ISSN 1098-0121. Disponível em: <http://link.aps.org/doi/10.1103/PhysRevB.89.165314>. Citado 3 vezes nas páginas 26, 27, and 81.

VOLOVIK, G. *The Universe in a Helium Droplet*. Clarendon Press, 2003. (International Series of Monographs on Physics). ISBN 9780198507826. Disponível em: <https://books.google.com.br/books?id=cbngYQWAiDEC>. Citado 2 vezes nas páginas 72 and 73.

WAHL, P. et al. Kondo temperature of magnetic impurities at surfaces. *Phys. Rev. Lett.*, American Physical Society, v. 93, p. 176603, Oct 2004. Disponível em: <https://link.aps.org/doi/10.1103/PhysRevLett.93.176603>. Citado na página 40.

WATTS, J. D. et al. Magnetic impurities as the origin of the variability in spin relaxation rates in cu-based spin transport devices. *Phys. Rev. Materials*, American Physical Society, v. 3, p. 124409, Dec 2019. Disponível em: <https://link.aps.org/doi/10.1103/PhysRevMaterials.3.124409>. Citado na página 28.

WEINBERG, S. *The Quantum Theory of Fields: Volume 1, Foundations*. Cambridge University Press, 1995. ISBN 9781139643245. Disponível em: <https://books.google.com.br/books?id=V7ggAwAAQBAJ>. Citado 2 vezes nas páginas 64 and 157.

WHITTAKER, E.; WATSON, G. *A Course of Modern Analysis*. Cambridge University Press, 1996. (A Course of Modern Analysis: An Introduction to the General Theory of Infinite Processes and of Analytic Functions, with an Account of the Principal Transcendental Functions). ISBN 9780521588072. Disponível em: <https://books.google.com.br/books?id=ULVdGZmi9VcC>. Citado na página 167.

WILCZEK, F. Majorana returns. *Nature Physics*, Nature Publishing Group, v. 5, n. 9, p. 614–618, 2009. Citado na página 151.

WILSON, K. G. Renormalization group and critical phenomena. i. renormalization group and the kadanoff scaling picture. *Phys. Rev. B*, American Physical Society, v. 4, p. 3174–3183, Nov 1971. Disponível em: <https://link.aps.org/doi/10.1103/PhysRevB.4.3174>. Citado 2 vezes nas páginas 42 and 157.

WILSON, K. G. Renormalization group and critical phenomena. ii. phase-space cell analysis of critical behavior. *Phys. Rev. B*, American Physical Society, v. 4, p. 3184–3205, Nov 1971. Disponível em: <https://link.aps.org/doi/10.1103/PhysRevB.4.3184>. Citado 2 vezes nas páginas 42 and 157.

WILSON, K. G. The renormalization group: Critical phenomena and the kondo problem. *Rev. Mod. Phys.*, American Physical Society, v. 47, p. 773–840, Oct 1975. Disponível em: <https://link.aps.org/doi/10.1103/RevModPhys.47.773>. Citado 4 vezes nas páginas 39, 53, 61, and 157.

WINKLER, R. *Spin-orbit Coupling Effects in Two-Dimensional Electron and Hole Systems*. Springer, 2003. (Physics and Astronomy Online Library, Nº 191). ISBN 9783540011873. Disponível em: <https://books.google.com.br/books?id=LQhcSCuzC3IC>. Citado 2 vezes nas páginas 119 and 121.

Wolf, S. A.; Chtchelkanova, A. Y.; Treger, D. M. Spintronics—a retrospective and perspective. *IBM Journal of Research and Development*, v. 50, n. 1, p. 101–110, 2006. Citado na página 121.

YAFET, Y. Ruderman-kittel-kasuya-yosida range function of a one-dimensional free-electron gas. *Phys. Rev. B*, American Physical Society, v. 36, p. 3948–3949, Sep 1987. Disponível em: <https://link.aps.org/doi/10.1103/PhysRevB.36.3948>. Citado 2 vezes nas páginas 109 and 125.

YOSHIDA, M.; WHITAKER, M. A.; OLIVEIRA, L. N. Renormalization-group calculation of excitation properties for impurity models. *Phys. Rev. B*, American Physical Society, v. 41, p. 9403–9414, May 1990. Disponível em: <https://link.aps.org/doi/10.1103/PhysRevB.41.9403>. Citado na página 78.

YOSIDA, K. Magnetic properties of cu-mn alloys. *Phys. Rev.*, American Physical Society, v. 106, p. 893–898, Jun 1957. Disponível em: <https://link.aps.org/doi/10.1103/PhysRev.106.893>. Citado 2 vezes nas páginas 27 and 109.

ZEE, A. *Quantum Field Theory in a Nutshell*. Princeton University Press, 2003. ISBN 9780691010199. Disponível em: <https://books.google.com.br/books?id=85G9QgAACAAJ>. Citado 3 vezes nas páginas 49, 157, and 161.

ZHANG, G.-M.; HEWSON, A.; BULLA, R. Majorana fermion formulation of the two channel kondo model. *Solid State Communications*, v. 112, n. 2, p. 105 – 108, 1999. ISSN 0038-1098. Disponível em: <http://www.sciencedirect.com/science/article/pii/S003810989900294X>. Citado na página 80.

ZHANG, H. et al. Retracted article: Quantized majorana conductance. *Nature*, v. 556, n. 7699, p. 74–79, Apr 2018. ISSN 1476-4687. Disponível em: <https://doi.org/10.1038/nature26142>. Citado na página 26.

ZHANG, H. et al. Retraction note: Quantized majorana conductance. *Nature*, Mar 2021. ISSN 1476-4687. Disponível em: <https://doi.org/10.1038/s41586-021-03373-x>. Citado na página 26.

ZITKO, R.; PRUSCHKE, T. Energy resolution and discretization artifacts in the numerical renormalization group. *Phys. Rev. B*, American Physical Society, v. 79, p. 085106, Feb 2009. Disponível em: <https://link.aps.org/doi/10.1103/PhysRevB.79.085106>. Citado na página 78.

ZUBAREV, D. N. DOUBLE-TIME GREEN FUNCTIONS IN STATISTICAL PHYSICS. *Sov. Phys. Usp.*, v. 3, p. 320, 1960. Citado 2 vezes nas páginas 32 and 154.